Characterization of High-PGE Low-Sulphur Mineralization at the Marathon PGE-Cu Deposit, Ontario

by

Ryan Ruthart

A thesis
presented to the University of Waterloo
in fulfillment of the
thesis requirement for the degree of
Master of Science
in
Earth Sciences

Waterloo, Ontario, Canada, 2013

Author's Declaration

I hereby declare that I am the sole author of this thesis. This is a true copy of the thesis, including any required final revisions, as accepted by my examiners.

I understand that my thesis may be made electronically available to the public.

Abstract

The Marathon PGM-Cu deposit is hosted by the Coldwell alkaline complex, which consists predominantly of gabbro and syenite and was emplaced at 1108 Ma as part of the Mid-Continent Rift System. Mineralization at the Marathon PGM-Cu deposit is hosted by the Two Duck Lake Gabbro (TDLG), a fresh olivine-bearing gabbro. The Marathon deposit contains several zones of mineralization including the Basal Zone, the Main Zone and the W-Horizon. The W-Horizon is a high-grade PGE zone characterized by low S, low Cu/Pd and high Cu/Ni. The sulphide mineral assemblage is predominantly chalcopyrite and bornite. This contrasts with the Main Zone where the dominant sulphide mineral assemblage is chalcopyrite and pyrrhotite. The Main Zone contains higher S, higher Cu/Pd and shows a decrease in Cu/Pd and pyrrhotite/chalcopyrite from base to top.

Four drill holes were selected for detailed analysis to characterize the W-Horizon style of mineralization. Detailed petrographic study of the pristine and largely unaltered TDLG shows that wide spread hydrothermal alteration is not responsible for the mineralization. Detailed outcrop mapping shows that the TDLG intruded as a series of multiple intrusions in a dynamic magmatic system. Geochemical studies through the W-Horizon show that the mineralization is not the result of crystallization in a layered intrusion. The results of geochemical assays and electron microprobe analysis of olivine grains show that the chemistry through the TDLG hosting the W-Horizon is erratic. This data supports the TDLG intruding as a series of sills in a dynamic conduit environment.

The calculated sulphide metal tenors for the W-Horizon are higher than can be explained by closed system R Factor models. Multistage dissolution upgrading in an open system is examined as the process forming the W-Horizon. This model is able to produce the sulphide metal tenors observed in the W-Horizon. Sulphur loss also affects grades and tenors and was examined through geochemical and petrological data. The change in sulphide mineral assemblage from a pyrrhotite and chalcopyrite (S-rich) to chalcopyrite and bornite (S-poor) supports S-loss. Whole rock S and Se contents are also analyzed to investigate S loss, a lower S/Se indicates that sulphur has been removed from the system. Average S/Se values are $\sim$800 for the W-Horizon, $\sim$1980 for the Main Zone and $\sim$1700 in unmineralized samples. The very low S/Se observed within the W-Horizon supports S-loss.

Sulphur loss in a dynamic magmatic conduit system is proposed for the formation of the W-Horizon mineralization. In this model sulphur undersaturated basaltic magma interacted with an immiscible sulphide liquid in a magma conduit, resulting in the dissolution of sulphide into the basaltic melt and PGE enrichment.

Acknowledgements

Stillwater Canada Inc. generously provided me with a project and financial support for this study. This study was also funded by a NSERC grant from Dr. Robert Linen.

This project would not have been possible without my advisors: Dr. Robert Linnen (University of Waterloo and University of Western Ontario), Dr. Iain Samson (University of Windsor) and Dr. David Good (Stillwater Canada Inc.). It was great to work with such a dedicated team and I benefited greatly from the variety of backgrounds and specialties each of them possesses. Dr. Robert Linnen was especially helpful turning my drafts into a flowing and comprehensive document, to the benefit of the rest of the advisory panel.

I would like to thank Stillwater Canada Inc. and their staff for providing me with work during the field season, allowing me to gain further experience in exploration geology in addition to gathering samples for this project. Without Rachel I am not sure if I would have been able to distinguish between all the gray rocks after my first summer in Marathon. Yanan for the help in the electron microprobe lab at the University of Toronto and Melissa and Iain for help with the LA-ICP-MS work at the University of Windsor lab.

I thank my family who helped me throughout my degree: Mom, Dad, Rob, Amber, Jesse, Rosalie and Emily. All my friends, especially Ryan, Lisa, Jon, Jess and everyone from the 'Hardrock Cafe' who provided me great discussions and interludes from work. I would also like to thank my girlfriend Katrina, who has been extremely patient and helpful while I took too long to finish this project.

Without support from all these wonderful people I would not have been able to complete this project and I cannot thank you all enough.

Table of Contents

List of Tables

List of Figures

Chapter 1

Introduction

1.1 General Introduction

The platinum group elements are a valuable and scarce resource important in modern society. The average platinum and palladium prices in July 2012 were 1,427.00 USD/oz and 579.14 USD/oz respectively (Johnson Matthey website July 2012). Global platinum supply in 2011 was 6,480,000 ounces and palladium supply was 7,360,000 ounces (Butler, 2012). The primary uses for platinum in 2011 were automobile catalytic converters (50%), jewelry (26%), industrial (19%) and investment (2%) (Butler, 2012). Primary palladium uses in 2011 were nearly identical with automobile catalytic converters (52%), industrial (30%) jewellery (11%) and investment (3%) (Butler, 2012). Globally the production of platinum and palladium are predominantly from magmatic sulphide deposits which are located within a limited number of regions (Naldrett, 2011). Platinum production occurs predominantly out of South Africa (75%) followed by Russia (13%), North America (5%) and Zimbabwe (5%) (Butler, 2012). Palladium production is led by Russia (47%) followed by South Africa (35%), North America (12%) and Zimbabwe (4%) (Butler, 2012).

The Marathon PGM-Cu deposit is a magmatic sulphide deposit hosted by the Coldwell Complex, the largest alkaline igneous intrusion in North America. Exploration in the Coldwell Complex has been ongoing since the 1920s. A detailed exploratory drilling program was conducted at the Marathon PGM-Cu property by Anaconda in 1963 and led to the delineation of a large copper deposit. Since then the property has changed hands several times and is currently owned by Stillwater Canada Inc. The latest resource estimate for the deposit is 94.3 million tonnes measured with an average of 0.846 g/t Pd, 0.243 g/t Pt, 0.088 g/t Au and 0.262% Cu and an additional 20.5 million tonnes indicated with an average of 0.451 g/t Pd, 0.160 g/t Pt, 0.062 g/t Au and 0.140% Cu. The total contained metal (measured + indicated resource) is 2,950,000 oz Pd, 869,000 oz Pt, 316,000 oz Au and 618 million lb Cu. Approximately 62% of the value of the deposit comes from the precious metals (Pd+Pt+Au) compared to 38% from Cu (using July 2012 average prices, Pd (580 USD/oz) and Pt (1427 USD/oz) from Johnson Matthey website, Au (1592.8 USD/oz) from the London Bullion Market Assocation website and Cu (7591.9 USD/mt) from the London Metal Exchange website).

Magmatic sulphide deposits are broadly divided into two main types, those which the primary value comes from Cu and Ni and those which it comes from PGE. The Cu and Ni rich deposits tend to be sulphide-rich containing 20 to 90 percent sulphide whereas the PGE rich deposits tend to be sulphide-poor containing between 0.5 to 5 percent sulphide (Naldrett, 2011). The Marathon PGM-Cu deposit is a PGE-rich sulphide-poor deposit. This class of deposits has been further divided by Naldrett (2004, 2011) into 6 groupings based on the magma type associated with the deposit. The Marathon PGM-Cu deposit is classified as PGE-3 tholeiite related using Naldrett's classification scheme. The Marathon PGM-Cu deposit has also been classified as a strata-bound type deposit (Barrie et al., 2002).

The major mineralization zones at the Marathon PGM-Cu deposit have been divided into three distinct zones: the Footwall Zone, the Main Zone and the W-Horizon. The Footwall Zone occurs at the contact between the TDLG and the footwall occurs as net-textured to semi-massive sulphides which are characterized by low Cu/S ratios. The Main Zone, occurring above the Footwall Zone in the TDLG is the thickest and most continuous zone of mineralization. It is characterized by disseminated interstitial sulphide minerals (ranging from trace up to 5 modal %). The W-Horizon is a lens of high PGE low S mineralization occurring above the Main Zone. It was first noted by Marathon-PGM during diamond drilling programs conducted from 2004 to 2006. The W-Horizon is the focus of this study.

Numerous studies have been conducted on the Marathon PGM-Cu deposit over the years detailing the petrography, sulphide mineralogy, geochemistry, platinum group minerals and potential models for the formation of the deposit. Both a magmatic and hydrothermal origin for the mineralization have been proposed and it is a controversial subject in the published literature. This is the first study that focuses on the W-Horizon.

Hydrothermal models for the Marathon PGM-Cu deposit are detailed in Ohnenstetter et al. (1991), Watkinson and Ohnenstetter (1992), Watkinson and Jones (1996), Dahl et al. (2001), Barrie et al. (2002) and Samson et al. (2008). Common to these models is initial formation of the mineralization through magmatic processes. Subsequent interaction with Cl-rich fluids (saline and oxidized fluids have also been proposed) remobilizes Cu and PGE from the lower parts of the deposit to higher levels where they are deposited. Another related model for the mineralization is zone refining (Dahl et al., 2001; Barrie et al., 2002). In this model source areas of crystalline or nearly crystalline rocks are fluxed by a volatile rich fluid which depletes the incompatible elements (including Cu and PGE) and transports them from the source. The volatile rich fluxing fluid becomes further enriched in incompatible elements as it passes through and scavenges incompatibles from more rocks. When sulphur saturation occurs within the fluxing fluid both sulphur and the incompatible elements are deposited. Key evidence for these models includes an observed increase in alteration minerals associated with mineralization (Ohnenstetter et al., 1991; Watkinson and Ohnenstetter, 1992; Watkinson and Jones, 1996; Dahl et al., 2001; Barrie et al., 2002; Samson et al., 2008), an observed association of mineralization and pegmatitic gabbro (Dahl et al., 2001; Barrie et al., 2002), complexly zoned crystals of atokite-zvyagintsevite and hollingworhite which were interpreted to have a hydrothermal origin (Watkinson and Ohnenstetter, 1992) and the distribution of metals (high Cu and high Pd) which is unusual for a magmatic deposit (Barrie et al., 2002).

A magmatic origin for the Marathon PGM-Cu deposit is detailed in Wilkinson (1983), Good and Crocket (1989), Good and Crocket (1990), Good (1992), Good and Crocket (1994), Good (2010) and Good (2012 in press). In these models the Two Duck Lake Gabbro intrudes into the felsic country rock leading to assimilation. This causes S-saturation either through the addition of S from the country rock or contamination triggering S-immiscibility. Although hydrous minerals are observed in association with mineralization, the hydrous minerals are not pervasive and typically occur in cm-scale zones, consistent with post-mineralization formation from deuteric fluids (Good and Crocket, 1994). Results of whole rock geochemistry and major element mineral chemistry showed that the coarse grained Two Duck Lake Gabbro and the pegmatitic Two Duck Lake Gabbro had the same composition (Good and Crocket, 1994). Cu and Pd rich mineralization with low amounts of Ni can be modeled by early crystallization of olivine prior to sulphur saturation. The metal abundances can further be explained by sulphide dissolution upgrading in a magmatic conduit system which would enrich the sulphides in Pd and to a lesser extent Cu (Good, 2010).

1.1.1 Deposits Sharing Similar Characteristics

The Skaergaard intrusion is interpreted to represent fractional crystallization of a closed igneous system (McBirney, 1996). It contains the Platinova Reef, which is similar in some regards to the W-Horizon as it contains low amounts of S and cannot be readily identified by texture or mineral assemblages in the field (McBirney, 1996; Andersen et al., 1998; Nielsen et al., 2005). Ten PGE-rich zones (>0.5 ppm Pd) within a stratigraphic sequence of 60 m with a lateral continuity over 23 km^2 have been successfully identified using geochemical assays for metals. Electron microprobe of plagioclase grains across the intrusion have shown that anorthite content in plagioclase decreases smoothly up through the intrusion with no erratic jumps associated with mineralization (Toplis et al., 2008).

The Sonju Lake Intrusion located in the Duluth complex is another example of closed system fractional crystallization associated with a PGE-horizon. Fractional crystallization is shown by smooth cryptic variations in the composition of olivine and augite crystals determined from electron microprobe (Miller, 1999). Saturation of sulphide in the closed system is interpreted to have resulted from fractional crystallization and settling of the sulphide liquid left strong depletion signatures above the mineralization.

Layering at the Stillwater Complex was identified using major element geochemistry and major element mineral chemistry(Todd et al., 1982). Using these methods over 17 cyclic units ranging from 50-150 m were reported in the Stillwater Complex. Major element mineral chemistry of plagioclase and olivine was used through a transect of the J-M Reef to asses for cyclic mineral variation. Plagioclase showed a gradual upward trend of decreasing anorthite content through the J-M Reef. Olivine showed an abrupt change from Fo_{81}-Fo_{88} to Fo_{60}-Fo_{74} just below the J-M Reef (Todd et al., 1982). Another study by Keays et al. (2012) showed an increase of MgO (from whole rock geochemistry) at the reef contact that was interpreted to indicate a fresh pulse of magma.

Multiple pulses of magma through a conduit system have been proposed for many magmatic Ni-Cu-(PGE) deposits including Norilsk (Naldrett, 1992; Arndt et al., 2003; Arndt, 2011), Voisey's Bay (Li and Naldrett, 1999; Naldrett and Ripley, 2009; Ripley and Li, 2011), Jinchaun (Li and Ripley, 2011; Song et al., 2011), the Thunder Bay North deposit (Chaffee et al., 2012), the Eagle Deposit (Ripley and Li, 2011; Ding et al., 2012) and the Partridge River Intrusion (Taib, 2001; Thériault et al., 2000; Ripley et al., 2007). A magmatic conduit system has also been proposed for the Marathon PGM-Cu deposit based on modeling of trends in metal ratios (Good, 2010). Common themes for magmatic conduit deposits include evidence for large volumes of extrusive magma, cyclic or erratic trends in major element and mineral chemistry resulting from recharge events, the transport of sulphide liquid through conduits and physical traps which allow for the sulphides to settle out and collect. These key criteria will be used to evaluate the data gathered from the W-Horizon for evidence of a magmatic conduit system.

Sulphur dissolution upgrading (Kerr, 2005) is a process which occurs in magmatic conduits. After the formation of sulphide liquid, new pulses of sulphur-undersaturated magma pass through the system. The sulphur undersaturated magma interacts with the sulphur liquid and dissolves some of the sulphide while at the same time upgrading the tenor of the remaining sulphide. This model has been proposed to explain the very high PGE tenors observed at Bushveld (Kerr, 2005), Norilsk (Kerr 2005 and Arndt 2011), Stillwater (Keays et al., 2012) and the Marathon PGM-Cu deposit (Good, 2010). The PGE tenors in the W-Horizon will be modeled to determine if they could have formed from sulphur dissolution upgrading.

1.2 Research Objectives

The major goals of this project are to: characterize the W-Horizon mineralization and compare it to the other mineralization zones at the Marathon deposit; determine the physical conditions of emplacement of the W-Horizon; and determine if the W-Horizon mineralization was formed through magmatic and/or hydrothermal processes. For this project four, diamond drill holes intersecting the W-Horizon were studied and sampled in detail. Complete sample suites intersecting the W-Horizon and the surrounding unmineralized rock were logged in detail and sampled for geochemical assay and the production of polished thin sections.

Characterization of the W-Horizon will be done using drill core logging, silicate and sulphide mineral petrography, whole rock geochemistry and mineral chemistry. The petrography and sulphide mineral assemblage of the Two Duck Lake Gabbro hosting the W-Horizon mineralization will be described in detail and compared to the other mineralized zones. Whole rock geochemistry will be used to compare the W-Horizon mineralization to the previously studied zones, and assess for chemical evidence of hydrothermal alteration. Both major and trace element mineral chemistry will be determined by electron microprobe and LA-ICP-MS to examine for changes between the various mineralized zones and unmineralized TDLG. Trace element mineral chemistry was analyzed using LA-ICP-MS. Trace element mineral chemistry is not affected by crystal re-equilibration and is useful for interpreting crystallization histories.

The physical conditions of emplacement will be assessed using whole rock geochemistry and mineral chemistry. Evidence for fractional crystallization, cryptic layering or cyclic injections within the TDLG will be assessed using major element geochemistry and examining for systematic changes. Olivine grains were analyzed for major element composition using an electron microprobe as these compositions remain unaffected by changes in modal mineral abundances.

Chapter 2

Geology

2.1 Introduction

The Marathon deposit is located on the north shore of Lake Superior on the eastern edge of the Coldwell Alkaline Intrusive Complex (Fig. 2.1). The Coldwell Complex formed at approximately 1108 Ma as part of the mid-continent rift system of North America (Heaman and Machado, 1992).

2.2 The Mid-Continent Rift System of North America

The mid-continent rift system (MCR) of North America is an aborted Proterozoic rift, and is one of the largest known continental rifts in the world (Heaman and Machado, 1992). The MCR is over 2300 km in length and extends from Lake Superior south-west to central Kansas (Green, 1983) (2.1 inset map). The majority of the MCR rocks are covered by Paleozoic sedimentary strata but are exposed in the Lake Superior area. The MCR intruded rocks of the Archean Superior Province of the Canadian Shield (2.7 Ga) and the Early Proterozoic Southern Province (1.9 Ga) (Van Schmus and Bickford, 1981). Keweenawan volcanism associated with the rift took place between 1108 and 1087 Ma (Palmer and Davis, 1987). During this time voluminous amounts of magma were erupted, estimated between 300,000 km^3 (Green, 1983) and 850,000 km^3 (Hutchinson et al., 1990), making it the most voluminous major Precambrian mafic magmatic event in North America (Heaman and Machado, 1992). The rates of eruption are estimated to have been between 0.2-0.6 km^3/year producing Phanerozoic flood basalt provinces (Davis and Paces, 1990). Similar tectonic settings and types of igneous activity are located in the Gregory-Kavirondo Rifts of East Africa and the Kangerdlugssuaq area of East Greenland (Mitchell and Platt, 1978).

Major tholeiitic intrusions associated with the MCR include the Duluth Complex (Minnesota), the Mellon Complex (Wisconsin), the Logan Sills (Ontario) and the Coldwell Complex (Ontario) (Heaman and Machado, 1992). Plutons located off-axis of the northern flank of

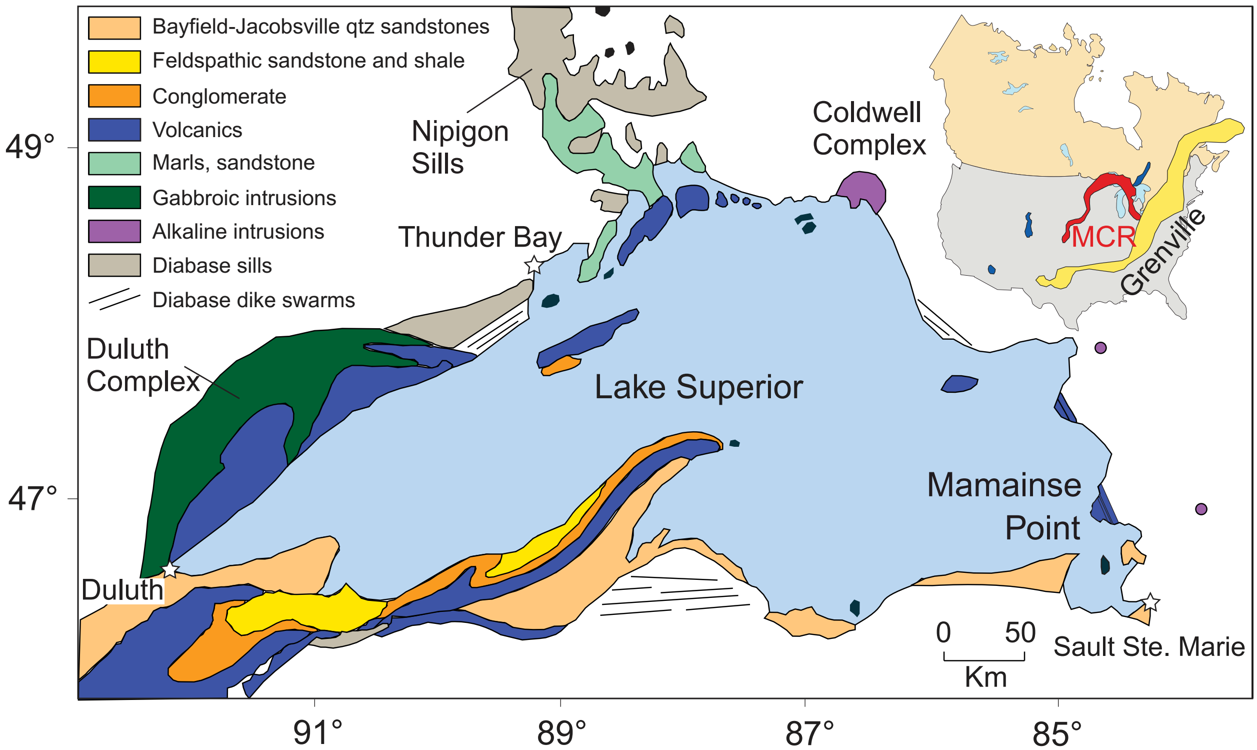

Figure 2.1: Generalized geologic map of the of the Lake Superior region showing the Coldwell Complex with the mid-continent rift gravity anomaly highlighted in the inset map. Modified from Swanson-Hysell et al. (2009).

the MCR include the Coldwell, Prairie Lake, Killala Lake and Chipman Lake intrusions (Heaman and Machado, 1992).

2.3 The Coldwell Complex

The Coldwell Complex, the largest alkaline intrusion in North America, is approximately 28 km in diameter and has a surface area of 580 km^2 (Mitchell and Platt 1977, Shaw 1997, Heaman and Machado 1992). It was emplaced at 1108 $\pm$ 1 Ma during the early stages of the mid-continent rift system of North America (Heaman and Machado, 1992). The Coldwell Complex is unusual in that it contains oversaturated, saturated and undersaturated rocks. Rocks of the Schreiber-White Lake Archean metavolcanic-metasediment are truncated by the Coldwell Complex (Mitchell and Platt, 1978). On the eastern edge of the complex the contact with the Archean rocks has a regular arcuate shape, whereas on the west the contact is irregular and faulted. The rocks within 50 m of the contact are metamorphosed to pyroxene hornfels grade. The configuration of the Coldwell Complex shows that it was emplaced as sheet like bodies during cauldron subsidence (Walker et al., 1993). Early work by Lilley (1964) interpreted the Coldwell Complex as a funnel shaped body of gabbro, which crystallized by fractional crystallization, and was later intruded by nepheline syenites. Later work by

Puskas (1967) reinterpreted the complex as a large lopolith. Detailed field studies conducted by Puskas (1970), Mitchell and Platt (1977), Mitchell and Platt (1982), and Mitchell et al. (1993) have shown that the Coldwell Complex actually consists of three overlapping ring intrusions which they termed Centres (Fig. 2.2). The rocks to the western portion of the complex are characterized by multiple breccias and show extensive metasomatism. The rocks on the eastern portion of the complex contain low amounts of xenoliths and metasomatism, and were interpreted to represent a deeper level of the complex by Mitchell and Platt (1978).

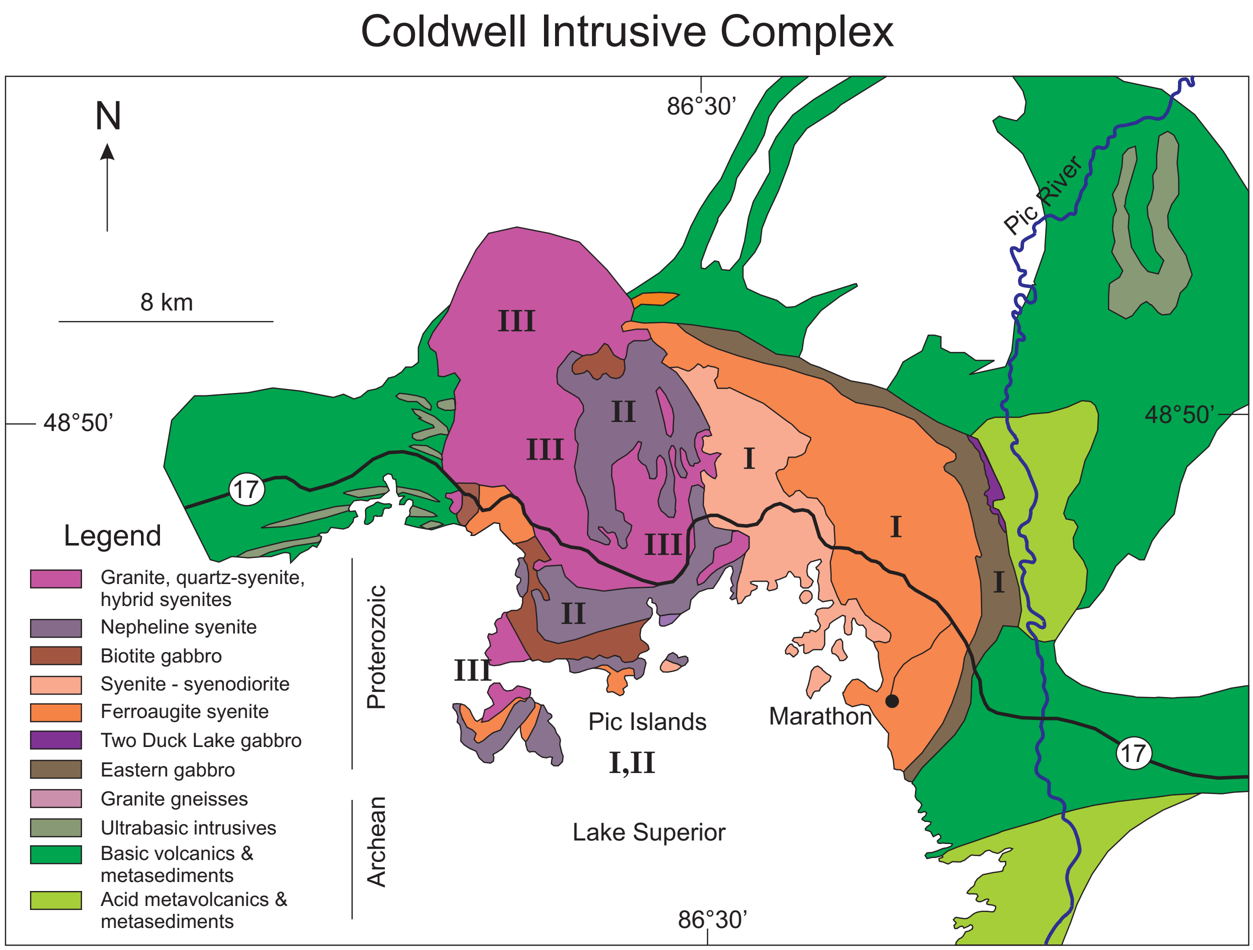

Figure 2.2: Geology of the Coldwell Complex, northwestern Ontario, showing the three overlapping intrusive centres (I, II and III). The Two Duck Lake Gabbro intrusion is shown along the eastern margin of the Coldwell Complex. Modified from Mulja and Mitchell (1991)

Centre I is the oldest unit, consists of saturated alkaline rocks with peralkaline over-saturated residua and is located in the eastern portion of the Coldwell Complex (Mitchell and Platt, 1977). The oldest unit within this Centre is the Eastern Gabbro, which rims Centre I along the eastern and northern boundaries. The Marathon deposit is hosted within Centre I. The gabbros were intruded by the ferroaugite syenites that make up the bulk of Centre I. The gabbros and syenites commonly show igneous layering and rarely contain breccias. Mineralogical studies have shown iron enrichment in the form of the minerals fayalite, ferroaugite, ferrodenite-hastingsite and ferrorichterite (Mitchell and Platt, 1977).

Centre II is composed of undersaturated alkaline rocks. Biotite gabbro has been intruded by several phases of nepheline and natrolite syenites (Mitchell and Platt, 1982). Texturally these rocks display variable textures, and in outcrop breccia zones, layering and evidence of recrystallization are apparent. The dominant mafic phase amphibole which ranged from magnesian hastingsitic hornblende to hastingsite to hastingsitic hornblende to ferroedenitic hornblende. Pyroxenes were observed to occur as corroded diopside cores surrounded by amphibole and less commonly as acmitic hedenbergite overgrowth rims on iron-rich amphiboles (Mitchell and Platt, 1982). The nepheline syenites are silica over saturated and contained feldspars which lacked microcline twinning and perthites and also exhibited extensive high sub-soludius ion exchange with Na-rich fluids (Mitchell and Platt, 1982). Extensive dike swarms of lamprophyres and analcite tinguaties are also associated with this intrusion.

Centre III rocks are alkaline with oversaturated residua. The order of intrusion in this centre was magnesiohornblende syenite, contaminated ferro-edenite syenite, ferro-edenite syenite and quartz syenite (Mitchell et al., 1993). This centre is characterized by a wide variety of amphibole compositions ranging from magnesiohornblende through ferro-edenite and ferrorichterite. Magnesiohornblende syenites are composed of alkali feldspar, amphibole, minor biotite, quartz and accessory minerals. The ferroedenite syenites are composed of alkali feldspar, quartz, minor biotite, magnetite-ilmenite and accessory minerals (McLaughlin and Mitchell, 1989). The contaminated ferro-edenite syenite is composed of alkali feldspar, amphibole, biotite, accessory minerals and contains abundant xenoliths. Quartz syenites are composed of alkali feldspar, amphibole, minor quartz and accessory minerals (McLaughlin and Mitchell, 1989). This centre shows evidence of multiple intrusions, contamination and brecciation of preexisting plutons (Mitchell et al., 1993). Rocks of this centre were observed to have intruded into most other phases in the complex (Mitchell and Platt, 1978).

2.4 Summary of Previous Work

Exploration around the Marathon property has been ongoing since the 1920's. In 1963 Anaconda acquired the Marathon property and a systematic exploratory diamond drilling program led to its development as a copper resource. Since then numerous studies on the property have been published. A key controversy in the literature has been whether the mineralization has a magmatic or hydrothermal origin. No detailed studies of the W-Horizon mineralization have been published. Below is a detailed summary of the major works published on the Marathon PGM-Cu property.

Wilkinson (1983) conducted a detailed study of the Two Duck Lake Gabbro within the Bamoos Lake area of the Marathon PGM-Cu deposit. Initial work included detailed mapping and sample collection. Samples were assayed for major and base precious metals by atomic absorption and optic emission. Using polished thin sections Wilkinson compiled a detailed description of the petrography of the gabbro, the sulphide minerals and the platinum group minerals. His work concluded that the mineralization at the Marathon PGM-Cu deposit was of magmatic in origin. He proposed that after intruding, the TDLG assimilated some of the wall rock material leading to the addition of H_2O and CO_2 volatiles. The increase in f_{O_2} caused precipitation of the massive layers of magnetite. The f_{S_2} increased in response to the formation of magnetite and led to the precipitation of sulphide minerals within the TDLG. These late stage volatiles were attributed as the cause for the localized, patchy alteration minerals associated with some of the sulphide minerals.

Good and Crocket (1989) conducted sulphur isotopic analysis on samples of TDLG from the Marathon PGE-Cu deposit, and gabbro from the MacRae occurrence (a near-by mineralized gabbro located within the Coldwell Complex). The results of the analysis showed that both the Marathon PGE-Cu deposit and the MacRae occurrence had $\delta^{34}S$ near 0, and were indistinguishable from magmatic values. The footwall which the TDLG intruded was not analyzed for comparison to the samples of TDLG. However since both deposits had values near 0 it was concluded that similar ranges of $\delta^{34}S$ inherited from the Archean basement was unlikely and interpreted to support a magmatic origin for both deposits.

Good and Crocket (1990) conducted detailed mapping, sample collection and whole rock geochemistry to investigate the origin for the mineralization. Their detailed petrographic work showed that the sulphides in the TDLG occurred interstitial to fresh silicates and as disseminated grains associated with hydrous minerals (biotite, chlorite, amphibole and altered plagioclase and calcite). Calculations of the PGE tenor to 100% sulphides showed that there were no fractionation trends that separated the most altered samples from the fresh samples, and it was concluded that the origin of the mineralization was magmatic.

Ohnenstetter et al. (1991) conducted a study of zoned hollingworthite (RhAsS) crystals in samples of TDLG. The samples were collected from coarse grained to pegmatitic TDLG and were analyzed by electron microprobe and scanning electron microscope. Hollingworthite crystals were observed in close association with chalcopyrite. They observed three stages of zoning within the hollingworthite crystals: 1) initial growth of an Ir and As-rich hollingworthite; 2) partial resorption of this phase and precipitation of near end-member hollingworhite; 3) resorption of hollingworthite along the edges of grains and cracks, outer rims enriched in Pd, Os or Ru, and depletion of Pd and Ni. The observed zoning was interpreted to be too complex to have formed from the exsolution of a magmatic sulphide and to have resulted from variations in the compositions of fluids. The proposed model was the dissolution of pyrrhotite by a saline fluid leading to its enrichment in S. Precipitation of this fluid resulted in the alteration of original silicates and oxides, the modification of sulfides through the replacement of Fe minerals by chalcopyrite and the precipitation of Pt-group minerals.

Watkinson and Ohnenstetter (1992) conducted a petrographic study of the TDLG and an electron microprobe study to determine the composition of PGM in the TDLG. The PGM in the TDLG were observed as: 1) inclusions in or adjacent to postcumulus sulphides (chalcopyrite and cubanite), 2) in chalcopyrite or pentlandite along sulphide-oxide grain boundaries, 3) in the rim of plagioclase grains with chalcopyrite, in veinlets along the contacts of chalcopyrite with other minerals, or 5) in veins cutting magnetite that is partly altered. The majority of PGM were located as isolated grains within chalcopyrite. They also observed that the highest PGE grades were in coarse grained to pegmatitic rocks, however the coarsest grains rocks did not contain the highest grades. A close relationship of PGM with mica and apatite, and PGM with the alteration assemblage chlorite + actinolite + epidote + sericite +

calcite was noted. The electron microprobe revealed that most of the PGM had homogeneous compositions, whereas atokite-zvyagintsevite and hollingworhite were intricately zoned. They concluded that the mineralization at the Marathon PGE-Cu deposit was hydrothermal in origin based on: 1) unusual Cu-rich sulphide mineral assemblage dominated by chalcopyrite which is uncommon for a magmatic sulphide assemblage, 2) replacement of pyrrhotite by chalcopyrite 3) association of PGM with alteration minerals. The proposed model was an early precipitation of magmatic sulphides followed by alteration by a fluid (derived from magmatic sources and the breakdown of felsic metavolcanic xenoliths from the footwall). The fluid transported PGE and Cu, possibly as chloride complexes, to refine the original sulphide minerals.

Good (1992) conducted a detailed study on the Marathon PGE-Cu deposit. The study involved detailed mapping and sampling, whole rock geochemical assays for major and trace elements, precious metals assays and major element mineral chemistry using electron microprobe. He concluded that a magmatic origin for the sulphides at the Marathon PGE-Cu deposit was consistent with the geochemical and petrographic evidence. The observed enrichment in Cu and depletion in Ni and Ir was explained by his model. In the model the TDLG was emplaced as a crystal mush containing plagioclase, olivine and sulphide liquid. Sulphide saturation was attained in a lower magma chamber through the assimilation of S-bearing Archean country rock. The sulphide liquid equilibrated with fractionated silicate melt which was depleted in Ni and Ir. During the intrusive event the sulphide liquid crystallized into a monosulphide solution which resulted in an enrichment in Cu, resulting in the Main Zone. The Basal Zone, which contains more S and less Cu, was deemed to be a later phase which gathered metals from a PGE and Cu depleted source.

The work of Good and Crocket (1994) continued on the work of Good (1992) and the results supported a magmatic origin for the Marathon PGE-Cu deposit. This study involved detailed petrography, major element mineral chemistry by electron microprobe and whole rock geochemistry. The TDLG samples studied contained predominantly primary unaltered minerals, and there was an absence of extensive alteration minerals. Hydrous minerals, where observed, were in small centimeter scale zones consistent with local migration of chalcophile elements over very short distances in a deuteric fluid. The sulphide minerals were observed to be primarily in contact with anhydrous silicate minerals and magnetite. Whole rock geochemistry and mineral chemistry showed that there were no significant differences between coarse grained TDLG and the more hydrous pegmatitic TDLG. Whole rock geochemistry also showed that there was a significant positive correlation between chalcophile elements and sulphur, which is consistent with a magmatic origin. If the ore was formed from hydrothermal processes a loss in element proportions typical of magmatic control would be expected.

Shaw (1994 and 1997) focused on the Eastern Gabbro, examining field relationships, whole rock chemical composition and major element mineral compositions by electron microprobe. Modal layering was observed within the Eastern Gabbro, the layers dip between 20 and 60 degrees towards the center of the complex. The predominant layering of the Eastern Gabbro in the Bamoos Lake area were meter-scale planar layers that laterally discontinuous over distances of 5 to 10 m. Folded and slumped layers of varying thickness were also observed.

Major element mineral chemistry revealed trends of both normal and reversed fractional crystallization in the gabbro. The intrusion of the gabbro was interpreted to have occurred as a large ring dyke system into an active ring fault system through multiple injections of magma. Using mineral-melt equilibria Shaw concluded that the parental magma for the Eastern Gabbro had a subalkaline parentage with a Mg# of 0.42-0.49.

Watkinson and Jones (1996) investigated PGM grains and fluid inclusions located in chalcopyrite and cubanite grains in the TDLG of the Marathon deposit. He observed that the PGM were commonly located on broken irregular surfaces of Cu-Fe-S minerals. Halite daughter minerals and quenched brine were also observed in and around fluid inclusions. PGM grains in fractures cutting altered titanomagnetite that had undergone oxyexsolution were interpreted to indicate a highly oxidized environment. In highly oxidizing conditions brines of deuteric or mixed origins could interact with previously crystallized magmatic sulphides and remobilize the PGE from the lower parts of the intrusion to a higher level where they reacted with a strong temperature gradient. He concluded that the PGE enrichment was due to this zone refining process and occurred at subsolidus temperatures.

Dahl et al. (2001) presents data collected from a detailed 1:200 mapping program of the TDLG centered around Two Duck Lake. In his mapping Dahl separates the TDLG into three distinct zones, the lower sub-unit, the middle sub-unit and the upper sub-unit. The lower zone is described as a fine to medium grained hornblende gabbro to monzonite, hydrous silicates are pervasive and it contains disseminated sulfides (2-3%). The middle sub-unit is described as a coarse grained to pegmatitic olivine gabbro with numerous pods of pegmatitic gabbro and granophyre, hydrous silicates occurred only locally, and trace amounts of sulfides were observed. The upper sub-unit is described as mainly coarse to very coarse grained olivine gabbro to diorite with hypidiomorphic to poikilitic textures, hydrous silicates occurred in a greater abundance than the middle zone and it contained disseminated sulphides (up to 5 vol%). The lower and upper sub-units were similar in that they both contained a greater abundance of hydrous silicates, sulfide minerals and xenoliths. The observed increase of hydrous silicates, pegmatitic zones, granophyre and xenoliths were interpreted to support the segregation and local remobilization of hybrid magmas enriched in silica, alkalies and volatiles. These magmas along with a base and precious metal enriched fluid phase migrated from the bottom to the top of the intrusion. This process was accompanied by hydrothermal alteration and remobilization along the intrusion boundaries during cooling of the TDLG and concentrated sulphide and PGE mineralization in the foot wall (Footwall Zone) and the hanging wall (Main Zone).

Barrie et al. (2002) published the results of a detailed relogging and assaying study from diamond drill core of the Marathon PGM-Cu deposit. They observed that primary magmatic textures were common in all of the mineralized zones and were best developed in medium and coarse grained gabbro where sulphides were interstitial to cumulus silicate phases with low amounts of alteration minerals. The ubiquitous, undisturbed, net-textured sulphides observed in the rocks indicated that the initial metal enrichment was due to accumulation of immiscible sulphide in a magmatic system. Very coarse to pegmatitic gabbro were observed to contain interstitial primary magmatic sulphides which commonly contained partial replacement textures with cumulus and intercumulus silicate minerals. The pegmatitic textures and increase in alteration minerals were interpreted to be consistent with crystallization in a fluid rich melt. The highest Cu and Pd values were observed to be displaced from the highest S values in the upper zones of the ore stratigraphy. The combination of pegmatitic textures associated with mineralization, alteration minerals in some of the mineralized zones and displacement of Cu and Pd from S led the authors to propose a zone refining model for the Marathon deposit. In this model the intrusion of the gabbro caused the release of volatile rich fluids from the felsic volcanic footwall unit, this fluid was then fluxed up through the gabbro. As the fluid rose it became enriched in incompatible elements, sulphur and metals and caused the depletion of incompatible elements in the residual gabbro. As the fluxing fluid rose it eventually reached S saturation and precipitated sulphide, chalcophile elements and caused the coarse grained to pegmatitic textures.

Good (2010) presented a 3D deposit model for the Marathon PGE-Cu deposit generated using logs and assays from diamond drill holes. Using base metal to PGE ratios he proposed that the multistage dissolution upgrading model of Kerr and Leitch (2005) can explain the observed trends. Magma conduits feeding the deposit are the source of sulphur undersaturated magma required for the dissolution upgrading model. After initial sulphide saturation the sulphide liquid became trapped in troughs in the magma conduit. New pulses of sulphur undersaturated magma intruded through the conduit system and upgraded the previously formed sulphide liquid. Dissolution upgrading reproduces the metal ratios observed in the deposit: a maximum Cu in sulphide tenor near 35 wt% Cu and extreme enrichment in Pd (tenor values up to 3.5 wt% Pd observed) and to a lesser extent Pt.

Good et al. (submitted) presents results of a geochemical and petrographical study of the Two Duck Lake Gabbro and the Eastern Gabbro spanning the eastern and northern rims of the Coldwell Complex. The Eastern Gabbro is shown to be chemically similar across the 20 km strength length in both major element chemistry and REE concentrations and chondrite normalized patterns. The REE patterns of the TDLG are distinct from those of the Eastern Gabbro. The detailed petrographic study showed that the Layered Gabbro and massive Eastern Gabbro are texturally distinct from the coarse grained to pegmatitic, heterogeneous TDLG.

2.5 Geology of the Marathon Deposit

The Marathon deposit is located within Centre I on the eastern rim of the Coldwell Complex, within the Eastern Gabbro (Fig. 2.3). The major geologic units in this area strike north-south and consists of a Rheomorphic Intrusive Breccia (RIB) at the contact with the Archean footwall host, the Eastern Gabbro and the Two Duck Lake Gabbro the intrudes the Eastern Gabbro at or near the RIB.

A generalized geologic cross section outlining the geometry of Marathon deposit is shown in Figure 2.4. The Two Duck Lake Gabbro intruded above the RIB and follows troughs and basins within it. Xenoliths of the Eastern Gabbro commonly occur within the Two Duck Lake Gabbro. The Eastern Gabbro lies above the Two Duck Lake Gabbro. The Main Zone mineralization is located at the base of the Two Duck Lake Gabbro, and the thickness of the mineralization typically increases in troughs in the footwall. The W-Horizon mineralization is also located within the Two Duck Lake Gabbro above the Main Zone mineralization. The separation between the two mineralized zones is variable and can range from less than a metre to decimetres.

2.5.1 Rheomorphic Intrusive Breccia

The Rheomorphic Intrusive Breccia (RIB) occurs at the base of the Eastern Gabbro contact and strikes north-south and dips to the west at 20 to 60° (Good, 1992; Shaw, 1994). The unit can be matrix or clast supported, with clasts ranging in size from 1 cm to greater than 1 m across (Fig. 2.5 D). Clasts in the area of the Two Duck Lake Gabbro are predominantly composed of fine grained gabbro and intermediate volcanic rocks of Archean age. Elsewhere in the Coldwell Complex the clasts are more variable including massive quartz, magnetite-rich iron formation and mafic volcanics. The shape of clasts ranges from sub-rounded to angular and granitic rinds are present on clast margins, clasts are stretched and boudinaged and the matrix displays flow fabrics (Shaw, 1994). These features are interpreted as evidence of thermal remobilization.

2.5.2 Eastern Gabbro

The Eastern Gabbro is a ring dike that forms an arc shaped unit and strikes for 33 km with a width up to 2.5 km. To the northwest the Eastern Gabbro is truncated by late quartz syenites. The Eastern gabbro is comprised of several units: Gabbronorite, Layered Gabbro and Layered Magnetite Olivine Cumulate.

2.5.2.1 Gabbronorite

The oldest subunit in the Eastern Gabbro is Gabbronorite. It is located between Bamoos Lake and Two Duck Lake where it occurs as dykes within the Archean footwall, as xenoliths in younger gabbro, and as clasts within the rheomorphic intrusive breccia. The dykes that intruded Archean volcanic rocks are vertical with a north strike traceable up to 100 m and can be up to 6 m thick (Shaw, 1994).

The composition and texture of the Gabbronorite is variable including olivine-plagioclase gabbronorite, fine to medium grained olivine gabbronorite, olivine gabbro, poikilitic gabbro and gabbronorite (Fig. 2.5 A and 2.7 A). Contacts between the subunits are gradational over 5-10 cm intervals. Weakly developed layering is common in the gabbronorite xenoliths and is defined by pyroxene, olivine and magnetite oikiocrysts in the fine grained (< 1 mm) gabbro and Gabbronorite. The layering is also defined by feldspar phenocrysts in the gabbronorite (Shaw, 1994).

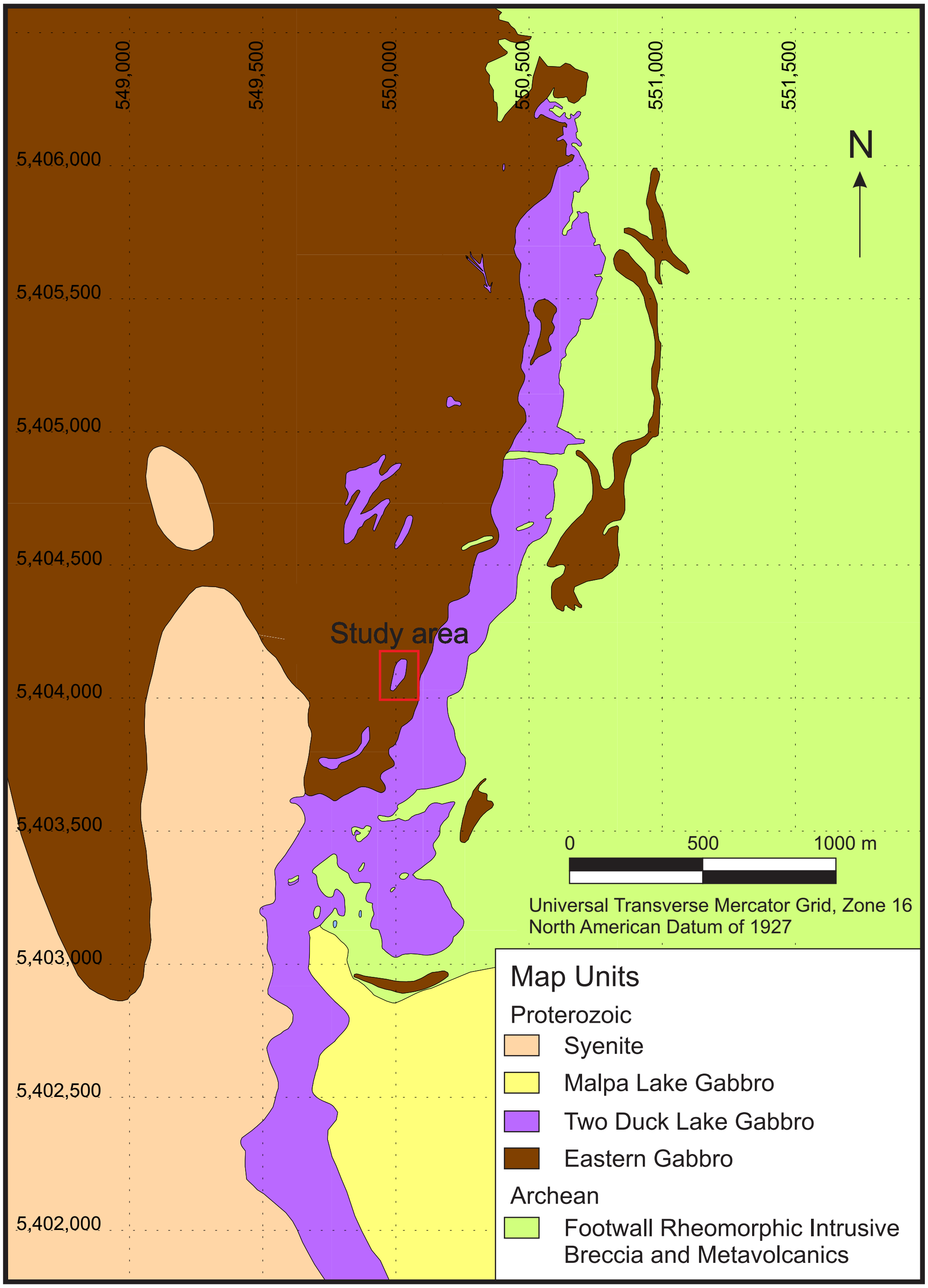

Figure 2.3: Geology of the Marathon deposit. The area the samples were taken from for this study is highlighted. Coordinates are shown in UTM. Map produced from Marathon-PGM internal data set.

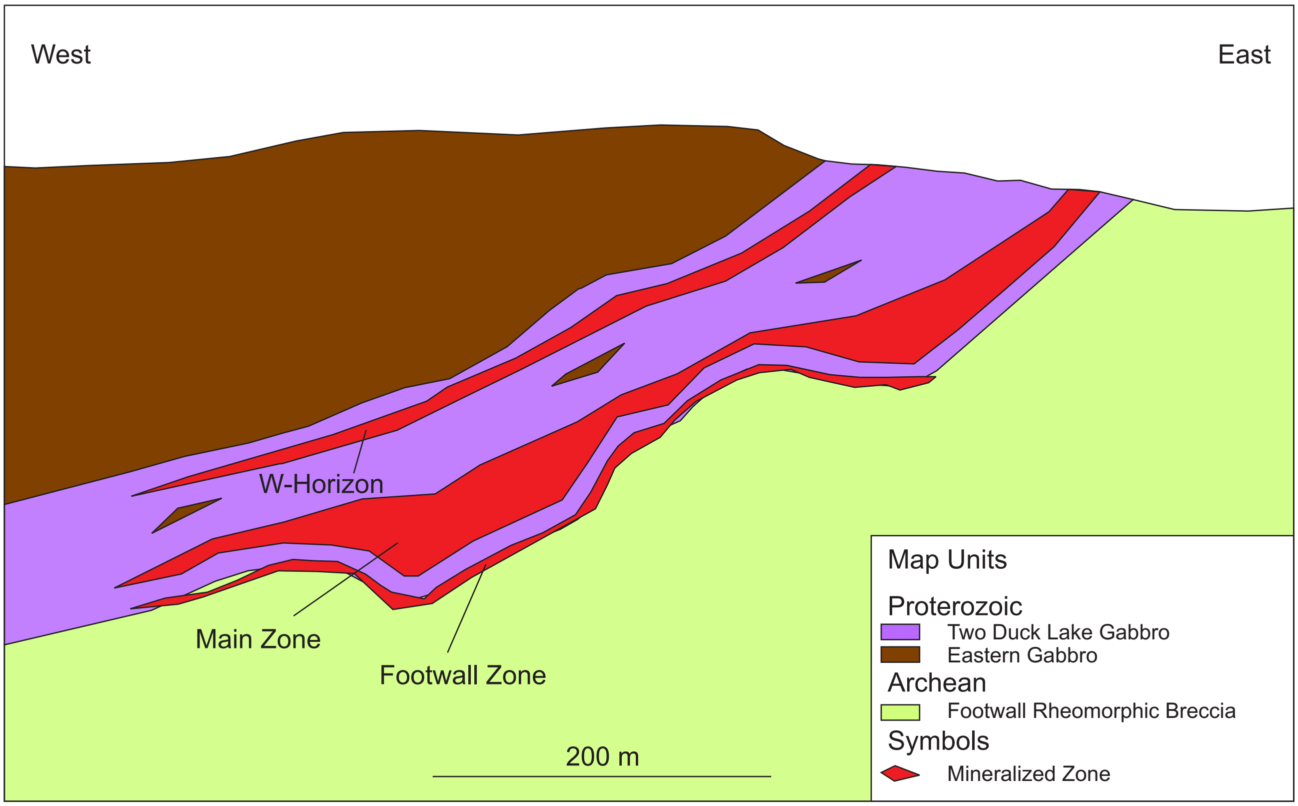

Figure 2.4: Generalized cross-section looking north showing the major units and mineralization zones of the Marathon deposit. The contact between the Two Duck Lake Gabbro and the Rheomorphic Intrusive Breccia dips between 20-60° to the west. The Footwall Zone occurs at the interface of the footwall and the TDLG and the mineralization can be hosted within either unit. The Main Zone mineralization is above the contact between the Two Duck Lake Gabbro and the footwall. The thickness of the Main Zone mineralization increases at troughs in the footwall. The W-Horizon mineralization occurs above the Main Zone mineralization within the Two Duck Lake Gabbro. Horizontal scale is exaggerated to show relationships between mineralized zones.

2.5.2.2 Layered Gabbro

The Layered Gabbro forms the majority of the Eastern Gabbro and consists of olivine, clinopyroxene, magnetite and plagioclase (Shaw, 1994). Olivine, clinopyroxene and magnetite crystallized first as cumulate minerals, with later anhedral plagioclase grains that fill the interstices. Contacts with the Archean country rock are vertical to steeply dipping to the west and are shallow dipping with the younger iron-rich augite syenite. The unit ranges from massive to layered, and there are several layering styles. Layers are laterally discontinuous over a few to tens of meters, they are rhythmic with layers between a few centimeters and meters in thickness, contacts are sharp to gradational, and structures such as cross beddings, slump features, and folds are present in localized zones (Fig. 2.5 B). The layers are defined by variations in modal percent plagioclase between leucocratic layers (60-80% plagioclase) to mesocratic and melanocratic layers (20-35% plagioclase). The layers strike parallel to the eastern contact of the unit and the dip ranges from 20° to 60° towards the centre of the Coldwell Complex (Shaw, 1994). Within the area of Bamoos Lake pyroxene and magnetite oikiocrystic anorthosite and anorthositic blocks which range in size from a few cm to more than a 1 m are common.

2.5.2.3 Layered Magnetite Olivine Cumulate

The Layered Magnetite Olivine Cumulate (LMOC) was observed to the west of and stratigraphically above the Two Duck Lake Gabbro by Shaw (1994). The LMOC occurs predominantly within the Layered Gabbro and consists of alternating gradational layers of medium to coarse grained magnetite and olivine cumulates with interstitial plagioclase. The massive magnetite cumulate layers contain 25-95% magnetite. Thickness of the unit ranges from a few cm up to 10's of m.

2.5.3 Two Duck Lake Gabbro

The Two Duck Lake Gabbro (TDLG) intruded the layered gabbro in the area south of Bamoos Lake. Based on textural and geochemical evidence the TDLG is considered a separate intrusion from the Eastern Gabbro. The intrusion strikes north-south, can be traced for over 6 km, and ranges in thickness between 50 and 250 m. The Two Duck Lake intrusion forms an anastomosing or bifurcating series of dikes or sills that cut the preexisting gabbros (Fig. 2.5 F); see also (Good, 2008). Local bands of mafic minerals observed in outcrop have been interpreted to represent accumulations of minerals from crystal settling processes occurring during the intrusion of a crystal mush, as described by Marsh (2004), Marsh (2006) and Marsh (2007). Examples of these zones of crystal sorting are shown in Figure 2.6. Figure 2.6 A and B show a 2 x 2 m outcrop of TDLG, overall the composition is that of a gabbro but on a localized scale different units can be picked out. This texture is unlikely to result from the intrusion of three different magmatic phases (clinopyroxenite, gabbro, and pegmatitic gabbro), but rather are interpreted to represent zones where crystals (gabbro) have accumulated and interstitial melt has accumulated or forced into open space (clinopyroxenite). Figure 2.6 C

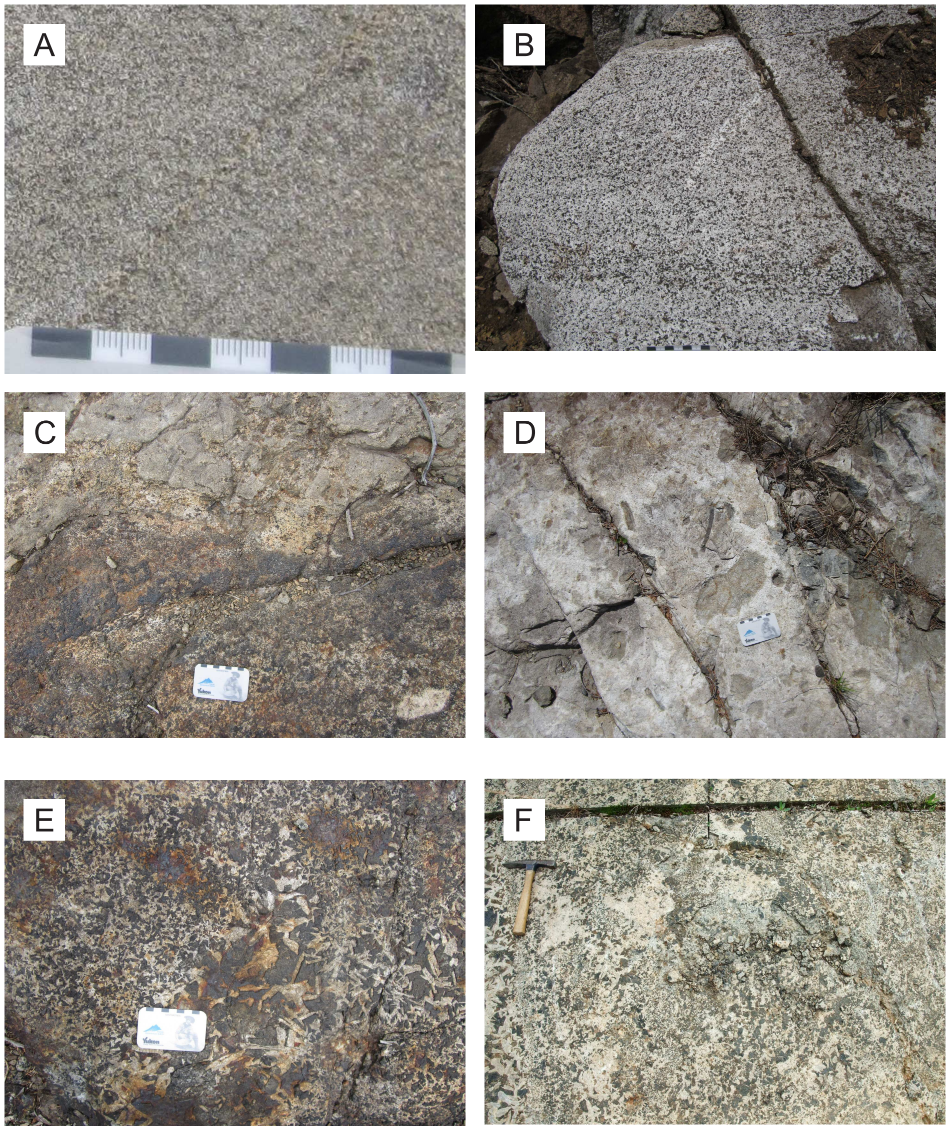

Figure 2.5: Photographs of rock textures seen in outcrop. Scale card is approximately 8 cm wide, hammer is approximately 30 cm long. A) Fine grained Eastern Gabbro with cumulate texture. B) Coarse grained equigranular Eastern Gabbro exhibiting layering (running right to left in photo). C) Layer of magnetite-olivine cumulate within fine grained Eastern Gabbro. D) Rheomorphic intrusive breccia exhibiting rounded and angular clasts.E) Vari-textured of coarse grained and pegmatitic Two Duck Lake Gabbro. F) Chaotic anastomosing stringers of TDLG indicating a dynamic intrusive environment.

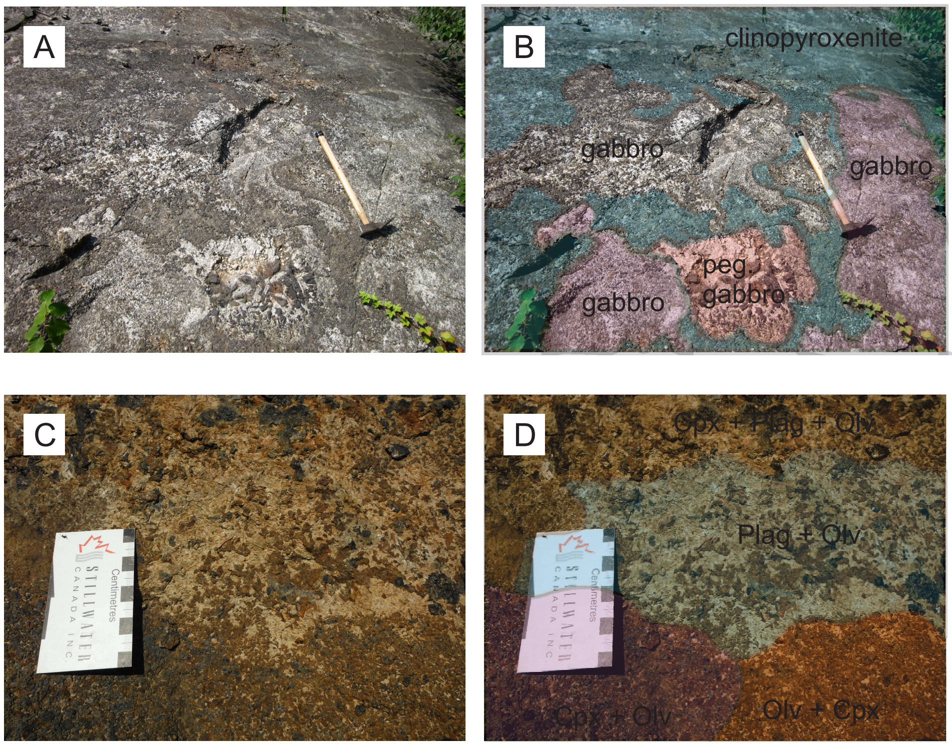

Figure 2.6: Photographs of rock textures exhibiting crystal sorting in outcrop. Scale card is approximately 8 cm wide, hammer is approximately 60 cm long. A) Outcrop of Two Duck Lake Gabbro showing complex relationships and zoning. B) Same photo as A highlighting the different rock compositions on a localized scale. Overall the entire area is classified as Two Duck Lake Gabbro, but within the 2x2 m area several sub units can be observed including clinopyroxenite, gabbro and pegmatitic gabbro. C) Close up of Two Duck Lake Gabbro showing the contact between four phases. D) Same photo as D highlighting the different compositions on a localized scale. The top section is composed of clinopyroxene (Cpx), plagioclase (Plag) and Olivine (Olv) and is the typical TDLG composition. Below this is a zone of predominantly Plag + Olv. The bottom right of the photo is a zone of Olv + Cpx. The bottom left of the photo is a zone of Cpx + Olv.

and D show a zoom in of a typical contact in a zone where crystal sorting is interpreted. Here over a 15 x 15 cm area the overall composition is a gabbro but there are four distinct phases. Again these are interpreted to represent zones of physical sorting and the different compositions are merely the results of accumulations of different mineral phases.

Also observed within outcrop the local bands of mafic minerals within the TDLG are cross-cut by younger generations of TDLG. The chaotic intrusive nature of the TDLG is important in the interpretation of whole rock and mineral chemistry data. The TDLG intrudes into the Layered Gabbro Series, the LMOC and the RIB. The TDLG is the host of the mineralization at the Marathon deposit.

Based on the observations of this study, and those of Wilkinson (1983), Good and Crocket (1990), Good (1992) and Dahl et al. (2001) the Two Duck Lake Gabbro predominantly has an ophitic texture (Fig. 2.5 D and 2.7 C). This texture is extremely important as it allows the TDLG to be easily distinguished from coarse grained Eastern Gabbro rocks which are otherwise similar in appearance. The order of crystallization for major minerals is plagioclase, olivine and clinopyroxene. Plagioclase grains are tabular, and typically have well defined euhedral to subhedral crystal shapes. Olivine grains are typically subhedral to anhedral. Both of these minerals are encased by large irregular anhedral oikocrysts of pyroxene. Modal composition of the major minerals is consistent on the mesoscopic scale with modal mineral abundances of plagioclase $\geq$ clinopyroxene $>$ olivine. On the microscopic scale the modal mineral abundances can be highly variable. Minor minerals include iron oxides (magnetite and ilmenite), biotite and apatite.

In his 2002 publication Tucker Barrie recommended that the use of the name Two Duck Lake Gabbro be abandoned. This was because of a lack of chemical, isotopic and mineralogical distinctions between the two units. At the time the major distinction between the two units was based on textural evidence, with the important ophitic texture of the TDLG separating it from the cumulate texture of the Eastern Gabbro. Trenching and mapping since then has revealed abundant textural evidence that the TDLG is a separate intrusive phase. In addition a recent lithogeochemistry study by Good et al. (submitted) have shown that there is a clear distinction between the units and ended this controversy.

The TDLG is typically medium to coarse grained, however there is a continuous range in crystal size from the groundmass to phenocrysts. Although there is a heterogeneous grain size distribution, clinopyroxene grains are generally the largest followed by plagioclase then olivine. Within the TDLG there are pegmatitic zones which form irregular pods ranging from a few centimeters to a few meters in size. Grain sizes within the pegmatitic pods can be up to 10 cm in size (Fig. 2.7 D). Minor cumulate zones of feldspathic clinopyroxenite with associated apatite were also observed within the TDLG (this study).

2.5.3.1 Feldspathic Clinopyroxenite

Feldspathic clinopyroxenite occurs locally within the TDLG and only comprises a minor proportion of the TDLG. This unit is typically thin (decimeter scale), exhibits gradational boundaries and is commonly intermixed with the TDLG. In hand sample these (Fig. 2.7

E) zones have a mottled texture, and the plagioclase are milky white in colour with visible quartz/K-feldspar intergrowths and range in size from 1 to 3 cm. Apatite rich zones are commonly green and have a sugary appearance. Typically these feldspathic clinopyroxenite zones are coarse grained with a modal abundance in decreasing order of clinopyroxene, plagioclase, K-feldspar, quartz, apatite, olivine and magnetite. Clinopyroxene is anhedral and subangular and is a cumulate phase.

2.5.4 Malpas Lake Gabbro

The Malpas lake Intrusion is centered near Malpas Lake, in the south central portion of the Eastern Gabbro. Limited exposure of cross-cutting relationships indicates that the Malpas Lake Intrusion is younger than the Layered gabbro. This unit is dominantly a blocky feldspar porphyritic, fine to medium grained massive gabbro. Sub-trachytic zones occur and a weak layering is present locally within this unit.

2.5.5 Syenite Dikes

Late quartz syenite and augite syenite dikes cut all of the gabbro units, but overall form only a minor component at the Marathon deposit.

2.6 Mineralization at the Marathon Deposit

The Cu-PGE mineralization at the Marathon deposit is hosted by the Two Duck Lake Gabbro as shallow dipping sub parallel lenses that follow the contact with the footwall RIB. Mineralization occurs three major zones of disseminated sulphides: the Footwall Zone, the Main Zone and the W-Horizon (Wilkinson 1983, Good 1992, Good and Crocket 1994, Dahl et al. 2001, Barrie et al. 2002 and Good 2010). The most recent published definitive resource study by Marathon-PGM (Murahwi et al., 2010) estimated the total tonnage of the deposit at 114.8 million tonnes (measured and indicated). The measured resource has an average grade of 0.26% Cu, 0.85 g/t Pd, 0.24 g/t Pt, and 0.088 g/t Au.

The location of the mineralized zones in relation to the rock units is shown in Figure 2.4. The Footwall Zone is located in both the Footwall RIB and the TDLG at the contact between the two units. The Main Zone mineralization occurs on the bottom of the TDLG and the thickness of the zone has been shown to increase in troughs within the footwall (Good, 2010). The W-Horizon is located above the Main Zone mineralization and is also hosted within the TDLG. A 3D block diagram cross section looking east is shown in Figure 2.8. This figure highlights the diamond drill holes (DDH) used in this study. Of note is the absence of a large continuous sheet of Main Zone mineralization below drill holes DDH-306, DDH-369 and DDH-441. Two 3D block diagrams looking at the deposit from above and below are shown in Figure 2.9 which also highlight the drill holes selected in this study. The view from the bottom looking up in Figure 2.9 B clearly shows the discontinuity of the Main Zone below three of the study drill holes.

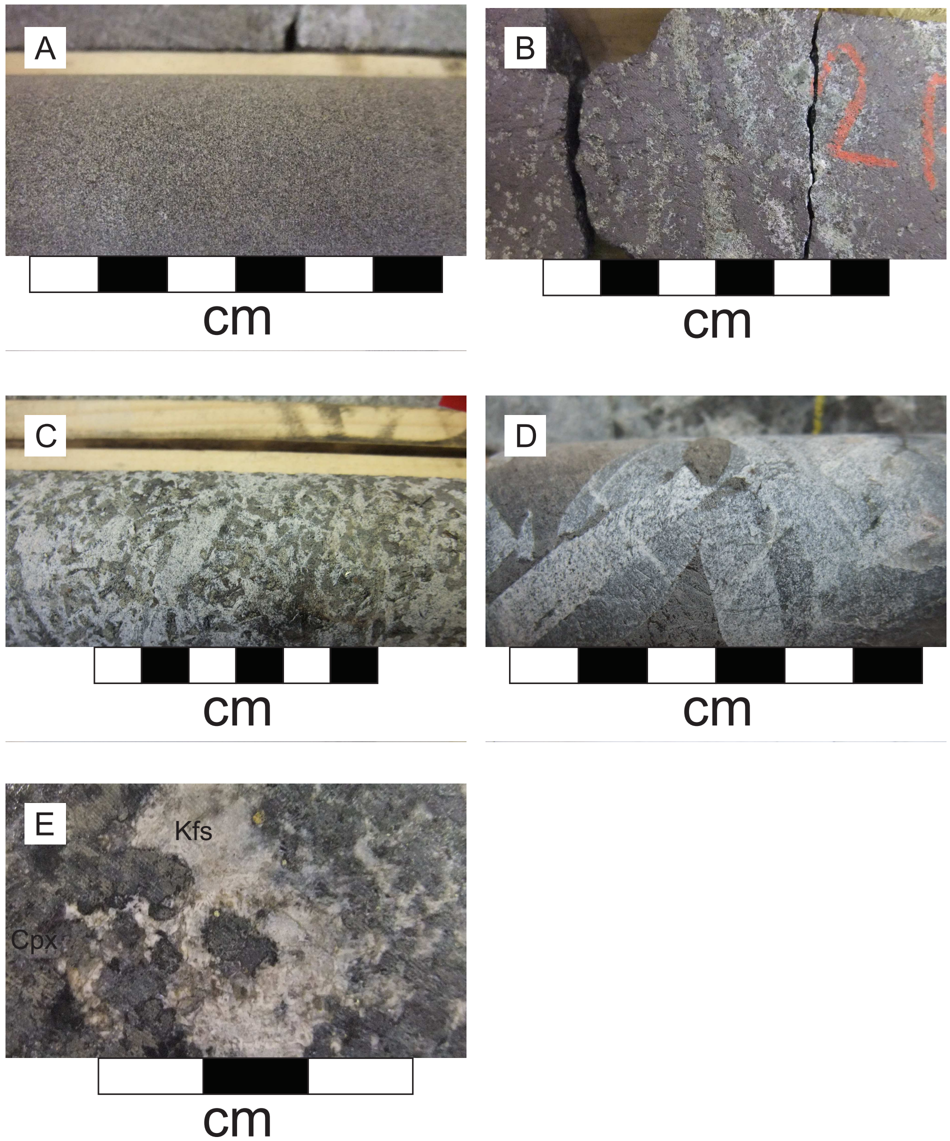

Figure 2.7: Photographs of rock textures seen in drill core. A) Fine grained Eastern Gabbro. B) Layered magnetite-olivine cumulate, banding is visible. C) Representative texture of coarse grained Two Duck Lake Gabbro, plagioclase (white), clinopyroxene (grey) and olivine (green) are visible, ophitic texture is defined by clinopyroxene. D) Two Duck Lake Gabbro exhibiting pegmatitic grain size, plagioclase (white) and clinopyroxene (grey) are visible. E) Photograph of a feldspathic clinopyroxenite in drill core. The dark grey colour is clinopyroxene and the opaque white colour is predominantly K-feldspar with graphic quartz intergrowths.

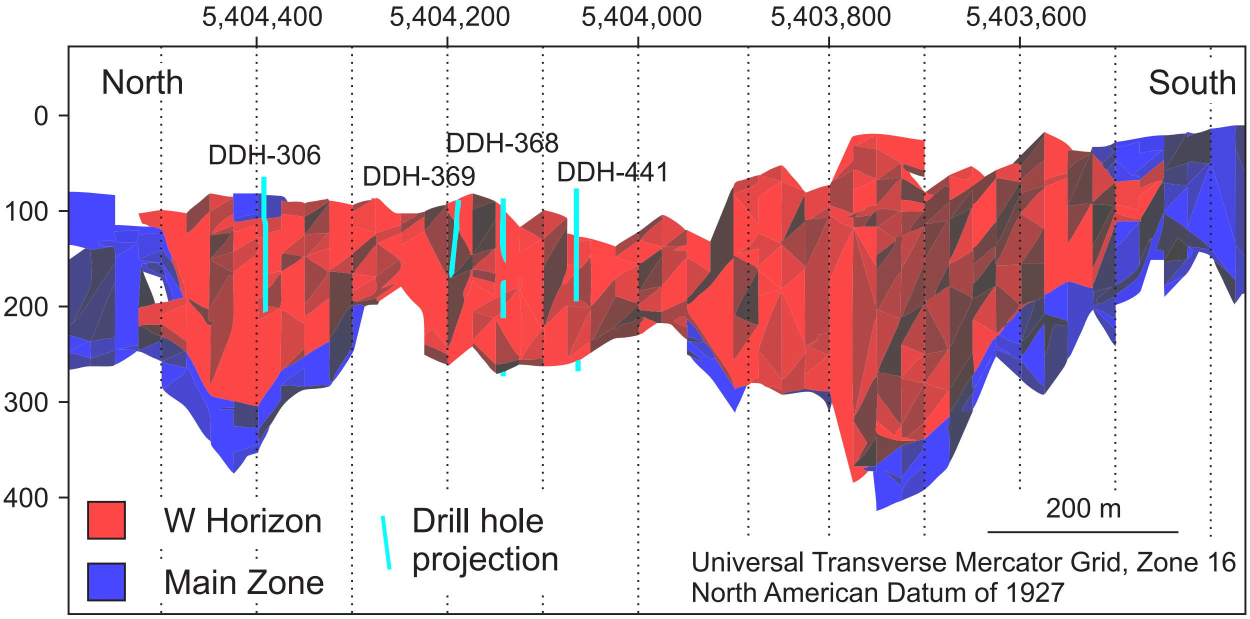

Figure 2.8: 3D block diagram of the Marathon deposit looking east showing the Main Zone, W-Horizon and the drill holes selected for use in this study. Three of the drill holes (DDH-368, DDH-369 and DDH-441) are located within the gap where there is little to no Main Zone mineralization beneath them. Produced using Marathon-PGM internal data set.

2.6.1 The Footwall Zone

The Footwall Zone is located at the contact between the Two Duck Lake Gabbro and the Rheomorphic Intrusive Breccia, the mineralization can be hosted by either unit. The sulphide minerals are pyrrhotite > chalcopyrite >> pyrite > pentlandite (Good (1992). The sulphides are commonly disseminated but can occur net-textured and as semi-massive blebs (up to 10 cm). The sulphide grains are interstitial and anhedral.

2.6.2 The Main Zone

The Main Zone is the thickest and most continuous zone of mineralization at the Marathon deposit. The mineralization has an average thickness of 35 m, and ranges between 4 and 183 m (Marathon-PGM internal data). The Two Duck Lake Gabbro is host to the Main Zone mineralization. Sulphides are disseminated within the host rock and are interstitial to silicate grains. The abundance of sulphide minerals is between trace and 5 modal% and can be as high as 7 modal% (Wilkinson, 1983), (Good, 1992), (Good and Crocket, 1994) and (Dahl et al., 2001). The dominant sulphide minerals are chalcopyrite and pyrrhotite, with minor amounts of bornite, pentlandite and pyrite. The ratio of chalcopyrite to pyrrhotite changes from ccp > po at the top to po > ccp at the bottom. Corresponding with the change in chalcopyrite:pyrrhotite, the ratio of PGE/Cu increases from base to top. The PGM within the Main Zone have been observed in association with hydrous minerals particularly chlorite and

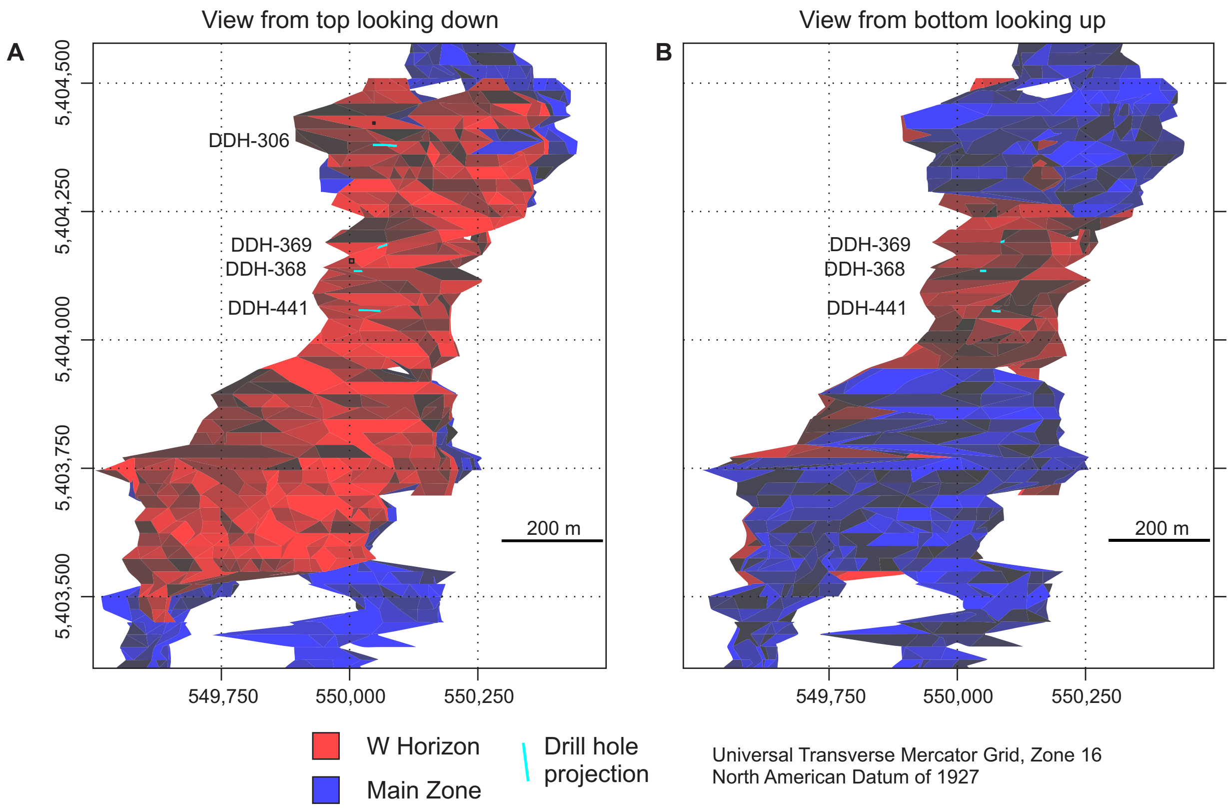

Figure 2.9: 3D block diagram of the Marathon deposit from top and bottom view points showing the Main Zone, W-Horizon and the drill holes selected for use in this study. Three of the drill holes (DDH-368, DDH-369 and DDH-441) are located within the gap where there is little to no Main Zone mineralization beneath them. Produced using Marathon-PGM internal data set.

actinolite within the Main Zone (Ohnenstetter et al., 1991), (Watkinson and Ohnenstetter, 1992). (Watkinson and Jones, 1996), (Dahl et al., 2001) and (Barrie et al., 2002). (Good, 1992) and (Good and Crocket, 1994) have shown the the hydrous minearls only occur at the local scale and are the formation is likely explained by post magmatic deuteric fluids. The ratio of Pd/Ir ratio from base to top is constant (Good, 1992). It is expected that Ir is much less soluble than Pd and Cu in a hydrous fluid (Wood, 1987) and Mountain and Wood (1988). The constant Pd/Ir ratio indicates that if it occurred hydrothermal remobilization was only at the hand specimen scale.

2.6.3 The W-Horizon

The W-Horizon, which is the focus of this study, forms a nearly continuous sheet of mineralization striking north-south for over 1 km between 5,403,450 mN and 5,404,500 mN (UTM Grid, Zone 16, NAD27). It dips easterly and extends for over 300 m down dip. The thickness of the W-Horizon is highly variable and ranges from 1 m (this study) to up to 30 m (Good (2008) and unpublished Marathon PGM internal data). The majority of the W-horizon overlies the Main Zone mineralization, however to the south there is a "gap" where there is no underlying mineralization (as shown in Figures 2.8 and 2.9).

The W-Horizon is characterized by low sulphur contents, high Cu/Pt, high Cu/Pd and low S/Se ratios (Good (2010) and this study). The dominant sulphide mineralogy is chalcopyrite and bornite ± minor pyrrhotite and pentlandite. The W-Horizon can only be recognized by geochemical assay. The TDLG host is a heterogeneous unit and no particular texture, composition or modal mineral assemblage/abundances was associated with the mineralization. The only notable difference from Main Zone mineralization is the change in sulphide mineral assemblage to chalcopyrite and bornite. It is difficult to identify the sulphide mineral assemblage within W-Horizon hand samples because they occur in trace amounts. The average grade in the W-Horizon exceeds 1 g/t (Pt + Pd) and has a characteristic Cu/Pd weight ratio of less than 3,500 (Murahwi et al., 2010). Within this study (including DDH-306, DDH-368 and DDH-369) the high grade W-Horizon intersections have an average Cu/Pd < 215. The highest grade intersection reported in the W-Horizon is from DDH M-07-239 with 107 g/t Pt+Pd+Au, 1.05 g/t Rh and 0.02% Cu over 2 m (Puritch et al., 2009). The thickest intersection in this study was from DDH-306 and was 8 m with an average grade of 10.8 ppm Pt, 19.4 ppm Pd, and 0.33 wt% Cu (this study). Modeling of drill hole data has shown that in general the mineralized zones thicken in basins and thin or pinch over crests of the footwall (Good, 2010).

Chapter 3

Methodology

3.1 Study Diamond Drill Hole Selection Criteria

Study of the W-Horizon mineralization was conducted using samples from four diamond drill holes: DDH-306, DDH-368, DDH-369 and DDH-441. A map of the surface geology and collar locations is shown in Figure 3.1. Diamond drill holes DDH-368, DDH-369 and DDH-441 are located within the gap (as described in Section 2.6.3 Figure 2.9) and are not underlain by Main Zone mineralization. There is a small pocket of Main Zone style mineralization beneath the W-Horizon in DDH-368, but this zone is not continuous between neighbouring drill holes (Fig. 3.2). Diamond drill holes within the gap were chosen for study to minimize interferences, such as upward remobilization, that could be caused by close proximity to the Main Zone, where the mineralization style is distinct and different from the W-Horizon. Diamond drill hole DDH-306 is located north of the gap and has contiguous Main Zone mineralization below the W-Horizon and was selected to test the hypothesis that the W-Horizon is unrelated to Main Zone mineralization (Fig. 3.3). Since the focus of this project was the W-Horizon and only limited Main Zone samples were taken they are not considered to represent the Main Zone as a whole.

The drill holes selected for study capture a variety of W-Horizon mineralization styles based on the amount Pt + Pd, sulphide mineralogy (presence or absence of bornite and pyrrhotite), total amount of sulphur, element ratios, and horizon thickness. Table 3.1 summarizes the styles, i.e., different prominent sulphide minerals, different Cu/Pd and different S content, that were sampled.

3.1.1 Diamond Drill Hole 306

A simplified stratigraphy of DDH-306 is shown in Figure 3.5, outlining mineralized zones and sample locations. This drill hole intersects very high grade W-Horizon mineralization ($>$ 10 ppm Pt + Pd) with high sulphur contents ($>$ 0.25 wt% S is considered high S in the W-Horizon). This drill hole was collared in Eastern Gabbro for 130 m, and then intersected

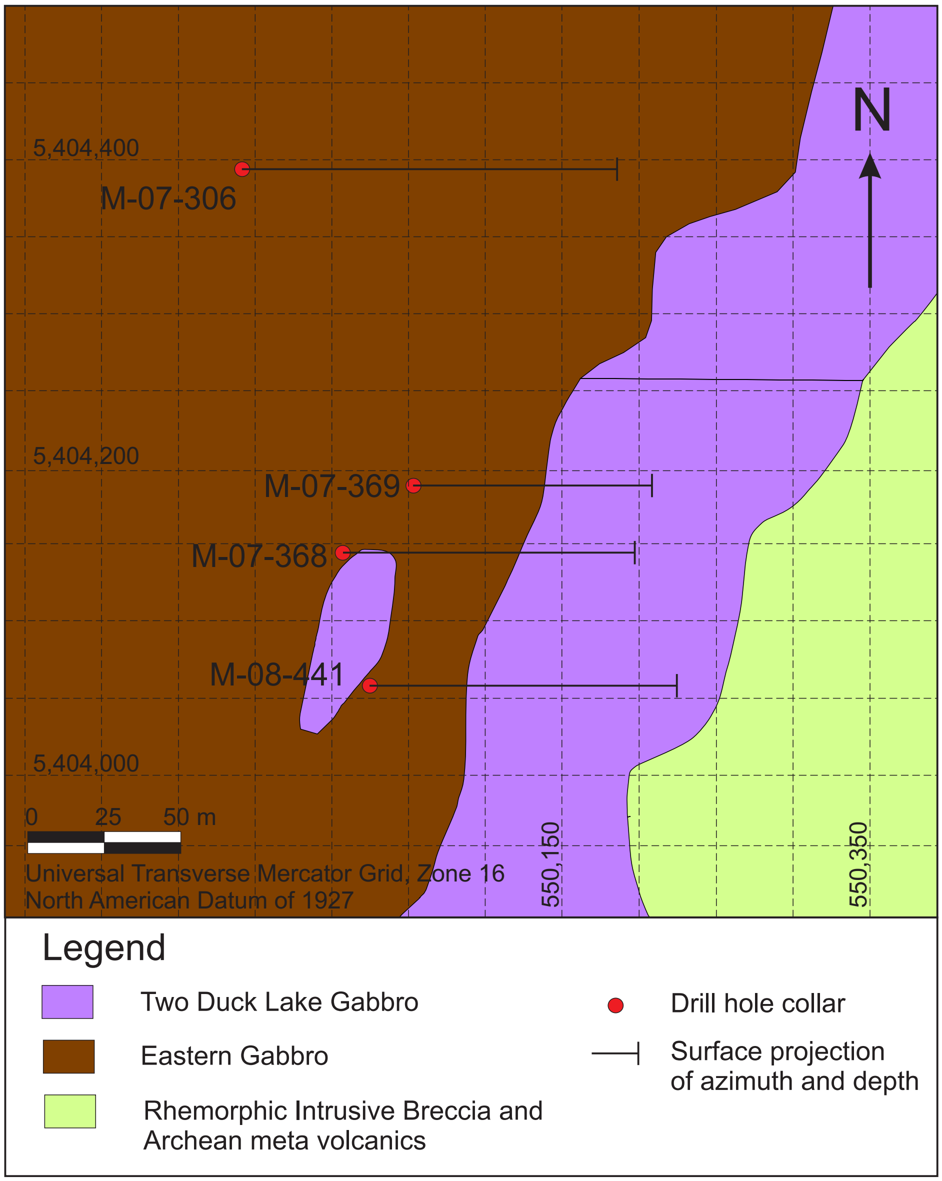

Figure 3.1: Detailed map showing study diamond drill hole collar locations, azimuth, and depth projections.

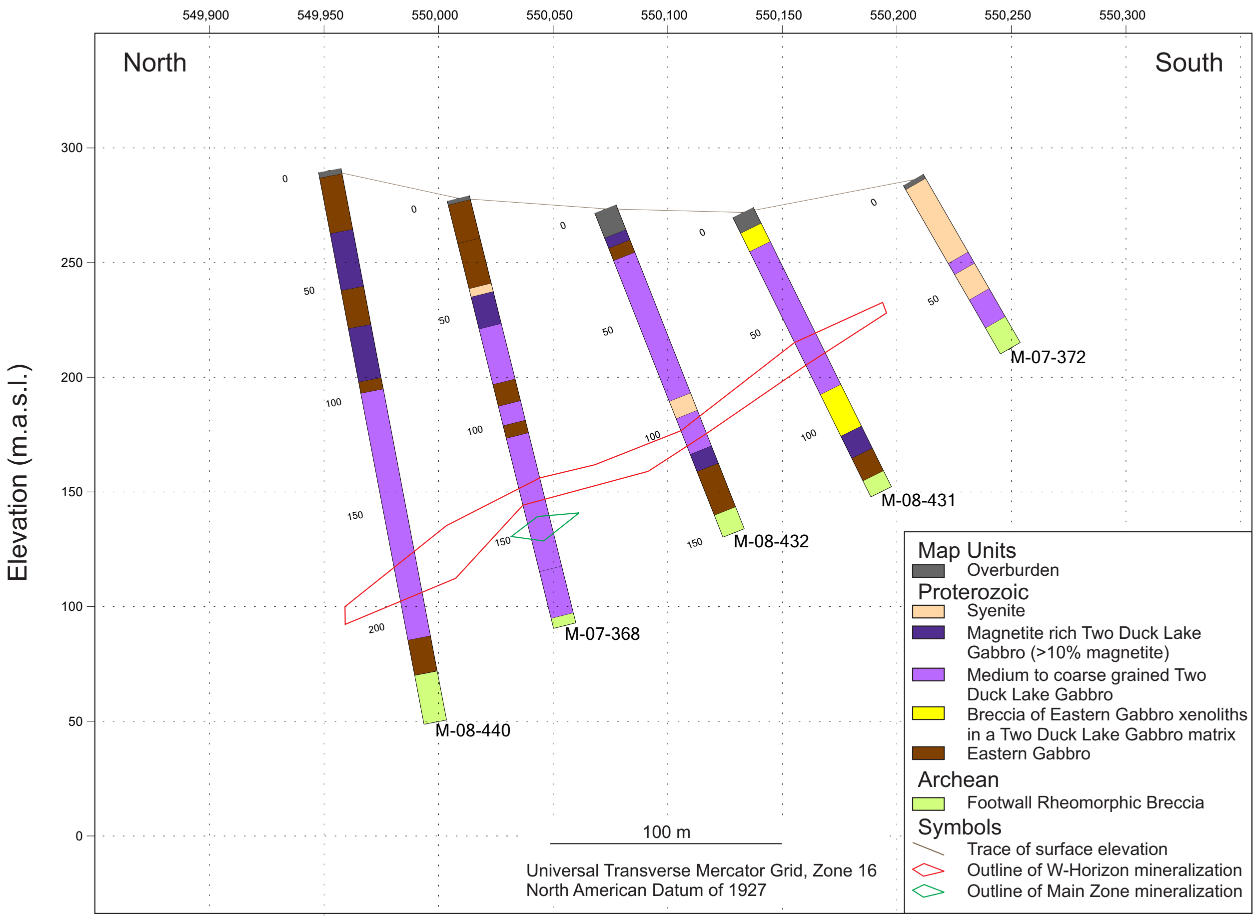

Figure 3.2: Cross section looking east containing DDH-368 and neighbouring diamond drill holes. The Main Zone and W-Horizon mineralized zones are highlighted. This cross section highlights the small zone of Main Zone-style mineralization at the bottom of DDH-368 and shows that it is not continuous between neighbouring drill holes.

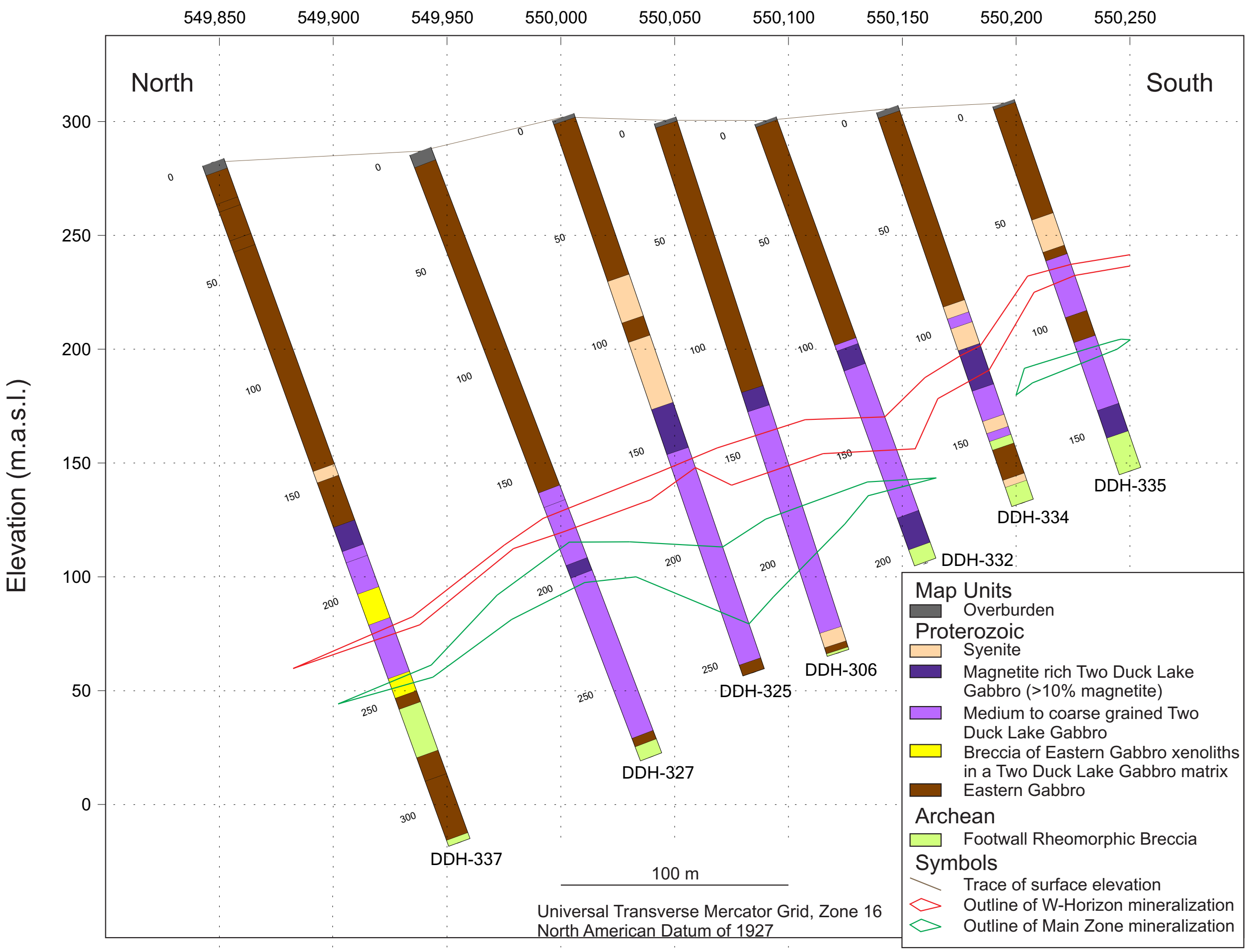

Figure 3.3: Cross section looking east containing DDH-306 and neighbouring diamond drill holes. The Main Zone and W-Horizon mineralized zones are highlighted.

100 m of coarse grained Two Duck Lake Gabbro. The W-Horizon is located 20 m below the upper contact in the TDLG package, and the Main Zone is located 30 m above the lower contact. The bottom of the hole intersects a syenite dike, fine grained Eastern Gabbro and ends in Footwall RIB. This drill hole intersects very high grade W-Horizon mineralization with an average of 30 ppm Pt+Pd over an eight meter intersection. Locally Pt+Pd is > 50 ppm. Copper values within this intersection average 0.33 wt% which is typical for the deposit but high for the W-Horizon. The average value of Cu/Pd for this intersection is 215. Throughout this intersection the average modal abundance of sulphide minerals is 2-3%, and the average S over the interval is 0.24 wt%, which is also high compared to the other W-Horizon intersections. The sulphide minerals in this intersection are chalcopyrite, bornite ± trace pentlandite and pyrrhotite (Fig. 3.4 A).

There is a 10 m thick lens of Main Zone mineralization below the W-Horizon mineralization in DDH-306. It has much lower Pt + Pd (1.4 ppm average) and slightly higher average Cu (0.37 wt%) than the W-Horizon intersection in this drill hole. The values of Cu/Pd (4360) and S (0.49 wt%) are also higher in the Main Zone lens compared to the W-Horizon. The sulphide minerals in this zone are chalcopyrite and pyrrhotite with trace amounts of pentlandite (Fig. 3.4 B).

3.1.2 Diamond Drill Hole 368

A simplified stratigraphy of DDH-368 is shown in Figure 3.6, outlining mineralized zones and sample locations. This drill hole intersects moderate-grade W-Horizon mineralization with moderate sulphur. The top 50 m of this drill hole intersects Eastern Gabbro containing stringers and dikelets of Two Duck Lake Gabbro (20%). Two Duck Lake Gabbro is then intersected for 125 m and within this zone of Two Duck Lake Gabbro there are two large xenoliths of anorthositic gabbro with poikilitic magnetite and a fine grained gabbro with poikilitic clinopyroxene. The W-Horizon mineralization is intersected within this unit at 130 m and a small lens of Main Zone mineralization (at 142 m) is below the W-Horizon, separated by 10 m of barren TDLG.

The lens of W-Horizon Mineralization is one meter thick. Over this interval the average amount of Pt + Pd is 9 ppm, Cu is low at 0.084 wt% and Cu/Pd is 164. The typical modal abundance of sulphide minerals over this intersection is 0.5%, and the average S is 0.08 wt%. The sulphide minerals in this intersection are chalcopyrite and bornite (Fig. 3.4 C).

Below the W-Horizon mineralization in DDH-368 there is a lens of Main Zone style mineralization. This Main Zone mineralization was not intersected by neighbouring diamond drill holes. The Main Zone style mineralization is not continuous over its 22 m intersection. It contains low amounts of Pt + Pd (0.86 ppm average) and Cu (0.092 wt% average). The Cu/Pd ratio is very high in this intersection and averages 6070. Sulphide mineral abundance in this zone were typically from trace to 1 modal % and the average amount of S is 0.13 wt%. In addition within this intersection there are abundant amounts of mafic-rich cumulates, dominantly composed of pyroxene, olivine, hornblende and apatite. The sulphide minerals in this zone include chalcopyrite and pyrrhotite ± very trace amounts of bornite and pentlandite (Fig. 3.4 D).

3.1.3 Diamond Drill Hole 369

A simplified stratigraphy of DDH-369 is shown in Figure 3.7, outlining mineralized zones and sample locations. This drill hole intersects two zones of W-Horizon mineralization, both of which are moderate- to high-grade mineralization with no visible to trace amounts of sulphide minerals. The top 8 m of this hole intersects Eastern Gabbro, followed by a zone of olivine-magnetite cumulate for 8 m and then a mixed zone of fine grained Eastern Gabbro with stringers and dikelets of Two Duck Lake Gabbro. The next unit is 90 m of coarse grained Two Duck Lake Gabbro. The W-Horizon intersections are within this unit of TDLG at depths of 85 and 122 m. From 50-70 m the unit has been strongly faulted and strongly chlorizited and sericitized gabbro with abundant hematite is pervasive through the interval. The fault is post-magmatic without any visible offset and did not affect the mineralization relative to the lower W-Horizon intersection. Below the faulted zone the Two Duck Lake Gabbro is pristine and unaltered. The upper W-Horizon intersection is 2 m thick and has an average of 8.1 ppm Pt + Pd. This intersection has nil to trace visible sulphides, an average of 0.05 wt% S, 0.03 wt% Cu and a Cu/Pd ratio of 84, the lowest in the study. The sulphide minerals present are chalcopyrite and trace bornite. The lower W-Horizon intersection is 4 m thick and has an average of 10.3 ppm Pt + Pd. There is 0.06 wt% Cu in this interval and the average Cu/Pd is 202. This intersection has trace visible sulphides and an average of 0.09 wt% S. The sulphide minerals present are chalcopyrite and trace bornite (Fig. 3.4 E).

3.1.4 Diamond Drill Hole 441

A simplified stratigraphy of DDH-368 is shown in Figure 3.8, outlining mineralized zones and sample locations. The average value of Cu/Pd in DDH-441 is 3620 and can be as high as 7000. Values this high are above the cutoff typically used for the W-Horizon (Cu/Pd < 3500). The high values of Cu/Pd also coincides with the lowest Pt + Pd values for W-Horizon samples in this study. The samples from this drill hole are considered representative of low grade W-Horizon material. This drill hole is collared in fine-grained Eastern Gabbro for 30 m. This is followed by 130 m of coarse grained ophitic Two Duck Lake Gabbro with a small zone of coarse-grained Eastern Gabbro and fine-grained Eastern Gabbro before the hole ends in Footwall RIB. The W-Horizon intersection is at 140 m depth and 10 m thick. It has low grade Pt + Pd (1.0 average) and moderate Cu (0.29 wt%). The modal sulphide mineral abundance is 1-2% the average S is 0.3 wt%. The sulphide minerals also differ from the other W-Horizon intersections in this study. Chalcopyrite and pyrrhotite are the major minerals, with trace amounts bornite and pentlandite (Fig. 3.4 F).

3.2 Sample Collection

The samples used in this project were collected from diamond drill core produced during exploration projects conducted by Marathon-PGM from 2007 to 2008. The drill tubes used in the exploration projects were NQ size with a 75.8 mm diameter and produce drill core

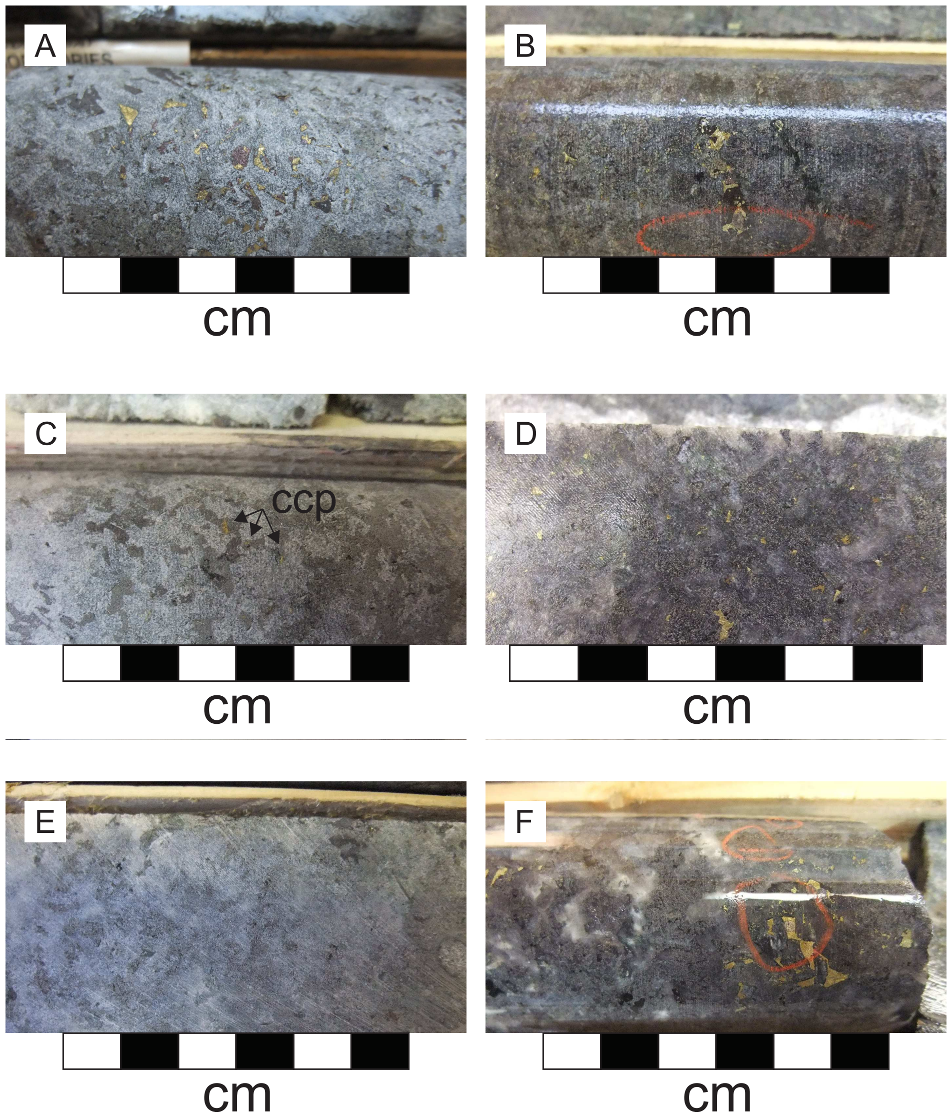

Figure 3.4: Photographs of mineralization from drill core. A) W-Horizon mineralization from DDH-306 showing 3-5% fine to medium grained chalcopyrite (brassy-yellow) and bornite (purple) within ophitic Two Duck Lake Gabbro. B) Lower Zone mineralization from DDH-306 showing 3-5% fine to medium grained chalcopyrite and pyrrhotite (silver) within ophitic Two Duck Lake Gabbro. C) W-Horizon mineralization from DDH-368 showing trace fine to medium grained chalcopyrite (ccp) within Two Duck Lake Gabbro. D) Lower Zone mineralization from DDH-368 showing 2-3% fine to medium grained chalcopyrite within Two Duck Lake Gabbro. E) W-Horizon mineralization from DDH-369 with very-trace chalcopyrite (not visible in photograph) within Two Duck Lake Gabbro. F) W-Horizon mineralization from DDH-441 showing 3-5% chalcopyrite and pyrrhotite within Two Duck Lake Gabbro.

Table 3.1: Summary of metals and sulphide mineralogy in mineralized samples

Hole ID	Length (m)	Cu (%)	Pt (ppm)	Pd (ppm)	S (wt%)	Cu/Pd	Sulphide Minerals
W-Horizon Mineralization							
DDH-306	8.0	0.33	10.8	19.4	0.24	215	ccp, bn ± pn
DDH-368	0.6	0.084	3.5	5.5	0.08	164	ccp, bn
DDH-369	2.0	0.031	2.3	5.8	0.05	84	ccp ± trace bn
DDH-369	4.0	0.066	2.6	7.7	0.09	202	ccp ± trace bn
DDH-441	10.0	0.285	0.22	0.83	0.3	3620	ccp, po, ± bn, pn
Lower Zone Mineralization							
Hole ID	Length (m)	Cu (%)	Pt (ppm)	Pd (ppm)	S (wt%)	Cu/Pd	Sulphide Minerals
DDH-306	10	0.37	0.28	1.1	0.49	4360	ccp, po ± pn
DDH-368	22	0.092	0.25	0.61	0.13	6070	ccp, po, ± trace bn, pn

Values are averages for the mineralized zone

with a 47.6 mm diameter. At the time of drilling Marathon-PGM split (using a diamond saw blade) the core longitudinally and sent 2 m long samples for analysis by chemical assay. After selecting samples from the half core it was sawed again longitudinally producing a quarter of the original core for use in this study. From each sample at least one 20x40x10 mm block was sawed and used to produce a polished thin section with the remainder used for chemical assay analysis.

The same sampling procedure was used for all of the drill holes in this study. The location of W-Horizon mineralization was identified from the assays conducted by Marathon-PGM. Continuous samples between 30-50 cm long were taken through the W-Horizon mineralization. The exact size and the position of each sample were chosen in an attempt to analyze homogeneous samples based on silicate mineralogy, texture, sulphide mineralogy and abundance. In addition, 50 cm bracket samples were taken at 5-10 m intervals in the unmineralized Two Duck Lake Gabbro above and below the W-Horizon. The purpose of these samples was to establish a lithogeochemical baseline of the non-mineralized unit.

The sample size was chosen in order to accurately identify the thickness of the W-Horizon and to test for subtle layering within the W-Horizon. This allowed for the identification of the W-Horizon as a continuous unit or several small lenses of high grade material. The high resolution correlation of Pt+Pd with silicate and sulphide minerals as well as textures is also possible with the small sample size.

3.2.1 Whole Rock Geochemistry

The samples taken from the drill core were used for analysis whole rock geochemistry by chemical assay at either Geosciences Laboratories (Sudbury, Ontario) or Activation Laboratories (Ancaster, Ontario). The details of this work are presented in Chapter 5: Geochemistry.

3.2.2 Thin Section Analysis

The polished thin sections were used to study silicate mineralogy, textures and alteration by transmitted light microscopy. Reflected light microscopy was also used to study the sulphide mineralogy, textures and relationships between the sulphide, silicate, and platinum group mineral grains. The details of this work are presented in Chapter 4: Petrography.

Electron microprobe was used to analyze the major elements in the major silicate minerals in the Two Duck Lake Gabbro. Laser ablation inductively coupled plasma mass spectrometry (LA-ICP-MS) was also used to analyze the olivine and pyroxene grains in the TDLG for trace element chemistry. The details of this work are presented in Chapter 6: Mineral Chemistry.

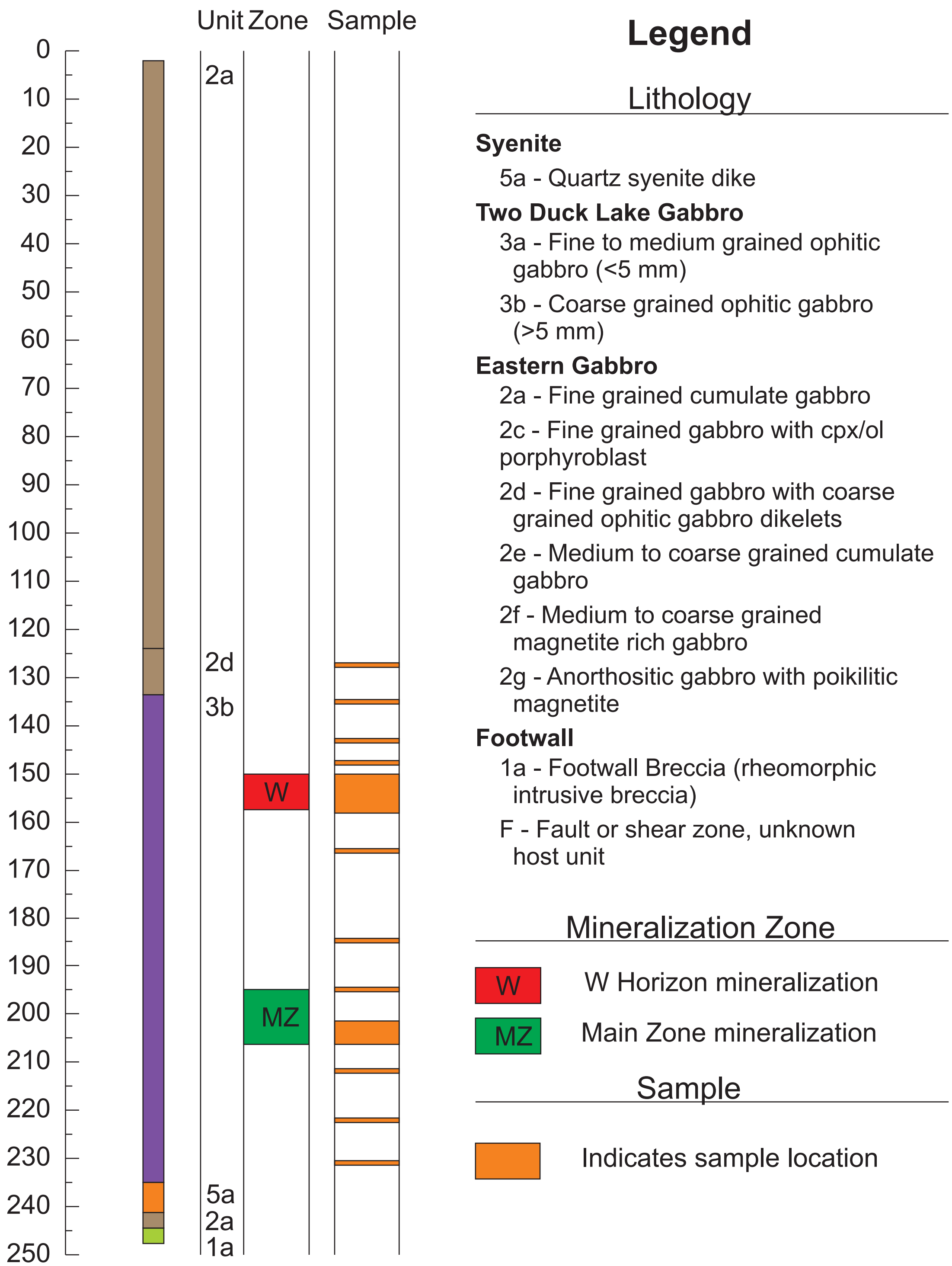

Figure 3.5: Diamond Drill Hole 306, showing geology, mineralized zones and sample locations.

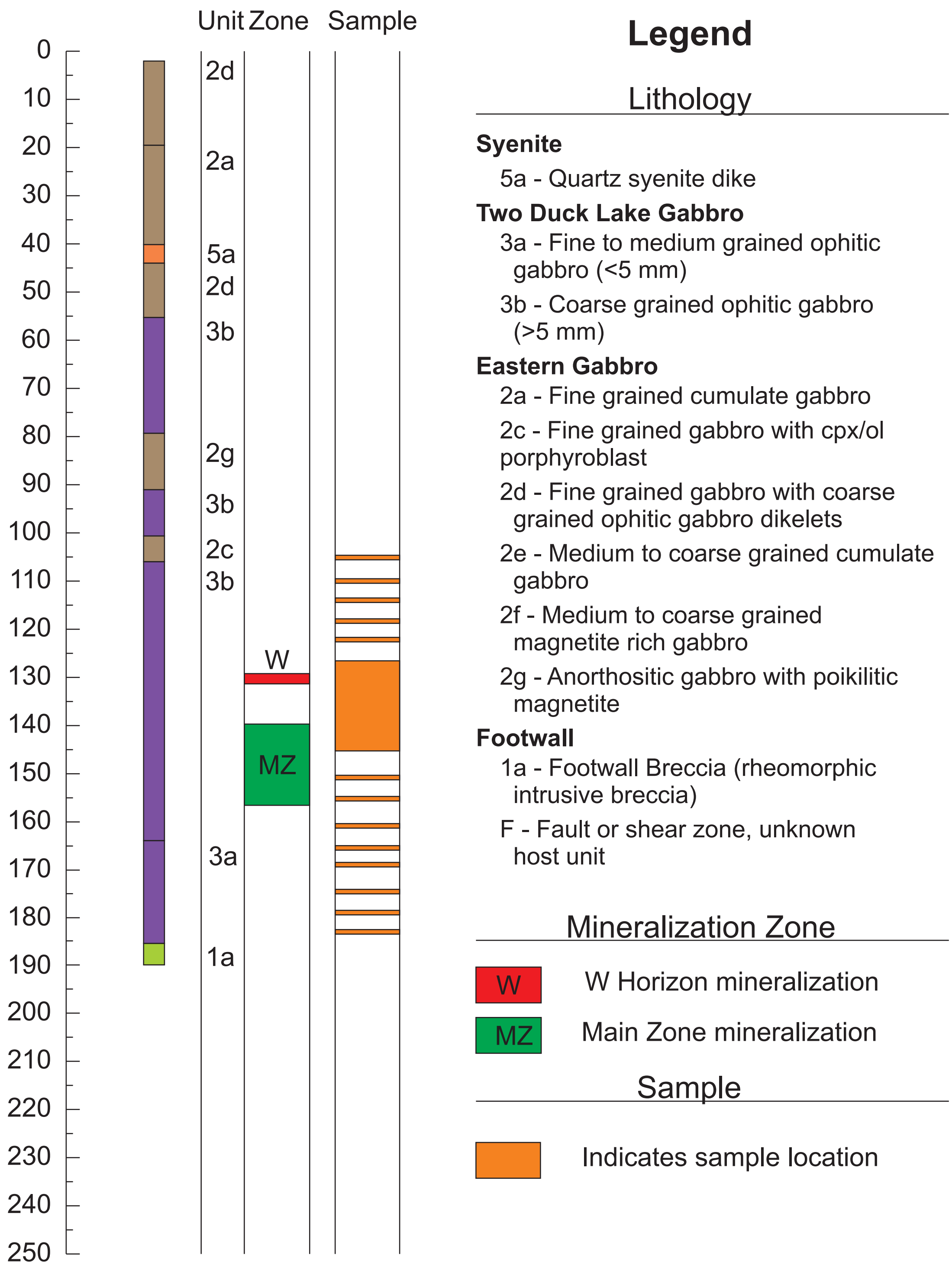

Figure 3.6: Diamond Drill Hole 368, showing geology, mineralized zones and sample locations.

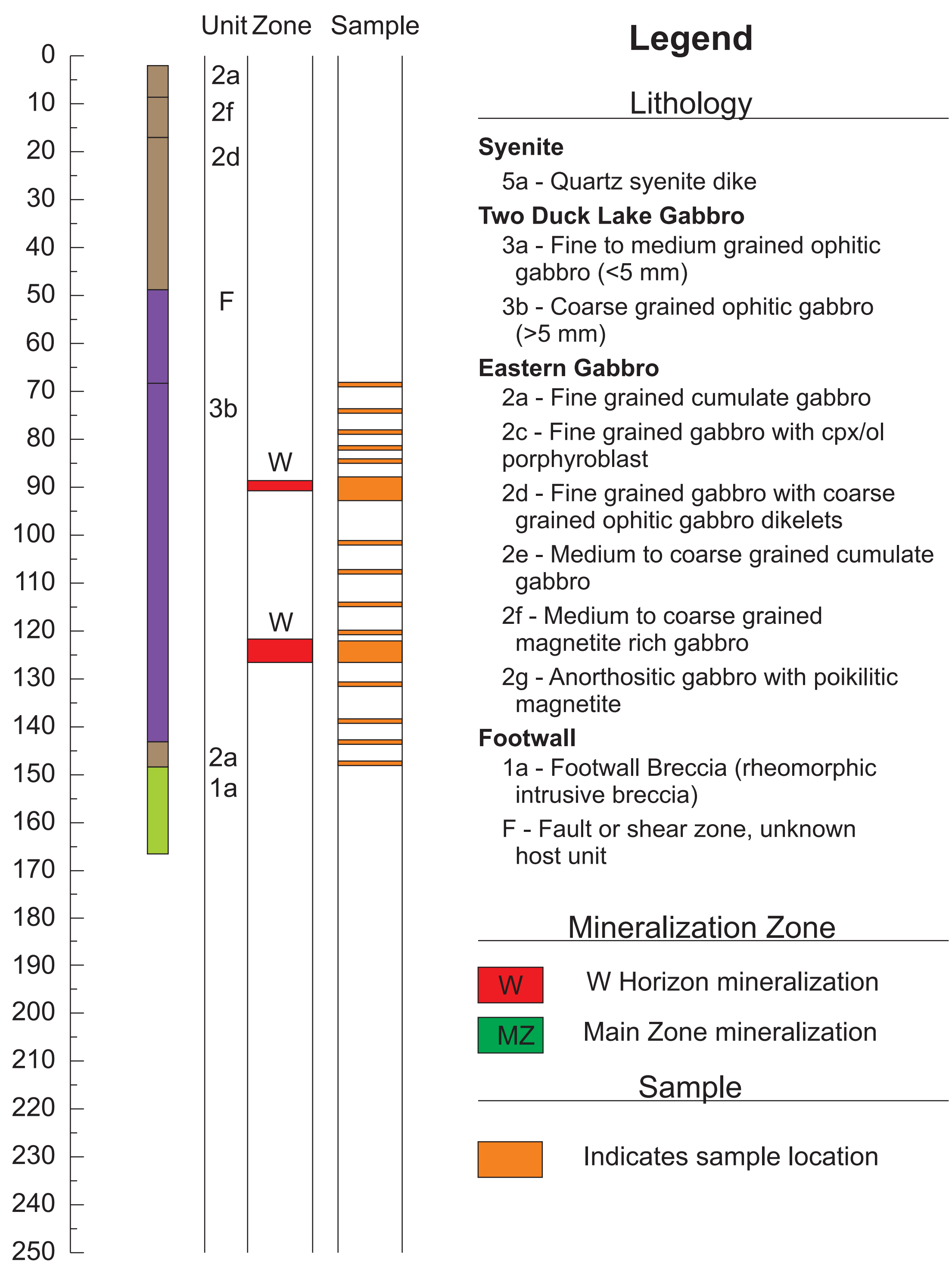

Figure 3.7: Diamond Drill Hole 369, showing geology, mineralized zones and sample locations.

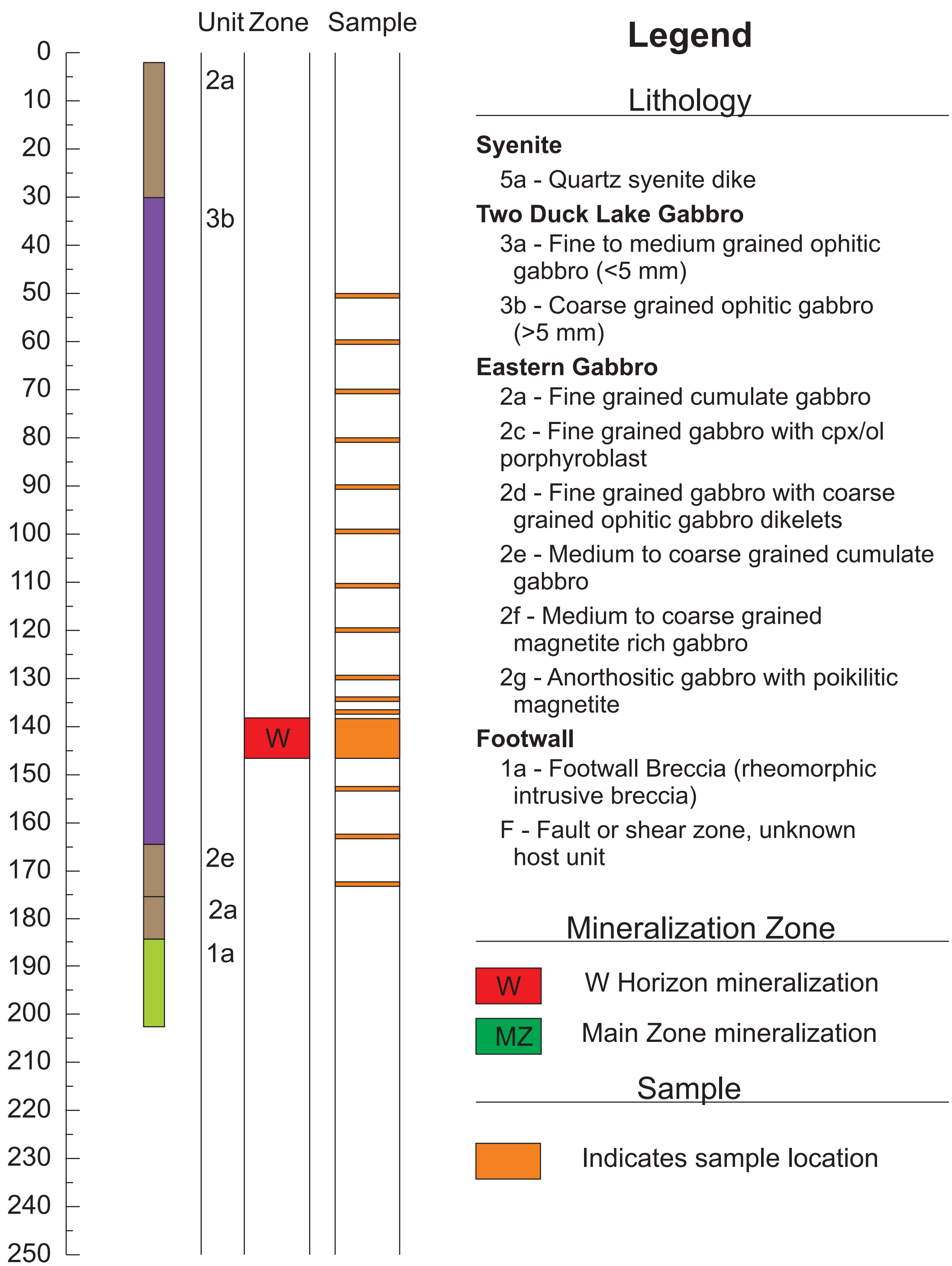

Figure 3.8: Diamond Drill Hole 441, showing geology, mineralized zones and sample locations.

Chapter 4

Petrography

4.1 Introduction

The Main Zone and W-Horizon mineralization are hosted within the Two Duck Lake Gabbro (TDLG). This section summarizes the observations of the TDLG made during this study and details differences pertaining to the mineralized zones. The primary silicate mineralogy and textures between unmineralized, Main Zone and W-Horizon samples were very similar. The petrography of the sulphide and platinum group minerals are distinct between the Main Zone and W-Horizon. Observations in this study showed that the sulphide minerals in the W-Horizon were predominantly interstitial and associated with anhydrous silicate minerals, similar to the observations published in Puritch et al. (2009). The samples of the Main Zone in DDH-306 and the Main Zone style mineralization in DDH-368 were similar to previous studies with sulphide minerals associated with both pristine gabbro as well as the hydrous mineral assemblage of chlorite, actinolite, sericite, calcite and hornblende (Good and Crocket, 1990, Good, 1992; Watkinson and Ohnenstetter, 1992; Watkinson and Ohnenstetter, 1992; Watkinson and Jones, 1996; Dahl et al., 2001; Barrie et al., 2002).

4.2 Petrography of the Two Duck Lake Gabbro

The Two Duck Lake Gabbro (TDLG) is an orthocumulate and the samples studied exhibit a characteristic subophitic to ophitic texture, which is consistent with previous studies of the Marathon deposit (Good, 1992, Good and Crocket, 1994 and Shaw, 1997). The order of crystallization is plagioclase, olivine and clinopyroxene respectively. Early formed plagioclase and olivine oikocrysts are partially or completely enclosed in larger clinopyroxene crystals, demonstrating the subophitic to ophitic texture of the TDLG (Fig. 4.1 A-B). This texture is distinct from the adcumuluate texture seen in the Eastern Gabbro.

The abundance, occurrence and distribution of the major minerals of the TDLG were observed to be consistent among unmineralized, Main Zone and W-Horizon samples. Samples from the Main Zone have a slight increase in the amount of hydrous minerals, particularly in association with the feldspathic clinopyroxenite.

Modal mineral abundance is consistent at outcrop scale and includes in decreasing order plagioclase, clinopyroxene and olivine. On the thin section scale the modal mineral abundance can be highly variable. The grain size of the TDLG is typically coarse grained (0.6-6.0 cm), but ranges from fine-grained to pegmatitic. The order of mineral size from largest to smallest is typically clinopyroxene, plagioclase and olivine. Zones of very coarse grained to pegmatitic ($>$ 6 cm, up to 12 cm) with crystals of clinopyroxene up to 12 cm, plagioclase up to 10 cm and olivine up to 5 cm were observed. These zones are typically gradational to the medium to coarse grained TDLG and range in width from centimeters to meters. Previous studies (Watkinson and Ohnenstetter, 1992, Watkinson and Jones, 1996, Dahl et al., 2001 and Barrie et al., 2002) proposed that the pegmatitic gabbro was predominantly associated with mineralization, however analysis of the Marathon-PGM data set has had contradictory results. The presence of pegmatitic TDLG was observed in drill core intersecting the W-Horizon, however pegmatitic gabbro accounted for $< \sim 5\%$ of the W-Horizon samples in this study. Overall the abundance of pegmatitic gabbro was not correlatable to mineralization in the samples analyzed for this study.

Plagioclase grains are typically tabular and have a euhedral to subhedral grain shape. The subhedral grains are commonly scalloped and have irregular rounded boundaries (Fig. 4.1 B-C). Plagioclase grains commonly display optical zonation seen in extinction patterns under cross polarized light. Secondary plagioclase is present locally along the grain boundaries in contact with sulphides, or along fine grained sulphides that penetrate the plagioclase along cleavage. Microprobe analyses of the secondary plagioclase have shown that these secondary plagioclase grains can have a higher anorthite (An) content than the host plagioclase grain (See Section 6.1.1.2).

Olivine grains are subhedral, subrounded-subangular, and optically homogeneous. Olivine grains in contact with plagioclase exhibit both straight boundaries along tabular plagioclase grains parallel to plagioclase cleavage (4.1 B) and rounded boundaries (4.1 C). Poikilitic olivine grains up to a few centimeters across encasing plagioclase crystals were also observed within the TDLG. Olivine crystals are commonly rimmed by a thin mm-thick veneer of clinopyroxene.

Clinopyroxene crystals are interstitial to plagioclase and olivine, anhedral and optically homogeneous. The subophitic to ophitic nature of the clinopyroxene grains is demonstrated by optical continuity between separate grains when viewed under cross polarized light.

Magmatic accessory minerals that are common and ubiquitous throughout the TDLG are magnetite-ilmenite aggregates, biotite and apatite. Interstitial magnetite-ilmenite is common throughout the TDLG. Primary, magmatic magnetite-ilmenite is common as an interstitial mineral (Fig. 4.1 C), and rarely as poikilitic magnetite. The primary magnetite-ilmenite forms complex intergrowths of magnetite and ilmenite exsolution bands. The bands have two typical occurrences, as thick exsolution bands within magnetite and as fine scale needle-like exsolution lamellae within magnetite bands. Microprobe work shows appreciable TiO_2 in both magnetite (average 11.4 wt% TiO_2) and ilmenite (average 49.5 wt% TiO_2) (see Section 6.1.6).

Biotite is common throughout the TDLG and occurs interstitially between the major silicate phases, rimming magnetite grains and rimming sulphide grains.

4.2.0.1 Feldspathic Clinopyroxenite

Feldspathic clinopyroxenite occurs locally within the TDLG and exhibits gradational boundaries. This unit is typically thin (decimeter scale) and is commonly intermixed with the TDLG. The feldspathic clinopyroxenite occurred within unmineralized and Main Zone samples and was not associated with W-Horizon mineralization. The increase in abundance of hydrous minerals within the Main Zone predominantly occurred in association with samples of feldspathic clinopyroxenite. Typically these feldspathic clinopyroxenite zones are coarse grained with a modal abundance in decreasing order of clinopyroxene, plagioclase, K-feldspar, quartz, apatite, olivine and magnetite. Clinopyroxene is anhedral and subangular and is a cumulate phase. It commonly contains orthopyroxene lamellae. The quartz and K-feldspar are usually intergrown with a graphic texture and occur within plagioclase differentiates or as single crystals within the mafic cumulates. This texture was also reported in Good (1992) within what was described as late stage felsic differentiates. Apatite in the feldspathic clinopyroxenite occurs within clinopyroxene and plagioclase, and is euhedral, angular, and fine to medium grained. Apatite interstitial to magnetite grains was also observed (Fig. 4.2 A).

Hydrous and secondary minerals are most common within the feldspathic clinopyroxenite. Common hydrous minerals include hornblende, calcite, tremolite, chlorite and actinolite. The hydrous minerals typically occur in clusters and are described in the next section.

4.2.1 Alteration

Overall the TDLG samples examined in this study are unaltered and do not contain large scale zones of low temperature hydrothermal alteration. However, local development of secondary minerals on the thin section scale does occur. Hydrous mineral abundances are highest within the feldspathic clinopyroxenite. These minerals include sericite, chlorite, tremolite, serpentine, actinolite and calcite. Sericite has typically replaced plagioclase. Tremolite and chlorite commonly occur together with calcite as replacements of clinopyroxene. Actinolite formed as a replacement of clinopyroxene. Small degrees of serpentinization of olivine along grain boundaries and fractures are common in olivine, and less commonly olivine grains are completely serpentinized.

No spatial relationships relating alteration minerals with the W-Horizon samples were observed. Main Zone samples in this study showed an increase in alteration minerals associated with sulphide minerals relative to the W-Horizon, although the alteration minerals were not ubiquitous throughout the Main Zone and primary magmatic sulphide minerals were also observed. This finding is similar to those reported in (Good and Crocket, 1990), (Good, 1992), (Watkinson and Ohnenstetter, 1992), (Watkinson and Ohnenstetter, 1992), (Watkinson and Jones, 1996), (Dahl et al., 2001) and (Barrie et al., 2002). Main Zone samples of this study had similar abundances of localized alteration minerals as observed in unmineralized samples of TDLG.

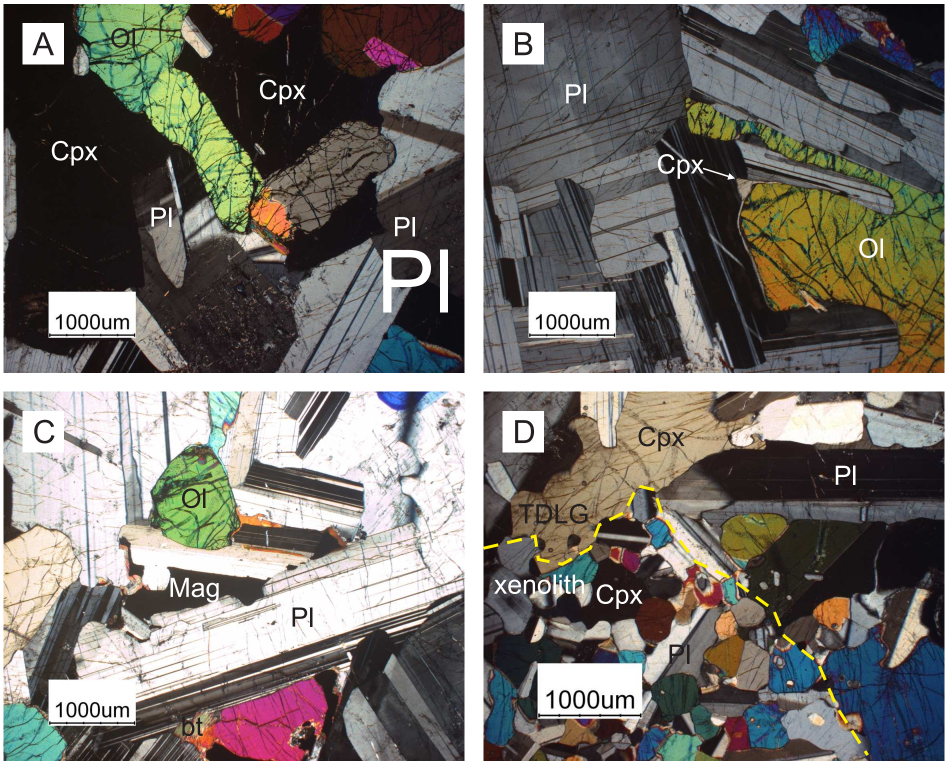

Figure 4.1: Photomicrographs of silicate minerals in thin section taken under cross polarized light. A. Representative ophitic texture of the TDLG. The black clinopyroxene (Cpx) grain exhibits continuous extinction and encases olivine (Ol) and plagioclase (Pl) grains. B. Representative texture of the TDLG showing the scalloped irregular Pl grain boundaries. The Ol grain is wrapped around earlier formed Pl. A fine veneer of Cpx rims the Ol. C. Representative TDLG showing interstitial magnetite (Mag) and biotite (Bt). D. Contact (highlighted with yellow dashed line) between a fine grained gabbro xenolith (lower left corner) and TDLG (upper right corner).

4.2.2 Xenoliths

The occurrence of xenoliths were rare in this study and they formed $< 5\%$ of the samples. The xenoliths are fine-grained gabbro comprising plagioclase, clinopyroxene, olivine and magnetite. The contacts between xenoliths are typically sharp, although some do appear partially assimilated or resorbed (Fig. 4.1 D). In thin section, the contacts do not show rims of any sort. An example of the contact between a xenolith and the host TDLG is shown in Figure 4.1 D.

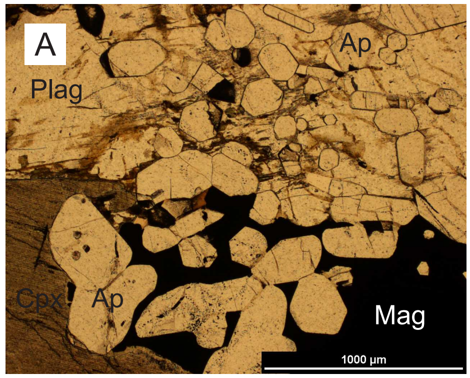

Figure 4.2: Photomicrograph of the feldspathic clinopyroxenite. A) Photomicrograph under plain polarized light of a polished thin section of feldspathic clinopyroxenite. Euhedral to subhedral apatite cluster occurring within clinopyroxene, feldspar and magnetite grains.

4.3 Petrography of the Mineralization

The principle sulphide minerals at the Marathon deposit are chalcopyrite and pyrrhotite. Trace amounts of bornite, pentlandite, marcasite and pyrite occur irregularly. The major sulphide mineral assemblage in the W-Horizon is chalcopyrite and bornite, which is distinct from chalcopyrite and pyrrhotite which dominate in the Main Zone. This section characterizes the sulphide mineral assemblages and silicate associations within the two zones.

4.3.1 W-Horizon Sulphides

The sulphide minerals in the W-Horizon are chalcopyrite > bornite > ± pentlandite > ± pyrrhotite. The sulphide minerals of the W-Horizon are predominantly interstitial to silicate minerals and a minor component is within silicate grains as inclusions. The interstitial sulphide grains were observed to be in contact with plagioclase > olivine > clinopyroxene > hydrous minerals > accessory minerals which is consistent with results reported in Good (1992) for the Main Zone. When interstitial to silicate phases the grain shapes of the sulphide minerals are controlled by the silicate minerals. The chalcopyrite grains have a wide range of sizes ranging from very fine grained to coarse grained (up to 10 mm). Sulphide inclusions in silicate minerals (predominantly chalcopyrite blebs) are hosted in plagioclase > olivine ≥ clinopyroxene > hydrous silicates > accessory minerals. No correlation between the ratio of chalcopyrite and bornite to PGE grades was noted.

4.3.1.1 W-Horizon Chalcopyrite

Chalcopyrite is the dominant sulphide mineral in the W-Horizon and predominantly occurs as an interstitial mineral to silicate grains. The grain boundaries of the silicate minerals control the shape of the chalcopyrite (Fig. 4.3 A-C). The other sulphide minerals which occur within the W-Horizon almost exclusively occur as part of larger chalcopyrite grains.

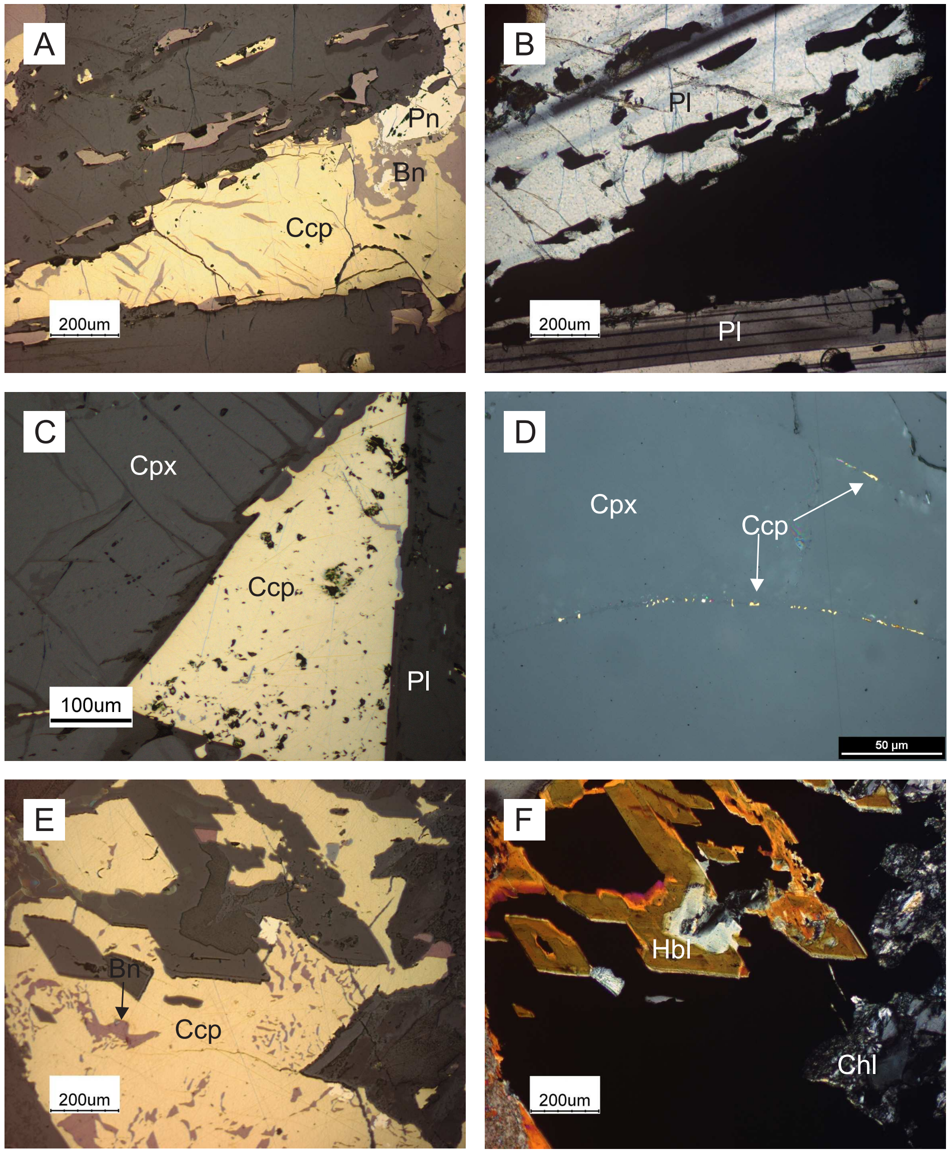

Figure 4.3: Photomicrographs of sulphide minerals in the W-Horizon from polished thin sections. Unless otherwise noted images are taken using reflected light. (**A**) Chalcopyrite (Ccp) grain with bornite (Bn) exsolution under reflected light. The shape of the large grain is controlled by the two bounding plagioclase (Pl) grains. Smaller grains of ccp have penetrated along Pl cleavage. (**B**) Cross polarized image of A, showing Pl crystal and cleavage control on the shape of the small penetrating sulphide grains. (**C**) A large Ccp grain bounded by Cpx and Pl demonstrating the control of silicate minerals on sulphide grain shape. (**D**) Several chains of disseminated chalcopyrite blebs within clinopyroxene (Cpx) (**E**) Ccp in a localized zone of hydrous silicates (hornblende (Hbl) and chlorite (Chl)). The Hbl is euhedral and appears to truncate Bn exsolution within the Ccp. (**F**) Cross polarized image of E, showing euhedral grains of Hbl and Chl.

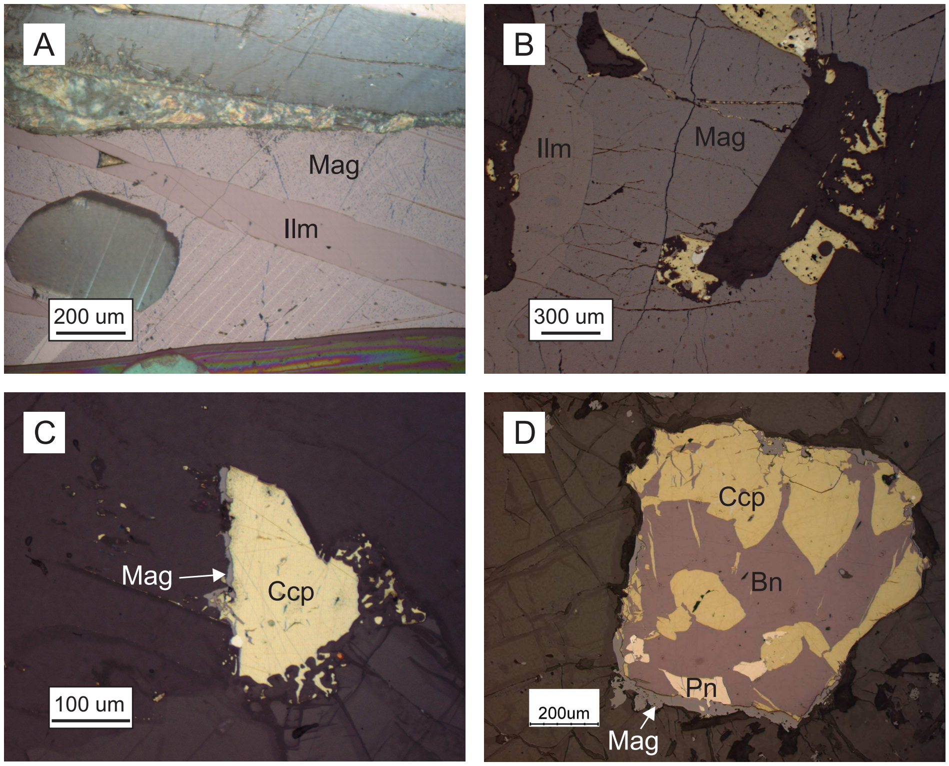

Figure 4.4: Photomicrographs of magnetite (Mag) in the W-Horizon from polished thin sections. Images were taken using reflected light. (**A**) Typical primary Mag within the TDLG showing a thick ilmenite (Ilm) exsolution band within the Mag, in addition there are fine Ilm bands (light grey) throughout the Mag grain. (**B**) A typical Mag grain from the TDLG showing a coarse Ilm band on the left. (**C**) A Mag rim on a chalcopyrite (Ccp) grain from the W-Horizon, the Mag rim does not contain any Ilm exsolution bands. (**D**) A Ccp grain containing granular bornite (Bn) and pentlandite (Pn) from the W-Horizon. Along the rim of the Ccp grain there is a band of Mag which does not contain any Ilm.

The chalcopyrite that is present as inclusions in plagioclase occurs along cleavage planes and its shape is controlled by the plagioclase mineral structure (Fig. 4.3 A-B). The inclusions are typically small (< 250 μm) and commonly emanate from nearby larger (>4 mm) chalcopyrite grains. Secondary plagioclase is typically associated with the sulphides and electron microprobe work, discussed below, has shown that the secondary plagioclase can be more calcic than the primary plagioclase.

The shapes of chalcopyrite grain inclusions within clinopyroxene and olivine are anhedral and are not controlled by structure of the host mineral (Fig. 4.3 D). It occurs in these minerals as very fine disseminated grains (< 10 μm) throughout the silicate grain. The disseminated grains often form continuous chains or lines through the silicate mineral. Larger (~ 100 μm) chalcopyrite grains within clinopyroxene and olivine are less common, and are usually associated with grain boundaries between other silicates. In addition to the inclusions thin (< 10 μm) sulphide filled fractures were also observed within clinopyroxene and olivine.

Chalcopyrite grains within hydrous silicates (chlorite, tremolite, hornblende, and calcite) are uncommon in the W-Horizon. The timing relationship between hydrous minerals and sulphide minerals is ambiguous. Figures 4.3 E-F shows a photomicrograph of euhedral chlorite and tremolite grains intergrown with a chalcopyrite grain exhibiting bornite exsolution.

Chalcopyrite is commonly rimmed by secondary magnetite within the W-Horizon. Figure 4.4 A and B shows typical magnetite from the TDLG not associated with sulphide minerals. This magnetite contains large bands of ilmenite exsolution as well as very fine disseminated bands of ilmenite. The magnetite which is observed to rim chalcopyrite within the W-Horizon does not contain any ilmenite (Fig. 4.4 C-D). Electron microprobe analyses, discussed below, has confirmed this observation and shown that this magnetite is chemically distinct from the primary magmatic magnetite and contains very low amounts of Ti.

4.3.1.2 W-Horizon Bornite

Bornite within the W-Horizon occurs almost exclusively within chalcopyrite grains as either fine exsolution lamella or as granular masses. Exsolution lamellae are the predominant form of bornite, and occur as elongate bands less than 50 μm in width. The location, orientation and abundance of the bands are random and irregular within the chalcopyrite grains (Fig. 4.5 A and B). The granular masses of bornite coexist with chalcopyrite grains which may or may not contain bornite exsolution (Fig. 4.5). Bornite has been rarely observed as individual crystals up to 300 μm across without chalcopyrite as shown in Figure 4.5. Independent crystals of bornite (crystals only in contact with silicate minerals) have the same occurrence and habit as chalcopyrite, and exhibit grain shape controlled by silicate minerals. It is likely that the independent crystals of bornite connect to chalcopyrite in another plane (not observed on the thin section plane). Correlation between the presence of bornite and magnetite rims on sulphides were not observed.

4.3.1.3 W-Horizon Pyrrhotite

Pyrrhotite is absent in high grade W-Horizon samples ($>$ 10 ppm Pt + Pd) and was not observed in samples from DDH-306, DDH-368 and DDH-369. Only samples from the low grade W-Horizon in DDH-441 contained pyrrhotite. The pyrrhotite occurs as granular masses within larger chalcopyrite grains and is commonly located in the core of the chalcopyrite (Fig. 4.6). In chalcopyrite grains containing pyrrhotite, bornite was absent.

4.3.1.4 W-Horizon Pentlandite

Pentlandite is present in essentially all W-Horizon samples studied for this project either as subrounded granular masses in chalcopyrite (Fig. 4.7) or as exsolution lamellae within pyrrhotite. Pentlandite grains up to 2 mm in width were observed within chalcopyrite. Boundaries with the host chalcopyrite are typically irregular and slightly rounded. Grains of pentlandite were either solid grains (Fig. 4.7 C, D and F) or contained fine exsolution

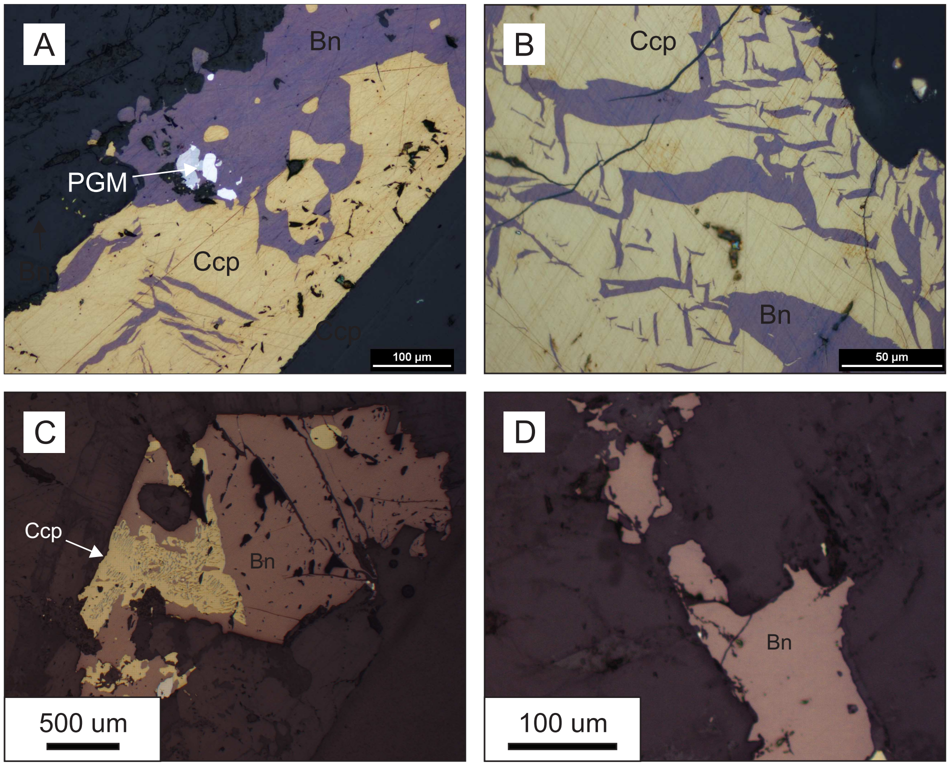

Figure 4.5: Photomicrographs of bornite in the W-Horizon from polished thin sections. Images were taken using reflected light. (**A**) Exsolution lamellae of bornite (Bn) within a chalcopyrite (Ccp) grain. There is no preferred orientation to the Bn lamellae and the right side of the photo contains less Bn than the left. (**B**) Exsolution lamellae of Bn within a Ccp grain showing the random orientation and distribution of Bn. The centre of the grain has a zone with low Bn abundance, and there is no concentration of Bn along the edge of the grain. (**C**) A large grain of Ccp-Bn. The right side of the grain is composed of granular Bn and contains very little Ccp. The left side of the grain has a large section of Ccp which contains very fine exsolution lamellae of Bn. (**D**) Granular Bn occurring with very little Ccp interstitial to silicate grains.

bands of chalcopyrite (Fig. 4.7 A, B and E). Chalcopyrite grains containing pentlandite also commonly contained bornite as fine exsolution lamellae in either the chalcopyrite or in the pentlandite (Fig. 4.7 F). The semi-quantitative composition of the pentlandite from electron dispersive X-ray spectroscopy (EDX) is approximately 44 At% S, 22 At% Fe, 2 At% Co, and 32At% Ni. In the low grade W-Horizon samples which do contain pyrrhotite, pentlandite is also present as exsolution bands or ‘‘pentlandite eyes” in the pyrrhotite.

4.3.2 Main Zone Sulphides

This section describes the Main Zone samples from DDH-306 and the Main Zone-like samples from DDH-368, and is a small sample set. The typical sulphide mineral assemblage in the Main Zone samples of this study are chalcopyrite > pyrrhotite > bornite ≥ pentlandite >

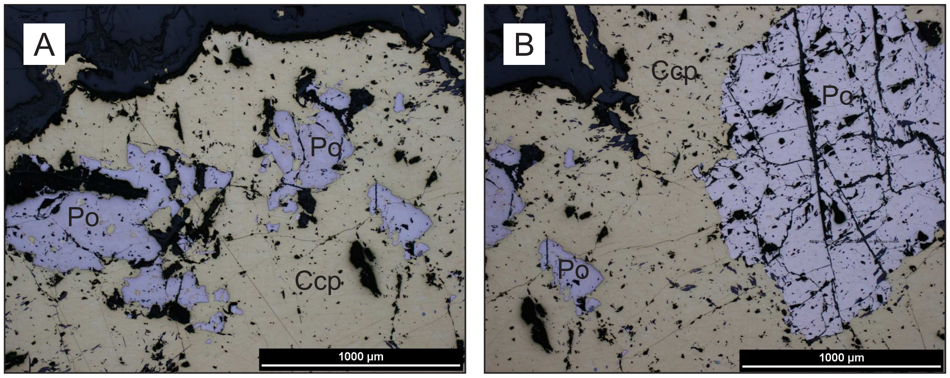

Figure 4.6: Photomicrographs of pyrrhotite in the W-Horizon from polished thin sections. Images were taken using reflected light. (**A**) Grain of Ccp with three Po cores taken from the low grade W-Horizon in DDH-441. (**B**) A core of Po within a larger Ccp grain taken from the low grade W-Horizon in DDH-441.

pyrite. Trace amounts of bornite are present in some of the thin sections from the Main Zone samples in this study. The sulphides have variable grain size ranging from very fine grained to coarse grained. Chalcopyrite is generally coarser in the Main Zone than W-Horizon, and can be up to 2 cm. The chalcopyrite/pyrrhotite is variable, with chalcopyrite >> pyrrhotite. This places it in the upper end of chalcopyrite/pyrrhotite range of 0.8 to 2.8 reported for the Main Zone by Good and Crocket (1994). Chalcopyrite grains also occur surrounded by localized patches of hydrous silicates (a combination of amphibole, biotite, chlorite, epidote, and carbonate (Fig. 4.8 C-D). The hydrous silicates typically have a subhedral to euhedral shape and penetrate the sulphide minerals giving them a ragged appearance. Secondary magnetite rimming chalcopyrite was observed in the Main Zone as in the W-Horizon, although with less abundance. Pyrrhotite typically forms the core of chalcopyrite grains (Fig. 4.8 A-B). Pentlandite occurs in association with chalcopyrite, as in the W-Horizon, and samples containing pyrrhotite can contain pentlandite exsolution lamellae.

The silicate association of sulphide minerals changes slightly between the Main Zone and the W-Horizon. In Main Zone samples the sulphide minerals are predominantly interstitial to silicate mineral grains, in order of abundance, plagioclase, clinopyroxene, olivine, actinolite, chlorite, biotite, sericite, magmatic magnetite and magmatic biotite. Sulphide minerals occurring with alteration minerals (actinolite, chlorite, biotite and sericite) are more commonly intergrown rather than interstitial. A minor amount of sulphide grains are also located within the silicate minerals. Sulphide grains associated with plagioclase exhibit shapes controlled by plagioclase grain boundaries commonly penetrated along cleavage (4.8 A-B). Chalcopyrite within clinopyroxene and olivine are similar in appearance to the W-Horizon, occuring as subrounded grains disseminated throughout the silicate grains.

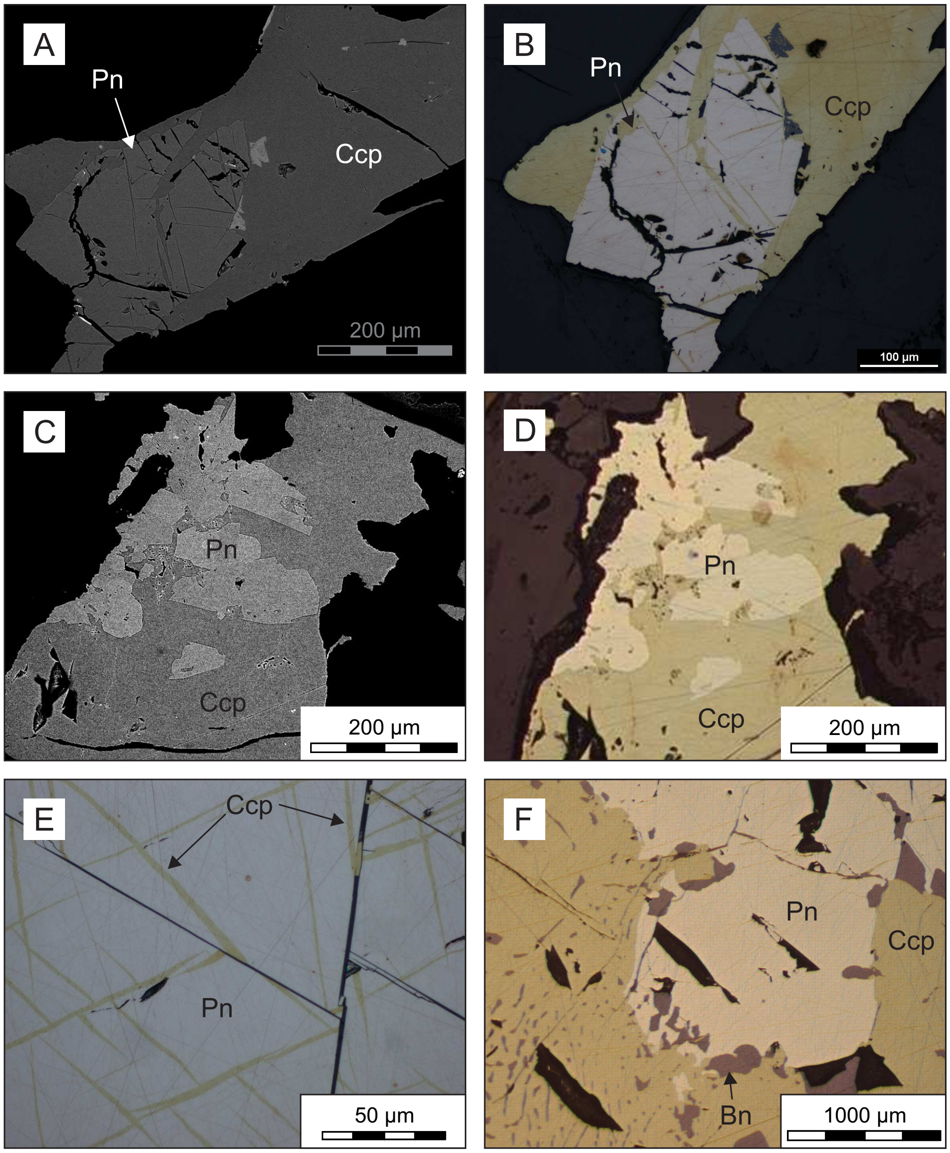

Figure 4.7: Photomicrographs of pentlandite in the W-Horizon from polished thin sections. (**A**) Backscatter image of pentlandite (Pn) in a chalcopyrite (Ccp) grain. The Pn has angular to rounded contacts with the Ccp. The Pn grain has a regular fracture pattern which is filled by Ccp. (**B**) Reflected light image of A showing the Pn grain within Ccp. (**C**) Backscatter image of granular Pn in a Ccp grain. The Pn grains are subrounded within the Ccp. (**D**) Reflected light image of C showing granular Pn within Ccp. (**E**) High magnification image of Pn within a larger Ccp grain. The Pn contains abundant fine fractures of Ccp. (**F**) Reflected light image of Pn in Ccp. The Pn occurs as a large granular mass within a larger Ccp grain. Bornite exsolution lamellae are abundant within the Ccp and granular Bn occurs along the boundaries and within the Pn grain.

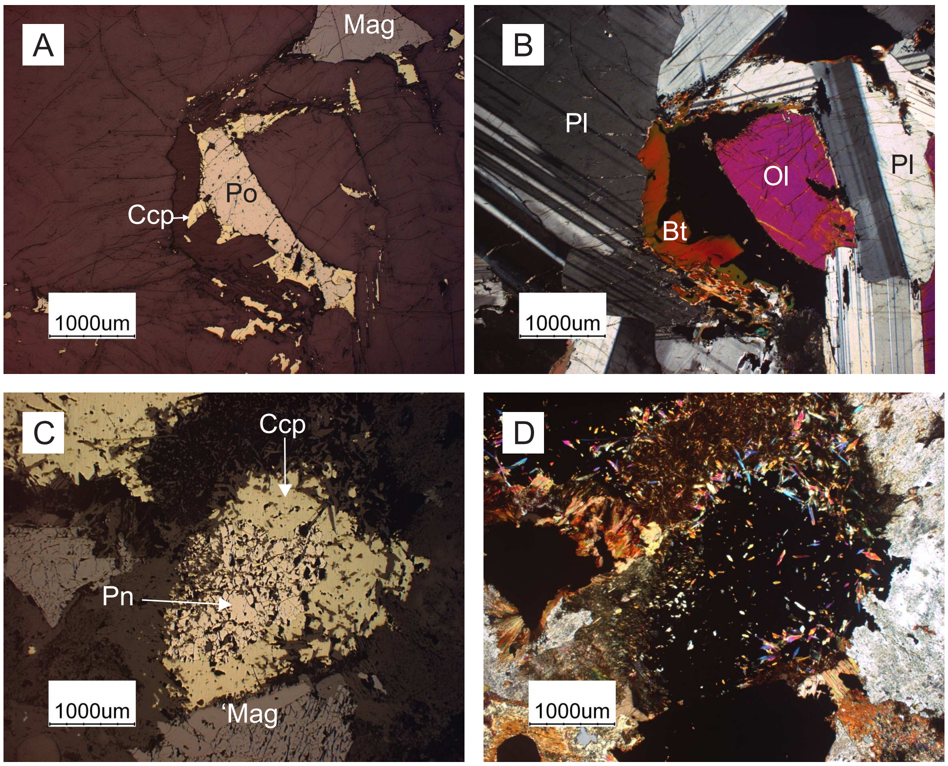

Figure 4.8: Photomicrographs of the Main Zone Sulphides from polished thin sections. (**A**) A sulphide grain with a pyrrhotite (Po) core rimmed by chalcopyrite (Ccp) under reflected light. The sulphide grain is interstitial to the silicate minerals. There are finer extensions of the Ccp grain penetrating along plagioclase (Pl) cleavage in surrounding grains. (**B**) Cross polarized light image of A showing Ccp and Po interstitial to silicate grains. (**C**) Chalcopyrite with a pentlandite (Pn) core within a localized zone of hydrous minerals. (**D**) Cross polarized light image of C showing chlorite, biotite and actinolite.

4.4 Platinum Group Minerals

A detailed study of the platinum group minerals (PGM) was beyond the scope of this study. The reader is referred to Puritch et al. (2009) which summarizes a detailed petrographic and SEM-EDS study conducted by Marathon-PGM. In the study 2,304 PGM grains were analyzed from 55 thin sections of Main Zone and W-Horizon mineralization. Summary tables showing the size distribution of PGM, PGM host mineral, and the dominant PGM Phases of the Main Zone and W-Horizon are reproduced in Tables 4.1 4.2 and 4.3.

The dominant hosts of platinum group minerals in W-Horizon samples from this study were sulphide minerals $>$ other platinum group minerals $>$ within plagioclase boundaries. The PGM hosts in the Main Zone samples from this study were sulphide minerals $\geq$ secondary alteration minerals (predominantly actinolite and chlorite) $>$ within plagioclase boundaries, similar to Puritch et al. (2009). The PGM host phases in the W-Horizon reported in Puritch et al. (2009) were sulphides (53.7%) $>$ plagioclase boundaries (25%) $>$ other PGMs (16.5%) $>$ secondary hydrous silicates (predominantly chlorite and serpentine)(4.3%). The PGM host phases in the Main Zone samples reported in Puritch et al. (2009) were secondary alteration minerals (predominantly actinolite and chlorite) (38%), $>$ sulphides (34.9%) $>$ plagioclase boundaries (22.4%) $>$ other PGMs (4.36%).

The grain size of PGM within the Main Zone and W-Horizon is similar with approximately 60% of PGM grains $<$ 60 um (Puritch et al., 2009). The suite of PGM between the W-Horizon and Main Zone were also shown to contrast greatly. The W-Horizon is dominated by zvyagintsevite, palladinite and telargpalite where as the Main Zone is dominated by kotulskite-sobolevskitess, mertierite-II, sobolevskite, kotulskite and sperrylite. The results of the PGM phase study are summarized in Table 4.3.

Although detailed identification of PGM was beyond the scope of this project a minor amount of work was conducted to identify the location of PGM grains within the W-Horizon samples. The findings agree with those reported in (Puritch et al., 2009), the majority of PGM are associated with sulphide minerals either within the sulphide grains (Fig. 4.9 A) or on the edges of grains (Fig. 4.9 B). The PGM either occur as individual grains or complex grain aggregates (Fig. 4.9 C). It is rare to find PGM grains associated only with silicate phases and in these cases it is possible that if viewed in 3D these PGM would be on the edge of a sulphide grain. In addition it is rare to find PGM associated with secondary alteration minerals (predominantly actinolite and chlorite). Lastly, it was observed in this study that the amount of PGM grains drastically increases when bornite exsolution lamellae occur within chalcopyrite.

Table 4.1: Dominant PGM Phases in the Main Zone Compared to the W-Horizon

Zone	No. of grains	< 5 microns (%)	5-10 microns (%)	10-20 microns (%)	> 20 microns (%)
Main	573	64.9	16.9	12.5	5.7
W-Horizon	1731	58.3	27.1	9.6	5

Reproduced from Puritch et al. (2009)

Table 4.2: Dominant PGM Phases in the Main Zone Compared to the W-Horizon

Zone	No. of grains	Plagioclase boundaries (%)	Sulphides (%)	Other PGM's (%)	Hydrous silicates (%)
Main	573	22.4	34.9	4.36	38
W-Horizon	1731	25	53.7	16.5	4.3

Reproduced from Puritch et al. (2009)

Table 4.3: Dominant PGM Phases in the Main Zone Compared to the W-Horizon

Mineral	Formula	W-Horizon	Main Zone
Zvyagintsevite	$(Pd,Pt,Au)_3Pb$	41.8 %	-
Palladinite	(Pd,Cu,Au)O	15.5 %	-
Telargpalite	$(Pd,Ag)_3Te$	5.5 %	-
Skaergaardite	PdCu	3.9 %	-
Kotulskite, Pb-rich	Pd(Te,Bi,Pb)	3.8 %	-
Isoferroplatinum	$(Pt,Pd)_3(Fe,Cu)$	3.7 %	-
Keithconnite, Pb-rich	$Pd_{3\text{-}x}(Te,Pb,Sb)$	3.5 %	-
Tetraferroplatinum	PtFe	3.4 %	-
Plumbopalladinite	Pd_3Pb_2	1.2 %	-
Vysotskite	PdS	1.2 %	-
Laflammeite	$Pd_3Pb_2S_2$	1.1 %	-
Atokite, Pb-rich	$(Pd,Pt)_3(Sn,Pb)$	0.9 %	-
Au, Ag and alloys		7 %	3.3 %
Stilwaterite	Pd_8As_3	0.4 %	0.9 %
Arsenopalladinite	$Pd_8(As,Sb,Pb)_3$	0.3 %	1.7 %
Cotunnite, Ru-rich	$(Pb,Ru)Cl_2$	-	2.1 %
Hessite	Ag_2Te	-	3.7 %
Hollingworthite	(Rh,Pt,Pd)AsS	0.2 %	5.6 %
Sperrylite	$PtAs_2$	1.1 %	6.3 %
Kotulskite	Pd(Te,Bi)	-	9.9 %
Sobolevskite	PdBi	0.1 %	10.1 %
Mertierite-II	$Pd_8(Sb,As,Pb)_3$	0.3 %	16.1 %
Kotulskite-Sobolevskitess	$Pd_2Te(Bi,Pb)$	0.2 %	34.9 %

Reproduced from Puritch et al. (2009)

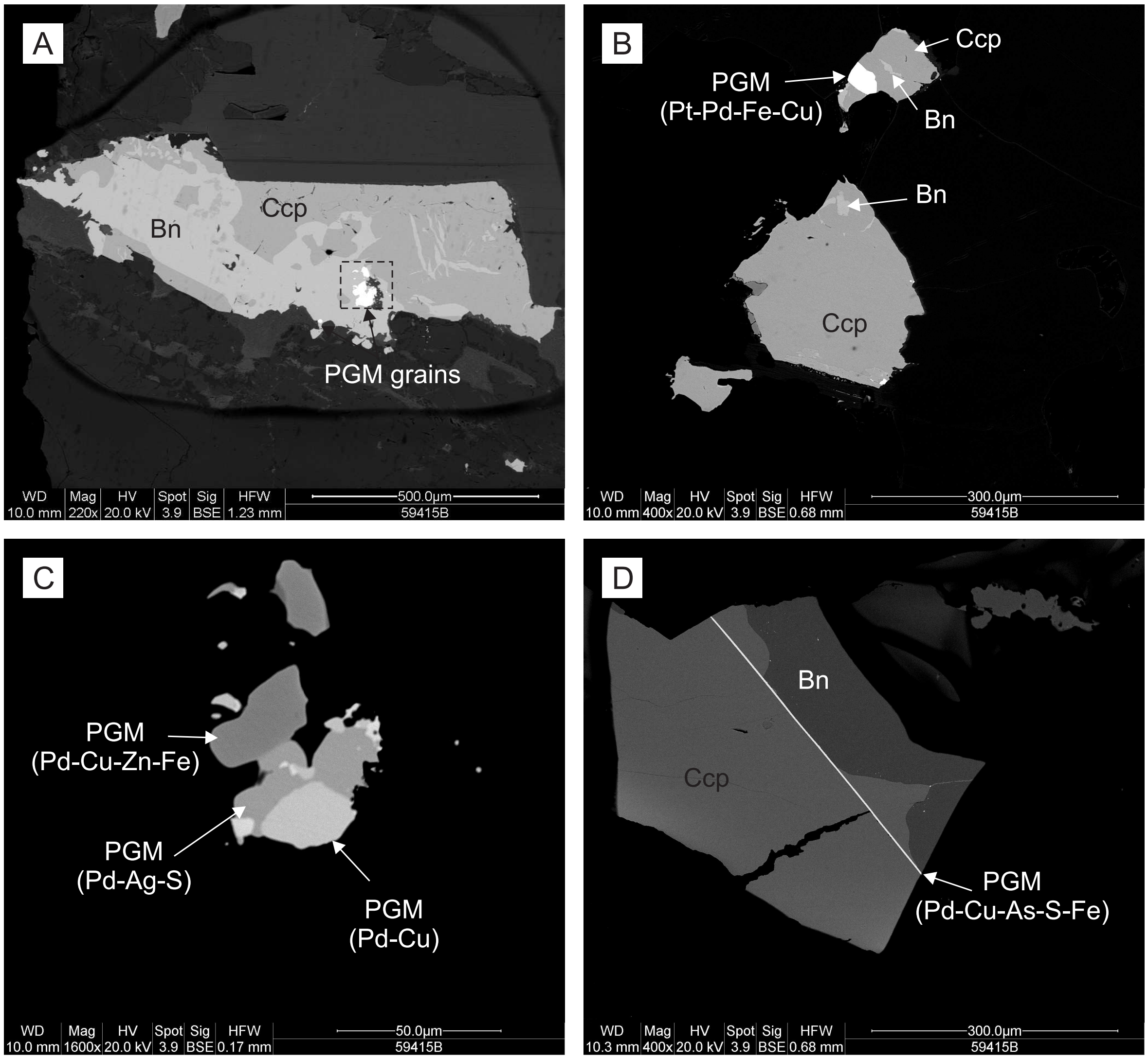

Figure 4.9: SEM backscatter images of platinum group minerals in the W-Horizon. (**A**) Chalcopyrite grain (grey) with bornite exoslution bands (lighter grey) and a cluster of PGM minerals (white) within the bornite. The highlighted area is shown in panel C. (**B**) Two chalcopyrite grains with small amounts of bornite exosolution lamellae. The top grain of chalcopyrite has a PGM grain (Pt-Pd-Fe-Cu) on the edge. (**C**) Magnified image of the PGM grain in panel A that shows the complex intergrowth of multiple PGM minerals. (**D**) Grain of chalcopyrite with granular bornite. A band of PGM (Pd-Cu-As-S-Fe) cross-cuts the bornite.

Chapter 5

Geochemistry

In this study the geochemistry of unmineralized, Main Zone, and W-Horizon samples were examined for trends related to mineralization processes. Major elements, trace elements, gold, platinum and palladium were analyzed. The analyses were carried out at two commercial labs, Geosciences Laboratories (Geo Labs), Sudbury and Activation Laboratories Ltd. (Actlabs), Ancaster, Ontario. The samples from DDH-368 were analyzed at Geo Labs where as DDH-306, DDH-369 and DDH-441 were analyzed at Actlabs. The raw data from all geochemical analyses are given in Appendix IV.

5.1 Analytical Techniques

All drill core samples used in geochemical analysis were first ground into a powder. Geo Labs samples were ground using high chrome steel mills and the powder passed through a minus 100 mesh (149 microns). This method of preparation is expected to contaminate samples with approximately 150 ppm Cr and 0.1% Fe. Actlabs samples were ground using a mild steel mill. Samples were crushed to a nominal minus 10 mesh (1.7 mm), mechanically split (riffle) and then pulversized to at least 95% minus 150 mesh (105 microns). Iron contamination of up to 0.2% is expectect, the use of a steel mill does not add any Cr or Ni contamination.

Major elements at Geo Labs were analyzed by X-ray fluorescence spectrometry (XRF). Samples were prepared by first conducting a loss on ignition at 100 °C under nitrogen atmosphere, followed by 1000°C under an oxygen atmosphere until a constant weight% was determined. The sample was then fused with a lithium borate flux to produce a glass bead for analysis. Major elements at Actlabs were analyzed by Inductively Coupled Plasma Mass Spectrometry (ICP-MS). To prepare samples they mixed them with a flux of lithium metaborate and lithium tetraborate and fused in an induction furnace. The glass bead was then dissolved into a solution of 5% nitric acid.

Trace elements at Geo Labs were analyzed by dissolution in a multi acid digest (hydrofluoric, hydrochloric, nitric and perchloric acid) in a closed vessel to promote total dissolution, then analyzed by ICP-MS. Trace elements at Actlabs were also analyzed by ICP-MS using the glass bead prepared for major element chemistry.

Samples for S analysis at Geo Labs conducted by combustion of the sample in an oxygen rich environment and then measuring S was by infrared absorption. The samples for Se and Te were prepared by digestion in concentrated acids (hydrofluoric, hydrochloric, nitric and perchloric), and then analyzed by ICP-MS. The samples used to analyze for S, Se and Te at Actlabs were prepared by digestion in aqua regia at 90°C in a digestion block for 2 hours. The solution was then analyzed by ICP-MS.

Gold, platinum and palladium were analyzed by lead fire assay with a ICP-MS finish at both labs.

No samples were analyzed at both labs. Results for major element chemistry and trace element chemistry were similar between two labs. A comparison between major and trace element analytical results between the two labs is shown in Fig. 5.1. This figure compares major elements, rare earth elements and high field strength elements. The results two labs overlap the same range indicating that the data sets can be compared.

5.2 Major and Trace Element Lithogeochemistry

A summary of the major element chemistry for unmineralized and mineralized zones of each drill hole is shown in Table 5.1. A box and whisker plot summarizing the major element chemistry for unmineralized, Main Zone, W-Horizon and samples from Good (1992) is shown in Figure 5.2. The results of major element lithogeochemistry from this study show similar ranges to those reported in Good (1992). The major element lithogeochemistry are also consistent between unmineralized, Main Zone and W-Horizon samples. Main Zone samples have slightly elevated Al_2O_3, MnO and CaO whereas the W-Horizon samples reveal a decrease in P_2O_5. The dominant control on major element chemistry is modal mineral abundance, which can be highly variable because of the small sample size. Clinopyroxene is the major control on CaO and Mg#, and plagioclase controls Na_2O and Al_2O_3. Due to its low abundance, olivine does not exhibit a strong control on major element chemistry. Magnetite and ilmenite are the major controls on TiO_2.

Harker differentiation diagrams are shown in Figure 5.3. It is expected that an evolving igneous system with an SiO_2 range of 42-52 wt%, will show the following trends with increasing SiO_2; increasing Al_2O_3, Na_2O, K_2O and decreasing MgO, FeO, CaO and TiO_2 (Winter, 2001). Linear correlations in these diagrams are weak. In this sample suite the Harker diagrams show the following relationships with increasing SiO_2; increasing Al_2O_3, Na_2O, and CaO and decreasing FeO. MgO differentiation diagrams are shown in Figure 5.4. This set of diagrams demonstrates the following relationships with decreasing MgO; increasing SiO_2, Na_2O and Al_2O_3 and decreasing FeO. Al_2O_3, Na_2O and Fe_2O_3 all show linear trends on the Harker and MgO differentiation diagrams, and are therefore considered to be indicators of fractionation trends.

Major and trace element down hole plots are shown in Figures 5.5-5.8 with the mineralized zones highlighted. Within mineralized zones the results look more erratic compared to the unmineralized zones. This is actually caused by the increased number of samples analyzed

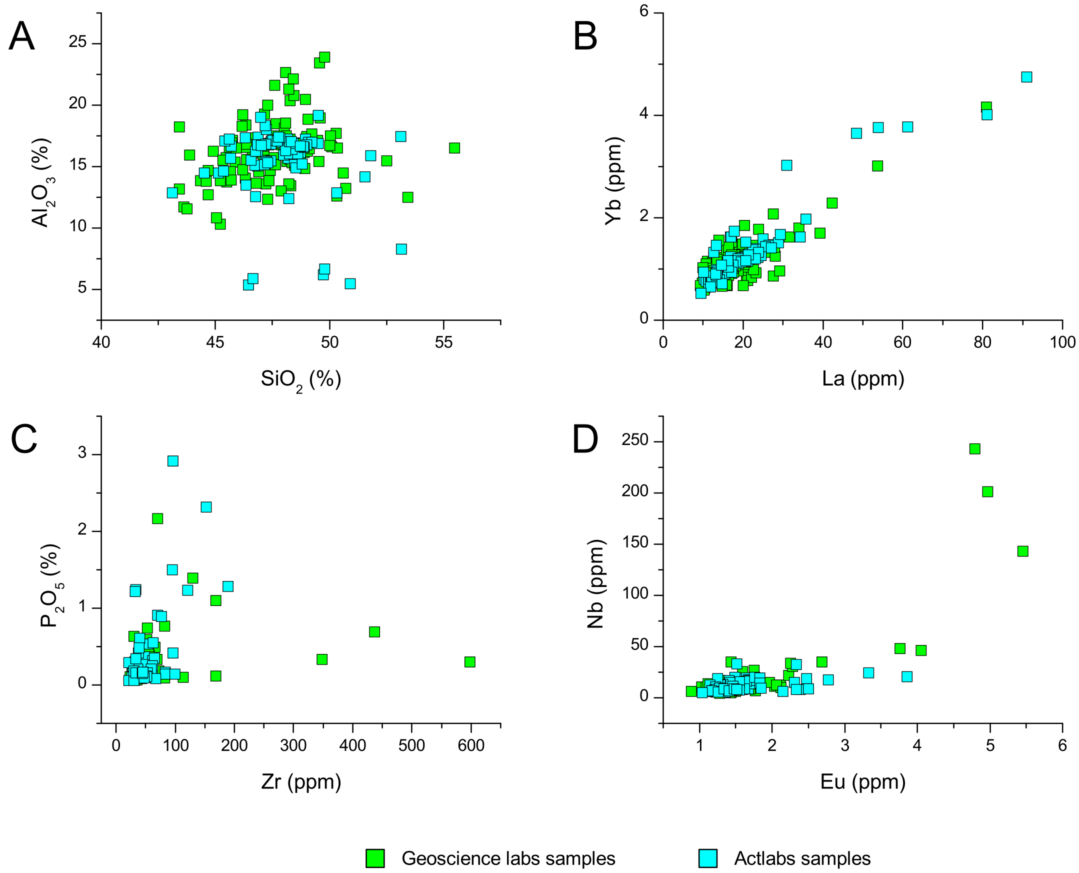

Figure 5.1: Major and trace element comparison between the two analytical laboratories used displaying overlapping ranges. (**A**) Comparison of major elements (SiO_2 and Al_2O_3). (**B**) Comparison of light rare earth elements to heavy rare earth elements (La and Yb). (**C**) Comparison of high field strength elements (Zr and P). (**D**) Comparison of rare earth elements vs. high field strength elements (Eu and Nb).

within the mineralized zones relative to the unmineralized zones, and the small amount of material used in each analysis. Both TiO_2 and P_2O_5 show a wide range of values. This is caused by variable modal abundances of apatite and magnetite, predominantly within the feldspathic peridotite. Each drill hole will be examined in the following section.

Overall the trace element chemistry trends follow shifts in the major element chemistry. The most obvious of these trends are caused by magnetite, plagioclase and clinopyroxene. The abundance of magnetite is shown by positive correlations of TiO_2, V and these values generally have opposite trends to SiO_2. Plagioclase control on trace elements is observed in a strong positive correlation between Al_2O_3, Na_2O and Sr. Incompatible elements Zr, Nb and Y show a strong positive correlation and generally correlate with increases in P_2O_5. Shaw (1994) demonstrated that clinopyroxene represents trapped interstitial liquid and is the major control on CaO. The abundance of CaO generally shows a positive correlation with the incompatible trace elements.

Table 5.1: Major Element Composition by Zone

	Unmineralized N = 100			306 W-Horizon N = 19			368 W-Horizon N = 5			369 W-Horizon 1 N = 5		
	Min	Max	Avg	Min	Max	Avg	Min	Max	Avg	Min	Max	Avg
SiO_2	43.11	55.49	47.83	44.68	49.57	47.54	44.51	48.72	47.75	44.6	47.64	46.42
TiO_2	0.27	1.82	0.78	0.17	1.65	0.54	0.59	1.37	0.77	0.4	0.71	0.57
Al_2O_3	8.27	19.18	15.97	10.31	23.42	17.61	14.47	16.23	15.63	13.82	20.02	16.22
Fe_2O_3	6.90	23.15	11.85	6.74	18.54	10.96	10.95	16.29	12.4	9.47	13.56	11.71
MnO	0.12	0.36	0.19	0.09	0.29	0.17	0.18	0.22	0.19	0.14	0.21	0.18
MgO	2.21	13.94	7.31	3.42	14.22	7.20	7.92	8.88	8.36	4.92	9.28	7.27
CaO	5.70	14.32	12.17	8.47	14.93	11.83	12.07	14.35	12.62	9.44	12.92	11.1
Na_2O	1.49	5.41	2.44	1.29	3.42	2.49	1.97	2.22	2.10	1.56	2.82	2.14
K_2O	0.28	2.36	0.53	0.24	0.76	0.49	0.35	0.4	0.38	0.35	0.54	0.41
P_2O_5	0.06	2.17	0.29	0.07	0.77	0.17	0.21	0.53	0.29	0.10	0.20	0.15
LOI	-1.75	6.45	0.81	-0.52	2.8	0.21	-0.32	0.22	0.02	2.45	5.11	3.38
	369 W-Horizon 2 N = 9			441 W-Horizon N = 18			306 Main Zone N = 13			368 Main Zone N = 15		
	Min	Max	Avg	Min	Max	Avg	Min	Max	Avg	Min	Max	Avg
SiO_2	47.3	50.35	48.47	45.71	53.44	48	43.88	50.11	46.52	45.42	51.55	47.93
TiO_2	0.51	0.94	0.7	0.34	1.38	0.73	0.51	1.69	1.09	0.51	1.82	0.96
Al_2O_3	12.33	17.67	15.16	12.52	23.93	17.09	13.84	20.76	16.27	5.37	18.99	12.44
Fe_2O_3	8.12	12.35	9.97	4.14	14.37	10.70	9.61	16.75	12.72	10.07	17.68	13.38
MnO	0.14	0.21	0.17	0.06	0.21	0.16	0.12	0.27	0.18	0.16	0.32	0.22
MgO	4.74	8.76	6.91	2.23	8.85	6.50	3.45	6.80	5.47	6.26	9.41	8.14
CaO	11.64	15.21	13.42	8.64	14.21	12.43	9.76	13.55	11.91	10.18	16.76	13.55
Na_2O	1.7	3.43	2.36	1.9	3.77	2.51	2.00	3.09	2.54	1.21	2.74	1.90
K_2O	0.31	0.73	0.48	0.26	2.11	0.52	0.29	0.44	0.35	0.30	0.96	0.51
P_2O_5	0.10	0.23	0.13	0.07	1.10	0.19	0.07	0.63	0.19	0.06	2.92	0.74
LOI	0.64	2.09	1.34	0.02	1.23	0.6	0.46	7.04	1.61	-0.06	1.30	0.63

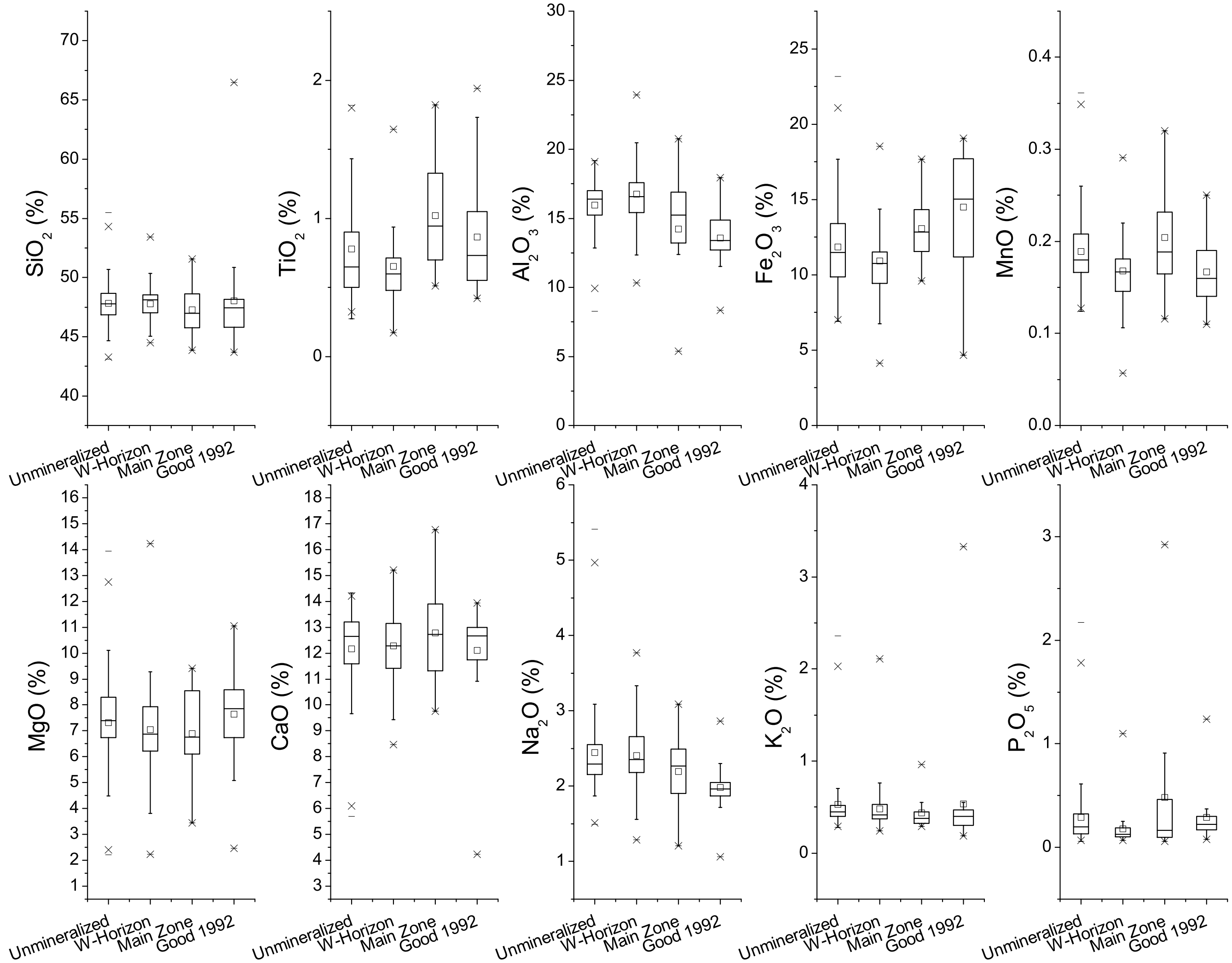

Figure 5.2: Box and whisker plot summarizing the major element chemistry of the TDLG grouped by unmineralized, W-Horizon and Main Zone samples. The box is divided into the 25 and 75 percentile range, also shown are the mean, 1% and 99% percentile values and the minimum/maximum.

5.3 Down Hole Lithogeochemistry

5.3.1 DDH-306

The major and trace element lithogeochemistry is shown in Figure 5.5 and the log is in Figure 3.5. Three distinct packages can be defined based on the Mg#, and the major and trace elements elements show similar behaviour in these intervals. From the base of the drill hole to the top of the Main Zone is the first package (the apparent erratic results within the mineralized zone are a result of the increased samples as described above). From the top of the Main Zone through unmineralized zone 2 the assays are consistent with a Mg# increasing smoothly to higher values. From the base of the W-Horizon to the top of the drill hole there is no clear trend. The overall patterns of the trace elements mirror the major elements. Magnetite control is evident by the positive correlation of TiO_2 and V. Plagioclase control is shown through positive correlation of Al_2O_3 and Sr. Incompatible elements Zr, Nb, and Y show a strong positive correlation with each other and also parallel the overall trends exhibited by CaO which correlates with the amount of trapped liquid. A spike in P_2O_5 (corresponding with a sample of feldspathic clinopyroxenite) at 158 m is reflected by increases in Ti, V, Nb and Y.

5.3.2 DDH-368

The major and trace element lithogeochemistry is shown in Figure 5.6 and the log is in Figure 3.6. Three distinct packages can be defined based on the Mg#, and the other elements show similar behaviour in these intervals. From the base of the intrusion to the base of the Main Zone the Mg# increases smoothly. Within the Main Zone there is no clear trend. Above the Main Zone there is a second package of smoothly increasing Mg# to the base of the W-Horizon. Within the W-Horizon there is no clear trends and above the Mg# decreases up-section.

Overall the trace element patterns mirror those observed within the major elements. Magnetite control is evident by the positive correlation of TiO_2 and V. Trace elements compatible with magnetite show negative correlation with SiO_2. Plagioclase control is shown through a positive correlation of Al_2O_3 and Sr. Incompatible elements Zr, Nb, and Y show a strong positive correlation with each other and also parallel the overall trends exhibited by CaO which correlates with the amount of trapped liquid. The incompatible trace elements are highest at the bottom of this drill hole and decrease towards the top. The largest increases in trace element abundance, particularly Zr, Nb and Y, occur in conjunction with increases in the amount of apatite. This trend is observed within unmineralized zone 3, and the Main Zone. Above the W-Horizon to the top of the samples the values remain relatively constant.

5.3.3 DDH-369

The major and trace element lithogeochemistry is shown in Figure 5.7 and the log is in Figure 3.7. The results from this drill hole do not show strong trends overall.

Incompatible trace element (Ba, Nb, Zr and Y) abundances smoothly increase from the top of W-Horizon 2 to the base of W-Horizon 1.

Magnetite control is evident by the positive correlation of TiO_2 and V. Trace elements compatible with magnetite show negative correlation with SiO_2. Plagioclase control is shown through the positive correlation of Al_2O_3 and Sr. Incompatible elements Zr, Nb, and Y show a strong positive correlation with each other but not with CaO as was observed in the previous drill holes. Samples containing elevated P_2O_5 and trace elements correspond to feldspathic clinopyroxenite. The normal fractionation trend observed through unmineralized zone 2 is also observed in the trace elements with TiO_2, V, K_2O, Rb, Sr, and Ba increasing whereas Zr and Y both decrease.

5.3.4 DDH-441

The major and trace element lithogeochemistry is shown in Figure 5.8 and the log is in Figure 3.8. Overall the results from this drill hole are near-constant and do not vary greatly up section. As observed in the previous drill holes the results are the most erratic within the W-Horizon. As was observed in the previous drill holes magnetite control is evident by the positive correlation of TiO_2 and V. Trace elements compatible with magnetite show negative correlation with SiO_2. Plagioclase control is shown through the positive correlation of Al_2O_3 and Sr. Incompatible elements Zr, Nb, and Y do not show a strong positive correlation with each other or CaO which was also observed in DDH-369. Generally samples containing apatitic feldspathic clinopyroxenite or syenite dikes correlate with increases in trace elements.

5.3.5 Down Hole Summary

The major element chemistry is variable between adjacent drill holes of the study and is not correlatable. Trends indicating fractional crystallization in a closed system include increasing SiO_2 and decreasing Mg# with depth. These trends which represent fractionation in a closed magmatic system are not observed over large intervals but rather as small zones separated by breaks. All of the drill holes displayed an increase in variation of adjacent samples within the mineralized zones. This irregularity is due to the increased sampling density within the mineralized zones. Drill holes DDH-306, DDH-368 and DDH-369 each showed several distinct packages based predominantly on Mg# whereas the composition in DDH-441 remained constant. The scale of the trends is variable from small several meter sections to entire drill holes. The appearance of apatitic feldspathic peridotite also does not correlate to any changes in composition either above or below these zones. The apatitic feldspathic peridotite correlates with the largest major shifts in trace element chemistry, compatible elements decrease and incompatible elements increase in abundance.

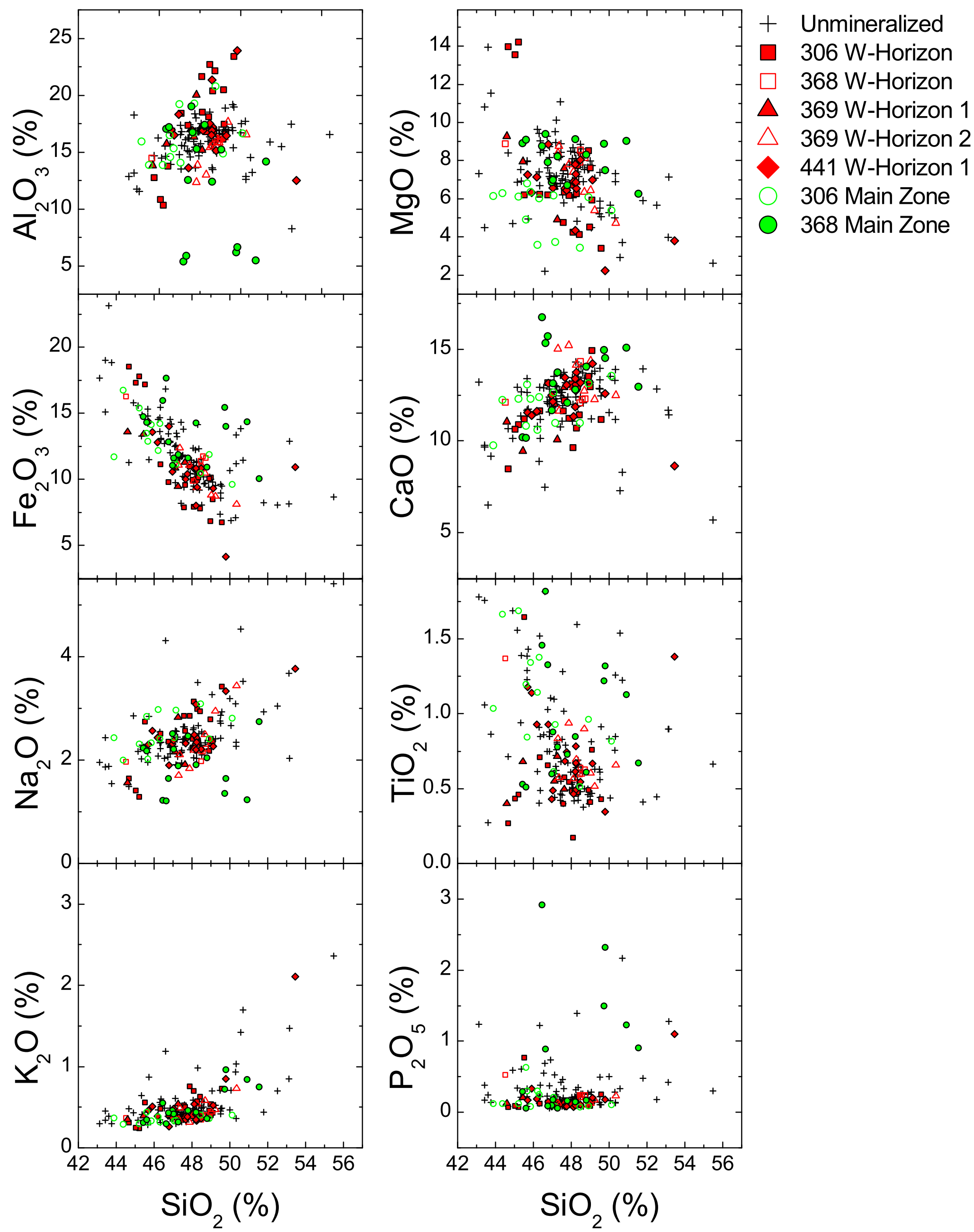

Figure 5.3: Harker diagrams plotting SiO_2 vs. major oxides (in weight %) for all samples. Linear correlations with major elements and SiO_2 are weak. The best correlation for linear trends indicating an evolving magmatic system are shown for Fe_2O_3, CaO and Na_2O_3. The remaining diagrams do not exhibit strong linear correlations with SiO_2.

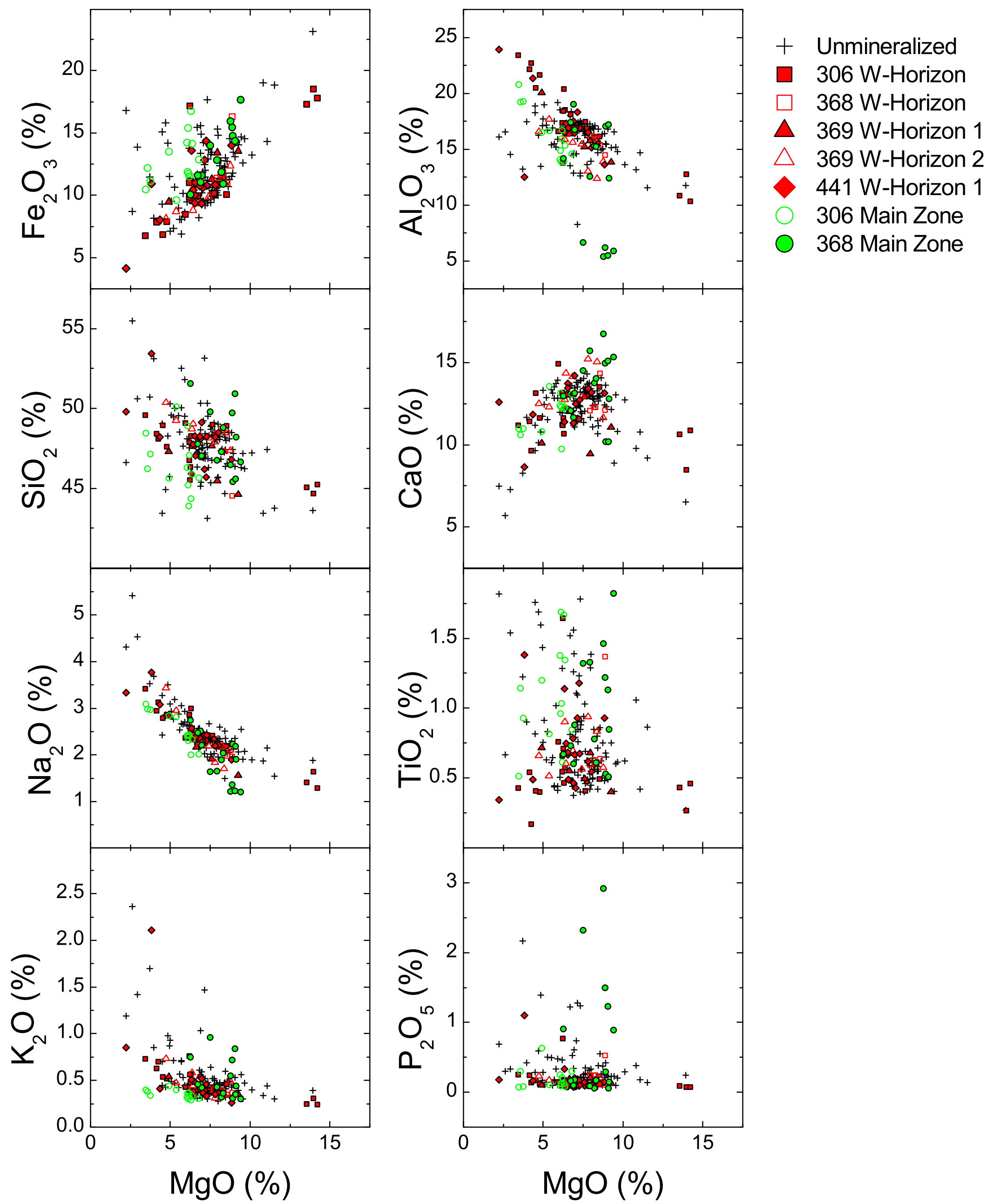

Figure 5.4: MgO differentiation diagrams for major elements. MgO is used as a differentiation index, samples having a lower MgO are expected to be move evolved. Overall correlations with major elements and MgO are weak. Weak linear correlations indicating an evolving magmatic system are shown for Fe_2O_3, Al_2O_3 and Na_2O. A wide spread is shown for TiO_2 and P_2O_5 due to zones of cumulate magnetite and apatite.

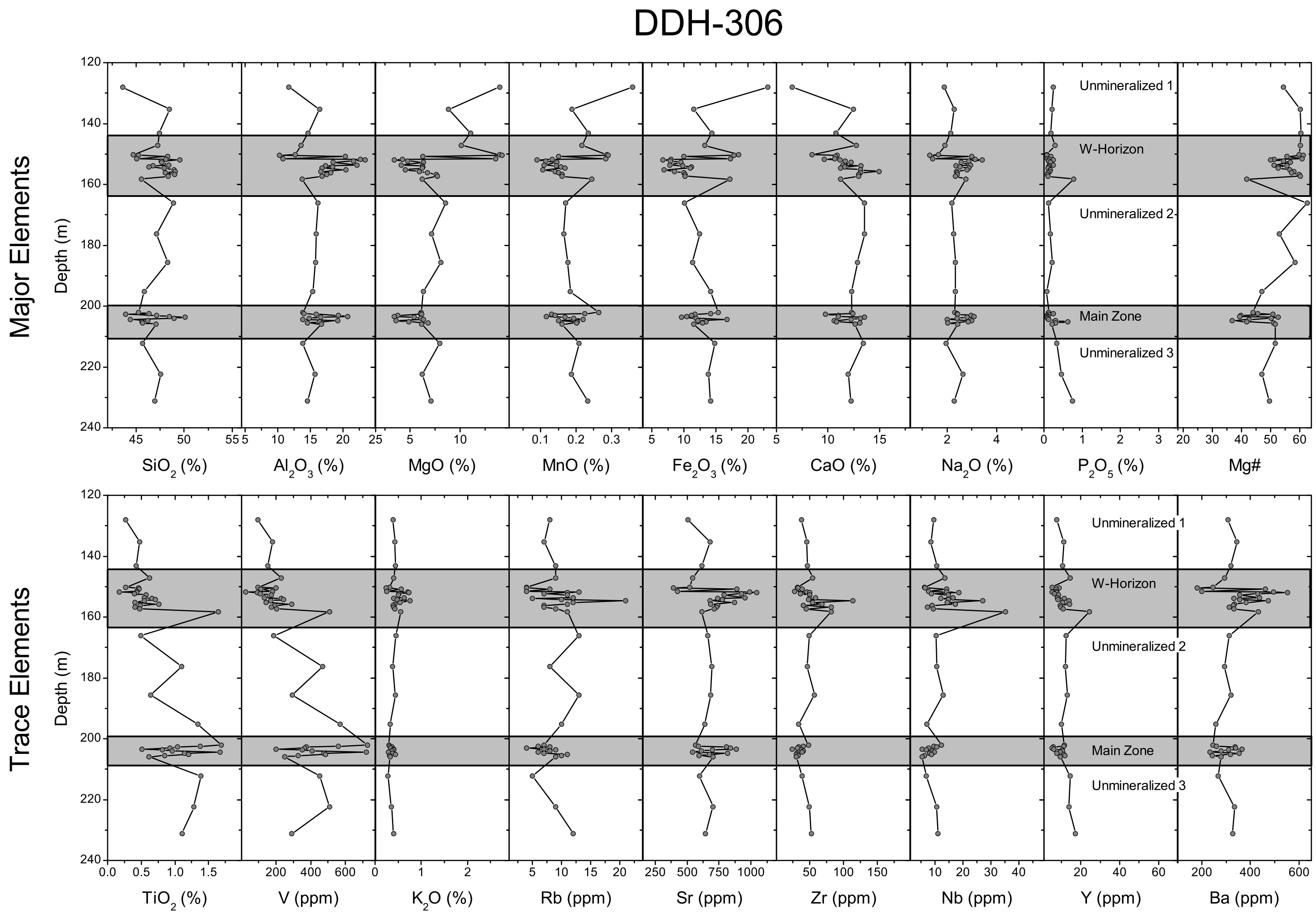

Figure 5.5: Down hole major element and trace element plots for DDH-306. Mineralized zones are highlighted in grey.

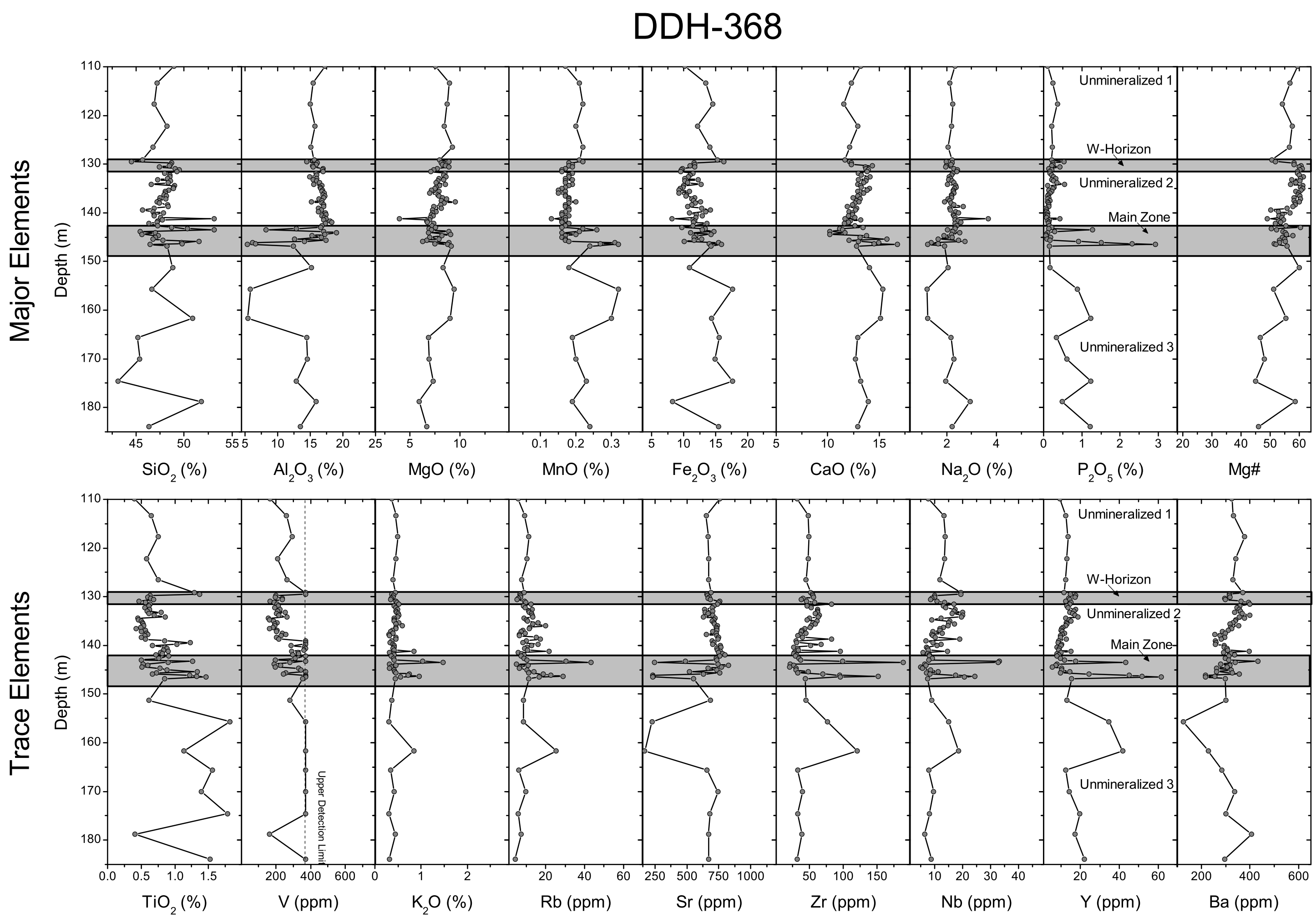

Figure 5.6: Down hole major element and trace element plots for DDH-368. Mineralized zones are highlighted in grey.

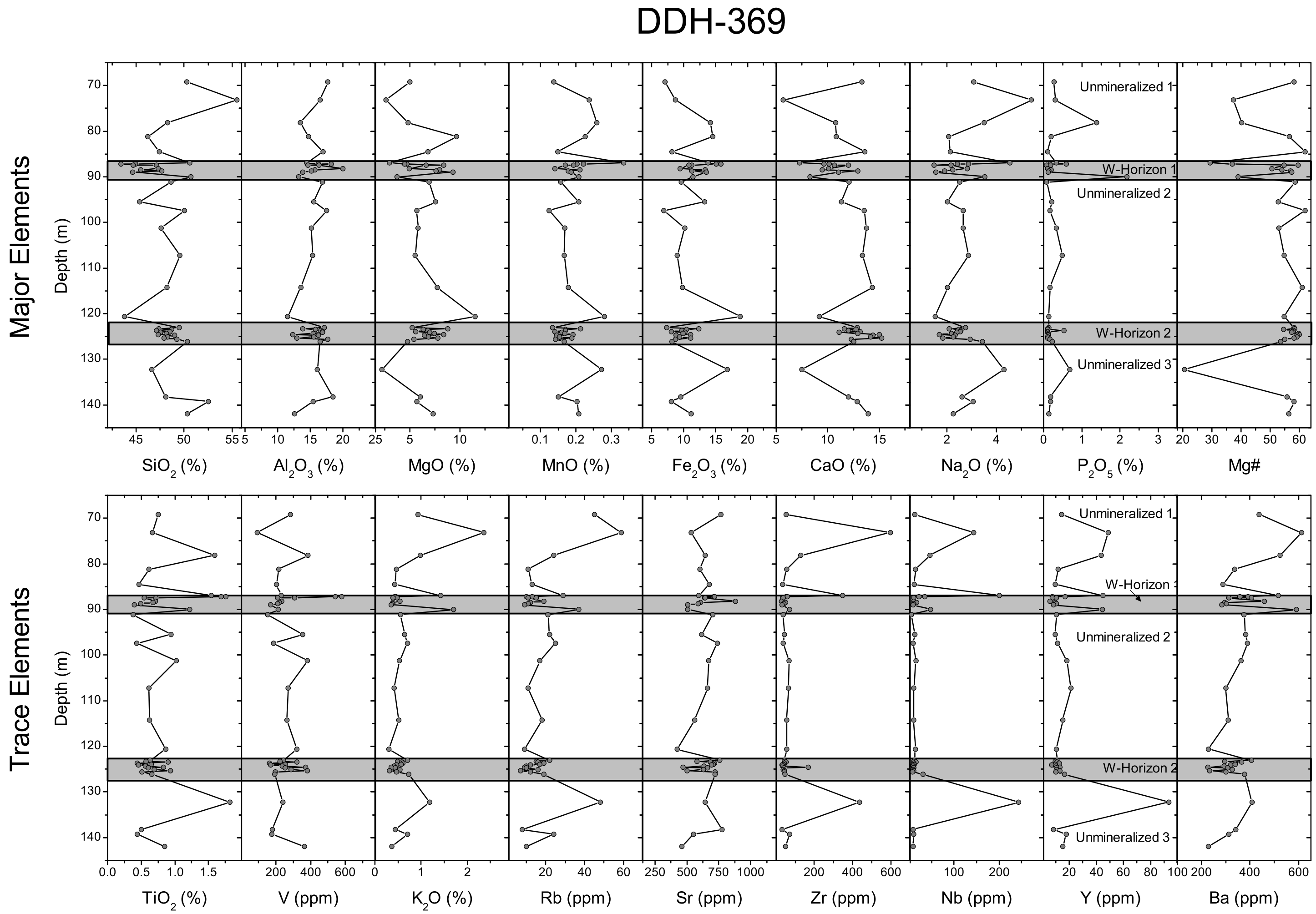

Figure 5.7: Down hole major element and trace element plots for DDH-369. Mineralized zones are highlighted in grey.

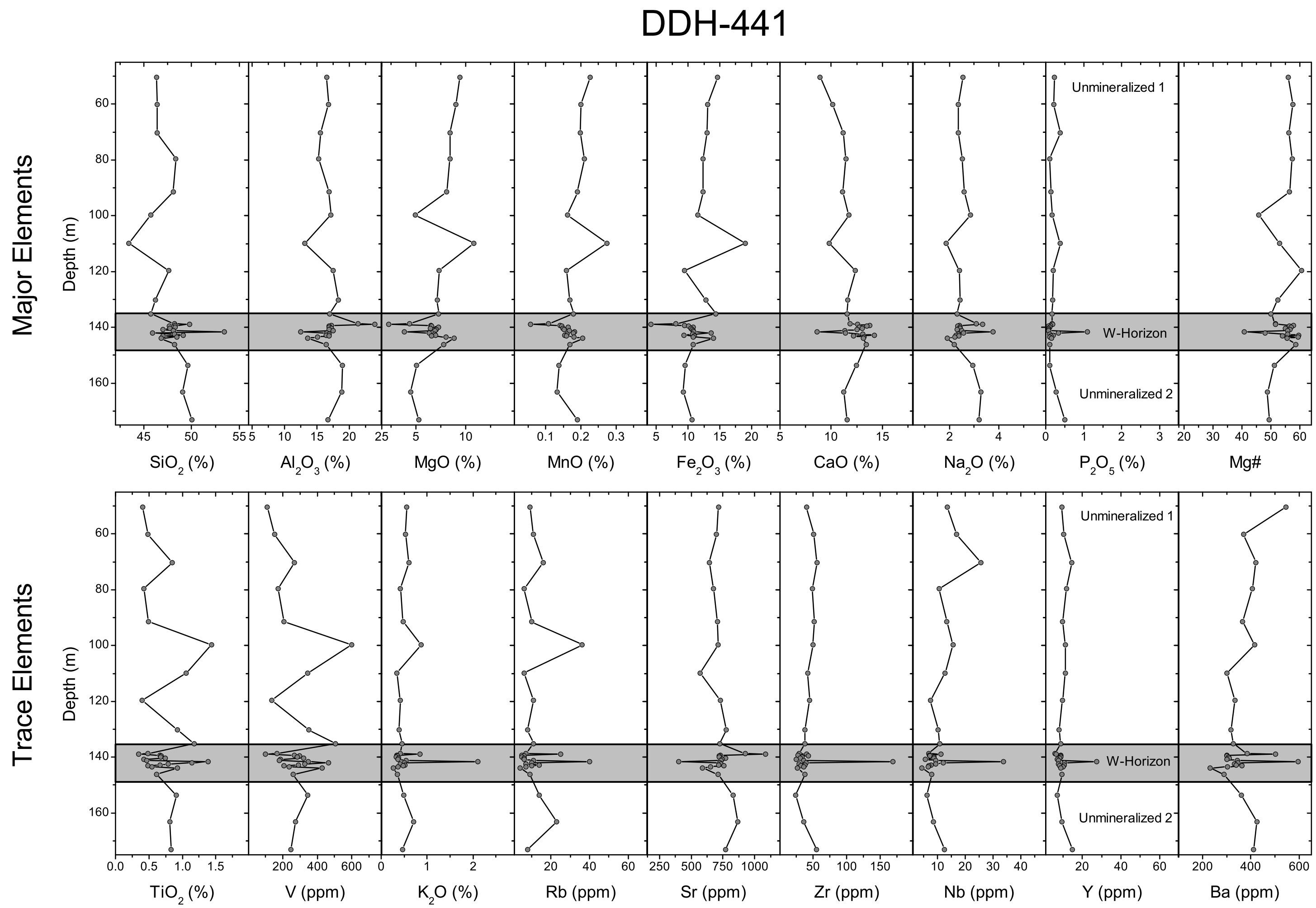

Figure 5.8: Down hole major element and trace element plots for DDH-441. Mineralized zones are highlighted in grey.

5.4 Rare Earth Elements

Analysis of the rare earth elements (REE) were conducted for all samples as described in the methodology section. The europium anomaly (Eu*) was also calculated using the method of Weill and Drake (1973). Eu* was calculated as Eu(CN)-[[Sm(CN)+Gd(CN)]/2] using chondrite normalized values from Sun and McDonough (1989)). Plagioclase preferentially incorporates Eu into its structure as a substitute for Ca resulting in a higher value of Eu relative to Sm and Gd in the normalized REE diagram. Where Eu* is positive it indicates the presence of plagioclase, where it is negative it indicates that plagioclase has been removed from the system. The partitioning of REE elements into apatite can also cause a negative value for Eu* due to the partition coefficients (crystal/liquid) of Sm, Eu and Gd which are 14.6, 9.6 and 15.8 respectively (Paster et al., 1974).

The values of La, La/Yb and Eu* are summarized by drill hole and zone as a box and whisker plot in Figure 5.9. Overall the REE results are consistent between the mineralized zones. Three samples of feldspathic pyroxenite with high amounts of apatite produce the apparent increase in La and Eu* within DDH-368 Main Zone. The values of La, La/Yb and Eu* are presented in Figure 5.10 to summarize the major trends in rare earth elements (REE). There are no consistent trends for the REE above or below mineralized zones or within mineralized zones. Increases in La and negative values of Eu* generally correlate with P_2O_5, an indicator of samples of feldspathic peridotite. The value of La/Yb remains relatively unchanged in the high P_2O_5 samples in DDH-368, DDH-368 and DDH-441, indicating a control by apatite (partition coefficients of 8.6 and 8.1 respectively Paster et al. (1974)). Within DDH-306 this ratio increases slightly with the increase in Eu*.

A chondrite normalized REE plot is shown in Figure 5.11 summarizing different zones of the study. The range of unmineralized Two Duck Lake Gabbro samples shows a typical REE pattern and shows a positive europium anomaly due to cumulate plagioclase. At low REE abundances the europium anomaly is positive and with increasing REE abundances it diminishes and then becomes negative.

The average of the Main Zone (green circles) and W-Horizon samples fall directly within the zone defined by unmineralized Two Duck Lake Samples. The unmineralized samples of the feldspathic peridotite overlay the Two Duck Lake Gabbro samples directly at a higher REE values. The mineralized Main Zone samples of feldspathic peridotite plot within the range of the unmineralized samples.

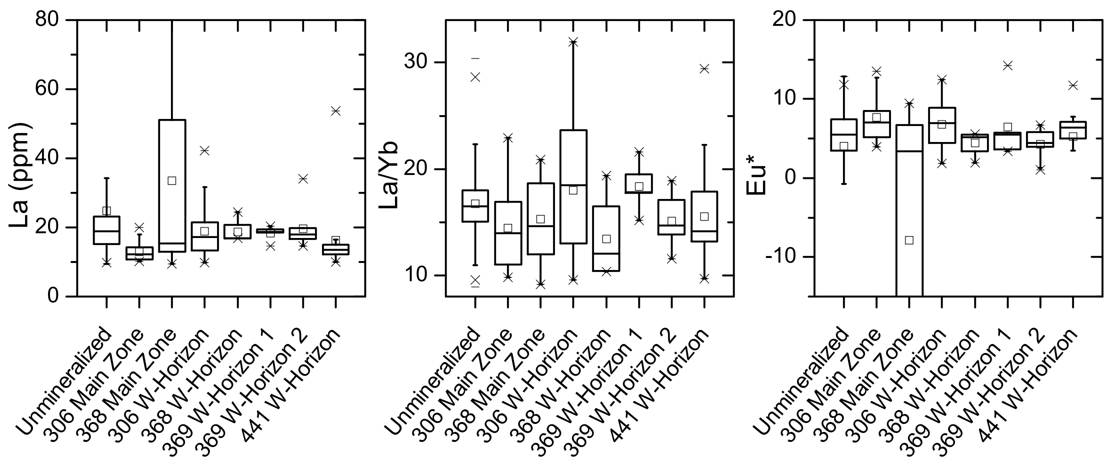

Figure 5.9: Box and whisker plot summarizing the rare earth element chemistry major element chemistry of the TDLG grouped by unmineralized, W-Horizon and Main Zone samples. The box is divided into the 25 and 75 percentile range, also shown are the mean, 1% and 99% percentile values and the minimum/maximum. The higher values of samples from DDH-368 are due to different lab analysis techniques. This figure demostrates the considerable overlap of major element chemistry within the TDLG and highlights a lack of sysematic REE changes in respect to mineralizaiton.

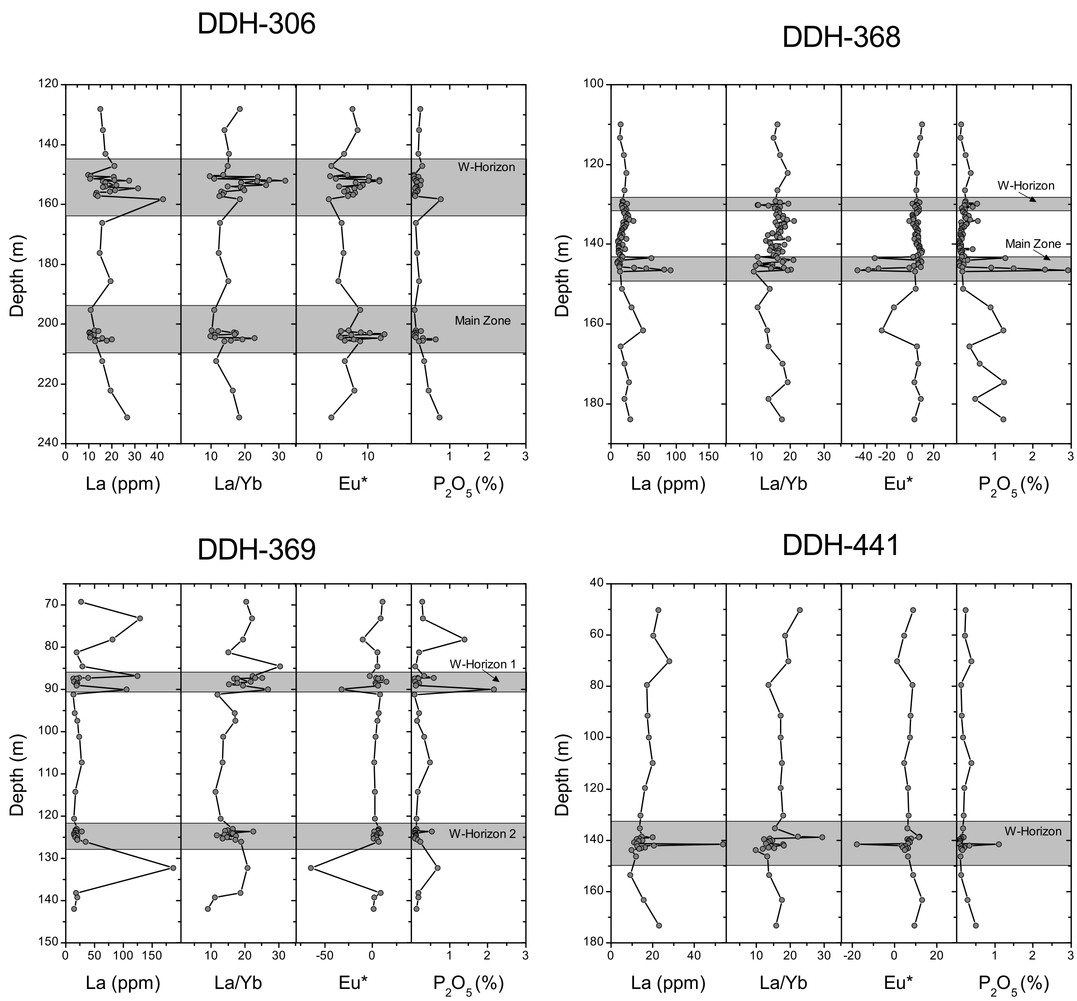

Figure 5.10: Rare earth element variation with depth for DDH-306, DDH-368, DDH-369, DDH-441.

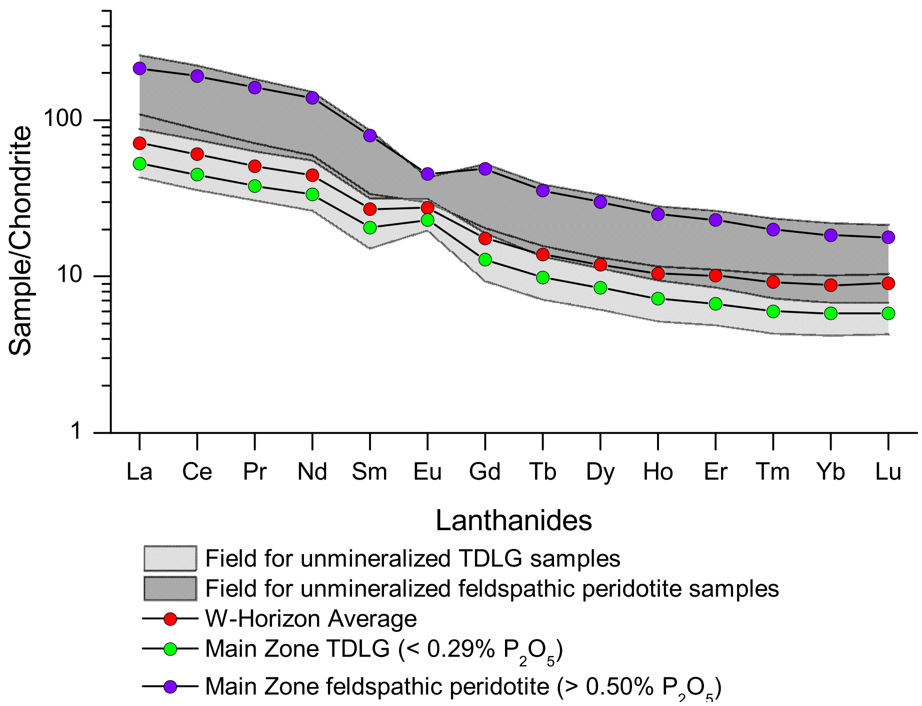

Figure 5.11: Chondrite normalized REE plot using values from (Sun and McDonough, 1989). Fields for the unmineralized samples of Two Duck Lake Gabbro and feldspathic peridotite are shown in light grey and dark grey. The average values for W-Horizon (red) and Main Zone (green) fall within the field defined by the unmineralized average. The average value of Main Zone samples within feldspathic peridotite (purple) fall within the range for unmineralized samples of feldspathic peridotite.

5.5 Metals

The variation of whole rock metal content Ni, Cu, Pt, Pd, Au and S are summarized in Table 5.2 and down hole plots are shown in Figures 5.12 and 5.13. The unmineralized samples contain low levels of Ni, Cu, Pt, Pd, Au and S. The mineralized zones are defined by increases of Cu, Pt, Pd, Au and S relative to the unmineralized samples. The mineralized horizons show consistently higher grades across the entire width of mineralization (i.e., there are no repetitive cycles or gradations within zones) although there is some variation in the total amount of metals in each sample.

In unmineralized samples the average amount of Ni is 110 ppm, and is a reflection of Ni in the olivine present within the gabbro. Within the mineralized zones, Ni is slightly elevated (average 200-250 ppm, locally up to 500 ppm) with the highest values occurring in samples that contain visible pentlandite (DDH-306 Main Zone and W-Horizon, DDH-441 W-Horizon). Analyses of Cu in DDH-306 had a detection limit of 1.4 ppm and DDH-306, DDH-369 and DDH-441 had a detection limit of 0.01 ppm. Copper in the unmineralized samples average 0.015 wt%, in the low S W-Horizon samples (DDH-368 and DDH-369) it ranges from 0.04-0.08 wt% and is around 0.30 wt% in both DDH-306 and DDH-441 (high S W-Horizon and high S low grade W-Horizon). The average amount of Cu in Main Zone samples from this study is 0.38 wt% and 0.15 wt% in DDH-306 and DDH-368 respectively, which is significantly lower than the average Main Zone value of 0.83 wt% reported in Good (1992).

The Main Zone samples of DDH-306 and DDH-368 average approximately 0.25 ppm Pt and 0.80 ppm Pd, which is again lower than the average Main Zone values of 0.55 ppm Pt and 1.72 ppm Pd reported in Good (1992). The W-Horizon in DDH-306 has the highest Pt and Pd grades, averaging 8.5 ppm Pt and 9.8 ppm Pd, with samples up to 29 ppm Pt and 23 ppm Pd. Drill holes DDH-368 and DDH-369 have similar W-Horizon Pt and Pd grades, in the range of 2-4 ppm Pt and 3-7 ppm Pd and can locally exceed 11 ppm Pt and 24 ppm Pd. The lowest Pt and Pd grades from W-Horizon samples came from DDH-441, where averages of 0.22 ppm Pt and 0.83 ppm Pd and local maximums of 1.0 ppm Pt and 3.2 ppm Pd occur.

Table 5.2: Average Metal Content Summary

	Num. Samples	Average Ni (ppm)	2σ Ni (ppm)	Average Cu (wt%)	2σ Cu (wt%)	Average Pt (ppm)	2σ Pt (ppm)	Average Pd (ppm)	2σ Pd (ppm)	Average Au (ppm)	2σ Au (ppm)	Average S (wt%)	2σ S (wt%)
Unmineralized													
M-07-306	9	121	125	0.01	0.03	0.01	0.03	0.04	0.05	0.01	0.03	0.04	0.05
M-07-368	55	127	51.8	0.01	0.03	0.09	0.26	0.12	0.44	0.04	0.23	0.03	0.06
M-07-369	25	69.3	85.5	0.02	0.03	0.08	0.28	0.24	0.89	0.01	0.02	0.05	0.04
M-08-441	11	100	118	0.01	0.02	0.02	0.04	0.05	0.23	0.00	0.01	0.03	0.03
Main Zone													
Good 1992	14	260	260	0.83	1.0	0.55	0.70	1.72	2.8	0.12	0.18	1.70	1.9
M-07-306	13	255	227	0.38	0.37	0.29	0.42	1.10	1.7	0.09	0.12	0.49	0.64
M-07-368	15	159	100	0.14	0.20	0.22	0.39	0.67	1.2	0.10	0.16	0.20	0.30
W-Horizon													
M-07-306	19	200	155	0.33	0.57	10.78	20.62	19.38	22.73	1.56	3.87	0.24	0.42
M-07-368	5	172	38.0	0.08	0.07	4.90	8.35	4.07	2.25	0.20	0.33	0.08	0.07
M-07-369 1	5	128	73.4	0.04	0.07	3.11	5.11	7.65	8.86	0.17	0.35	0.05	0.06
M-07-369 2	9	88	66.4	0.07	0.13	2.92	6.46	8.50	16.72	0.29	0.64	0.09	0.13
M-08-441	18	222	259	0.30	0.54	0.23	0.41	0.86	1.51	0.09	0.18	0.32	0.53

[1] 2σ is the 2σ standard deviation of the sample population

Figure 5.14 shows the relationship between mineralization, Mg# and geochemical indicators of the feldspathic pyroxenite. Plots A and B show Mg# vs. Cu and Pt + Pd. In the Cu plot there is overlap between both mineralization zones and no clear relationship between Cu and Mg#. The plot of Mg# vs. Pt + Pd also shows no unique trend for either zone, with the W-Horizon samples clustering at the higher end of the Mg# range. These plots show no correlation between evolved samples (using Mg# as a proxy for evolution) and base or precious metals.

Figure 5.14 C and D show Eu* vs. Cu and Pt + Pd, with negative values of Eu* indicating samples of feldspathic pyroxenite. Samples with negative Eu* values only contain low Cu values and have negligible values of Pt + Pd. Figure 5.14 E and F compare P_2O_5 with Cu and Pt + Pd, with high P_2O_5 values shown to correlate with samples of feldspathic pyroxenite. Samples with high P_2O_5 values correlate with low values of Cu, Pt and Pd. These two sets of graphs show that the feldspathic pyroxenite samples, which contained the highest amount of secondary hydrous minerals, do not correlate with mineralization and contain insignificant amounts of PGE.

Plots of Cu vs. Pd and Pt are shown in Figure 5.15. There are two distinct groupings of the ratios: Main Zone and DDH-441 W-Horizon (Main Zone group) and the W-Horizon samples from DDH-306, DDH-368 and DDH-369 (W-Horizon group). The Main Zone group has high Cu/Pd and Cu/Pt values, generally $>$ 1000:1 whereas the W-Horizon group has low Cu/Pd and Cu/Pt ratios, and are $<$ 500:1 overall. The ratio of Pd/Pt is shown in Figure 5.16. All of the samples have Pd/Pt ratios $>$ 1:1 and in the high grade W-Horizon samples Pd/Pt ratios $>$ 3:1 are common. Figure 5.17 is a plot of Cu/Pd vs. Pd/Au. This figure again shows the grouping of the Main Zone group samples, which cluster at high Cu/Pd and low Pd/Au values. The W-Horizon group clusters at low Cu/Pd and high Pd/Au. It is also shown that there is a trend between the two styles of mineralization, with low grade W-Horizon (DDH-441) mineralization bridging the gap between the Main Zone and higher grade W-Horizon.

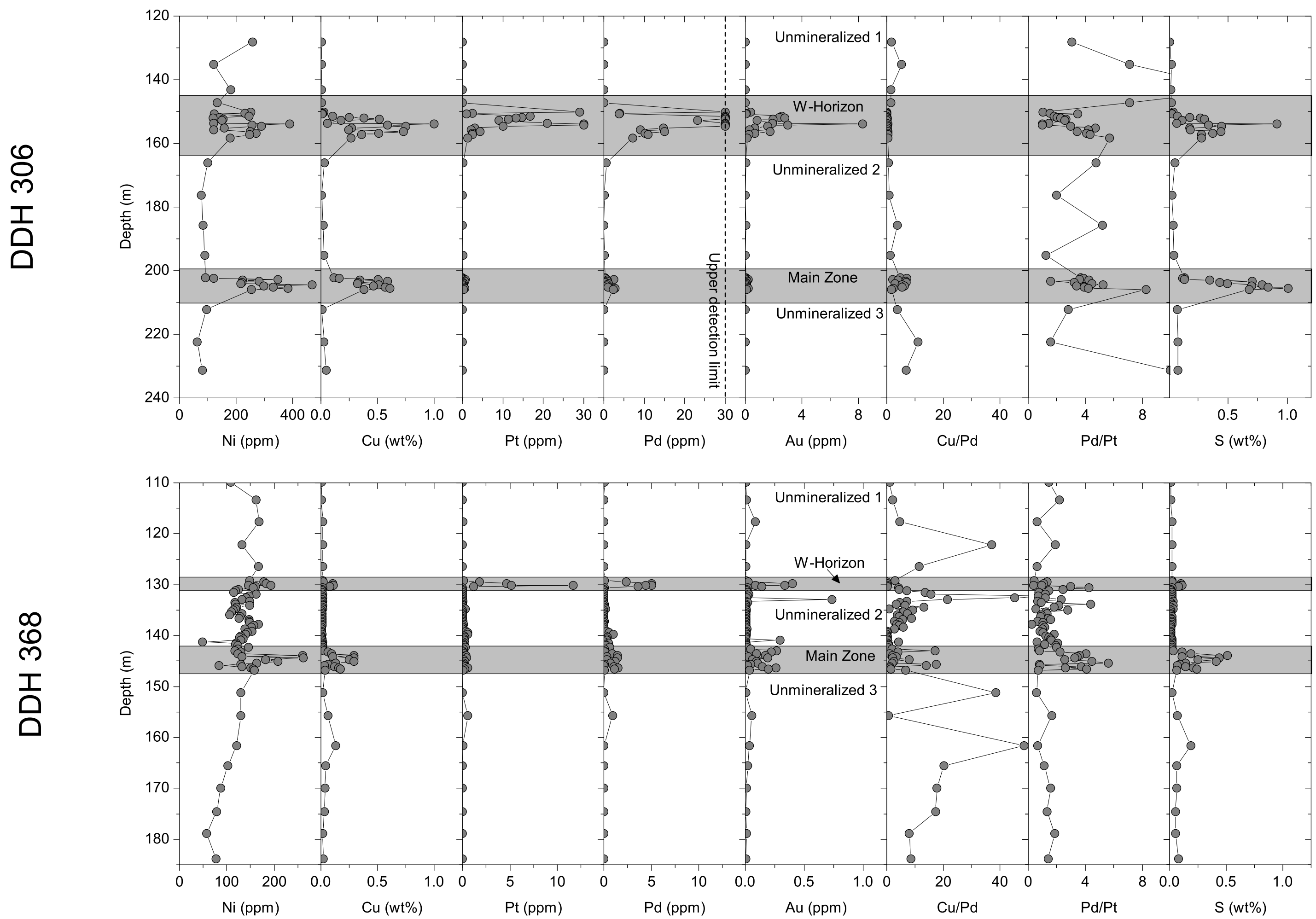

Figure 5.12: Metals, S, and Se vs. depth for DDH-306 and DDH-368. Dashed lines delineate mineralized zones.

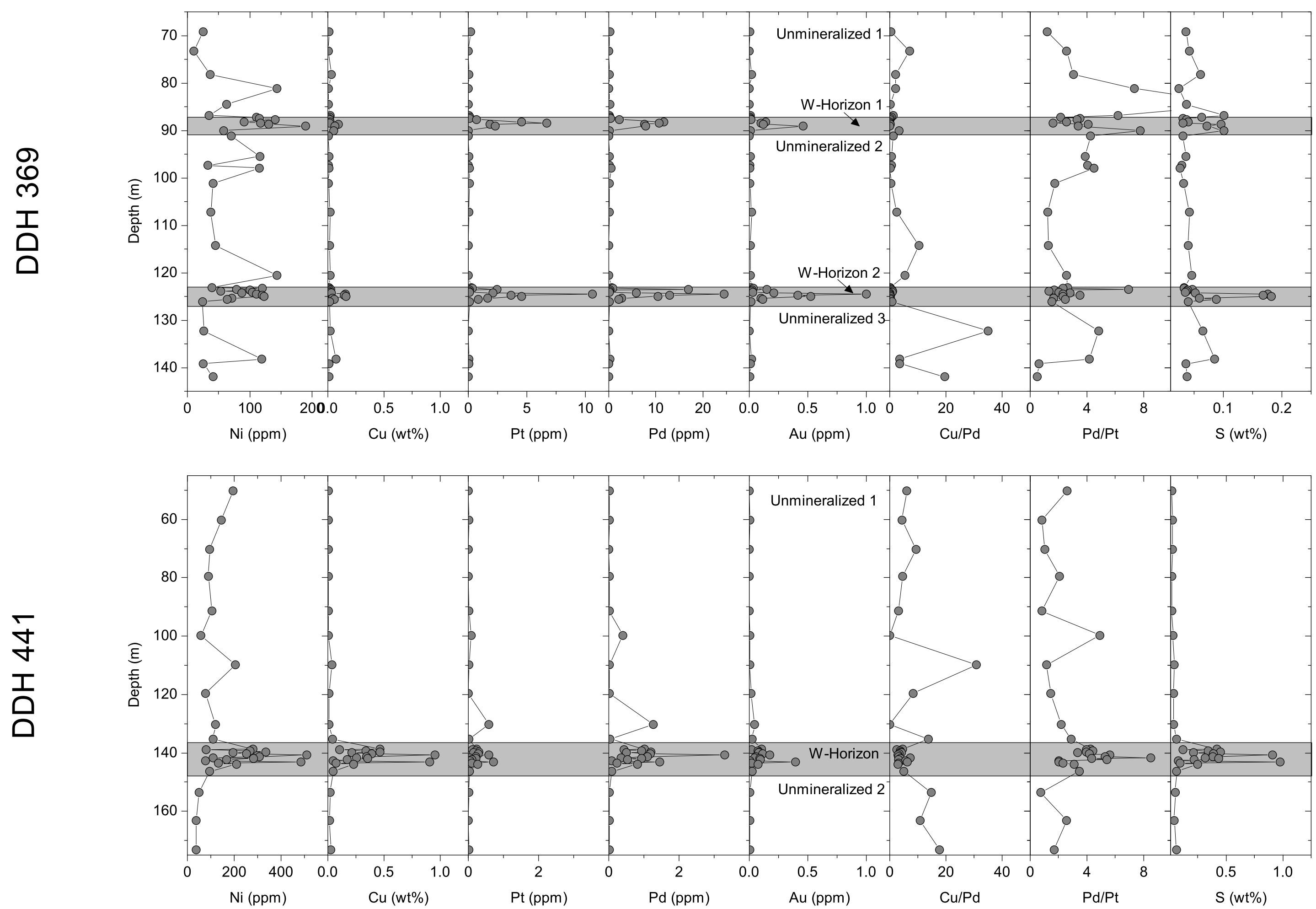

Figure 5.13: Metals, S, and Se vs. depth for DDH-369 and DDH-441. Dashed lines delineate mineralized zones.

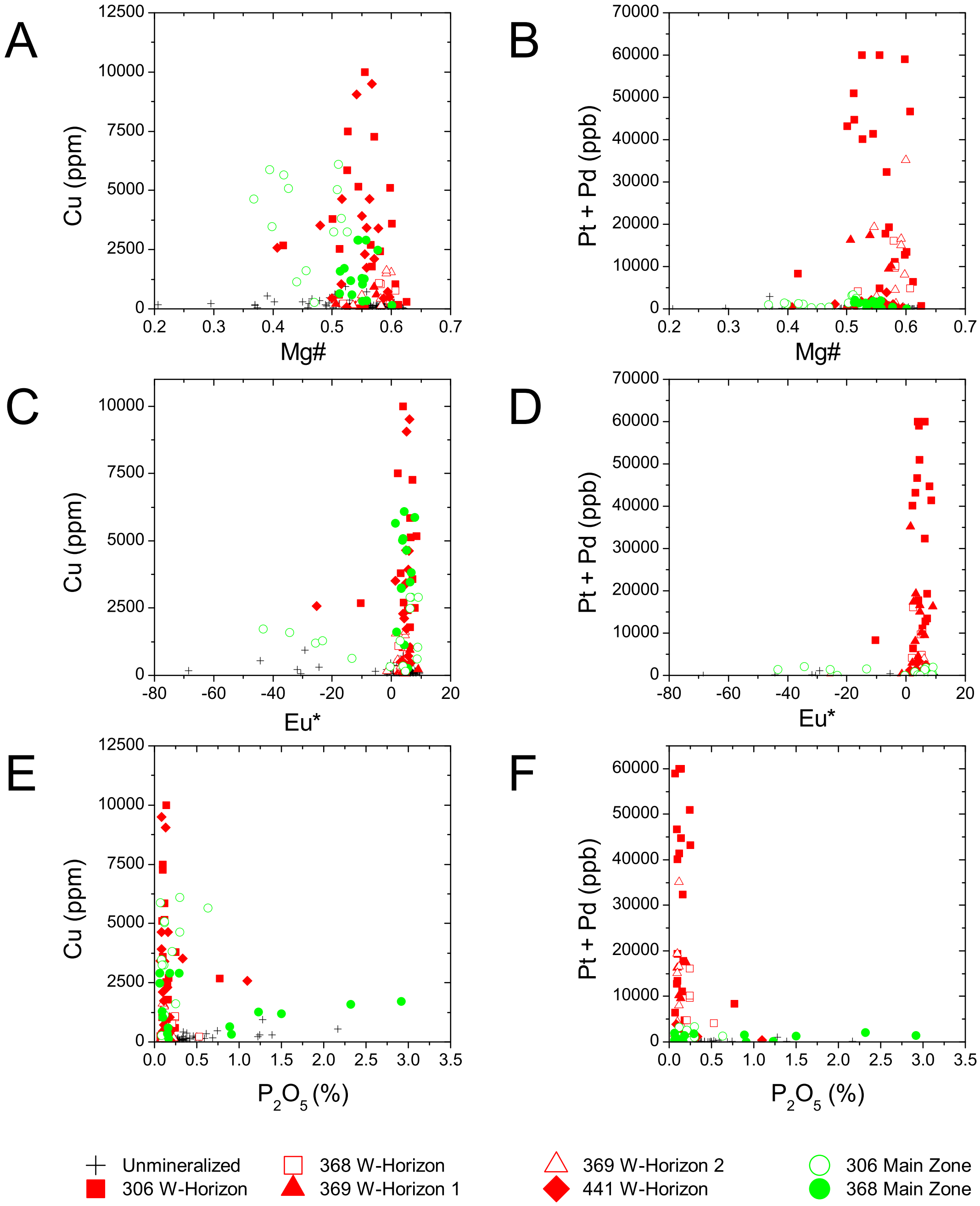

Figure 5.14: Base and precious metals vs. Mg#, Eu* and P_2O_5 (**A**) Plot of Cu. Vs. Mg#, using Mg# as an indicator for primitive magma. (**B**) Plot of Pt+Pd vs. Mg# showing overlap between the W-Horizon and Main Zone Samples. (**C**) Plot of Cu vs. Eu*. Positive values of Eu* correlate with typical Two Duck Lake Gabbro samples and negative values correlate with samples of apatitic feldspathic clinopyroxenite. (**D**) Plot of Pt+Pd vs. Eu*, showing overlap between the W-Horizon and the Main Zone samples. (**E**) Plot of Cu vs. P_2O_5. High values of P_2O_5 correlate with samples of feldspathic pyroxenite. (**F**) Plot of Pt+Pd vs. P_2O_5. High values of P_2O_5 correlate with Pt and Pd barren samples.

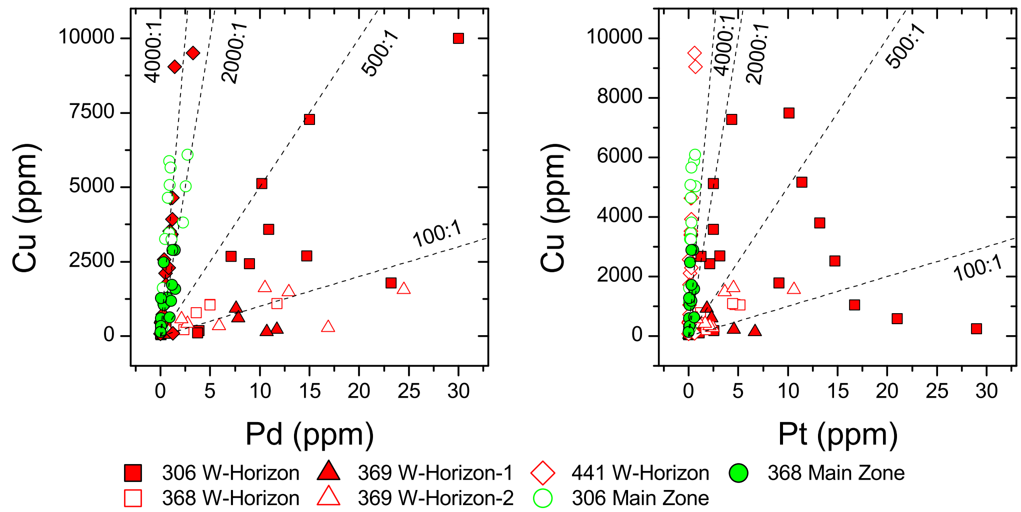

Figure 5.15: Cu vs. Pt and Pd plots. Dashed lines indicate Cu/Pd ratios. (**A**) Cu vs. Pd. Two distinct groups are shown with Main Zone and DDH-441 W-Horizon samples occurring at low Cu/Pd and the remaining W-Horizon samples occurring at higher Cu/Pd values. (**B**) Cu vs. Pt. Two distinct groups are shown with Main Zone and DDH-441 W-Horizon samples occurring at low Cu/Pt and the remaining W-Horizon samples occurring at higher Cu/Pd values.

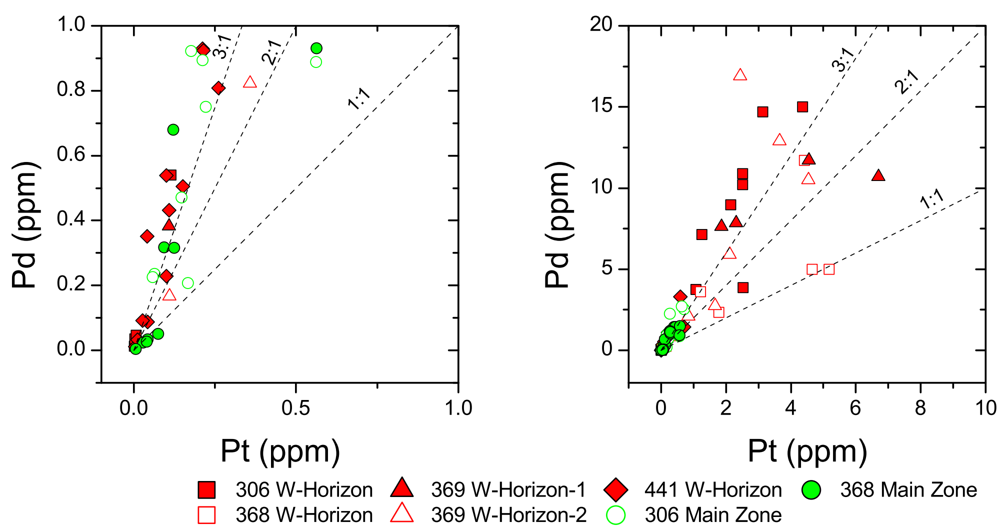

Figure 5.16: Pd vs. Pt plots, the left figure shows the low range and the right showing the high range of values, dashed lines to indicate Pd/Pt ratios. There is considerable overlap of the Pd/Pt values between the two mineralized zones and no distinct trend characteristic to either the Main Zone or is shown.

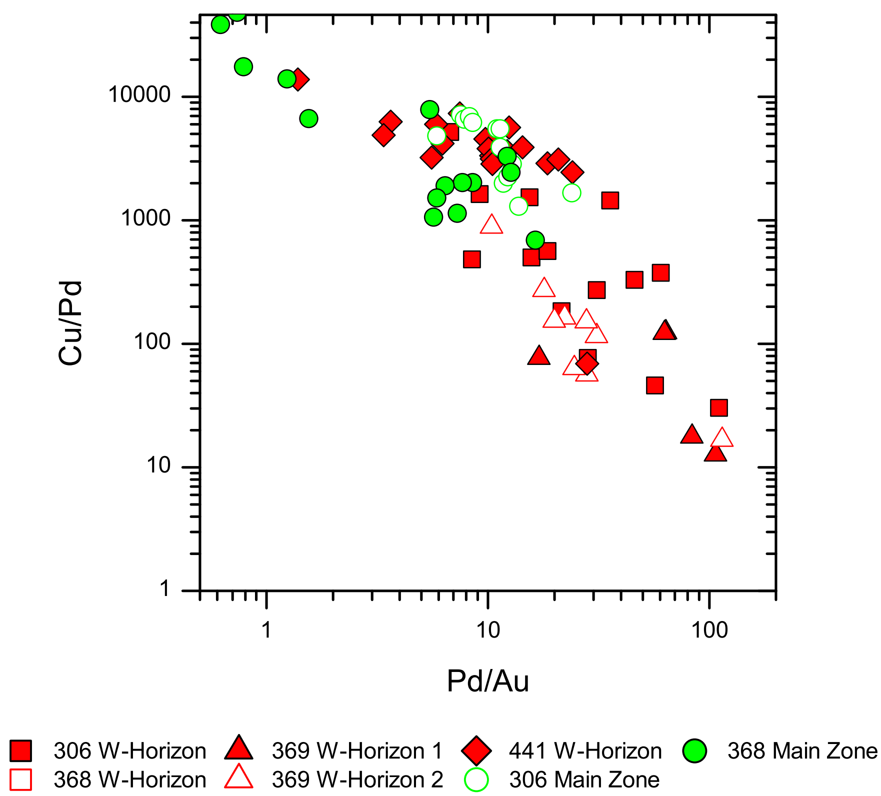

Figure 5.17: Cu/Pd vs. Pd/Au plot. Two distinct groupings are seen with Main Zone and DDH-441 W-Horizon mineralization at high Cu/Pd and low Pd/Au and high grade W-Horizon at low Cu/Pd and high Pd/Au values. There is a continuum between the two zones of mineralization indicating that the same initial process formed the zones and the W-Horizon samples were upgrading by another process.

5.6 Sulphur and Selenium

5.6.1 Introduction

Selenium and sulphur are highly siderophile elements. They are volatile and behave similar to other siderophile elements (such as Pt, Pd and Cu) in a magmatic system (Yi et al., 2000). Selenium is a trace element with an average crustal abundance of 0.050 ppm. The low abundance is attributed to removal from the upper mantle and crust during core segregation (Taylor and McLennan, 1985). Average S/Se values have been determined for various reservoirs and are shown in Table 5.3.

Within ore bodies it has been shown that essentially all of the Se is contained within sulphides (Hawley and Nichol (1959), Bethke and Barton (1971) and Cox et al. (2007). It is by this relation of Se and S that magmatic sulphide ore deposits have increased levels of Se relative to the primitive mantle. High concentrations of Se have also been reported in high temperature volcanic magmatic or hydrothermal ore deposits Bethke and Barton (1971). High S/Se values in Ni-sulphide ores have been used as evidence of the contribution of S from country rocks (Ripley et al. 2002 and Theriault and Barnes 1999). Where S/Se is subchondritic, it has been interpreted as evidence that the rocks have experienced S loss (Barnes et al., 2009).

Table 5.3: Average S/Se Values

Reservoir	S/Se	Reference
Primitive undifferentiated mantle	3333	(McDonough, 1995)
Chondrites	2500	(Dreibus et al., 1995)
Peridotites	3000	(Lorand and Alard, 2010)
MORB Basalts	4900-7300	(Auclair et al., 1987)

During crystallization of a silicate melt S and Se behave incompatibly along with lithophile elements such as La and Sm. Since they are both incompatible, the S/Se ratio in the liquid will remain constant with fractionation. If the silicate melt reaches S saturation and a sulphide liquid forms the siderophile elements (i.e., Se and Cu) will partition into the sulphide liquid whereas incompatible lithophile elements will remain in the silicate melt. Due to the high partition coefficients of S and Se into a sulphide liquid, S/Se will not change (Barnes et al., 2009). If the sulphide liquid segregates from the silicate melt it will change Se/La from that of the parental magma.

Since S and Se behave similarly in a silicate or sulphide liquid, specific conditions are required to change S/Se. Assimilation of an external S source (i.e., S-bearing country rock) that has a different S/Se than the parental magma can change the ratio. The degree of change will depend on the ratio of magma to assimilated S source and the S/Se in the magma compared to the new source. The loss of S has also been shown by several authors to lower S/Se . Dreibus et al. (1995) studied weathered meteorites and was able to show that the S/Se ratio decreased in strongly weathered rocks. Auclair et al. (1987) examined the distribution of S and Se in hydrothermal sulphide deposits and showed that S/Se ratios were lower in rocks which experience S loss. The affinity for O decreases from S to Se, and SO_2 and SO_3 are gasses that will volatilize or transport easily whereas SeO_2 is a solid that is relatively immobile.

5.6.2 Sulphur and Selenium Results

Figure 5.18 shows that there is a positive correlation between S and Se. The general trends show that S/Se is lower in the W-Horizon samples ($\sim$ 600-1000) than it is in the Main Zone Samples ($\sim$ 1000-1700) (Table 5.4), although there is some overlap between the two zones. In the low grade W-Horizon (DDH-441) S/Se is closer to the Main Zone samples and S/Se for DDH-368 Main Zone is closer to the W-Horizon values.

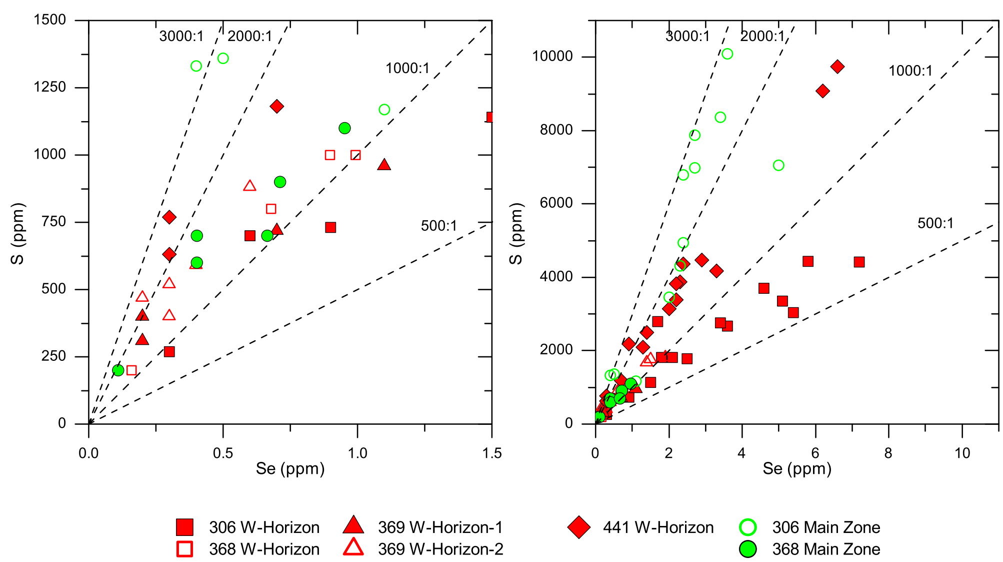

Figure 5.18: Plot of S vs. Se for all samples

5.6.3 Siderophile Elements trends and S, Se and S/Se

This section examines the trends of the siderophile elements and S, Se and S/Se. Each subsection shows plots of each of the siderophile elements. For each parameter the covariance was also calculated, the results are in Table 5.5. The covariance was calculated using the commercial software Origin.

Covariance is s measure used to show the correlation between two random variables. Covariance ranges between between -1 and +1. A value close to +1 means that the two parameters are positively correlated and a value close to -1 indicates a negative correlation.

Table 5.4: Element Ratios by Zone

	Zone							
	Unmin	306 W	368 W	369 W1	369 W2	441 W	306 M	368 M
S/Se (avg)	1130 ± 82	630 ± 36	1018 ± 76	680 ± 63	926 ± 70	1381 ± 45	1737 ± 385	977 ± 152
Cu/S (avg)	0.44 ± .03	1.67 ± .09	1.02 ± .05	1.28 ± .06	1.00 ± .02	1.01 ± .03	0.48 ± 0.1	0.86 ± .09
Cu/Se (avg)	438.1 ± 64.2	1060 ± 57.75	1047 ± 56.64	845.6 ± 48.76	929.6 ± 74.39	1406 ± 40.26	866.6 ± 275.9	1053 ± 126.8

Table 5.5: Covariance for S, Se, S/Se vs. Ni, Cu, Pt, Pd, Au Plots

	306 W	368 W	369 W-1	369 W-2	441 W	306 Main	368 Main
Ni vs. S	0.39	-0.29	0.042	0.27	0.86	0.53	0.78
Cu vs. S	0.92	0.99	0.99	0.99	0.98	0.63	0.91
Pt vs. S	-0.052	0.82	-0.18	0.53	0.51	0.033	0.47
Pd vs. S	0.61	0.21	-0.32	0.32	0.62	0.12	0.16
Au vs. S	0.20	0.13	-0.064	0.68	0.75	0.12	0.30
Ni vs. Se	0.51	-0.36	-0.13	0.58	0.86	0.13	-0.24
Cu vs. Se	0.91	0.99	0.99	0.96	0.99	0.45	0.93
Pt vs. Se	-0.076	0.93	0.66	0.38	0.88	0.011	-0.0030
Pd vs. Se	0.50	0.30	0.78	0.13	0.68	-0.089	-0.13
Au vs. Se	0.094	0.84	-0.42	0.56	0.71	-0.067	0.17
Ni vs. S/Se	0.02	-0.25	0.31	-0.036	0.27	0.22	-0.11
Cu vs. S/Se	0.15	0.62	0.65	0.39	0.33	0.02	0.63
Pt vs. S/Se	-0.044	0.72	0.27	-0.017	0.23	0.03	0.41
Pd vs. S/Se	0.15	0.41	0.95	-0.17	0.21	0.31	0.29
Au vs. S/Se	0.18	0.89	-0.26	0.11	0.09	0.22	0.64

5.6.3.1 The Highly Siderophile Elements (Au, Pt, Pd, Cu, Ni) and S

Plots comparing S vs. metal content are shown in Figure 5.19. Nickel correlates with S at S $\geq$ 2000 ppm, below this amount of sulphur the abundance of Ni is dominantly controlled by olivine rather than sulphide minerals. The highest Ni values were in the W-Horizon samples from DDH-306 and DDH-441 and the Main Zone samples from DDH-306 and DDH-368. Copper shows a strong positive correlation with S for all sample suites. The Cu/S value is variable depending on the mineralization style (Table 5.4). The average Cu/S is 0.44 $\pm$ 0.3 in unmineralized samples, the W-Horizon samples average $\sim$ 1, with the highest value in DDH-306 (167 $\pm$ 0.09), which corresponds to the highest amount of bornite in any of the samples. Barnes (2004) interpreted that Cu/S values close to 1 and low S/Se ratios represent samples that have undergone sulphur loss (Fig. 5.21). In the samples from DDH-306 Main Zone and DDH-368 Main Zone the Cu/S ratio is lower (0.50-0.80), which is explained by the presence of pyrrhotite. The precious metals show two distinct trends. Although the Main Zone and W-Horizon can have similar total Cu, the ratio of Cu/S is lower in the Main Zone.

The precious metals show two distinct trends for the W-Horizon and Main Zone samples. The Main Zone samples and DDH-441 W-Horizon have low Pt/S and Pd/S ratios and correlate directly with the amount of S. The W-Horizon samples from DDH-306, DDH-368 and DDH-369 have much higher Pt/S and Pd/S ratios and have been decoupled from S. These samples show a wide spread of Pt and Pd values over 100-4000 ppm S.

5.6.3.2 The Highly Siderophile Elements (Au, Pt, Pd, Cu, Ni) and Se

The general trends from S vs. Metals plots are mirrored in plots of Se vs. Metals (Fig. 5.20). Ni correlates positively with Se above 1 ppm Se, although there is a wide spread in the data. Again 306 and 441 W-Horizon and 306 Main Zone correlate the most with Ni. Copper shows a strong correlation between Se for all mineralized zones. Compared to S, Se vs. Cu does not show as much variation between the different mineralized zones, (Table 5.4) and Main Zone samples have lower Cu/Se than W-Horizon samples. The W-Horizon in 441 has the highest Cu/Se value, and 306 Main Zone has the lowest, the remainder of the mineralized zones Cu/Se is around 1000.

Plots of Pt and Pd vs. Se show that the two mineralized zones occur in distinct regions. The W-Horizon samples generally have higher precious metal/Se than the Main Zone samples. The samples from 441 W-Horizon tend to group with the Main Zone samples. W-Horizon samples from DDH-368, DDH-369 (1) and DDH-441 have higher correlation coefficients for Pt and Pd vs. Se compared to S.

5.6.3.3 The Highly Siderophile Elements (Au, Pt, Pd, Cu, Ni) and S/Se

Plots of the highly siderophile elements (Au, Pt, Pd, Cu and Ni) vs. S/Se are shown in Figure 5.21. For Ni there is no distinct trend with variations in S/Se. Copper shows a general increase with decreasing S/Se. Increasing amounts of Pt and Pd with decreasing S/Se are also observed in the W-Horizon samples. There is no discernible trend for Pt and Pd with S/Se within the Main Zone or W-Horizon samples from DDH 441. Again in all of the plots there are distinct differences in the trends between W-Horizon and Main Zone for precious metals vs. S/Se.

5.6.3.4 The Highly Siderophile Elements (Au, Pt, Pd, Cu, Ni) and Cu/S

Plots of the highly siderophile elements (Au, Pt, Pd, Cu and Ni) vs. Cu/S are shown in Figure 5.22. These plots were chosen to examine the relationship between the W-Horizon mineralization and the sulphide mineral assemblage. As described in the petrography section, the sulphide mineral assemblage changes from chalcopyrite and pyrrhotite dominant in the Main Zone to chalcopyrite and bornite in the W-Horizon. The ratio Cu/S is used as a proxy to increasing amounts of bornite in the sulphide mineral assemblage (the ratio of Cu/S in bornite is almost twice that of chalcopyrite). Main Zone and W-Horizon values of Cu/S overlap in the range of 0-0.9, whereas only W-horizon samples have values above 0.9. There are no trends for Ni vs. Cu/S. At very low values of Cu/S (< 0.5) Cu has a positive linear correlation with Cu/S. At values > 0.5 Cu/S there are no trends between Cu and Cu/S. The three highest Cu samples come from the mid-range of Cu/S (around 1.0 Cu/S) and are in W-Horizon samples. Both Pt and Pd show similar trends against Cu/S. Looking at all of the W-Horizon samples together there is not a single distinct trend relating high Pt and Pd values to high Cu/S values. Trends are apparent when looking at a single W-Horizon at a time. Within each individual W-Horizon there are clear trends showing increasing Pt and Pd with increasing Cu/S. The plots for Au again show overlap between the Main Zone and W-Horizon, with the exception of DDH-306 which has the highest Au values occurring at the upper range of Cu/S values.

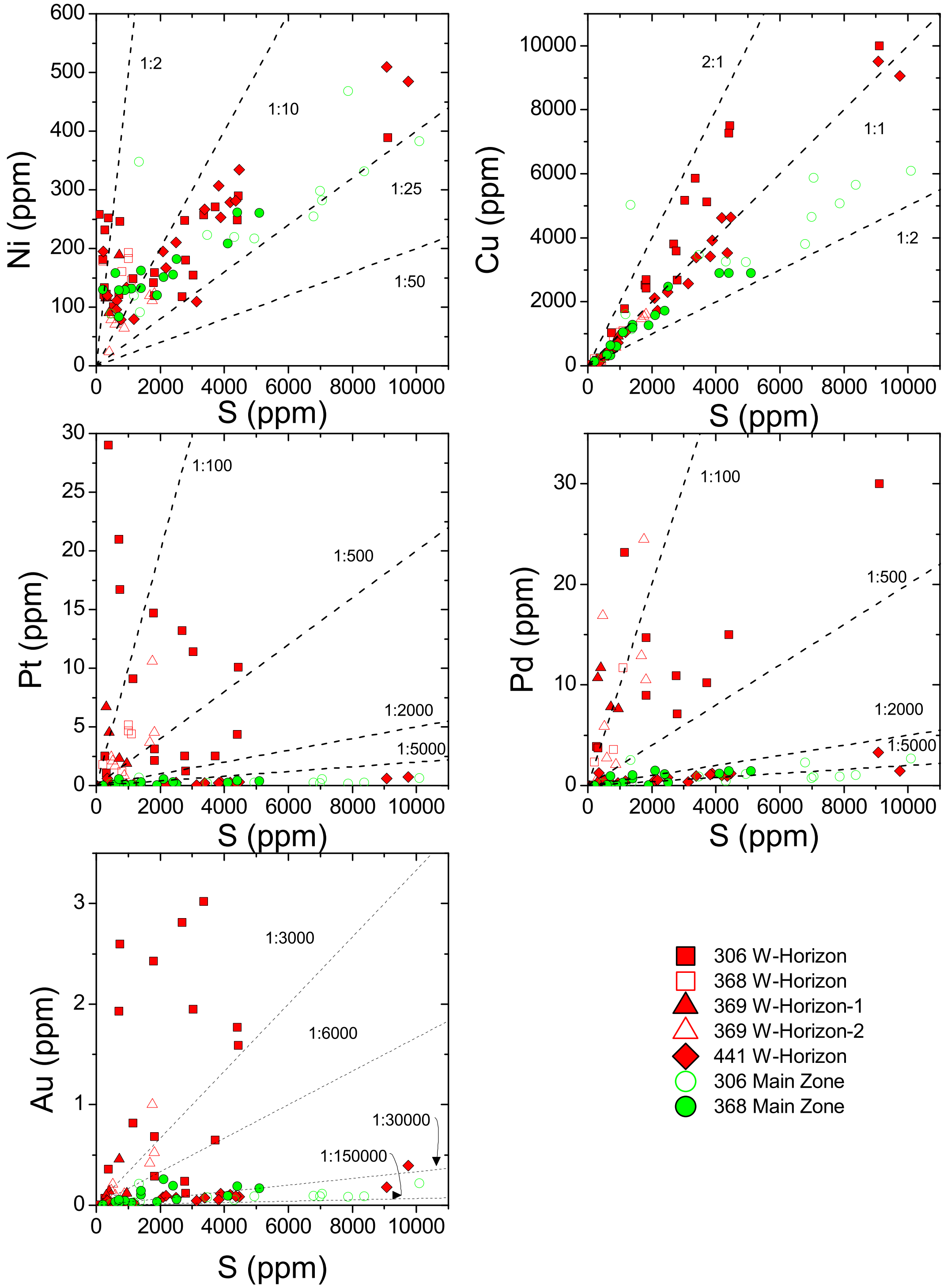

Figure 5.19: Plots of S vs. Ni, Cu, Pt, Pd and Au

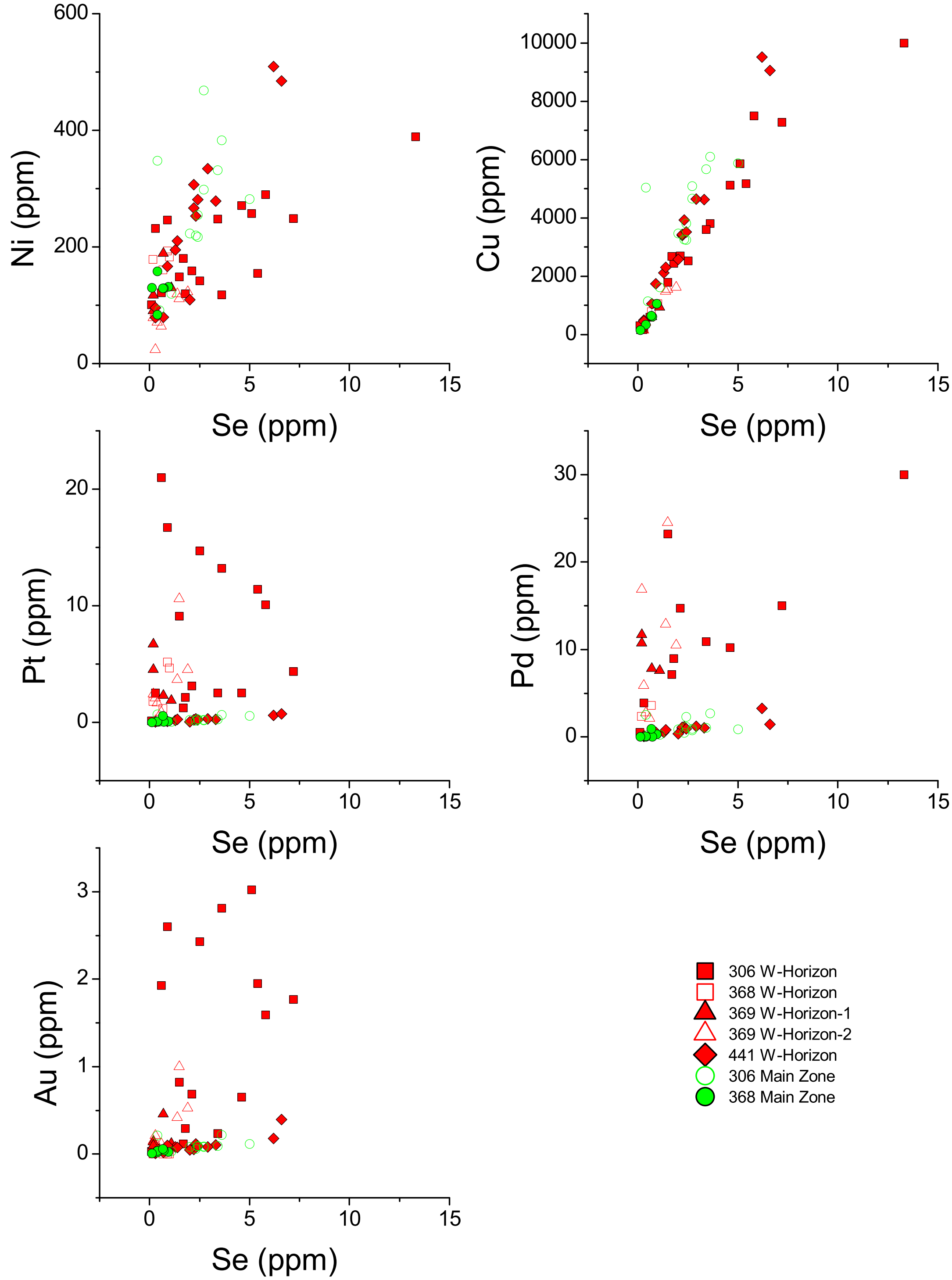

Figure 5.20: Plots of Se vs. Ni, Cu, Pt, Pd and Au

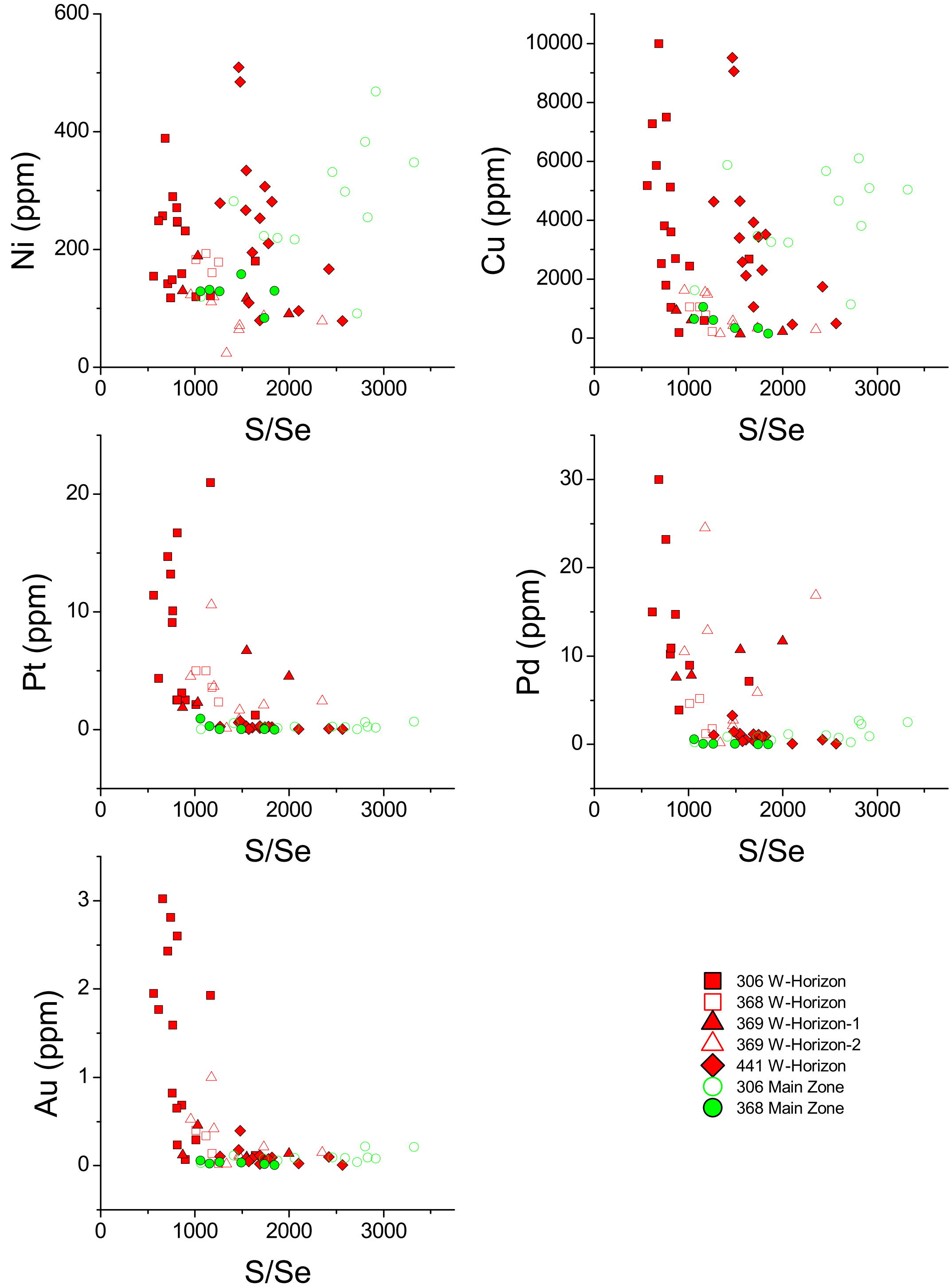

Figure 5.21: Plots of Se/Se vs. Ni, Cu, Pt, Pd and Au

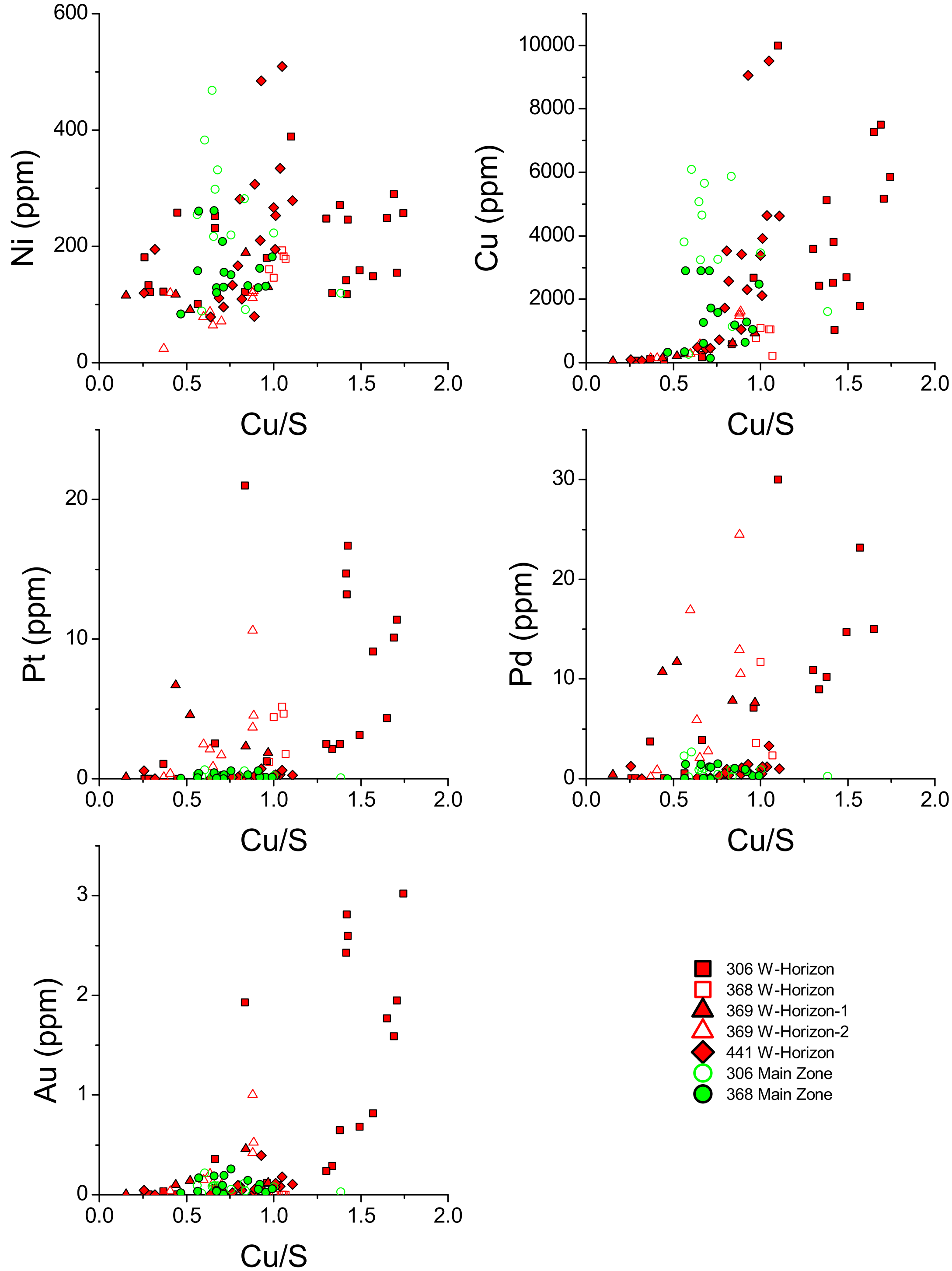

Figure 5.22: Plots of Cu/S vs. Ni, Cu, Pt, Pd and Au

Chapter 6

Mineral Chemistry

Mineral element chemistry was analyzed to examine for fractionation trends, cryptic layering and magma recharge events. Interpretation of whole rock geochemistry for these signatures is masked by the heterogeneous modal mineral abundances in the TDLG at the scale used for sampling. Analyses of major element mineral chemistry of olivine was conducted by electron microprobe. At constant magma compositions and P-T conditions mineral compositions such as Mg# are constant. The analysis of trace elements by LA-ICP-MS will allow for the examination of elements which are affected by fractionation e.g., Ni in olivine will decrease with fractionation.

6.1 Microprobe Analysis

6.1.1 Methodology

Grains of olivine, plagioclase, pyroxene and magnetite from polished thin sections of Two Duck Lake Gabbro were analyzed by electron microprobe. The analyses were conducted using a Cameca SX50 at the University of Toronto and a Cameca SX100 at the University of Michigan. The analyses were conducted in order to determine mineral compositional variations within the study drill holes and between mineralized units. Complete data sets are in Appendix V.

6.1.1.1 Olivine

Olivine grains from polished thin sections of DDH-306, DDH-368, DDH-369 and DDH-441 were analyzed by electron microprobe and olivine stoichiometry was calculated on the basis of four oxygens. Typically three grains per polished thin sections were analyzed. Initially both the core and rims of grains were analyzed, and after confirming compositional homogeneity of individual grains only cores were analyzed in subsequent analyses. The analyses of DDH-368 were conducted on a Cameca SX-50 at the University of Toronto and the analyses of DDH-306, DDH-369 and DDH-441 were conducted on a Cameca SX-100 at the University of Michigan. Machine operation conditions were the same at both facilities. Compositional analyses were acquired on an electron microprobe equipped with 3 tunable wavelength dispersive spectrometers. Olivine grains were analyzed for Si, Mg, Fe, Mn, Ca and Ni. Operating conditions were 40 degrees takeoff angle, and a beam energy of 15 keV. The beam current was 30 nA, and the beam diameter was 1 microns. Counting times were: 20 seconds for Si, Mg, Fe, 30 seconds for Mn, and 40 seconds for Ni, Ca. The off peak counting times were 20 seconds for Si, Mg, Fe, 30 seconds for Mn, and 40 seconds for Ni and Ca. Average detection limits were below 200 ppm for Mg, Si and Ca and below 380 ppm for Mn, Fe and Ni.

6.1.1.2 Plagioclase

Plagioclase grains from polished thin sections of DDH-306, DDH-368 and DDH-441 were analyzed by electron microprobe and plagioclase stoichiometry was calculated on the basis of 32 oxygens. Typically three grains per polished thin section were analyzed and the compositions of cores and rims were determined for each grain. The analyses were conducted on a Cameca SX-50 at the University of Toronto. Compositional analyses were acquired on an electron microprobe equipped with 3 tunable wavelength dispersive spectrometers. Plagioclase grains were analyzed for Na, Al, Fe, Ca, Si, K and Cu. Operating conditions were 40 degrees takeoff angle, and a beam energy of 15 keV. The beam current was 15 nA, and the beam diameter was 1 micron. Counting times were: 10 seconds for Cu, 20 seconds for Si, K, Ca, Na, 40 seconds for Sr, La, Al, and 60 seconds for Fe. The off peak counting times were: 8 seconds for Na, 10 seconds for Cu, 20 seconds for K, Ca, Si, 40 seconds for Sr la, Al, and 60 seconds for Fe. Average detection limits are less than 150 ppm for Si and Al, less than 300 ppm for Fe, K and Ca, and less than 350 ppm for Na.

6.1.1.3 Pyroxene

Pyroxene grains from polished thin sections of DDH-368 were analyzed by electron microprobe. Typically three grains were analyzed per polished thin section with one or two analyses per grain. The analyses were conducted on a Cameca SX-50 at the University of Toronto. Compositional analyses were acquired on an electron microprobe equipped with 3 tunable wavelength dispersive spectrometers. Pyroxene grains were analyzed for Na, Si, Mg, Al, Ca, Ti, Cr, Fe, Mn, Ni, and K. Operating conditions were 40 degrees takeoff angle, and a beam energy of 15 keV. The beam current was 15 nA, and the beam diameter was 1 microns. Counting times were: 10 seconds for Na, 20 seconds for Si, Mg, Al, Ca, Ti, Cr, 30 seconds for Fe, and 40 seconds for Mn, Ni, K. Off peak counting times were: 11 seconds for Si, 12 seconds for Na, Mg, Al, 20 seconds for Ca, Ti, Cr, 24 seconds for K, 30 seconds for Fe, and 40 seconds for Mn, Ni. Average detection limits are less than 250 ppm for Si, Mg and Al, and less than 350 for Na, Mn, Fe, and Ca.

6.1.1.4 Oxide Minerals

Oxide mineral grains (magnetite and ilmenite) from polished thin sections of DDH-306, DDH-368, DDH-369 and DDH-441 were analyzed by electron microprobe. Typically three grains were analyzed per polished thin section with one to two analyses per grain. The analyses were conducted on a Cameca SX-50 at the University of Toronto. Compositional analyses were acquired on an electron microprobe equipped with 3 tunable wavelength dispersive spectrometers. Oxide grains were analyzed for Mn, Fe, Ni, V, Cu, Nb, Ti, Cr, P, Mg and Al. Operating conditions were 40 degrees takeoff angle, and a beam energy of 20 keV. The beam current was 30 nA, and the beam diameter was 1 microns. Counting times were: 20 seconds for Mn, Fe, and 40 seconds for Al, Ni, Ti, Cr, Nb la, Mg, V, Cu, P. Off peak counting times were: 20 seconds for Mn, Fe, and 40 seconds for Al, Ni, Ti, Cr, Nb la, Mg, V, Cu, P. Average detection limits are less than 400 ppm for all elements.

6.1.2 Olivine Electron Microprobe Results

Olivine grains from polished thin sections of transects through each of the drill holes in this study were analyzed by electron microprobe. Analyses of the cores and rims of olivine grains showed that they are chemically homogeneous within individual grains. Samples from DDH-369 W-Horizon 1 were not analyzed due to a lack of fresh olivine grains. A summary of the olivine microprobe results are shown in Table 6.1.

The average Mg# for the complete suite of samples is 52.2% and the range is 47-59%. Good (1992) reported a slightly higher value of 56.9% ± 2.5% in his suite of Main Zone and unmineralized TDLG samples. Olivine grain compositions are consistent within a polished thin section, the difference in Mg# between grains was less than 2%. A box and whisker plot summarizing the olivine electron microprobe data is shown in Figure 6.1. This figure shows that the results from this study are all within the ranges reported by Good (1992) and that for most elements analyzed the results from unmineralized, W-Horizon and Main Zone samples overlap. Key differences between the zone include higher SiO_2, MgO, NiO, and lower FeO and CaO in the W-Horizon relative to the Main Zone.

The average Ni content of olivine is 620 ppm ($1\sigma = 220$ ppm) with a detection limit of $\sim$ 350 ppm Ni. This is higher than the value of 540 ± 140 ppm Ni reported by Good (1992), but the results of the two studies are within analytical error. Results for Ni in olivine grains on an individual slide were highly variable with differences up to 50% Ni. Compared to other sample groups the olivine in the W-Horizon has higher Ni contents and the Main Zone has higher Ca abundance and a lower Mg#.

6.1.3 Downhole Olivine Composition

6.1.3.1 DDH-306

This drill hole shows three distinct trends in Mg#: from the base of the drill hole up through the Main Zone, up through unmineralized zone 2, and from the base of the W-Horizon to the top of the drill hole. Each trend is characterized by overall increasing Mg# with increasing elevation and are separated by distinct jumps in Mg# to lower values. The bottom two trends show consistent NiO values, whereas the NiO increased near the base of the W-Horizon and decreases consistently to the top. Overall there is an increase in Mg# (45 to 55) from the base of the drill hole to the top correlating with an increase in Ni (0.04 to 0.12 %NiO).

6.1.3.2 DDH-368

This drill hole shows two distinct trends based on Mg# and Ni. From the base of this drill hole to the top of the the Main Zone mineralization the Mg# are consistent whereas there is a slight increase in Ni. At the base of unmineralized 2 there are three samples with anomalously low Mg# and Ni, which correspond to samples from a fine grained gabbro xenolith. Above the xenolith and to the top of the samples the Mg# decreases gradually while Ni increases gradually. Overall this drill hole has near-constant Mg# values while Ni increases slightly.

6.1.3.3 DDH-369

The results of this drill hole are characterized by a high amount of variability and do not show any distinct trends.

6.1.3.4 DDH-441

This drill hole shows two distinct trends. From the base of the drill hole to the top of the W-Horizon there is a general increase in Mg# corresponding with an increase in Ni. Within the W-Horizon the results become erratic, on average Mg# does not change and there is an overall increase in the amount of Ni in olivine. Above the W-Horizon Mg# and Ni show some slight variation but overall are constant.

Table 6.1: Results summary of olivine microprobe analyses

	Unmineralized			306 W Horizon			368 W Horizon			369 W Horizon 2		
no. grains	221			67			23			30		
no. analyses	307			120			42			60		
		Range			Range			Range			Range	
	Rep.	Min	Max	Rep.	Min	Max	Rep.	Min	Max	Rep.	Min	Max
SiO_2	35.51	34.05	36.69	35.82	33.75	36.67	35.04	34.64	35.64	35.88	35.18	36.55
MgO	25.63	19	28.46	24.96	17.55	27.75	26.81	24.91	28.48	26.11	22.6	27.7
MnO	0.49	0.49	1.09	0.711	0.545	1.42	0.577	0.495	0.676	0.693	0.586	0.789
FeO	38.97	34.21	45.97	38.42	35.16	47.24	37.2	35.54	39.8	37.47	35.91	41.79
NiO	0	0	0.12	0.12	0.024	0.15	0.081	0.051	0.11	0.079	0.035	0.11
CaO	0.065	0.032	0.10	0.09	0.043	0.17	0.062	0.038	0.13	0.14	0.039	0.18
Total	100.9	98.46	101.4	100.1	99.26	101	99.77	98.94	101.1	100.4	99.87	101.2
					number of ions on the basis of 4 oxygens							
Si	0.591	0.987	1.01	0.596	1	1.02	0.583	0.983	1	0.597	0.998	1.01
Mg	0.636	0.831	1.18	0.619	0.778	1.15	0.665	1.05	1.18	0.648	0.96	1.15
Mn	0.009	0.01	0.03	0.01	0.01	0.04	0.008	0.01	0.02	0.01	0.01	0.02
Fe	0.54	0.8	1.1	0.53	0.82	1.2	0.52	0.83	0.94	0.52	0.83	1
Ni	0	0	0.003	0.002	0.0006	0.003	0.001	0.001	0.003	0.001	0.0008	0.002
Ca	0.0009	0.001	0.006	0.002	0.001	0.005	0.001	0.001	0.004	0.003	0.001	0.005
Fo.	0.54	0.42	0.59	0.53	0.39	0.58	0.56	0.52	0.59	0.55	0.49	0.58
Fa.	0.46	0.4	0.57	0.46	0.41	0.59	0.44	0.41	0.47	0.44	0.42	0.51
Mg#	0.54	0.42	0.6	0.54	0.4	0.58	0.56	0.53	0.59	0.55	0.49	0.58

	441 W Horizon			306 Main Zone			368 Main Zone		
no. grains	78			15			16		
no. analyses	134			30			16		
		Range			Range			Range	
	Rep.	Min	Max	Rep.	Min	Max	Rep.	Min	Max
SiO_2	35.8	34.8	36.87	35.44	34.18	35.93	35.00	35	35.67
MgO	25.55	20.99	28.42	23.33	20.04	24.93	26.46	24.78	27.11
MnO	0	0	0.757	0.671	0.605	0.746	0.567	0.487	0.664
FeO	38.01	34.5	43.54	40.68	38.75	45.02	38.19	36.78	39.14
NiO	0.1	0.033	0.22	0.064	0.028	0.068	0.073	0.04	0.098
CaO	0.11	0.024	0.157	0.12	0.20	0.2	0.095	0.025	0.10
Total	100.2	99.42	100.9	100.3	99.71	100.9	100.8	99.78	101.1
					number of ions on the basis of 4 oxygens				
Si	0.596	1	1.02	0.59	0.999	1.01	0.59	0.991	1
Mg	0.634	0.907	1.16	0.579	0.875	1.05	0.657	1.05	1.14
Mn	0	0	0.02	0.009	0.01	0.02	0.008	0.01	0.02
Fe	0.53	0.79	1.1	0.57	0.91	1.1	0.53	0.86	0.93
Ni	0.001	0.0007	0.005	0.0009	0.0006	0.002	0.001	0.0009	0.002
Ca	0.002	0.0007	0.005	0.002	0.002	0.006	0.002	0.0008	0.004
Fo.	0.54	0.46	0.59	0.5	0.44	0.53	0.55	0.53	0.56
Fa.	0.45	0.4	0.53	0.49	0.46	0.55	0.44	0.43	0.47
Mg#	0.55	0.46	0.59	0.51	0.44	0.53	0.55	0.53	0.57

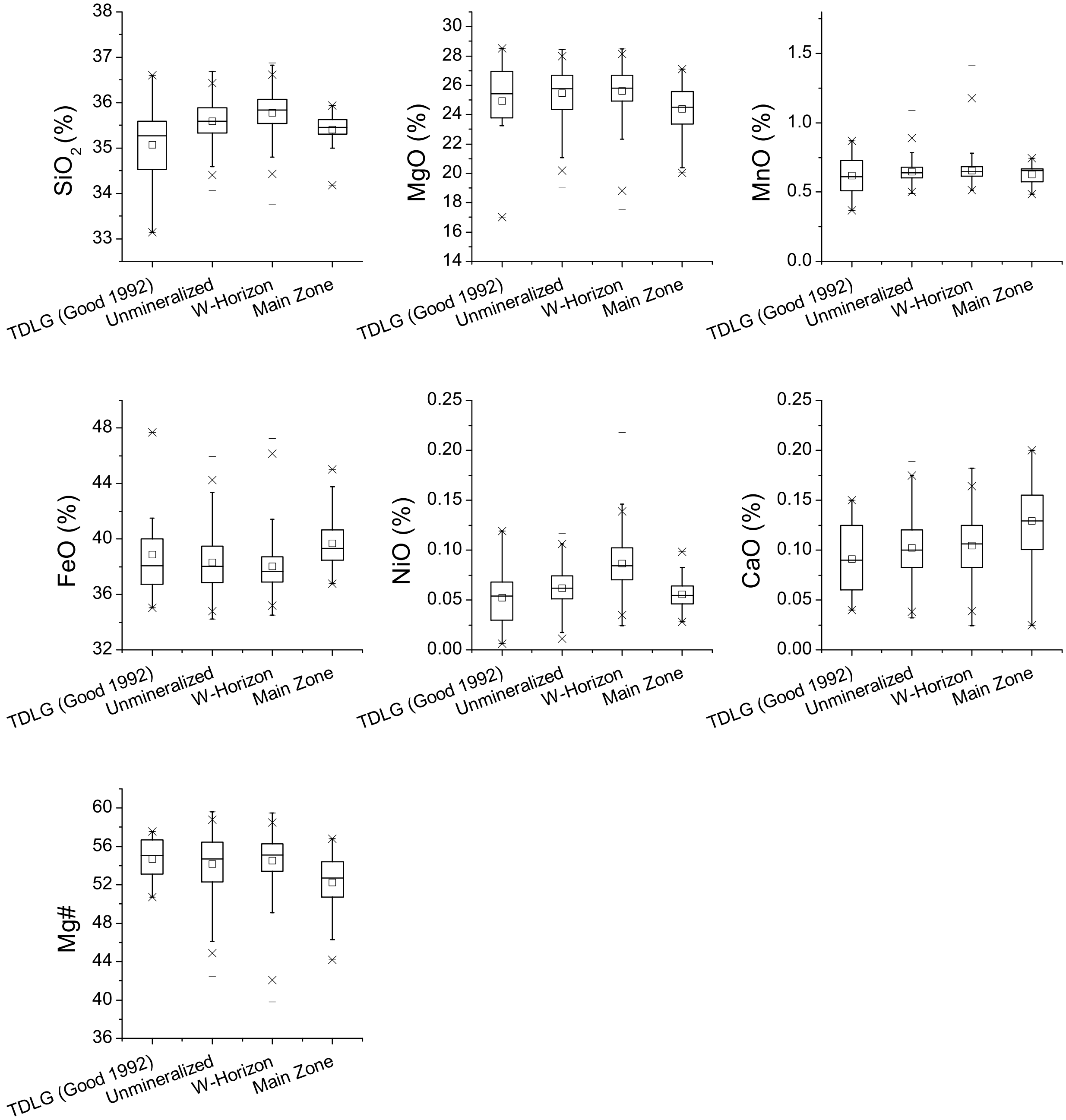

Figure 6.1: Box and whisker plot summarizing the major element chemistry of olivine grains in the TDLG. Samples are grouped into unmineralized, W-Horizon and Main Zone, samples from Good (1992) are included for comparison. The box is divided into the 25 and 75 percentile range, also shown are the mean (hollow square), 1% and 99% percentile values (X) and the minimum/maximum (-). This figure demostrates the considerable overlap of olivine grain major element chemistry within the TDLG and highlights a lack of systematic major element changes with respect to mineralizaiton.

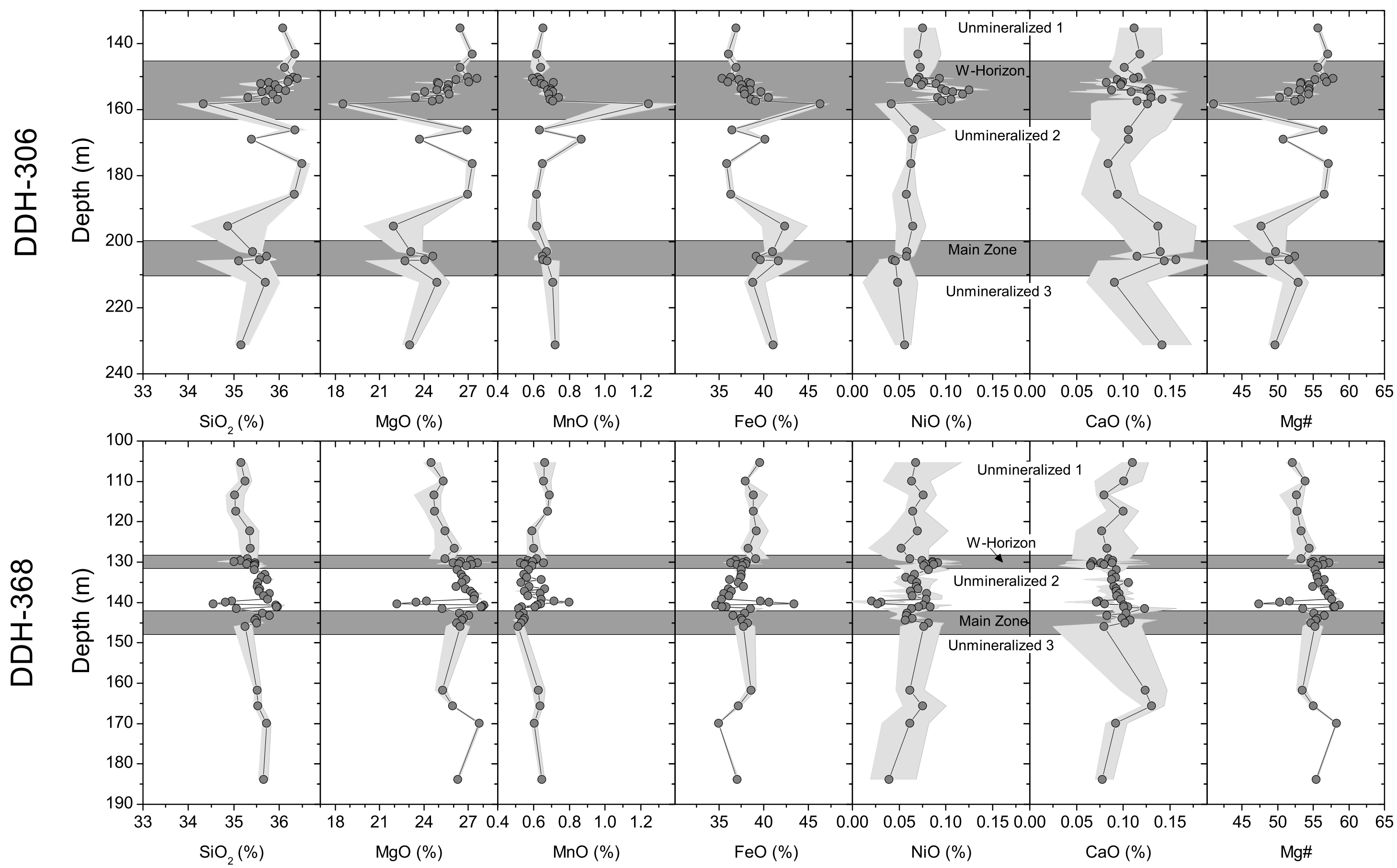

Figure 6.2: Olivine compositions from electron microprobe analyses of DDH-306 and DDH-368 plotted as a function of depth. Points represent the average value of the analyses for that sample. The shaded area denotes the range of values for each sample.

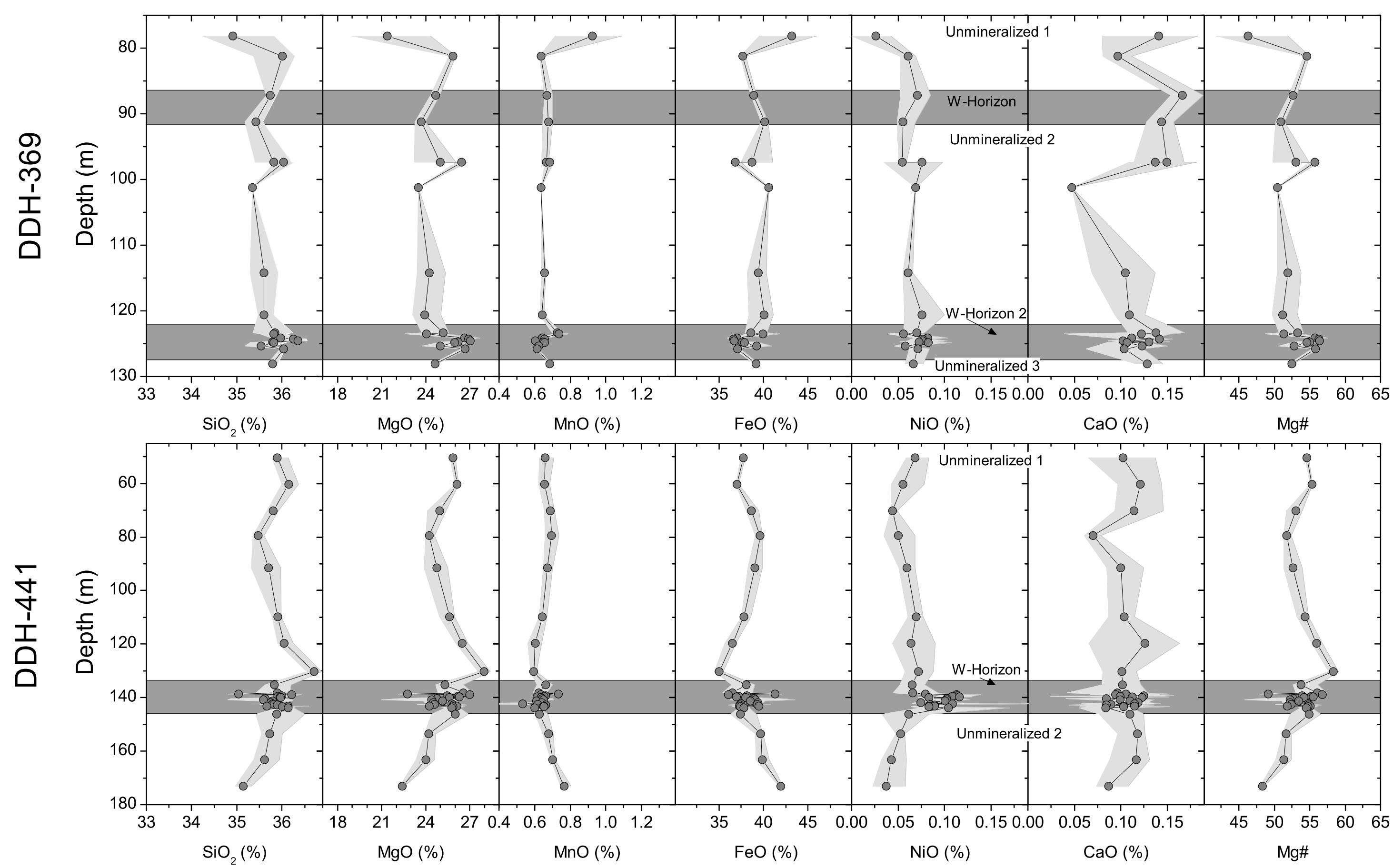

Figure 6.3: Olivine compositions from electron microprobe analyses of DDH-369 and DDH-441 plotted as a function of depth. Points represent the average value of the analyses for that sample. The shaded area denotes the range of values for each sample.

6.1.4 Plagioclase

Plagioclase grains from polished thin sections of DDH-306, DDH-368 and DDH-441 were analyzed by electron microprobe. Typically three grains were analyzed per slide with two analyses conducted on each grain. A suite of samples showing plagioclase composition stratigraphy were analyzed from DDH-368 as well as samples from DDH-306 Main Zone and DDH-441 W Horizon. A summary of the results is shown in Table 6.2. The composition of plagioclase grains is highly variable. The average composition is 59.6% An with a range of 41.1-73.7%. This range is in agreement with the range of 45.5-71.0% An calculated by Good (1992) for the Two Duck Lake Gabbro. The highest An compositions (>70%) tend to be from secondary plagioclase grains associated with chalcopyrite, although this is not always the case. Plagioclase grains commonly show chemical zonation with a Ca-rich core, and Ca decreases towards the grain boundaries. Zoned grains typically have compositional variations on the order of 5-10% An, with a maximum difference of 20% An observed.

The down-hole major element results from DDH-368 are plotted in Figure 6.5. The wide spread in plagioclase compositions on the sample scale is evident from the error bars. Down hole there is very little change in the range of plagioclase compositions, and there are no changes in the average plagioclase composition with mineralization.

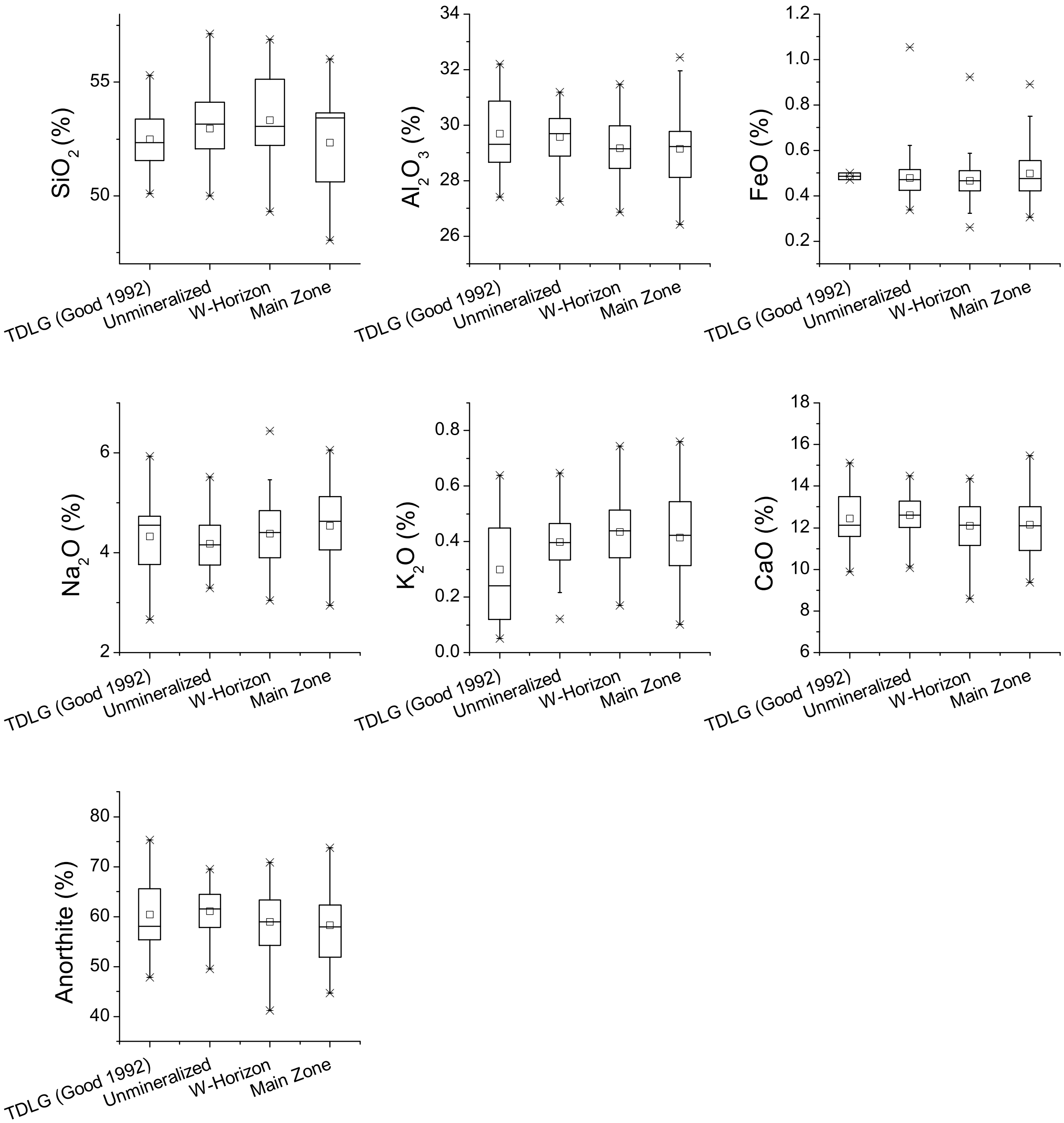

Figure 6.4: Plagioclase electron microprobe composition summary

Table 6.2: Results summary of plagioclase microprobe analyses

	Unmineralized			368 W Horizon			369 W Horizon			306 Main Zone			368 Main Zone		
no. grains	31			14			3			3			7		
no. analyses	84			62			9			8			23		
		Range			Range			Range			Range			Range	
	Rep.	Min	Max	Rep.	Min	Max	Rep.	Min	Max	Rep.	Min	Max	Rep.	Min	Max
SiO_2	52.68	50.1	55.29	53.16	49.98	66.82	53.4	51.13	54.58	56.41	53.51	64.21	52.64	49.29	56.89
Al_2O_3	29.58	27.25	31.19	29.46	18.22	31.47	29.34	28.18	31.17	27.53	18.68	29.44	29.16	26.41	32.44
FeO	0.49	0.18	1.1	0.46	0.11	0.92	0.5	0.41	0.67	0.34	0.15	0.47	0.52	0.32	0.89
Na_2O	4.19	3.3	5.51	4.49	0.651	5.47	4.45	3.77	5.1	6.05	0.373	6.44	4.22	2.94	5.77
K_2O	0.43	0.12	1.3	0.33	0.17	15	0.41	0.25	0.59	0.56	0.37	17	0.4	0.1	0.76
CaO	13	9.052	14.48	12.13	0.099	14.36	11.33	10.48	13.58	9.37	-0.022	11.69	12.62	9.471	15.48
Total	100.4	97.3	100.7	100.2	97.39	100.7	99.39	99.39	101	100.2	99.97	100.6	99.53	99.15	101.3
	based on 32 oxygens														
Si	24.6	23.4	25.8	24.9	23.4	31.2	25	23.9	25.5	26.4	25	30	24.6	23	26.6
Al	15.7	14.4	16.5	15.6	9.64	16.7	15.5	14.9	16.5	14.6	9.89	15.6	15.4	14	17.2
Fe	0.381	0.14	0.82	0.361	0.085	0.717	0.386	0.315	0.517	0.263	0.114	0.367	0.407	0.252	0.692
Na	3.11	2.45	4.09	3.33	0.483	4.05	3.3	2.8	3.78	4.49	0.277	4.78	3.13	2.18	4.28
K	0.357	0.101	1.09	0.276	0.141	12.4	0.344	0.207	0.488	0.462	0.308	13.7	0.331	0.085	0.631
Ca	9.29	6.47	10.3	8.67	0.071	10.3	8.1	7.49	9.71	6.69	-0.016	8.35	9.02	6.77	11.1
Ab	36	29	48	39	6.6	48	41	33	45	52	3.3	56	37	25	50
Or	2.4	0.7	8.1	1.9	0.99	93	2.5	1.4	3.4	3.2	2.1	97	2.3	0.59	4.3
An	62	47	70	59	0.52	71	57	51	66	45	-0.11	56	61	46	74

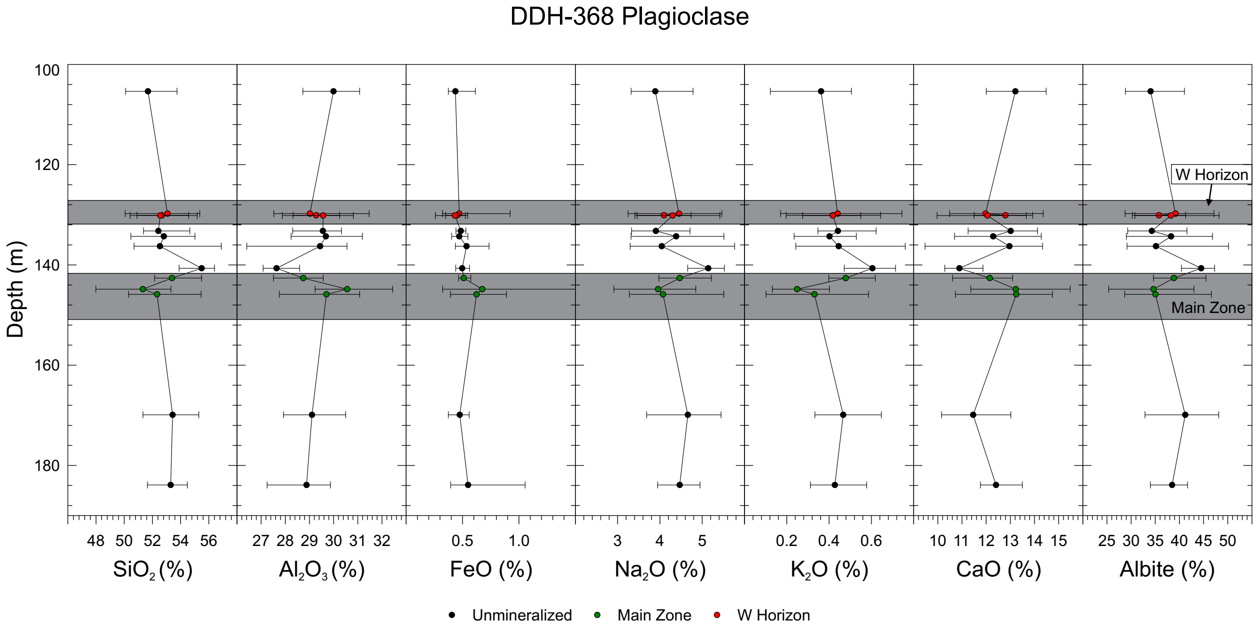

Figure 6.5: Plagioclase compositions from electron microprobe analyses of DDH-368 plotted as a function of depth. Points represent the average value of all the analyses for a sample. The lower and upper limits shown correspond the the minimum and maximum value returned for each sample. Mineralized zones are denoted.

6.1.5 Pyroxene

Pyroxene grains from polished thin sections of DDH-368 were analyzed by electron microprobe to produce a down hole transect. The results are summarized in Table 6.3 and Figure 6.6. The W-Horizon samples show elevated TiO_2, Al_2O_3 and Na_2O relative to the unmineralized and Main Zone samples collected in this study.

The down hole stratigraphy is shown in Figure 6.7. Overall the pyroxene compositions are erratic through the drill hole transect. From the top of the Main Zone to the base of the W-Horizon there is a slight increase in Mg#, in this interval olivine Mg# decreased. The down hole trends for clinopyroxene composition show similar erratic behaviour as observed in the olivine.

Pyroxene grains of Two Duck Lake Gabbro from this study all plot within the clinopyroxene field. It was reported by Good (1992) that orthopyroxene was observed within the TDLG but as a minor component and typically as rims on olivine grains. The only analysis that plotted in the orthopyroxene field from this study occurred in a sample of fine grained equigranular gabbro cumulate as rims on olivine grains. The composition of clinopyroxene falls within the field of diopside-augite and orthopyroxene within hypersthene (Fig. 6.8). Pyroxene grains are unzoned, and grains within a thin section showed average compositional difference of less than 4 mol% En.

Table 6.3: Results summary of pyroxene microprobe analyses of samples from DDH-368

	Unmineralized			368 W-Horizon			368 Main Zone			368 Orthopyroxene		
no. grains		25			9			11			3	
no. analyses		45			21			25			4	
		Range			Range						Range	
	Rep.	Min	Max	Rep.	Min	Max	Rep.	Min	Max	Rep.	Min	Max
SiO_2	51.15	49.93	52.58	50.36	50	51.98	51.19	49.04	52.66	52.2	51.86	52.2
TiO_2	0.76	0.29	0.9	0.89	0.58	0.95	0.75	0.31	0.84	0.3	0.16	0.3
Al_2O_3	2.88	1.56	3.66	3.17	2.26	4.12	2.63	0.972	3.98	0.811	0.638	0.923
FeO	9.64	8.68	11.8	9.55	8.73	9.97	9.54	7.41	14	22.3	22.3	24
MnO	0.261	0.18	0.38	0.188	0.188	0.336	0.289	0.151	0.514	0.652	0.603	0.652
MgO	13.84	12.75	14.71	13.64	13.36	14.39	13.51	11.31	14.79	20.86	20.13	20.86
CaO	20.72	18.04	21.96	21.4	20.91	21.7	20.86	17.33	23.74	1.511	1.184	1.547
Na_2O	0.326	0.204	0.43	0.346	0.201	0.442	0.297	0.157	0.407	0	0	0.0304
Total	99.57	98.25	100.2	99.54	99.13	100.5	99.08	97.69	100.4	98.62	98.42	98.99
based on 6 oxygen												
Si	1.919	1.887	1.959	1.896	1.877	1.937	1.93	1.876	1.979	1.98	1.974	1.986
Ti	0.043	0.017	0.051	0.05	0.033	0.054	0.043	0.018	0.047	0.017	0.0094	0.017
Al	0.13	0.068	0.16	0.14	0.099	0.18	0.12	0.044	0.18	0.036	0.029	0.041
Fe	0.3	0.27	0.37	0.3	0.27	0.31	0.3	0.23	0.45	0.71	0.71	0.76
Mn	0.0083	0.0058	0.012	0.006	0.006	0.011	0.0092	0.0047	0.017	0.021	0.019	0.021
Mg	0.77	0.72	0.82	0.77	0.75	0.8	0.76	0.65	0.83	1.2	1.1	1.2
Ca	0.83	0.73	0.88	0.86	0.84	0.87	0.84	0.71	0.94	0.061	0.048	0.063
Na	0.024	0.015	0.031	0.025	0.015	0.032	0.022	0.011	0.03	0	0	0.0022
Fe	15.84	14.03	19.41	15.58	14.12	16.31	15.81	11.62	23.54	36.3	36.3	39.13
Ca	43.62	38.66	45.2	44.74	43.8	45.65	44.28	37.24	47.67	3.153	2.47	3.227
Mg	40.54	37.6	44.21	39.68	39.2	41.46	39.91	33.57	42.71	60.55	58.4	60.55

Rep. - a sample with values close to the average was selected as the representative sample

6.1.6 Oxide Minerals

Oxide minerals from a selection of samples from DDH-306, DDH-368, DDH-369 and DDH-441 were analyzed by electron microprobe, the results are summarized in Table 6.4. As described in Section 4.3.1.1 there are two petrographically distinct types of Fe-oxide minerals. Magmatic Fe-oxide consists of magnetite with bands of ilmenite exsolution present throughout. The second type of Fe-oxide forms rims on chalcopyrite grains in the mineralized zones. Results from the microprobe analysis show that the petrographically distinct Fe-oxides are also chemically distinct. The magmatic Fe-oxide contains appreciable amounts of TiO_2, from 2-52%. The Fe-oxide rims on chalcopyrite were essentially pure Fe-end member, with trace amounts of TiO_2.

Table 6.4: Results summary of Fe-oxide microprobe analyses

	Magnetite			Ilmenite			FeO rims on chalcopyrite		
analys.	24			16			21		
	Avg	Min	Max	Avg	Min	Max	Avg	Min	Max
FeO	78.33	66.47	89.78	46.43	44.74	49.47	93.25	84.64	100.4
TiO_2	11.44	2.318	18.21	49.53	35.67	51.51	0.1478	0.01503	0.9613
Al_2O_3	2.96	0.207	10.3	0.686	0	9.67	0.212	0.00325	1.24
MgO	0.81	0	4.7	0.66	0.039	3.2	0.36	0	2.3
MnO	0.59	0.07	1.9	2.4	0.58	4	0.063	0	0.22
V_2O_3	1.02	0.35	2.3	0.078	0	0.21	0.052	0	0.9
Cr_2O_3	0.5	0.033	1.5	0.068	0	0.28	0.034	0	0.65
P_2O_5	0.0058	0	0.023	0.0039	0	0.016	0.0068	0	0.029
Total	95.7	89.1	99.6	99.9	99.1	101	94.2	88.3	101

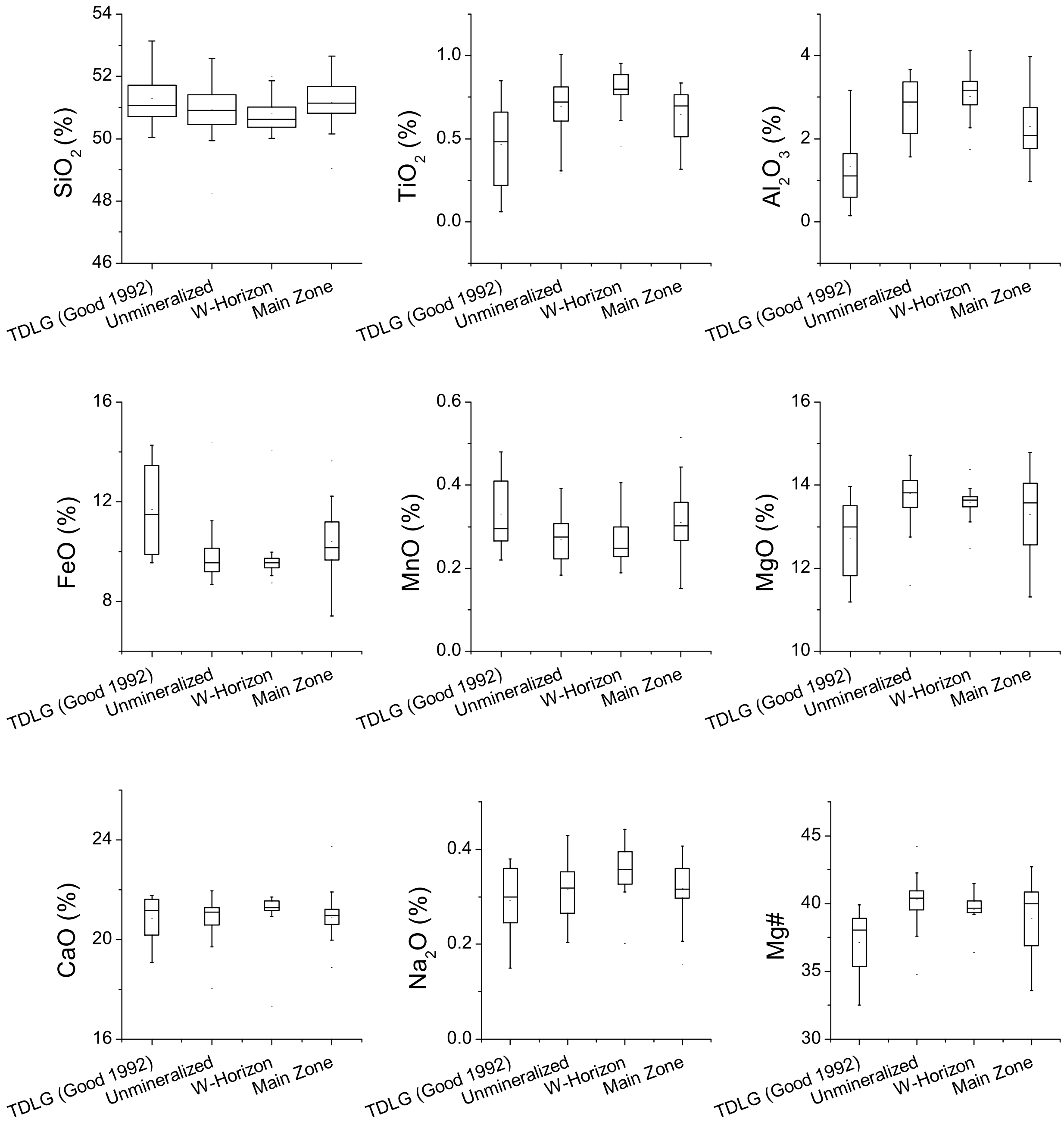

Figure 6.6: Clinopyroxene electron microprobe summary of samples from DDH-368

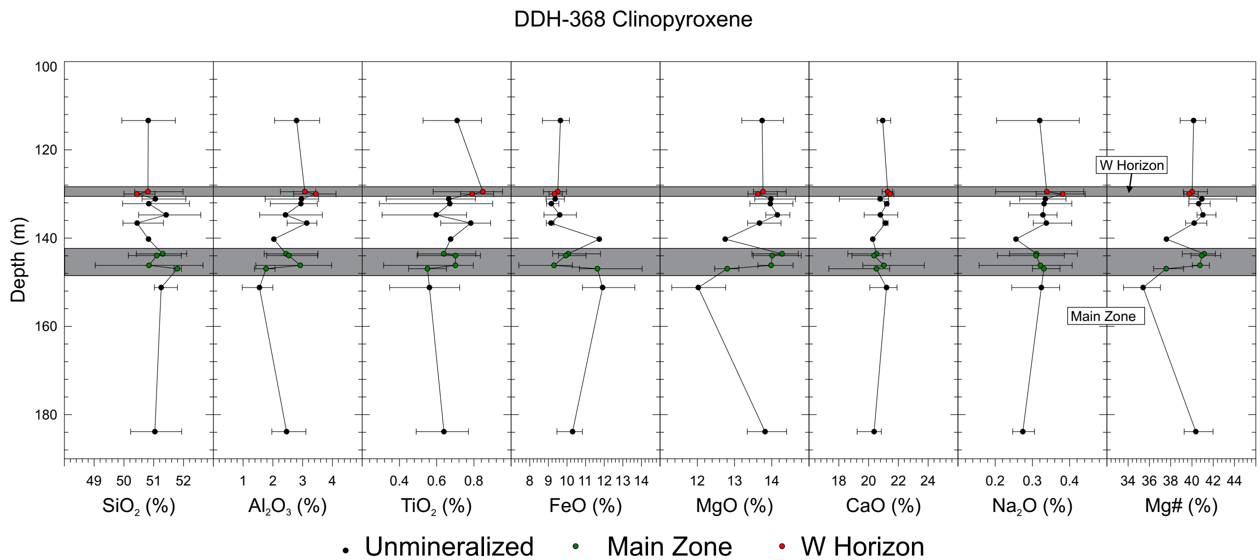

Figure 6.7: Clinopyroxene compositions from electron microprobe analyses of DDH-368 plotted as a function of depth. Points represent the average value of all the analyses for a sample. The lower and upper limits shown correspond the the minimum and maximum value returned for each sample. Mineralized zones are denoted.

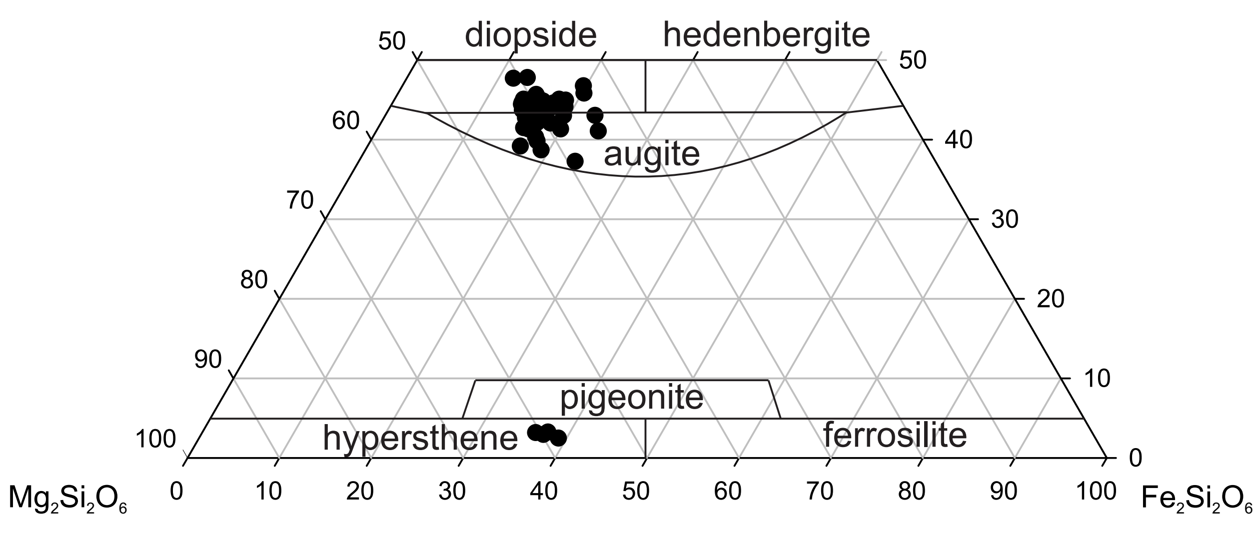

Figure 6.8: Ternary diagram for pyroxene composition. Clinopyroxene samples fall within the field of diopside-augite and orthopyroxene within the field of hypersthene.

6.2 Laser Ablation Inductively Coupled Plasma Mass Spectrometry

6.2.1 Methodology

Trace element mineral chemistry of olivine and clinopyroxene grains in polished thin sections were analyzed by Laser Ablation Inductively Coupled Plasma Mass Spectrometry (LA-ICP-MS) at the University of Windsor. Samples were selected from DDH-306, DDH-368, DDH-441 and three grains per polished thin section were analyzed. A complete stratigraphy transecting the mineralized zones in DDH-368 was analyzed. Only two and three polished thin sections were analyzed in DDH-306 and DDH-441, respectively. The samples were ablated using a Quantronix Integra-C Fs laser system at the fundamental wavelength of 785 nm. It is a regenerative and multi-pass Titanium-doped sapphire (Ti:sapphire) laser ablation system based on the Chirped Pulse Amplification (CPA) technique. The LA system operating conditions for sample analyses are summarized in Table 6.5. The ablation material was transported from the ablation cell to the ICP-MS using argon as the carrier gas and analyzed using a Thermo Electron X series II quadrupole ICP-MS. The data acquisition protocol was time-resolved analysis, the scanning mode was peak-jumping mode, dwell times were 10 ms for ^{7}Li ^{25}Mg ^{27}Al ^{29}Si, ^{31}P, ^{43}Ca, ^{44}Ca, ^{45}Sc, ^{47}Ti, ^{51}V, ^{53}Cr, ^{55}Mn, ^{59}Co, ^{60}Ni, ^{62}Ni, ^{65}Cu, ^{66}Zn, ^{75}As, ^{103}Rh, ^{106}Pd, ^{195}Pt, and ^{197}Au. The ICP-MS analyses were calibrated using a NIST610 glass standard from the National Institute of Standards and Technology. The average value of Si from electron microprobe analyses was used as an internal standard. Data was processed off-line using commercial software and an in-house written program based on Longerich et al. (1996). Complete data sets are in Appendix VI.

Detection limits were generally below 1 ppm for ^{45}Sc, ^{51}V, ^{55}Mn, ^{59}Co, ^{65}Cu, ^{66}Zn, ^{103}Rh, ^{106}Pd, ^{195}Pt, ^{197}Au, below 5 ppm for ^{7}Li, ^{27}Al, ^{45}Sc, ^{47}Ti, ^{53}Cr, ^{60}Ni, below 25 ppm for ^{25}Mg, ^{31}P, ^{61}Ni, ^{75}As, and below 200 ppm for ^{29}Si and ^{43}Ca. The results for ^{53}Cr in olivine were at or below detection limits for the majority of the analyses. Rh, Pd, Pt and Au contents were analyzed in olivine and clinopyroxene but the concentration of these elements were never above the detection limit.

6.2.2 Olivine Results

Olivine grains from samples forming a complete transect through the mineralized zones of DDH-368 were analyzed by LA-ICP-MS. The results are plotted in Figure 6.9. Compatible (Ni, Co, Zn) and incompatible elements (V, Sc, P) show opposite trends. The compatible elements show trends which parallel Mg# trends observed from the electron microprobe study of olivine grains. Lower Mg# samples have higher amounts of Ni, Co and Zn. A sample with anomalously low compatible trace elements occurs immediately above the Main Zone. The compatible trace elements then decrease to the base of the W-Horizon. Within the W-Horizon the trace element chemistry is again highly variable as was observed within the major element data set.

Table 6.5: LA-ICP-MS Machine Operating Conditions

	DDH-368	DDH-306	DDH-441
Rep. Rate (Hz)	100	100	100
Pin Hole Diameter [NIST] (mm)	2.5	2.5	2.5
Pin Hole Diameter [Sample] (mm)	1.5	2.5	2.5
Energy [NIST] (mJ)	0.03	0.025	0.025
Energy [Sample] (mJ)	0.012	0.025	0.025
Beam Width [NIST] (um)	22	20	20
Beam Width [Standard] (um)	17	20	20
Objective [NIST]	10x	10x	10x
Objective [Sample]	10x	25x	25x
High resolution on:	29Si, 44Ca	44Ca	44Ca
Monitor	As	As	As

Within the W-Horizon the Cu content in olivine were up to four times higher than the olivine in the Main Zone and unmineralized zones. The Cu increase occurs independent of the grains contact with chalcopyrite or silicate grains. The average value of Ni in olivine, 500 ppm, is slightly lower than was determined from electron microprobe.

The results of the down hole olivine trace element data are similar to the olivine major element data from microprobe analyses and show localized Mg# trends which do not correlate with mineralized horizons. A localized fractionation trend from the LA-ICP-MS data is shown between 130 and 140 m where compatible elements (Li, V, and Co) increase with depth. A second plot zoomed in to this interval and comparing the LA-ICP-MS analyses to select data from electron microprobe and whole rock geochemistry is shown in Figure 6.10. The whole rock data (Mg#) does not follow the trends in the LA-ICP-MS or electron microprobe data, and has two intervals of increasing Mg# over the same range. The electron microprobe data for olivine and clinopyroxene closely follow the LA-ICP-MS data. There is a divergence at around 140 m due to a xenolith of fine grained gabbro where the major element chemistry of the olivine and clinopyroxene diverge from the fractionation trend.

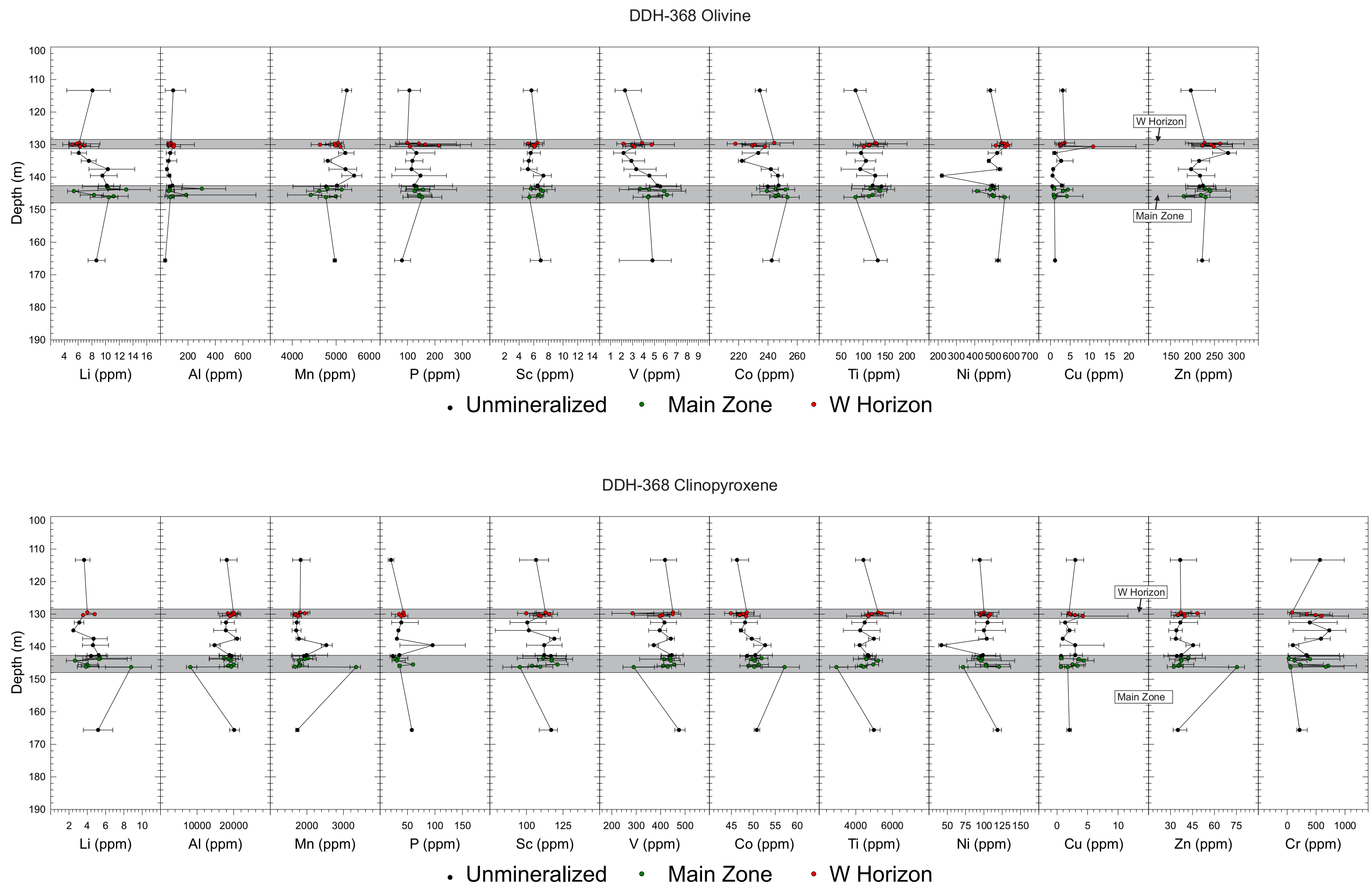

Figure 6.9: Olivine and clinopyroxene compositions from LA-ICP-MS from DDH-368 vs. depth. Points represent the average value of all the analyses for a sample. The lower and upper limits shown correspond the the minimum and maximum value returned for each sample. Mineralized zones are denoted.

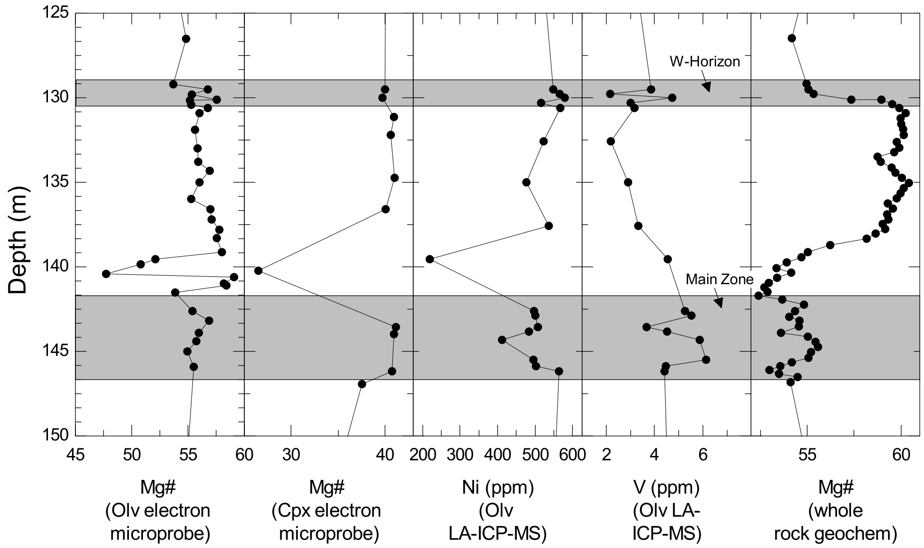

Figure 6.10: Whole rock geochemistry, microprobe and laser ablation results comparison for olivine

6.2.3 Clinopyroxene Results

Plots showing the results from the clinopyroxene LA-ICP-MS are shown in Figure 6.9. The results have similar patterns as those observed in olivine. Localized fractional crystallization trends are shown by Li, V, and Co, although the signal is not as strong in clinopyroxene as olivine. The increase of Cu clinopyroxene is lower than in olivine grains.

Clinopyroxene Cu values are the same, approximately ∼5 ppm, between the Main Zone and W-Horizon, with two samples in the W Horizon containing up to ∼10 ppm. The amount of Ni in clinopyroxene shows a high degree of variation with a range of over ∼110 ppm, the average value does not change appreciably with depth.

6.2.4 Copper in Olivine and Clinopyroxene

The LA-ICP-MS analyses conducted on DDH-368 only included ^{65}Cu. This led to ambiguity in the data set due to the possibility of interference with other elements. In order to confirm that the results were not influenced by interference a second run of analyses was conducted this time analyzing for both ^{63}Cu and ^{65}Cu. These results, shown in Figure 6.11, show a near 1:1 correlation indicating that the results were not caused by interference. An example spectrum from the ablation in Figure 6.12. The consistent level spectrum indicates that the Cu is present in the mineral structure and is not caused by micro-nuggets of Cu trapped within the mineral.

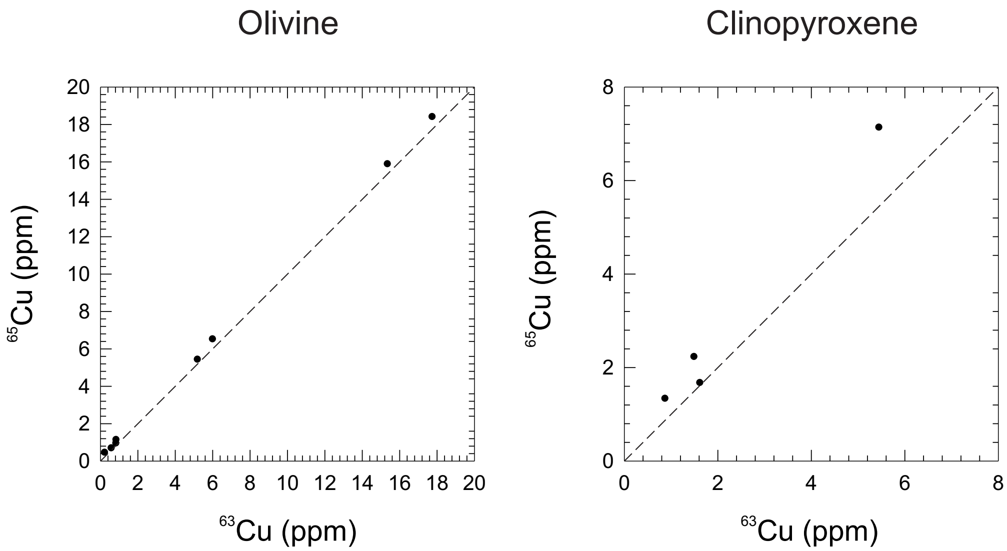

Figure 6.11: Plot showing ^{65}Cu vs. ^{63}Cu showing a near perfect correlation for the two elements in both olivine and clinopyroxene. Dashed line indicates a slope of 1:1.

6.2.5 Comparison between drill holes and mineralized zones

In addition to the suite of thin sections analyzed throughout DDH-368, an additional three thin sections from DDH-306 and three thin sections from DDH-441 were analyzed. A plot of Cu vs. Ni from the LA-ICP-MS analysis is shown in Figure 6.13 A.

These results show that for the sample set analyzed unmineralized and Main Zone samples have the lowest Ni in olivine. There is a large overlap between Main Zone and W-Horizon samples over the range of 500-650 ppm Ni in olivine. The highest results for Ni in olivine were all from W-Horizon samples. Trends for Cu in olivine are less distinct between the zones. Overall the sample set had less than 6 ppm Cu in olivine, a small amount of Main Zone and W-Horizon samples had elevated Cu in olivine, with samples from DDH-368 W-Horizon being the only samples with greater than 10 ppm Cu. There is no correlation shown between Cu and Ni in olivine for the data set analyzed. If the amount of Cu and Ni in olivine grains is the result of re-equilibration with sulphide minerals present within the sample there should be consistent trends relating Ni and Cu in olivine to Ni and Cu values from whole rock analysis. Figure 6.13 B plots Cu vs. Ni from whole rock geochemistry showing that the trends from LA-ICP-MS olivine data do not follow the mineralization and eliminating the possibility of re-equilibration with sulphide minerals.

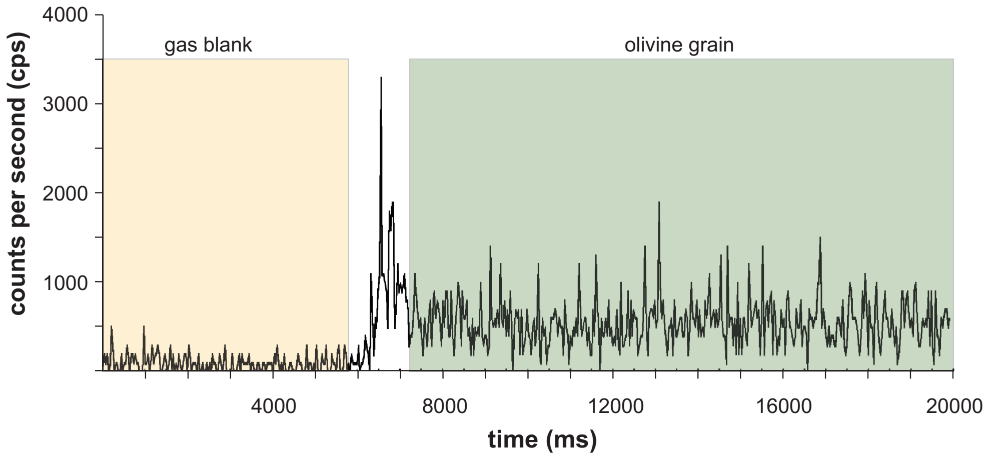

Figure 6.12: Representative LA spectra for the determination of Cu concentration from an olivine grain. The gas blank is highlighted in yellow and the olivine grain in green. There is a distinct continuous high signal from the olivine grain showing that the Cu is not the result of the nugget effect.

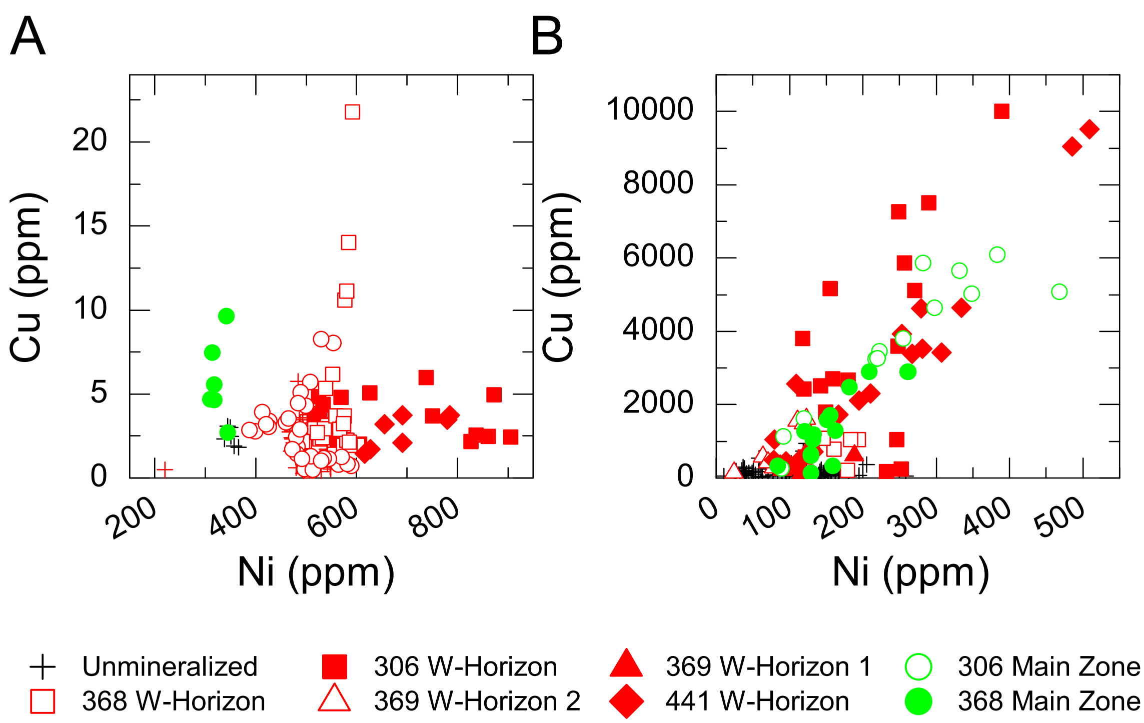

Figure 6.13: Ni vs. Cu ratios for mineralized horizons. A) Plot of Ni vs. Cu of olivine grains from the LA-ICP-MS study B) Plot of Ni vs. Cu using data from whole rock geochemistry.

Chapter 7

Sulphide Tenor and R-Factor Modeling

7.1 Sulphide Tenor

Comparing sulphide mineralization between magmatic sulphide deposits is complicated because styles of mineralization can differ (disseminated, semi-massive or massive) and there are a wide array of potential sulphide minerals. Calculating the sulphide tenor of mineralized samples is a commonly used method to normalize mineralization and aid comparison. This method has been described in great detail by Naldrett et al. (2000), Li (2001), Kerr (2001), and Kerr (2003). The sulphide tenor recalculates the grade of a sample as though it consists of 100 percent sulphides. This allows for the comparison of grades between different samples by removing the affects caused by variable amounts of sulphur.

The calculation of sulphide tenor requires that the proportion of S in the sulphide mineral assemblage is known, or can be estimated. If the modal abundance of all the sulphide minerals in a sample is known the proportion of S in the sulphide minerals can be calculated using each minerals stoichiometry. A detailed study by Kerr (2003) showed that it is reasonable to estimate the proportion of S in the sulphide mineral assemblage without greatly affecting results. In a typical magmatic sulphide assemblage of chalcopyrite-pyrrhotite-pentlandite the wt% S in the sulphide minerals can be approximated by the average value of 35.7 wt% S.

Within the W-Horizon the sulphide mineral assemblage is chalcopyrite and bornite whereas in the Main Zone it is chalcopyrite, pyrrhotite and bornite. The wt% S in chalcopyrite, bornite and pyrrhotite is 34.94, 25.25 and 36.5 respectively. Due to the lower wt% S in bornite using an average value of 35.7 wt% S in sulphide minerals is an over estimate, however due to the variable modal abundance of bornite in each sample it is not possible to calculate a precise wt% S for each sample analyzed. In a sample containing chalcopyrite:bornite in the ratio of 2:1 the actual wt% S is 31.88, a 10% difference. The values determined for sulphide tenor in this study are therefore the lower limit of the actual values.

The mass fraction of sulphur M_{sulf} is calculated by:

$$M_{\text{sulf}} = \frac{\text{measured S wt\% in sample}}{\text{assumed S wt\% in sulphide minerals}} \tag{7.1}$$

The sulphide tenor (X_{sulf}) represents a grade projection for a material consisting of 100 percent S. (X_{sulf}) is calculated by:

$$X_{\text{sulf}} = \frac{X_{WR}}{M_{\text{sulf}}} \tag{7.2}$$

where X_{WR} is the corrected wt% of metal X from the whole rock analysis, and M_{sulf} is the mass fraction of sulphide. The value of X_{WR} is calculated by subtracting the metals contained within silicate minerals from the total metals resulting from the assay. The average metal value from unmineralized low sulphur samples was calculated and represents the amount of metals contained within silicate minerals. This correction is particularly important when calculating Ni tenors in olivine bearing samples. The corrected wt% of metal X is calculated by subtracting the average value of that metal in unmineralzied rocks with low S values.

The sulphide tenor can also be calculated using a linear regression assuming that the analyses come from closely related samples, and that sulphide tenors are fairly constant. The sulphide tenor is then given by:

$$X_{\text{sulf}} = \left(\frac{\text{Me}}{S}\right)_R * Y \tag{7.3}$$

where $(M\text{e}/S)_R$ is the slope of the regression line for the metal being examined vs. sulphur, and Y is the sulphur content used for the calculation.

The potential errors involved in this calculation are discussed in great detail by Kerr (2003). The main sources of error are from the assumed value of wt% S in 100% sulphides, and the accuracy of the analysis for S, base metals and PGE. The errors are highest for samples which contain low sulphur, very low base metals and PGE, and base metal and PGE values higher than the standards used for instrument calibration. The samples from the W-Horizon and to a lesser extent the Main Zone fall under the categories of high error. Based on the work of Kerr (2003) it is estimated error on sulphide tenor calculations for the W-Horizon and Main Zone are 30-50%.

The sulphide tenor was calculated using two methods: 1) corrected whole rock data, calculated by subtracting the average metal value from unmineralized, low sulphur samples and 2) a graphical solution using a linear regression of metal vs. S data. For all of the calculations a value of 34.94 was used for the assumed wt% S in the sulphide mineral assemblage (Equation 7.1). As discussed above this led an over estimate of X_{sulf} in samples containing bornite. The results of the calculations are shown in Table 7.1 along with sulphide tenors calculated with data from Good (1992). A graphical comparison of the results is shown in Figure 7.1. The linear regressions used in the graphical method are shown in Figure 7.2. As described in Section 5.5 the ore grades observed in DDH-441 W-Horizon follow the trends of Main Zone samples. In order to calculate the linear regression samples from DDH-306, DDH-369 and DDH-368 W-Horizon are grouped as W-Horizon, and samples from DDH-306 and DDH-368 Main Zone and DDH-441 W-Horizon are grouped as Main Zone.

Table 7.1: Sulphide tenor (X_{sulf})

Sulphide tenor of ore samples in the Marathon deposit (metal values normalized to 100% sulphides)

	No. Samples	Ni (wt%)			Cu (wt%)			Pt (ppm)			Pd (ppm)			Au (ppm)		
		Min	Max	Avg.	Min	Max	Avg.	Min	Max	Avg.	Min	Max	Avg.	Min	Max	Avg.
Calculationed using corrected values[3]																
Basal Zone[1]	4	0.1	0.3	18	6	8	7.3	1	3	2.1	1	3	2.1	0	1	1
Main Zone[2]	28	0.3	5.7	1.1	13	130	28	2.2	460	83	4.6	660	81	1.1	55	13
Main Zone[1]	22	0.1	4	0.8	10	51	24	2	121	21	2	119	36	1	36	1
W-Horizon[1]	56	0.01	13	2.1	1.9	60	31	3	27000	1800	9.5	28000	3100	0.68	1200	120
Graphical Method																
Main Zone[2]	46	na	na	1.2	na	na	26	na	na	11	na	na	64	na	na	5.7
W-Horizon[2]	44	na	na	1.1	na	na	48	na	na	640	na	na	960	na	na	220

[1] Data from this study
[2] Data from Good (1992)
[3] Data from this study are corrected using unmineralized average, data from Good (1992) are corrected for Ni using calculated 95 ppm Ni in silicates
na Results not applicable to the graphical method

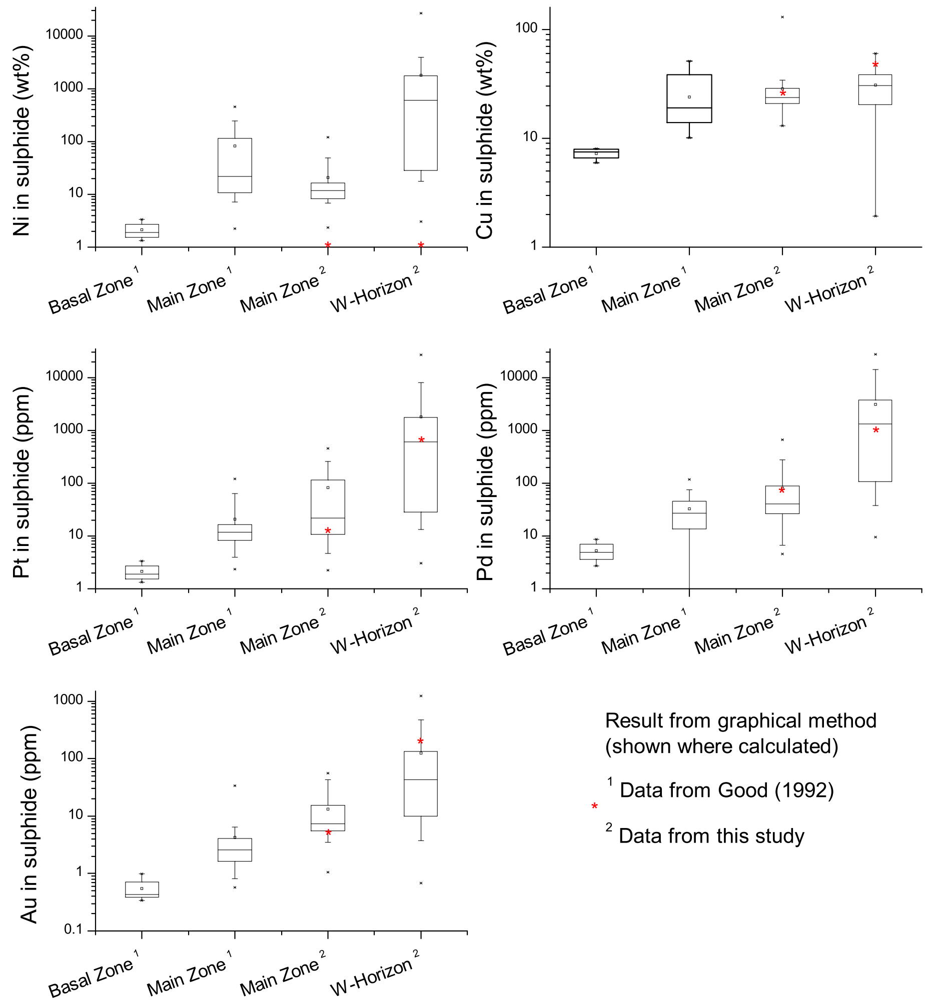

Figure 7.1: Box and whisker plot comparing the sulphide metal tenor between mineralization zones. The box is divided into the 25 and 75 percentile range. The red star marks the results from the graphical calculation.

The results of the sulphide tenor calculation shows a wide range of values for each mineralized zone. This range could be caused by several factors. The process which led to the enrichment of the sulphide liquid in PGE may have occurred to varying degrees within different parts of the deposit, resulting in different levels of enrichment. The micro nugget affect could cause values to be anomalously high if the PGE were concentrated within a sulphide grain analyzed in the assay (heterogeneous PGE distribution). The PGE may be concentrated in a phase other than sulphide. The range of tenor for the Main Zone calculated from this study broadly overlaps with those calculated from the Main Zone by Good (1992). The value of tenor between mineralized zones is W-Horizon $>>$ Main Zone $>$ Basal Zone. The tenor within the W-Horizon is generally higher than in the Main Zone at lower total S

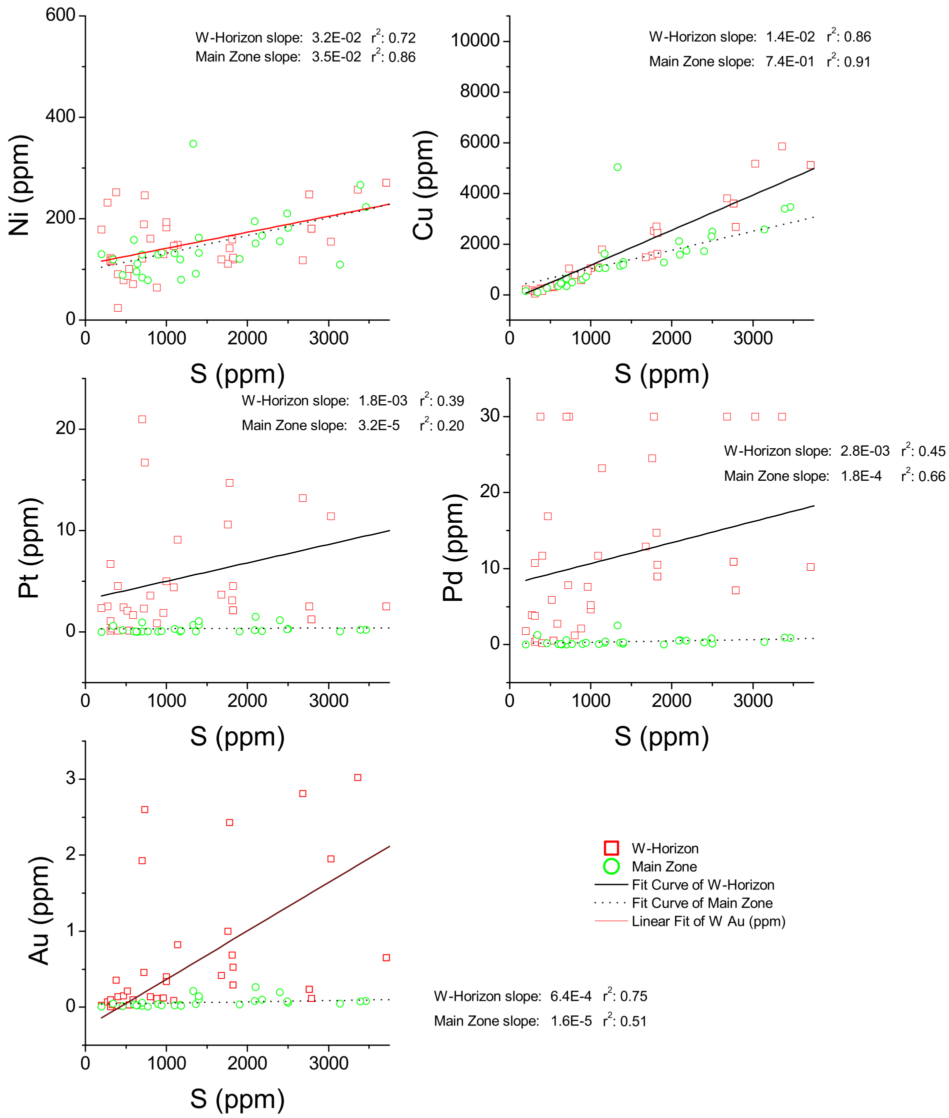

Figure 7.2: Metal vs. S linear regression plots. Samples from DDH-306, DDH-369 and DDH-368 W-Horizon are grouped as W-Horizon, and samples from DDH-306 and DDH-368 Main Zone and DDH-441 W-Horizon were grouped as Main Zone.

values.

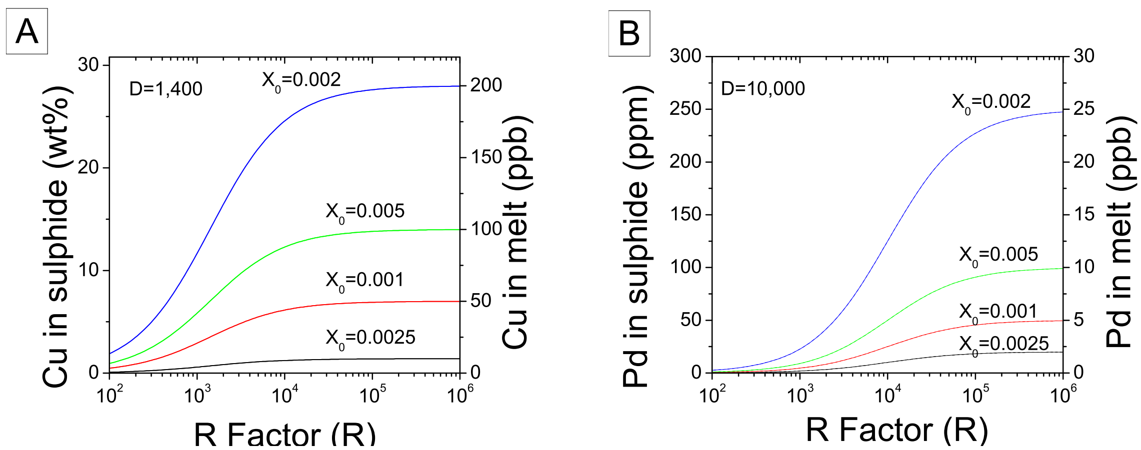

Figure 7.3: Closed system R Factor model results using various initial melt compositions

7.2 Modeling of Sulphide deposits using the R Factor

7.2.1 Closed System R Factor Model

The importance of the formation of an immiscible sulphide liquid in magmatic Cu-Ni ± PGE deposits has been well documented. Many research papers have been published modeling the extraction of base metals and PGE from silicate magma by immiscible sulphide liquids. A classic paper by Campbell and Naldrett (1979) introduced the concept of the R factor for modeling magmatic ore deposits. The R factor is the ratio of silicate magma to sulphide liquid within a magmatic system (Eqn. 7.4).

$$R = \frac{\text{mass of silicate magma}}{\text{mass of sulphide liquid}} \tag{7.4}$$

By increasing the ratio of silicate melt to sulphide liquid, the sulphide liquid is able to interact with more silicate melt (Fig. 7.4 closed system). As the sulphide liquid interacts with more silicate melt it is able to scavenge more metals (Ni, Cu, Pt, Pd, and Au) out of the melt and the sulphide metal tenor is upgraded (increased). The partition coefficient (D_{Me}) controls the amount of metal that can be partitioned into the sulphide liquid from the silicate melt and is defined as:

$$D_X = \frac{\text{weight \% X in sulphide liquid}}{\text{weight \% X in silicate melt}} \tag{7.5}$$

where X is the metal being examined. Metals that have high partition coefficients (i.e., Pt and Pd) are more efficiently scavenged from the silicate liquid than metals with low partition coefficients (i.e., Cu and Ni). The R factor is defined as:

Campbell and Naldrett (1979) derived the following equation to calculate sulphide tenor (X_{sulf}) in a closed system:

$$\frac{X_{\text{sulf}}}{X_0} = \frac{D(R+1)}{R+D} \tag{7.6}$$

where X_0 is the concentration of metal in the parent magma, X_{sulf} is the concentration of metal in the sulphide liquid, R is the R Factor, and D is the sulphide/silicate partition coefficient. A second equation to calculate the wt% of metal X remaining in the silicate magma is given by:

$$\frac{X_{\text{mag}}}{X_0} = \frac{(R+1)}{R+D} \tag{7.7}$$

where X_{mag} is the concentration of metal X in the silicate magma. As the R Factor increases the concentration of metal in the sulphide increases, up to the theoretical maximum which is given by $D \times X_0$. The limiting value is reached when $R \gg D$. As the R factor is increased and the maximum tenor of the sulphide liquid is achieved, the depletion of metals from the silicate magma decreases. In order to achieve the maximum enrichment of the sulphide liquid for metals with high partition coefficients very high R factors are required.

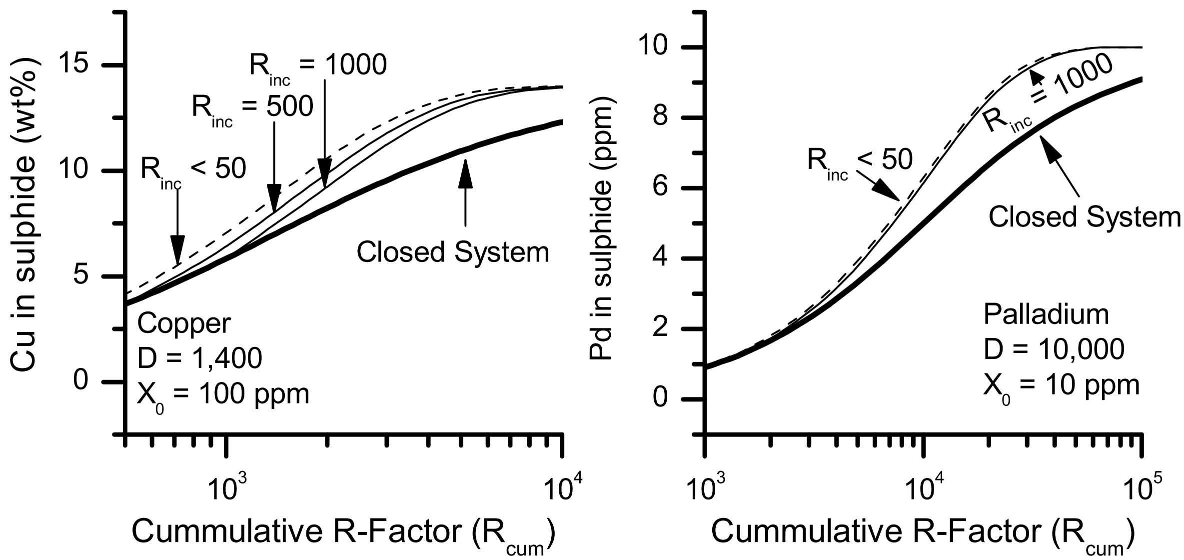

Figure 7.4: Sulphide metal tenors for closed and simple multistage upgrading models. Plots are shown for Cu (low partition coefficient) and Pd (high partition coefficient).

7.2.2 Simple Multistage Upgrading in an Open System

To achieve high sulphide tenor with lower R factors Naldrett and Lightfoot (1999) introduced the concept of simple multistage upgrading in an open system. In this open system model, the sulphide liquid comes into contact with multiple batches of silicate magma. After interacting with the sulphide liquid, the silicate magma then leaves the system. This process is then repeated with multiple batches of silicate magma. Through this process the R factor is increased stepwise. In this model, multiple small batches of silicate magma interact with the sulphide liquid instead of a single large batch. Smaller individual batches of magma interacting with the sulphide liquid are more realistic because the dense sulphide liquid is expected to settle within a magma chamber or conduit. Gravitational settling of the sulphide liquid will limit the amount of silicate magma that the sulphide liquid can interact with. This is exemplified by a large batch of magma entering a magma chamber containing settled sulphide liquid, the sulphide liquid will not interact with all of the incoming silicate magma.

In this model the incremental R factor (R_{inc}) is defined as the mass of each individual incoming batch of magma divided by the mass of sulphide liquid. The cumulative R factor (R_{cum}) is the accumulated mass of all magma batches divided by the mass of the sulphide liquid. Smaller values of R_{inc} represent conduit-like conditions whereas large values represent a magma chamber. Figure 7.4 shows the effect of different values of (R_{inc}), smaller values of (R_{inc}) lead to higher sulphide tenors at lower R. The equations assume that R_{inc} and X_0 remain constant over N batches of magma to simplify calculations.

$$R_{\text{cum}} = N R_{\text{inc}} \tag{7.8}$$

Detailed derivations of this model can be found in Kerr (2005). The equation they derived is:

$$\frac{X_{\text{sulfN}}}{X_0} = D \left[1 - \left(\frac{D}{R_{\text{inc}} + D} \right)^N \right] \tag{7.9}$$

It can be seen that (7.9) reverts to (7.6) when N = 1 such that there is only one batch of magma and $R = R_{\text{inc}}$.

In the simple multistage upgrading model the amount of sulphide liquid remains constant and does not change as it interacts with the silicate melt. For this to occur the incoming magma must be sulphur saturated. If the incoming magma was sulphur over saturated, and contained sulphide liquid, this would add to the sulphide liquid already present and the total amount would increase. If the incoming magma were sulphur undersaturated it would dissolve some of the sulphide liquid as it interacts.

7.2.3 Multistage Dissolution Upgrading in an Open System

The open system model was modified to include sulphur dissolution as a means of upgrading the sulphide tenor by Kerr (2005) Incoming silicate magma with a metal content high enough to form an ore deposit can not have previously undergone sulphide liquid formation and segregation. The formation and segregation of a sulphide liquid will deplete metals from the silicate magma, leaving it unable to upgrade the sulphide liquid. If the incoming silicate magma is not carrying an entrained sulphide liquid it will be sulphide undersaturated (Kerr, 2005). In a mafic magma, S solubility increases with temperature and FeO content of the silicate melt, and decreases with pressure (Li, 2001). The controls on S solubility make it so that a rising metal-bearing mafic magma is unlikely to have previously saturated a sulphide liquid. The interaction of a sulphur-undersaturated silicate magma with sulphide liquid will dissolve some of the sulphide liquid into the infiltrating silicate magma.

The dissolution upgrading process is envisaged as a three-step process (Kerr, 2005), a simplified cartoon depicting the process is shown in Figure 7.5. As a new batch of silicate magma enters the system the metals are partitioned from the silicate magma to the sulphide liquid and a portion of the sulphide liquid is then dissolved back into the silicate magma. The dissolution of the sulphide serves to enrich, or load, the metals into the silicate magma. Partitioning between the metal-enriched magma and the sulphide liquid takes place again. For this second partitioning, both the amount of metals in the magma (X_0) and the R factor have been increased. This allows the remaining sulphide liquid to be upgraded, or become more enriched in metals than possible before dissolution. Although the process has been broken into three phases, it is actually an equilibrium process and exchange occurs between the sulphide liquid and silicate melt simultaneously. The removal of PGE from the sulphide liquid as it dissolves could be limited by a low carrying capacity of the silicate liquid. Work by Blaine et al. (2005) shows that at fO_2 on the FMQ buffer and 1300 °C a mafic magma can dissolve < 10 ppb of Pt.

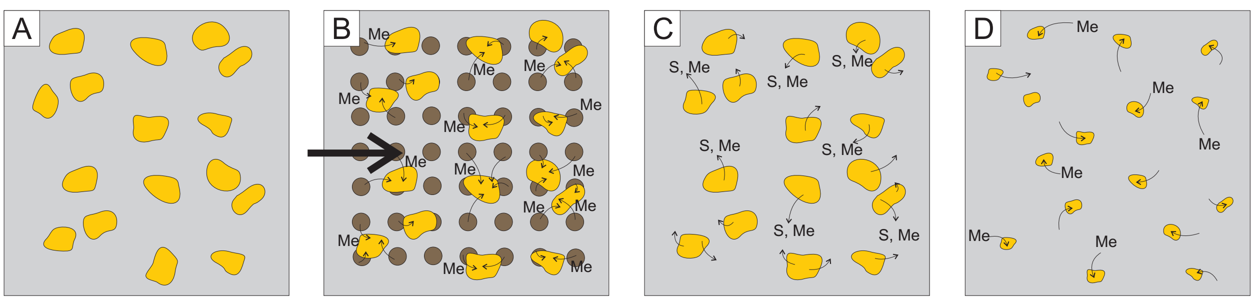

Figure 7.5: Cartoon illustration of the multistage dissolution upgrading process of Kerr (2005). A) Sulphide liquid (yellow) has formed within the silicate magma (grey). B) A new batch of metal bearing sulphur undersaturated magma (brown circles) enters the system. Metals are partitioned from the new magma into the sulphide liquid, enriching the sulphide metal tenor. C) The two magmas have mixed (grey) to form sulphur undersaturated magma, some of the S and metals from the sulphide liquid are dissolved back into the silicate magma. D) Due to dissolution of the sulphide liquid, the R factor has increased and metals are again partitioned into the sulphide liquid from the silicate magma. The total mass of sulphide has decreased and it has a higher sulphide metal tenor than originally.

The multistage-dissolution upgrading model introduces a new parameter, L, the incremental dissolution rate, or ‘‘loss factor’’. The loss factor is the proportion of the sulphide liquid that is dissolved by each discrete batch of magma entering the system and ranges between 0 (no loss), and 1 (all the sulphides are lost). Figure 7.6 shows the affects of loss factor on sulphide tenor. In the closed system model none of the sulphide liquid is dissolved. As the loss factor increases the amount of metal in the sulphide liquid is increased. As the loss factor becomes very large the increase in sulphide tenor decreases. Since the amount of sulphide is decreased by each successive batch of magma the R factor also increases. The R factor is now divided into two parts, the incoming incremental R factor (R'_{inc}) and the outgoing cumulative R factor (R_{cum}). The outgoing cumulative R factor is the total mass of silicate magma that has passed through the system divided by the amount of sulphide remaining.

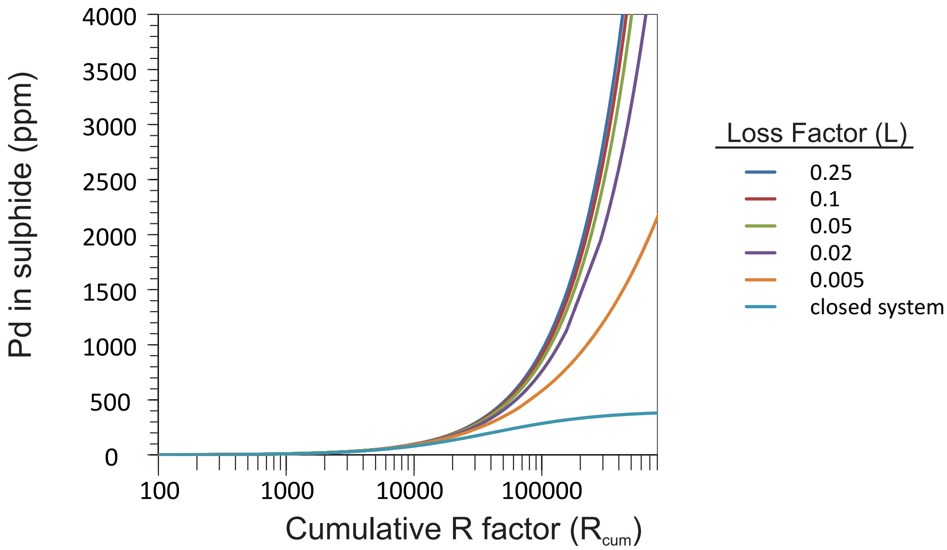

Figure 7.6: Loss factor dissolution plot. In the closed system model none of the sulphide liquid is dissolved. As the loss factor increases the amount of metal in the sulphide liquid is increased. As the loss factor becomes larger the increase in sulphide tenor decreases.

Dissolution of sulphide liquid into sulphur undersaturated silicate magma will increase the iron and sulphur content of the magma. It is expected that the increase in iron will be trivial where as the increase in sulphur could be significant. Ideally, if left in equilibrium, the unsaturated magma would dissolve sulphide liquid until it becomes saturated, but due to kinetic limitations the dissolution may not be complete. Using the mass fraction of sulphur in the sulphide liquid (FeS) as 0.365, the increase of sulphur in the silicate magma (ΔS) can be calculated using L and R_{inc}.

$$\Delta S = 0.365 \times (L/R'_{\text{inc}}) \times 10^6 \text{ppm} \tag{7.10}$$

The level of sulphur undersaturation in the magma is indicated by the ratio of L/R_{inc}. Using a range of sulphur solubility in mafic and ultramafic magmas from 800 to 2,000 ppm (Li, 2001) the value of L/R_{inc} could range from 0 (sulphur saturated magma) to 0.005 (e.g., $L = 0.5$ and $R'_{\text{inc}} = 100$. Values this low are unlikely, magma derived from partial melting of the mantle will contain some amount of sulphur.

The quantitative equations are derived in detail in Kerr (2005). The equation to calculate the amount of metal in the sulphide liquid after N batches of incoming magma is:

$$\frac{X_{\text{sulfN}}}{X_0} \cong \left(\frac{R'_{\text{inc}}D}{R'_{\text{inc}-LD}}\right)\left[1 - \left(\frac{D}{D + R'_{\text{inc}} - LD}\right)^N\right] \tag{7.11}$$

This equation has been simplified under the assumptions that $D \gg 1$ and $L \ll R'_{\text{inc}}$. It can be seen that equation (7.11) reverts to equation (7.9) when $L = 0$, indicating no sulphur dissolution. The calculation of the cumulative R factor after N batches of magma is given by:

$$R_{\text{cum}} = \frac{R'_{\text{inc}}}{L}\left[\left(\frac{1}{1-L}\right)^{N} - 1\right] \tag{7.12}$$

Systems modeled using open-system behaviour can achieve higher sulphide tenors than those modeled using closed-system behaviour. The higher sulphur metal contents come at the cost of lower total mass of sulphides. While the ore will be of higher grade, it will be a smaller ore body. Even with a small amount of dissolution upgrading the total mass of metals in the ore body decreases as a consequence of the higher grade. A potential consequence of dissolution upgrading is that if all of the sulphide liquid is dissolved back into the magma, the sulphide phase concentrating the metals no longer exists. This results in the metals being dispersed back into the magma.

7.3 Application to the Marathon Deposit

In this section the models introduced in Section 7.2 will be applied to the data from the Marathon deposit in an attempt to model the sulphide metal tenors calculated in Section 7.1 (Table 7.1). The Basal Zone (high sulphur low grade), Main Zone (moderate sulphur, moderate grade) and W-Horizon (low sulphur, high grade PGE) will be discussed. Research by Good (1992) showed the parental magma for the Two Duck Lake Gabbro has an olivine tholeiite composition.

Partition coefficients for the metals between sulphide liquid and silicate melt are shown in Table 7.2. There is a wide range of potential partition coefficients, particularly for Pt and Pd, which can range from 10^3 to 10^9. Due to the very large variation in partition coefficients, two groups will be examined separately. Low partition coefficients for Pt and Pd will include those up to 88,000 and high partition coefficients for Pt and Pd (by extension of its similar behaviour to Pt) will be those $> 10^7$.

Metal concentrations in the parental magma are unknown, and so the starting compositions used in the model are estimates. Average values of Ni and Cu in mafic magmas are generally < 200 ppm (Mungall, 2005). The concentrations of Pt and Pd within a mafic magma are also expected to be < 20 ppb (Crocket, 2002).

7.3.1 R Factor Model using low D values

Using the partition coefficients and initial magma composition described above, there was no single R value which could model all the the sulphide metal tenors in a mineralized zone. This section discusses the variations in R factor which were able to reproduce the sulphide metal tenor observed.

Table 7.2: Values of Partition Coefficients for Magmas near 1200°C and Oxygen Fugacity near the QFM

	Cu	Ni	Os	Ir	Ru	Rh	Pt	Pd	Au	Reference
Cpx/silicate liquid							1.5			Gaetani and Grove (1997)
Olivine/silicate liquid				2						Brenan et al. (2005)
					2.2	1.9	< 0.01			Brenan et al. (2003)
Spinel/silicate liquid										Righter et al. (2004)
Sulphide/ silicate liquid	1383	800		14000				23000	15000	Peach et al. (1990)
			30000	26000	6400		10000	17000	1200	Fleet et al. (1999)
				35000				43000		Peach et al. (1994)
				450000				33000		Peach et al. (1994)
							9100	88000		Stone et al. (1990)
							$> 10^9$			Pruseth and Palme (2004)
							$> 10^7$			Fonseca et al. (2009)
Mss/sulphide liquid	0.2	0.6-1.5		5	10	4	0.05	0.1	0.005	Fleet et al. (1999)

Table modified from Mungall (2005)

7.3.1.1 Closed System Model

The results for the closed system model are shown in Table 7.3 A. The Ni sulphide tenor values calculated are higher than those observed in the Basal Zone, Main Zone and W-Horizon at $R \sim 200$. To produce the Ni sulphide tenor values observed a Ni-depleted source is used. A Ni-depleted magma is formed by the early crystallization of olivine prior to saturation of sulphide liquid. With the Ni depleted source, the Basal Zone Ni sulphide tenor is modeled with $R < 100$ and at higher R values ($R >$ 15,000) it reaches the maximum Ni sulphide tenor (1% Ni in sulphide) which is observed in the Main Zone and W-Horizon. The Cu sulphide tenor in the Basal Zone is reached at $R \sim$1,000. For both the Main Zone and W-Horizon the low range of Cu sulphide tenor (5-13% Cu in sulphide) is reached at low R values of 15,000. The maximum values for Cu sulphide tenor (26-32% Cu in sulphide) are above the maximum value calculated in the closed system model. Pt and Pd sulphide tenors in the Basal Zone are modeled at $R \sim$200. The Pt and Pd sulphide tenors in the Main Zone require a range of R from 1,000-15,000. Only the lower range of the W-Horizon Pt and Pd sulphide tenors can be modelled in a closed system at very high $R >$ 1,000,000.

The observed Pd/Pt ratio is also shown in Table 7.3. The ratio of Pd/Pt between the mineralized zones has an overall range of 2.1-3.5. The ratio of Pd/Pt calculated in the R factor model is dependent on the value of R and the ratio of metals in the source. At low values of R Pd/Pt is close to that of the parental magma. As R factor is increased the ratio shifts towards the element with the higher partition coefficient. Using the tholeiitic parental magma composition requires very high R factors to reproduce the Pd/Pt observed in all of the mineralized zones.

7.3.1.2 Simple Multistage Upgrading Model

The results from the simple multistage upgrading model are very similar to the closed system model. The results for the model were calculated using a $R'_{\text{inc}} = 100$, simulating a conduit-like environment with a high degree of sulphide liquid and silicate melt interaction. The results are shown in Table 7.3 B.

To calculate Ni sulphide tenors in the range observed for all mineralized zones, a Ni depleted source is needed. With the Ni depleted source, the Basal Zone Ni sulphide tenor is modeled with $R \sim 200$ and at higher R values ($R > 4{,}000$) it reaches the maximum Ni sulphide tenor (1% Ni in sulphide) which is observed in the Main Zone and W-Horizon. The Cu sulphide tenor in the Basal Zone is reproduced at $R < 1{,}000$ which is lower than the R from the closed system model. The Cu sulphide tenor produces the lower range observed in both the Main Zone and W-Horizon at R from 1,000-10,000 however the maximum value from the model is still lower than the maximum observed value. The Pt and Pd sulphide tenors observed in the Basal Zone are produced at R values of 100-200. Main Zone Pt and Pd sulphide tenors are calculated at R of 1,000-15,000. In the W-Horizon only the lower range of Pt and Pd are modeled at moderate R values (10,000-100,000) and the upper ranges are not produced by this model even at very high R of 1,000,000.

7.3.1.3 Multistage-dissolution Upgrading Model

The multistage-dissolution upgrading model is shown in Table 7.3 C using $L = 0.02$ and $R'_{\text{inc}} = 100$. Figure 7.7 A depicts the results graphically. As in the previous models the Ni sulphide tenor for the Basal Zone, Main Zone and W-Horizon require a Ni depleted source to model the observed values at low R values. The Cu sulphide tenor for the Basal Zone is again calculated at low R_{cum} ($R_{\text{cum}} < 100$). The Cu sulphide tenor observed in the Main Zone and W-Horizon reach the mid-upper range observed in samples. The maximum Cu sulphide tenor is 19% Cu in sulphide and occurs at $R = 25{,}000$, which is much lower than the previous model. The Pt and Pd sulphide tenors in the Basal Zone are calculated at $R \sim 100$. In the Main Zone, Pt and Pd sulphide tenor is calculated at values of R_{cum} ~1,000-7,500 (lower than the simple multistage model). The low range of the W-Horizon is achieved starting at R_{cum} ~7,500 and the mid-range of the Pt and Pd tenor is achieved at R_{cum} >250,000. However at R_{cum} values this high, most of the original sulphide has been removed, and the fraction of sulphide liquid remaining is only 2%. The ratio of Pd/Pt calculated is lower than observed in all mineralized zones. The ratio of Pd/Pt increases at higher R values, and at $R > 250{,}000$ the ratio is 1.8, which is approaching the observed value.

The multistage dissolution model using a higher loss factor ($L = 0.03$) is shown in Table 7.3 D and Figure 7.7 B. The results for Ni sulphide tenor are the same as in the previous model. The Cu sulphide tenor for the Basal Zone is again reached at $R_{\text{cum}} < 100$. The maximum value for Cu sulphide tenor is 24% Cu in sulphide at $R = 250{,}000$ which is close to the maximum value observed in both the Main Zone and W-Horizon. The Pt and Pd sulphide tenors in the Basal Zone are reached at $R_{\text{cum}} < 100$. The Main Zone upper limit is reached by relatively low R values of 10,000. The lower range of W-Horizon Pt and Pd tenors are reached at $R =$ 10,000 and the mid-range at $R > 250,000$. The high end of the W-Horizon values are still much higher than can be modelled by sulphur dissolution upgrading.

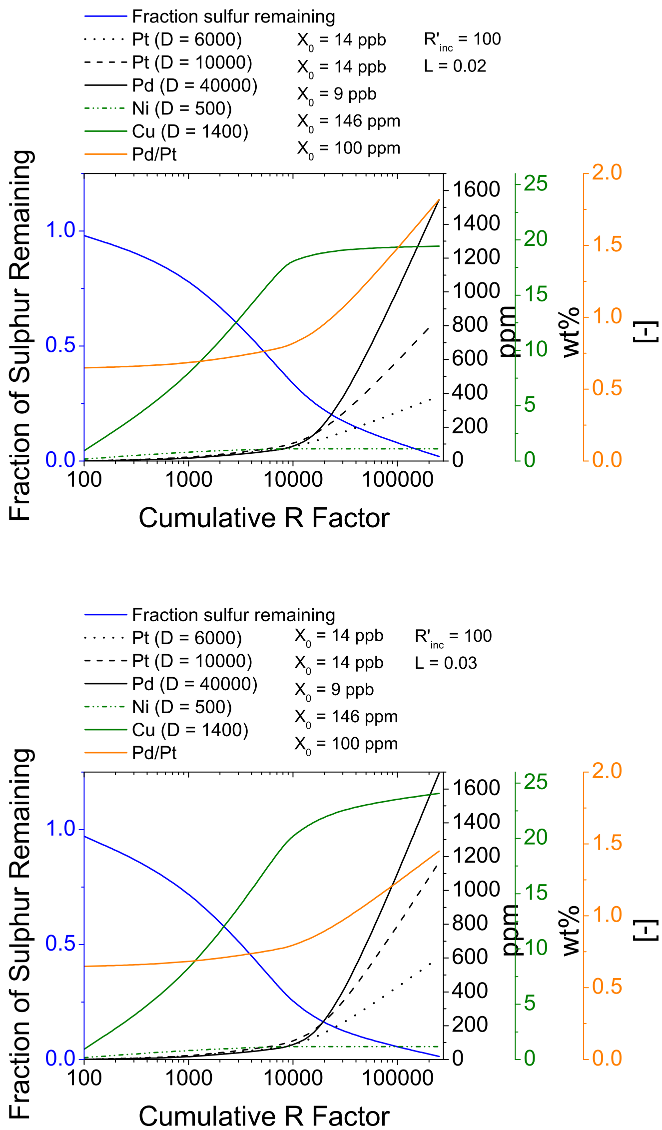

Figure 7.7: Multistage dissolution upgrading in an open system model using low partition coefficients. The colours of the curves correspond to the colour of axis.

Table 7.3: R Factor Modeling of Mineralization using low D values

Observed compositions (at 100% sulphide, Ni corrected for silicates)

	Ni (%)	Cu (%)	Pt (ppm)	Pd (ppm)	Pd/Pt
Basal Zone	0.1-0.3	6-8	1-3	1-3	2.1 ± 2.7
Main Zone	0-1	10-26	2-70	2-107	3.5 ± 1.5
W-Horizon	0-1	5-32	60-2600	133-3285	2.9 ± 1.7

Parental Magma Compositions

	Ni (ppm)	Cu (ppm)	Pt (ppb)	Pd (ppb)	Pd/Pt
Tholeiitic[1]	146	100	14	9	0.64
Tholeiitic[2]	20	100	14	9	0.64

Model results (metal concentrations in sulphides))

A. Closed System model using Tholeiitic[1] parental magma)

R Factor	Ni (D = 500) (%)	Ni[a] (D = 500) (%)	Cu (D = 1400) (%)	Pt (D = 10000) (ppm)	Pd (D = 40000) (ppm)	Pd/Pt
100	1.2	0.17	0.94	1.4	0.91	0.65
1000	4.9	0.67	5.8	12.7	8.8	0.69
15000	7.1	0.97	13	84	98.2	1.2
100000	7.3	1	14	127.3	257.1	2.02
1000000	7.3	1	14	138.6	346.2	2.5

B. Simple multistage upgrading model using Tholeiitic[1] parental magma (R'inc = 100))

R_{cum}	Ni (D = 500) (%)	Ni[a] (D = 500) (%)	Cu (D = 1400) (%)	Pt (D = 10000) (ppm)	Pd (D = 40000) (ppm)	Pd/Pt
100	1.2	0.17	0.93	1.4	0.9	0.65
1000	6.1	0.84	7	13.3	8.88	0.67
10000	7.3	1	14	88.2	79.5	0.9
100000	7.3	1	14	140	330.4	2.4
1000000	7.3	1	14	140	360	2.6

C. Multistage-dissolution upgrading model, Tholeiitic[1] parental magma (R'inc = 100 L = 0.02)

R_{cum}	f_{sulf}	Ni[a] (D = 500) (%)	Cu (D = 1400) (%)	Pt (D = 6000) (ppm)	Pt (D = 10000) (ppm)	Pd (D = 40000) (ppm)	Pd/Pt
100	0.98	0.17	0.93	1.38	1.39	0.898	0.65
1000	0.833	0.86	7.1	12.85	13.29	8.883	0.67
7500	0.4	1.1	17	68.67	80.85	63.11	0.78
10000	0.333	1.1	18	83.62	101.8	82.9	0.81
25000	0.167	1.1	19	144.7	201.4	194.7	0.97
250000	0.0196	1.1	19	384.4	849.9	1546	1.8

D. Multistage-dissolution upgrading model, Tholeiitic[1] parental magma (R'inc = 100 L = 0.03)

R_{cum}	f_{sulf}	Ni[a] (D = 500) (%)	Cu (D = 1400) (%)	Pt (D = 6000) (ppm)	Pt (D = 10000) (ppm)	Pd (D = 40000) (ppm)	Pd/Pt
100	0.97	0.17	0.93	1.38	1.39	0.898	0.65
1000	0.77	0.87	7.1	12.87	13.31	8.885	0.67
7500	0.31	1.2	19	71.51	82.97	63.55	0.77
10000	0.25	1.2	20	88.42	105.6	83.71	0.79
25000	0.12	1.2	23	164.6	219.4	199.4	0.91
250000	0.013	1.2	24	603	1168	1692	1.4

[a] Calculated with the Ni depleted Tholeiitic parental magma
[1] Using values from Kerr (2005) for the Tholeiitic parent of the Merensky Reef of the Bushveld Intrusion, South Africa
[2] Reduced amount of Ni in parental magma to model the Ni depleted sulphides

7.3.2 R Factor Model using high D values

The R factor models were computed using the high partition coefficients for Pt and Pd (D $= 10^7$). A prominent effect of using high partition coefficients is that the ratio of Pd/Pt becomes independent of the R factor. Unlike the previous modeling where Pd/Pt changes based on the R factor and the partition coefficients, partition coefficients this high always reproduce the Pd/Pt ratio of the source. Due to the independence of Pd/Pt on R factor, the parental magma composition was changed to reflect the average ratio observed in all of the mineralized zones. Since only the partition coefficients for Pt and Pd were changed the results for Ni and Cu are the same as in the previous section.

7.3.2.1 Closed System Model

In the closed system model (Table 7.4 A) the Pt and Pd sulphide tenors in the Basal Zone are reproduced using low R factors (< 100). The Main Zone is reproduced at $R \leq 15,000$. The lower range of the W-Horizon is modeled with $R = 15,000$ and the upper range with $R = 300,000$.

7.3.2.2 Simple Open System Model

The simple open system model (Table 7.4 B) reproduces the Basal Zone at $R \leq 100$. The Main Zone is reproduced at $R \leq 14,000$. The low end of the W-Horizon is calculated using $R = 95,500$ and the upper range at $R = 262,000$. As with the low partition coefficient model lower R values are required to model the mineralization.

7.3.2.3 Multistage-dissolution Upgrading Model

The multistage-dissolution upgrading model ($L = 0.02$ and $R'_{\text{inc}} = 100$) is shown in Table 7.4 C and Figure 7.8 A. The Main Zone is reproduced using $R = 13,900$. The low end of the W-Horizon is reproduced using $R = 90,600$ and the upper range using $R = 235,000$. The multistage-dissolution upgrading model ($L = 0.03$ and $R'_{\text{inc}} = 100$) is shown in Table 7.4 D 7.8 B. The Main Zone is reproduced using $R = 13,900$. The low end of the W-Horizon is reproduced using $R = 90,300$ and the upper range using $R = 234,000$.

Overall the main effect of changing to very high partition coefficients is that all of the models (closed system, simple multistage upgrading and multistage dissolution upgrading) produce much higher sulphide metal tenors. At the high range of R values ($\sim$ 250,000), the closed system values for Pd sulphide tenor are only 200 ppm lower than in the dissolution upgrading model. Using high partition coefficients multi-stage dissolution upgrading still produces the highest sulphide metal tenors for a given R value, however the difference between multi-stage dissolution upgrading and simple multistage upgrading is lower.

Table 7.4: R Factor Modeling of Mineralization using high D values

Observed compositions (at 100% sulphide, Ni corrected for silicates)

	Ni (%)	Cu (%)	Pt (ppm)	Pd (ppm)	Pd/Pt
Basal Zone	0.1-0.3	6-8	1-3	1-3	2.1 ± 2.7
Main Zone	0-1	10-26	2-70	2-107	3.5 ± 1.5
W-Horizon	0-1	5-32	60-2600	133-3285	2.9 ± 1.7

Parental Magma Compositions

	Ni (ppm)	Cu (ppm)	Pt (ppb)	Pd (ppb)	Pd/Pt
Tholeiitic[1]	146	100	5	14	2.8
Tholeiitic[2]	20	100	5	14	2.8

Model results (metal concentrations in sulphides))

A. Closed System model using Tholeiitic[1] parental magma)

R Factor	Ni (D = 500) (%)	Ni[a] (D = 500) (%)	Cu (D = 1400) (%)	Pt (D = 10^7) (ppm)	Pd (D = 10^7) (ppm)	Pd/Pt
100	1.2	0.17	0.94	0.5	1.4	2.8
1000	4.9	0.67	5.8	5	14	2.8
10000	7	0.95	12	49.5	139	2.8
100000	7.3	1	14	454.6	1273	2.8
300000	7.3	1	14	1154	3231	2.8

B. Simple multistage upgrading model using Tholeiitic[1] parental magma (R'inc = 100))

R_{cum}	Ni (D = 500) (%)	Ni[a] (D = 500) (%)	Cu (D = 1400) (%)	Pt (D = 10^7) (ppm)	Pd (D = 10^7) (ppm)	Pd/Pt
100	1.2	0.17	0.93	0.5	1.4	2.8
1000	6.1	0.84	7	5	14	2.8
14000	7.3	1	14	69.5	195	2.8
95500	7.3	1	14	455.4	1275	2.8
262000	7.3	1	14	1152	3227	2.8

C. Multistage-dissolution upgrading model, Tholeiitic[1] parental magma (R'inc = 100 L = 0.02)

R_{cum}	f_{sulf}	Ni[a] (D = 500) (%)	Cu (D = 1400) (%)	Pt (D = 10^7) (ppm)	Pd (D = 10^7) (ppm)	Pd/Pt
100	0.98	0.17	0.93	0.5	1.4	2.8
1000	0.83	0.86	7.1	5.0	14	2.8
13900	0.26	1.1	19	69.2	194	2.8
90600	0.052	1.1	19	448	1250	2.8
235000	0.021	1.1	19	1158	3241	2.8
250000	0.02	1.1	19	1231	3447	2.8

D. Multistage-dissolution upgrading model, Tholeiitic[1] parental magma (R'inc = 100 L = 0.03)

R_{cum}	f_{sulf}	Ni[a] (D = 500) (%)	Cu (D = 1400) (%)	Pt (D = 10^7) (ppm)	Pd (D = 10^7) (ppm)	Pd/Pt
100	0.97	0.17	0.93	0.5	1.4	2.8
1000	0.77	0.87	7.1	5.0	14	2.8
13900	0.19	1.2	21	69.3	194	2.8
90300	0.036	1.2	24	448	1250	2.8
234000	0.014	1.2	24	1157	3239	2.8
250000	0.013	1.2	24	1236	3460	2.8

[a] Calculated with the Ni depleted Tholeiitic parental magma
[1] Using values from Kerr (2005) for the Tholeiitic parent of the Merensky Reef of the Bushveld Intrusion, South Africa
[2] Reduced amount of Ni in parental magma to model the Ni depleted sulphides

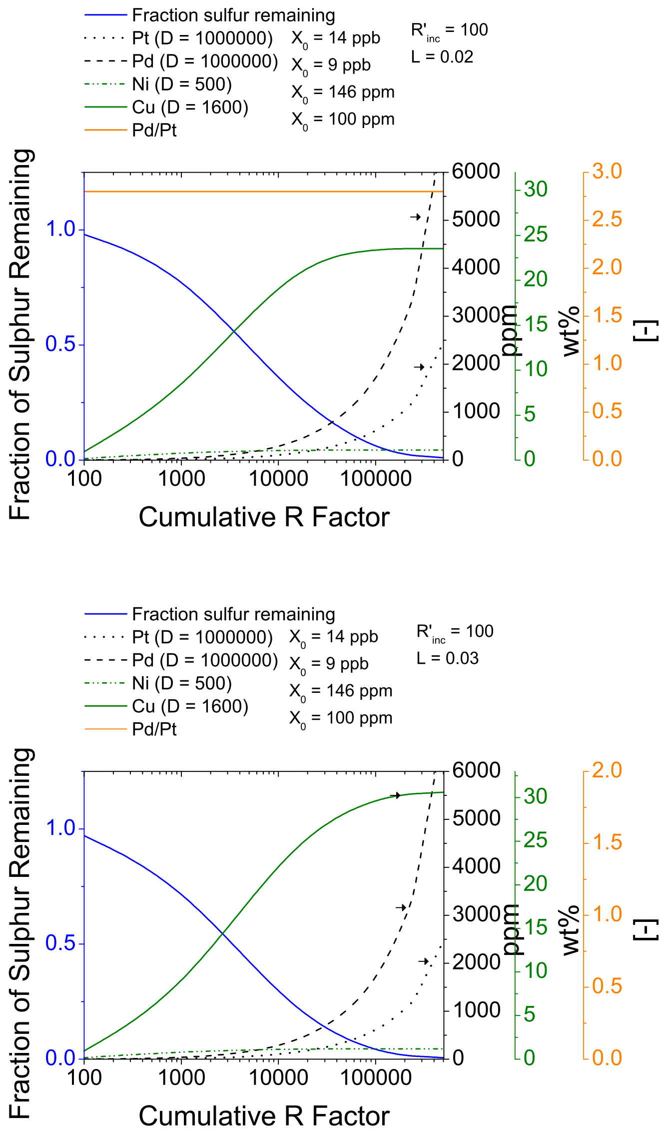

Figure 7.8: Multistage dissolution upgrading in an open system model using high partition coefficients. The colours of the curves correspond to the colour of axis.

7.3.3 Discussion of R Factor Modeling

The R factor model is commonly drawn upon to model sulphide tenors in magmatic sulphide deposits. It is clear from the results presented that the original closed system model gives values for the Basal Zone and Main Zone sulphides at reasonable R factors. In order to model the values of Pt and Pd in the W-Horizon, very high R factors are required, and these only calculate the minimum range of values of sulphide tenor observed. The simple open system multistage upgrading model produces higher results for sulphide tenor at the same R

factor as the closed system model.

The modeled values of Ni in sulphide are only close to the observed value at very low R factor values. Once R is greater than 200 the amount of Ni expected in the sulphide liquid is higher than observed. In order to account for this discrepancy the incoming magma could have been depleted in Ni prior to interacting with the sulphide liquid. A possible mechanism for this would be the crystallization of olivine in the magma chamber prior to entry in the conduit. Modeling the Ni sulphide tenor using a depleted Ni source reproduced observed values in all models, including multistage dissolution upgrading.

In the low partition coefficient calculations the observed high values of Pt and Pd sulphide tenors can only be produced using the multi stage dissolution upgrading model. As is shown in Table 7.3 section C and D at R_{cum} ~2,500-250,000 the model matches the mid range of the observed sulphide tenors. However at these high R_{cum} values only ~2% of the initial amount of sulphide liquid in the system remains.

The ratio of Pd:Pt is variable in the low partition coefficient models and depends on the R factor used in the calculation. If the parental magma had Pd:Pt of 1:2, then at higher R factors the modeled ratio reproduces the observed ratio of 3:1. By using the high partition coefficient models the dependence of the Pd:Pt ratio is removed and it is only based on the Pd:Pt in the parental magma. In order to model these results Pd:Pt in the parental magma needs to be changed to reflect the observed value.

The difference in R factor is lower between the dissolution upgrading and simple open system models using high Pd and Pt partition coefficients compared to low partition coefficients. The Cu sulphide tenor is not reproduced using the simple open system model. The Cu sulphide tenor only approaches observed values using the dissolution model. The use of the dissolution model is in agreement with the low modal abundance of sulphide minerals observed in the W-Horizon samples.

Chapter 8

Discussion and Conclusion

8.1 Marathon PGM-Cu Deposit Overview

The Marathon PGM-Cu deposit is located on the north shore of Lake Superior on the eastern margin of the Coldwell Igneous Complex. It was emplaced during the early stages of the mid-continent rift of North America as a ring dike structure. The formation of the mid-continent rift was a period of voluminous magmatic activity. Doming caused by thermal expansion and subsequent cauldron subsidence is attributed as a key process in the intrusion of the Eastern Gabbro (Shaw 1992). Repeated cycles of expansion created space for subsequent generations of gabbroic intrusions. The Two Duck Lake Gabbro (TDLG) intrusion occurred in the later stages of cauldron subsidence. This is supported by field evidence such as abundant Eastern Gabbro xenoliths within the TDLG and the chaotic geometry of the TDLG within the Eastern Gabbro. The TDLG is shown to swell and pinch in troughs and ridges within the footwall. Dikelets of TDLG emanate from the main body and stope into the Eastern Gabbro. Outcrops showing multiple generations of cross cutting TDLG are also observed.

The TDLG hosts the majority of the mineralization at the Marathon deposit. Overall the mineralogy of the TDLG is very consistent; the average composition is 60% plagioclase, 25% pyroxene, 6% olivine, 5% magnetite/ilmenite and accessory biotite and apatite. The TDLG has a characteristic ophitic texture, with subhedral to euhedral plagioclase and subhedral to anhedral olivine partially or fully enclosed within clinopyroxene grains. Grain size is predominantly medium (1 to 5 mm) to coarse (5 to 12 mm) and minor pegmatitic (1.2 to 8 cm) zones also occur. Pegmatitic zones comprise approximately 5-10% of the samples in this study. Transitions from medium grained to coarse grained material are both sharp and gradational. The TDLG samples are remarkably fresh, and the majority of secondary alteration and hydrous minerals observed are only present locally and within confined zones. The primary secondary alteration mineral assemblage is chlorite, epidote, sericite, amphibole and serpentine

The W-Horizon forms a continuous sheet that extends north-south for over 1 km and extends up to 300 m down dip to the east. Thickness of the zone is variable, between 1-30 m. Within diamond drill holes separate zones of W-Horizon mineralization are observed separated by unmineralized gabbro. The W Horizon is characterized by high Pt + Pd, low S, low Cu/Pd, high Cu/Ni and low S/Se. The Main Zone has higher S, higher Cu/Pd and higher S/Se. The separation between the W-Horizon and Main Zone is variable, and can range from 5 to 50 m.

8.2 Petrographic Observations

The detailed petrography of the W-Horizon shows that the W-Horizon and Main Zone have similar silicate mineral assemblages and abundances. The two zones have different silicate-sulphide relationships, sulphide mineral assemblages and platinum group mineral assemblages. The differences between the two zones supports the hypothesis that they formed through fundamentally different processes.

8.2.1 Silicate-Sulphide Relationships

The silicate-sulphide relationships between the W-Horizon and Main Zone samples differ. Within the W-Horizon sulphide minerals are predominantly interstitial (in decreasing order) to: plagioclase, clinopyroxene, olivine, oxide minerals and biotite. Main Zone sulphide minerals in this study are predominantly interstitial (in decreasing order) to: plagioclase, clinopyroxene, olivine, secondary alteration minerals, oxides and biotite. Previous studies Watkinson and Ohnenstetter (1992), Watkinson and Jones (1996), Dahl et al. (2001) and Barrie et al. (2002) observed the sulphide minerals in association with secondary alteration minerals and with pristine unaltered silicate minerals in the Main Zone.

8.2.2 Sulphide Mineral Assemblages

The sulphide mineral assemblage and the abundance of sulphide minerals contrast between the Main Zone and W-Horizon. The Main Zone contains more abundant sulphide minerals whereas the W-Horizon has higher PGE grades.

Within the Main Zone the sulphide mineral assemblage is chalcopyrite, pyrrhotite, pentlandite, bornite and pyrite. The ratio of chalcopyrite to pyrrhotite is higher at the top of the Main Zone with chalcopyrite>pyrrhotite and decreases down hole. Towards the bottom of the Main Zone, the ratio changes to pyrrhotite>chalcopyrite. Pentlandite, bornite and pyrite occur as a very minor component of the sulphide mineral assemblage. The grain size of sulphide minerals in the Main Zone is variable, ranging from fine grained (less than 1 mm) to coarse grained. Pyrrhotite and chalcopyrite typically occur in association with chalcopyrite replacing pyrrhotite along rims. Pentlandite is observed in both pyrrhotite, and chalcopyrite. Within pyrrhotite, pentlandite occurs as exsolution lamellae. In chalcopyrite, pentlandite occurs as granular masses with chalcopyrite filled fractures. Chalcopyrite grains with pentlandite are not observed to contain pyrrhotite. Bornite is rare within Main Zone samples, and most commonly occurred as exsolution lamellae within chalcopyrite grains. Pyrite is rare and occurs in association with heavily serpentinized olivine grains.

The W-Horizon sulphide mineral assemblage is chalcopyrite >= bornite > pentlandite > pyrrhotite. No correlation is observed between chalcopyrite:bornite with depth, or to total PGE grades. It should be noted that due to the trace amount of sulphide minerals typically present in the W-Horizon, a detailed petrographic study relating bornite abundance to PGE grades is not possible. Sulphide minerals in the W-Horizon are predominantly very fine to medium grained. Interstitial grains are larger than sulphide inclusions in silicate minerals. Bornite almost always occurs in association with chalcopyrite, either as intergrowths, or as fine exsolution lamellae (1 μm to 50 μm in width). Bornite is rarely observed as independent grains without associated chalcopyrite. Pentlandite occurs as granular masses within chalcopyrite, and contains chalcopyrite-filled fractures. Pyrrhotite is only observed in the low grade W-Horizon samples of DDH-441. The pyrrhotite in DDH-441 has chalcopyrite rims as observed in the Main Zone.

8.2.3 Platinum Group Minerals

A detailed study of the platinum group minerals within the W-Horizon is beyond the scope of this project. PGM identified from a limited amount of SEM work in this study are all associated with sulphide minerals. A detailed study of PGM shows that they are markedly different between the Main Zone and W-Horizon (Puritch et al., 2009). Within the Main Zone the PGM hosts are sulphide minerals >= hydrous silicate minerals > within plagioclase boundaries. The PGM assemblage is mainly dominated by Kotulskite-Sobolevskitess (34.9%), Mertierite-II (16.1%), Sobolevskite (10.1%) Kotulskite (9.9%), Sperrylite (6.3%), Hollingworthite (5.6%). Within the W-Horizon the dominant PGM hosts are sulphides (53.7%) > plagioclase boundaries (25%) > other PGMs (16.5%) > hydrous silicates(4.3%). The PGM assemblage is dominated by Zvyagintsevite (41.8%), Palladinite (15.5%), Au,Ag and Alloys (7%) and Telargpalite (5.5%). The grain size of PGM are similar between the two zones, with 60% of PGM grains < 60 μm in size.

8.3 Magmatic or Hydrothermal Origin for the W-Horizon

In the literature published on the Marathon PGM-Cu deposit both magmatic and hydrothermal origins have been proposed by previous studies which focused on the Main Zone and Footwall Zone mineralization. Key evidence for a hydrothermal model includes an observed increase in alteration minerals associated with mineralization (Ohnenstetter et al. 1991, Watkinson and Ohnenstetter 1992, Watkinson and Jones 1996, Dahl et al. 2001, Barrie et al. 2002 and Samson et al. 2008), an observed association of mineralization and pegmatitic gabbro (Dahl et al. 2001 and Barrie et al. 2002), complexly zoned crystals of atokite-zvyagintsevite and hollingworhite interpreted to have a hydrothermal origin (Watkinson and Ohnenstetter, 1992) and the distribution of metals (high Cu and high Pd) which is unusual for a magmatic deposit (Barrie et al., 2002). Although hydrous minerals are observed in association with mineralization in the Main Zone the hydrous minerals are not pervasive and are consistent with a post-mineralization formation from fluids (Good and Crocket, 1994). Results of whole rock geochemistry and major element mineral chemistry show that the coarse grained Two Duck Lake Gabbro and the pegmatitic Two Duck Lake Gabbro had the same composition (Good and Crocket, 1994). All mineralization at the Marathon deposit is Ni-poor and this is modeled by removal of Ni from the system by early crystallization of olivine.

Observations of the Main Zone in this study agree with those of Good (1992), Good and Crocket (1994) and Puritch et al. (2009). Although an increase in the amount of secondary alteration minerals within the Main Zone mineralization is observed, they are not pervasive and occur with primary magmatic sulphides. The W-Horizon sulphide minerals samples display primary magmatic textures and occur in predominantly pristine unaltered TDLG, supporting a magmatic origin.

Zone refining is proposed by Barrie et al. (2002) to model the Main Zone mineralization. In this model source areas of crystalline or nearly crystalline rocks are fluxed by a volatile rich fluid which depletes the incompatible elements (including Cu and PGE) and transports them from the source. The volatile rich fluxing fluid becomes further enriched in incompatible elements as it passes through and scavenges the incompatible from more rocks. When sulphur saturation occurs within the fluxing fluid both sulphur and the incompatible elements are deposited.

Zone refining is not suggested by this research because there is no evidence of the PGE being scavenged from the rocks below the W-Horizon, values of 10-20 ppb Pt and 10-50 ppb Pd are commonly observed in the TDLG below the mineralization. The two intersections of W-Horizon mineralization observed in DDH-369 are also not consistent with the zone refining model. These two zones are separated by unmineralized TDLG which does not show any signs of PGE-scavenging. If the lower W-Horizon was formed first the second zone refining fluid would have either deposited its metals into this zone or it would have dissolved all of the sulphide minerals and PGE into the fluid. In both cases the result would have been the formation of a single W-Horizon intersection. If the top W-Horizon was the first to form from zone refining all of the rocks below it would have been depleted in PGE and there would not have been a source for a second zone refining fluid to form the lower W-Horizon. Two separate zone refining events are unlikely as the source material for PGE would be depleted and a second zone refining event would not become enriched in metals.

8.4 Deposition as a PGM Reef

The W-Horizon is located within the centre of a thick package (up to 300 m thick) of gabbro, and is not associated with any distinct change in mineral assemblage or any notable change in whole rock geochemistry. The formation of the W-Horizon as reef-style mineralization is unlikely as there are no chemical changes observed to suggest changing conditions that may explain the trigger of sulphide saturation. The transition from ultra-mafic to mafic rocks is an example of conditions that could trigger sulphide saturation as described by Maier and Groves (2011)

Reef deposits such the Sonju Lake Intrusion (Miller, 1999) and the Skaergaard Intrusion Andersen et al. (1998) display PGE depletion above the reef. When sulphide liquid crystallizes it settles through the magma chamber, sequestering chalcophile elements as it descends. This creates a zone with PGE depletion above the reef. There is no depletion signature above the W-Horizon where values for Pt are commonly 10-20 ppb and Pd are 20-50 ppb. The ratio of Cu/Pd is an indicator of PGE scavenging from a melt and will increase as PGE are removed (Barnes et al., 1993). The value of Cu/Pd is only slightly elevated ~10 m above the W-Horizon in DDH-306, DDH-368, DDH-369 (W-Horizon 1 and 2), and 30 m above the W-Horizon in DDH-441. This shows that the magma above the W-Horizon is not extensively scavenged of PGE. A very high amount of scavenging is required to produce the high PGE values within the W-Horizon.

High grade zones with no vertical depletion signatures are explained by intrusion in a conduit-like or sill system with flow in a primarily horizontal direction. Upgrading in the horizontal direction will not leave traces of depletion above or below the mineralization.

8.5 Physical Emplacement Conditions

The textural and geochemical characteristics of the TDLG are best explained by a model in which the gabbros intrude as multiple stacked intrusions (or sills) in a dynamic conduit system during a period of prolonged magmatic activity. In outcrops of TDLG dynamic layering, bands defined by abrupt changes in modal composition and grain size, are visible. Similar bands are described at the Skaergaard Intrusion (McBirney and Nicolas, 1997) and the Partridge River Intrusion (Miller, 1999). These bands are also cut by younger generations of TDLG. Individual TDLG intrusive events were thin, typically on the meter-scale. Similar thin sills are also common in other intrusions such as the Partirdge River Intrusion in the Duluth Complex (Ripley et al., 2007).

The dynamic layering in the TDLG results in changes of modal mineral assemblage over small distances (centimeter to meter scale). The intrusion of a crystal slurry in a conduit system results in physical sorting of mineral phases. This explains the features observed in the TDLG such as changes in rock composition (such as pyroxenite, dunite and gabbro) over decimeter thick intervals and gabbroic rocks containing greater than 10 modal% apatite.

Multiple intrusions in a dynamic conduit system is also supported by the lithogeochemical results of the drill holes in this study. Results between adjacent drill holes were highly variable and major trends were not correlatable. None of the drill holes shows single continuous trends. Each drill hole has micro-trends, shown by smoothly varying parameters (such as Mg#) followed by breaks and a large change. These breaks mark the transition between new intrusive events. Increases in incompatible elements show a direct correlation to increased apatite, a process which can be explained by the accumulation of apatite (a phase which sequesters incompatible elements).

The results from the olivine microprobe analysis also support the intrusion of a crystal slurry from a large source. Large trends representing fractional crystallization in a large magma chamber (such as decreasing Mg# with increasing height) are not observed. Rather, within each drill hole several micro-trends (on the meter to decimeter scale) are seen in the olivine compositions. The breaks in the trends represent new pulses of magma into the system. Trends of increasing Ni at constant Mg# are caused by multiple intrusions of a magma from the same source rather than a internal fractionation of a single event. The Mg# of olivine grains is dependent on the temperature of the intrusive magma. Mg# trends show that the individual intrusive events corresponded with frequent temperature changes in the crystallizing magma, and the highest temperature olivine grains are not always at the top of a sill (e.g., DDH-306 and DDH-441). Reversals in Mg# (decreasing with increasing depth) are caused by slumping of accumulated olivine. Olivine grains collect on the edge of the conduit system, become unstable and slump into the channel. Slumping causes the later-formed olivine crystals from the top of the crystal pile to move to the bottom. This results in reversals of Mg#.

8.6 R Factor and Multi-stage Dissolution Upgrading

Modeling the sulphide metal tenors of the Main Zone is possible using the closed system or simple open system R factor models. These models are able to produce the low Ni sulphide tenors observed using a Ni-depleted source magma. These magmas had Ni removed by the early formation of olivine in the system. The low to medium range of Cu sulphide metal tenors are produced using moderate R values of 10,000. The higher range of Cu sulphide tenors are above the maximum values calculated using these models. The Pt and Pd sulphide tenors observed are calculated with higher R values in the range of 500,000.

The Ni and Cu sulphide tenors in the W-Horizon are similar to the Main Zone and can be modeled in the same manor. However, only the lower range of W-Horizon Pt and Pd sulphide metal tenors can be modeled using the closed system and simple open system R factor models. The average Pt and Pd sulphide metal tenors are much higher than can be produced by a closed system or simple multistage upgrading.

Another process is required to produce the very high Pt and Pd sulphide metal tenors observed in the W-Horizon. The multistage dissolution upgrading model of Kerr and Leitch (2005) produces the values observed in the W-Horizon. The mid-range of W-Horizon Pt and Pd tenors are modeled using accepted partition coefficients (10,000-40,000 for Pt and Pd), incremental batches of magma with an R factor of 100 and a sulphur loss factor of 2%. The low to mid range of the W-Horizon sulphide tenors are produced at R = 25,000-250,000, however the upper range of Pt and Pd tenors were at the upper limits of this model. Multistage dissolution upgrading also produces a low sulphur high tenor ore, which matches the observations of the W-Horizon.

8.7 Evidence for Sulphur Loss

The examination of S/Se ratios reveals distinct trends between Main Zone and W-Horizon samples. The ratio of S/Se is lower in the W-Horizon than the Main Zone, and is attributed to S-loss in the W-Horizon. As S is removed from the system, Se will remain in the sulphide liquid and increase S/Se ratio. A continuum is observed between Main Zone, low grade W-Horizon and high grade W-Horizon samples. This supports varying degrees of upgrading, depending on flow in the conduit system and the amount of upgrading undergone.

The change in mineral assemblage from S-rich, Cu-poor in the Main Zone to S-poor, Cu-rich in the W-Horizon also indicates that S-loss has occurred. Removal of sulphur from the system changes the sulphide mineral assemblage from chalcopyrite and pyrrhotite dominant in the Main Zone to chalcopyrite and bornite dominant in the W-Horizon. As S is removed while Cu increases the stable mineral assemblage changes to phases which contain more Cu (such as bornite from chalcopyrite). Within the W-Horizon bornite occurs as exsolution lamellae within chalcopyrite and pentlandite is observed within chalcopyrite. Both of these features are interpreted to represent the removal of S while Cu and Ni remain in the sulphide liquid.

Within Main Zone and W-Horizon samples chalcopyrite grains are commonly rimmed by magnetite. Electron microprobe analyses of these magnetite rims reveals that they contain very low levels of Ti, and are near Fe end-member. This contrasts with the magmatic magnetite within the TDLG, where Ti is ubiquitous and magnetite always occurs with ilmenite exsolution bands. No distinct trends of magnetite rim abundance are observed between the Main Zone and W-Horizon. The magnetite rims on chalcopyrite are interpreted to indicate that S-loss has occurred. As S is removed from the system, Fe is left behind and forms the Ti-depleted magnetite rims. Sulphur removal to form the magnetite rims occurs as a late stage event, after the crystallization of the sulphide minerals, and is not the same process which formed the W-Horizon. The presence of magnetite rims on chalcopyrite in both the Main Zone and W-Horizon, and a lack of correlation between magnetite rims and increased PGE supports magnetite rims formed by late stage sulphur removal.

8.8 Sulphide Tenor and Metal Ratios

The Main Zone and W-Horizon are easily distinguishable by their Pt and Pd sulphide metal tenors. The Ni sulphide metal tenor is similar between the two zones (up to 1% Ni in sulphide), as is the Cu sulphide tenor (average of 12% Cu in sulphide). The Pt sulphide tenor averages 11 ppm in the Main Zone and 600 ppm in the W-Horizon. The Pd sulphide tenor shows similar trends with an average value of 13 ppm in the Main Zone and $>$ 1,000 ppm in the W-Horizon. There is a high degree of variability in the sulphide metal tenors between the four drill holes of the study.

In plots of metals vs. S and Au/Pd vs. Pd/Cu, two distinct groups are observed. The high grade W-Horizon samples (DDH-306, DDH-368 and DDH-369) form one distinct group whereas DDH-306 Main Zone, DDH-368 Main Zone and DDH-441 W-Horizon form another. Some overlap between the two groups is observed, and results show a continuous trend. The overlap and smooth trend between the two groups of samples indicates that the upgrading process in the W-Horizon began on sulphide liquid with a similar composition to the Main Zone. Samples undergoing a high degree of upgrading have a stronger affinity for W-Horizon characteristics, and those with a low amount of upgrading have an affinity for Main Zone Characteristics (such as DDH-441 W-Horizon).

The accumulation of sulphide in the magmatic conduit system is not uniform throughout the deposit. Depending on the physical characteristics of sulphide liquid traps and flow dynamics the initial amount of sulphide liquid changes with location. The initial amount of sulphide liquid will then determine the sulphide metal tenors resulting from upgrading. This behaviour is seen in the plots of metals vs. Cu/S and Pt and Pd vs. S. There is no single trend in either of these plots, the highest grades in the sample suite do not occur at the highest Cu/S (a proxy for increasing bornite) or the lowest amount of S (representing S-loss). The trends are apparent within individual W-Horizon intersections where the highest Pt and Pd values occur at high Cu/S and low S values in that sample set. These variations are a result of the initial conditions of the sulphide liquid before upgrading and the magma flow history through the location.

As an example, consider two locations within the conduit containing sulphide, one with a higher initial amount of sulphide liquid than the other. Both undergo the same amount of sulphur dissolution upgrading so they upgrade their Pt and Pd sulphide metal tenor. The location containing a higher initial amount of sulphide will have maximum Pt and Pd values at higher S and lower Cu/S than the location which had a lower initial amount of S. A similar example is two locations with the same amount of initial sulphide, but one has a greater amount of flow through by upgrading magmas. The location with higher flow through will have higher Pd and Pt values at lower S and higher Cu/S. This is why samples from this study do not necessarily have the highest grades at the lowest S values, or with samples showing the highest amount of S-removal.

8.9 A Model for the W-Horizon

The TDLG was emplaced during the mid-continent rift system of North America, a period of voluminous magmatic activity. The first stage is the emplacement of a large magma chamber which serves as a reservoir for the intrusion. In this chamber both plagioclase and olivine crystallize to form a crystal mush. The early segregation of olivine removes Ni from the system, and causes the low Ni tenor in the sulphide ores.

The TDLG then intrudes into the country rock at shallow levels. The TDLG assimilates the S-bearing Archean felsic country rock to become contaminated. This forms a sulphide liquid within the silicate melt. The sulphide liquid pools and gathers near the base of the footwall. The TDLG continues to intrude as a crystal mush in a series of stacked sills in magma conduits. The pathway through the conduits that the intrusions take are variable and can be highly erratic. The unmineralized zones are formed when magma pulses do not interact with the sulphide liquid. Pulses of magma which interact with the sulphide liquid can transport it within the conduit system. Segregation and physical traps sequester the sulphide liquid within the conduit system forming localized zones enriched in sulphide liquid. When the pulses interact with the sulphide liquid it undergoes multistage dissolution upgrading. The end result is a zone containing trace sulphur and very high metal tenors. As this is a highly dynamic process in a complex environment not all zones had the same initial amount of sulphide and not all zones undergo the same amount of dissolution upgrading. This results in a highly variable ore, with inconsistent geochemistry and sulphide metal tenors.

8.10 Conclusion

The Two Duck Lake Gabbro hosts the Main Zone and W-Horizon. Within the TDLG there are no mineralogical or geochemical differences between the mineralized and unmineralized zones. The sulphide mineral assemblage, platinum group mineral assemblage and sulphide tenor differ between the Main Zone and W-Horizon. These differences indicate that a different process is responsible for the formation of the W-Horizon. As there is no evidence for large scale hydrothermal alteration in the W-Horizon, a magmatic model is proposed. The W-Horizon was formed by multistage dissolution upgrading in a dynamic system and is supported by the physical and chemical evidence.

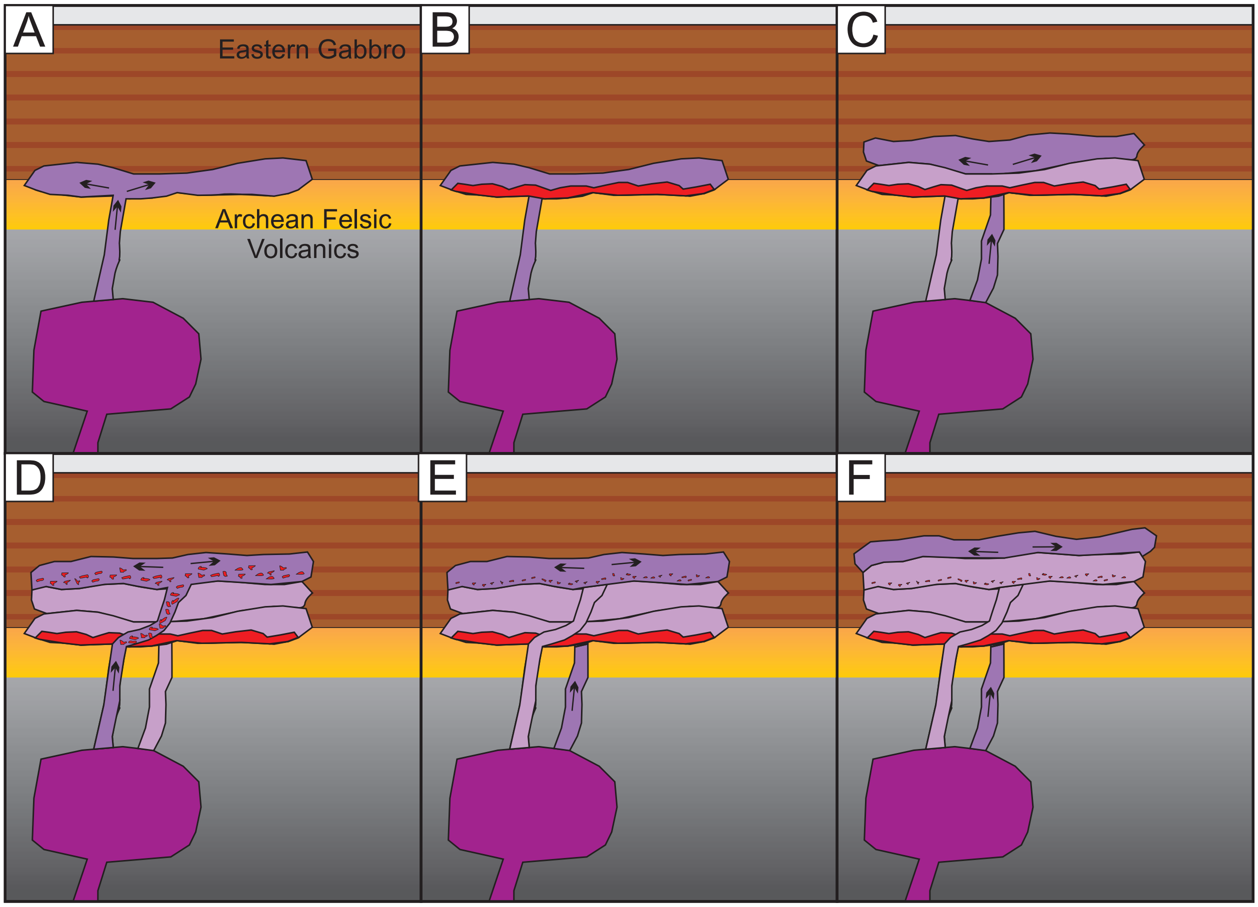

Figure 8.1: A simplified cartoon model for the formation of the W-Horizon. Dark purple depicts the magma pulse active in each panel and arrows depict magma flow.
(**A**) Emplacement of a low level magma chamber where plagioclase and olivine crystallize. This depletes the melt in Ni and forms a crystal mush. The crystal mush intrudes into higher levels into the Archean felsic volcanics. (**B**) The intruding magma assimilates the archean felsic volcanics and becomes sulphur saturated. (**C**) New pulses of magma intrude without interacting with the sulphur saturated melt forming unmineralized gabbro. (**D**) A pulse of magma intrudes through the sulphur saturated gabbro, picks up sulphide liquid and carries it into the conduit system where it collects in traps. (**E**) New pulses of sulphur undersaturated magma travel through the conduit containing previously deposited sulphide liquid. Interaction of the new magma with the sulphide liquid causes dissolution upgrading. The result is a lower total amount of sulphide liquid containing a higher PGE and Cu tenors and the addition of S into the silicate magma. (**F**) Subsequent pulses of magma intrude to higher levels and form sills of unmineralized gabbro.

References

Andersen, J., H. Rasmussen, T. Nielsen, and J. Ronsbo, 1998: The Triple Group and the Platinova gold and palladium reefs in the Skaergaard Intrusion; stratigraphic and petrographic relations. *Economic Geology*, **93 (4)**, 488--509.

Arndt, N., 2011: Insights into the Geologic Setting and Origin of Ni-Cu-PGE Sulfide Deposits of the Norilsk-Talnakh Region, Siberia. *Reviews in Economic Geology v. 17*, 199--215.

Arndt, N., G. Czamanske, R. Walker, C. Chauvel, and V. Fedorenko, 2003: Geochemistry and Origin of the Intrusive Hosts of the Norilsk-Talnakh Cu-Ni-PGE Sulfide Deposits. *Economic Geology*, **98**, 495--515.

Auclair, G., Y. Fouquet, and M. Bohn, 1987: Distribution of selenium in high-temperature hydrothermal sulfide deposits at 13 degrees North, East Pacific Rise. *Canadian Mineralogist*, **25 (4)**, 577--587.

Barnes, S., J. Couture, E. Sawer, and B. C., 1993: Nickel-copper occurrences in the Belleterre-Angliers Belt of the Pontiac Subprovince and the use of Cu-Pd ratios in interpreting platinum-group element distributions. *Economic Geology*, **88**, 1402--1418.

Barnes, S.-J., 2004: Platinum-group element distribution in the Main Zone and Upper Zone of the Bushveld Complex, South Africa. *Chemical Geology*, **208 (1-4)**, 293--317.

Barnes, S.-J., D. Savard, L. P. Bédard, and W. Maier, 2009: Selenium and sulfur concentrations in the Bushveld Complex of South Africa and implications for formation of the platinum-group element deposits. *Mineralium Deposita*, **44 (6)**, 647--663.

Barrie, C., A. MacTavish, P. Walford, R. Chataway, and R. Middaugh, 2002: Contact-type and magnetitite reeftype Pd-Cu mineralization in ferroan olivine gabbros of the Coldwell Complex, Ontario. *The geology, geochemistry, mineralogy and mineral beneficiation of platinum-group elements: Canadian Institute of Mining, Metallurgy and Petroleum Special*, **54 (l)**, 321--338.

Bethke, P. and P. Barton, 1971: Distribution of some minor elements between coexisting sulfide minerals. *Economic Geology*, **66 (1)**, 140--163.

Blaine, F., R. Linnen, F. Holtz, J. Gagnon, and G. Brugmann, 2005: Partitioning and vapour transport of Pt at magmatic conditions. *Abstracts of the 15th annual Vapor and the Transport of Metals Goldschmidt conference*, **10**, 736.

Brenan, J., W. McDonough, and R. Ash, 2005: An experimental study of the solubility and partitioning of iridium, osmium and gold between olivine and silicate melt. *Earth and Planetary Science Letters*, **237 (3-4)**, 855--872.

Brenan, J., W. McDonough, and C. Dalpé, 2003: Experimental constraints on the partitioning of rhenium and some platinum-group elements between olivine and silicate melt. *Earth and Planetary Science Letters*, **212 (1-2)**, 135--150.

Butler, J., 2012: *Platinum 2012*. Johnson Matthey Public Limited Company, Hertfordshire, 64 pp.

Campbell, I. and A. Naldrett, 1979: The influence of silicate: sulfide ratios on the geochemistry of magmatic sulfides. *Economic Geology and the Bulletin of the Society of Economic Geologists*, **74 (6)**, 1503--1506.

Chaffee, M., J. Miller, P. Hollings, G. Heggie, A. MacTavish, and B. Bandli, 2012: Petrographic and geochemical study of the hybrid rock unit associated with the Current Lake Intrusive Complex, Magma Metals Thunder Bay North Property. *Institute on Lake Superior Geology Proceedings, 58th Annual Meeting, Thunder Bay, Ontario, Part 1 - Proceedings and Abstracts, v. 58, part 1*, P. Hollings, Ed., Institute on Lake Superior Geology, 19--21.

Cox, R., L. Bédard, S.-J. Barnes, and M. Constantin, 2007: Selenium distribution in magmatic sulfide minerals. *Diversification de L'Exploration Minérale au Québec*, **418**.

Crocket, J., 2002: Platinum-group element geochemistry of mafic and ultramafic rocks. *The Geology, Geochemistry and Mineral Beneficiation of Platinum-Group Elements. Special Volume*, **54**, 177--210.

Dahl, R., D. Watkinson, and R. Taylor, 2001: Geology of the Two Duck Lake Intrusion and the Marathon Cu-PGE Deposit, Coldwell Complex, Northern Ontario. *Exploration and Mining Geology*, **10 (1-2)**, 51--65.

Davis, D. and J. Paces, 1990: Time resolution of geologic events on the Keweenaw Peninsula and implications for development of the Midcontinent Rift system. *Earth and Planetary Science Letters*, **97 (1-2)**, 54--64.

Ding, X., E. Ripley, and C. Li, 2012: PGE geochemistry of the Eagle NiCu(PGE) deposit, Upper Michigan: constraints on ore genesis in a dynamic magma conduit. *Mineralium Deposita*, **47 (1-2)**, 89--104.

Dreibus, G., H. Palme, B. Spettel, J. Zipfel, and H. Wanke, 1995: Sulfur and selenium in chondritic meteorites. *Meteoritics*, **30**, 439--445.

Fleet, M., J. Crocket, M. Liu, and W. Stone, 1999: Laboratory partitioning of platinum-group elements (PGE) and gold with application to magmatic sulfide-PGE deposits. *Lithos*, **47 (1-2)**, 127--142.

Fonseca, R. O., I. Campbell, H. S. C. ONeill, and C. M. Allen, 2009: Solubility of Pt in sulphide mattes: Implications for the genesis of PGE-rich horizons in layered intrusions. *Geochimica et Cosmochimica Acta*, **73 (19)**, 5764--5777.

Gaetani, G. and T. Grove, 1997: Partitioning of moderately siderophile elements among olivine, silicate melt, and sulfide melt: Constraints on core formation in the Earth and Mars. *Geochimica et Cosmochimica Acta*, **61 (9)**, 1829--1846.

Good, D., 1992: Genesis of the Marathon Cu-Platinum-Group Element Deposit, Port Coldwell Alkalic Complex, Ontario. Phd thesis, McMaster University, 203 pp.

Good, D., 2008: Geology of the Marathon Deposit. Tech. rep., Marathon-PGM Internal Report.

Good, D., 2010: Applying Multistage Dissolution Upgrading and 3d-GIS to Exploration at the Marathon Cu-PGE Deposit, Canada. *Abstracts, 11th International Platinum Symposium*, 1--4.

Good, D. and J. Crocket, 1989: PGE Study of the Geordie Lake and Marathon Cu-Ni-Precious Metal Deposits, Coldwell Alkalic Complex. *Geoscience Research Grant Program, Summary of Research 1988-1989, Ontario Geological Survey, Miscellaneous Paper 143*, 87--96.

Good, D. and J. Crocket, 1990: PGE Study: the MacRae and Marathon Copper-Precious Metal Deposits, Coldwell Complex. *Geoscience Research Grant Program, Summary of Research 1989-1990, Ontario Geological Survey, Miscellaneous Paper 150*, 87--96.

Good, D. and J. Crocket, 1994: Genesis of the Marathon Cu-Platinum-Group Element Deposit, Port Coldwell Alkalic Complex, Ontario: A Midcontinent Rift-Related Magmatic Sulfide Deposit. *Economic Geology*, **89 (1)**, 131--149.

Green, J., 1983: Geologic and geochemical evidence for the nature and development of the middle proterozoic (keweenawan) midcontinent Rift of north america. *Tectonophysics*, **94 (1-4)**, 413--437.

Hawley, J. E. and I. Nichol, 1959: Selenium in some Canadian sulfides. *Economic Geology*, **54 (4)**, 608--628.

Heaman, L. and N. Machado, 1992: Timing and origin of midcontinent rift alkaline magmatism, North America: evidence from the Coldwell Complex. *Contributions to Mineralogy and Petrology*, **110 (2)**, 289--303.

Hutchinson, D., R. White, W. Cannon, and K. Schulz, 1990: Keweenaw hot spot: Geophysical evidence for a 1.1 Ga mantle plume beneath the Midcontinent Rift System. *Journal of Geophysical Research*, **95 (7)**, 10--10.

Keays, R. R., P. C. Lightfoot, and P. R. Hamlyn, 2012: Sulfide saturation history of the Stillwater Complex, Montana: chemostratigraphic variation in platinum group elements. *Mineralium Deposita*, **47 (1-2)**, 151--173.

Kerr, A., 2001: The Calculation and Use of Sulfide Metal Contents in the Study of Magmatic Ore Deposits: A Methodological Analysis. *Exploration and Mining Geology*, **10 (4)**, 289--301.

Kerr, A., 2003: Guidelines for the calculation and use of sulfide metal contents in research and mineral exploration. *Current Research - Newfoundland. Geological Survey Branch*, **3 (1)**, 223--229.

Kerr, A., 2005: Self-Destructive Sulfide Segregation Systems and the Formation of High-Grade Magmatic Ore Deposits. *Economic Geology*, **100 (2)**, 311--332.

Li, C., 2001: Magmatic Ni-Cu versus PGE deposits: Contrasting genetic controls and exploration implications. *South African Journal of Geology*, **104 (4)**, 309--318.

Li, C. and A. Naldrett, 1999: Geology and petrology of the Voisey's Bay intrusion: reaction of olivine with sulfide and silicate liquids. *Lithos*, **47 (1-2)**, 1--31.

Li, C. and E. Ripley, 2011: The Giant Jinchuan Ni-Cu-(PGE) Deposit: Tectonic Setting, Magma Evolution, Ore Genesis and Exploration Implications. *Reviews in Economic Geology v. 17*, 163--180.

Lilley, F., 1964: An analysis of the magnetic features of the Port Coldwell intrusive. Ph.D. thesis, University of Western Ontario.

Longerich, H., S. Jackson, and D. Günther, 1996: Laser ablation inductively coupled plasma mass spectrometric transient signal data acquisition and analyte concentration calculation. *Journal of Analytical Atomic Spectrometry*, **11 (9)**, 899--904.

Lorand, J. and O. Alard, 2010: Determination of selenium and tellurium concentrations in Pyrenean peridotites (Ariege, France): New insight into S/Se/Te systematics of the upper in mantle samples. *Chemical Geology*, **278 (1-2)**, 120--130.

Maier, W. D. and D. I. Groves, 2011: Temporal and spatial controls on the formation of magmatic PGE and NiCu deposits. *Mineralium Deposita*, **46 (8)**, 841--857.

Marsh, B., 2004: A Magmatic Mush Column Rosetta Stone: The McMurdo Dry Valleys of Antarctica. *Eos, Transactions, American Geophysical Union*, **85 (47)**, 497--508.

Marsh, B., 2006: Dynamics of magmatic systems. *Elements*, 287--292.

Marsh, B., 2007: Magmatism, Magma, and Magma Chambers. *Treatise on geophysics Volume 6*, A. Watts, Ed., Elsevier, Amsterdam, chap. 7, 275--333.

McBirney, A., 1996: The Skaergaard Intrusion. *Layered Intrusions*, R. Cawthorn, Ed., Elsevier, Amsterdam, 147--180.

McBirney, A. and A. Nicolas, 1997: The Skaergaard layered series. Part II. Magmatic flow and dynamic layering. *Journal of Petrology*, **38 (5)**, 569--580.

McDonough, W., 1995: The composition of the Earth. *Chemical Geology*, **120 (3-4)**, 223--253.

McLaughlin, R. and R. Mitchell, 1989: Rare metal mineralization in the Coldwell alkaline complex, northwestern Ontario. *Geological association of Canada, Mineralogical Association of Canada, Program with Abstracts 14*, 1--1.

Miller, J., 1999: Geochemical evaluation of platinum group element (PGE) mineralization in the Sonju Lake Intrusion, Finland, Minnesota. *Minnesota Geological Survey Information Circular 44*, 31.

Mitchell, R. and R. Platt, 1977: Field guide to the aspects of the geology of the Coldwell Alkaline Complex. Tech. rep., Institute on Lake Superior Geology.

Mitchell, R. and R. Platt, 1978: Mafic mineralogy of ferroaugite syenite from the Coldwell alkaline complex, Ontario, Canada. *Journal of Petrology*, **19 (4)**, 627--651.

Mitchell, R. and R. Platt, 1982: Mineralogy and petrology of nepheline syenites from the Coldwell alkaline complex, Ontario, Canada. *Journal of Petrology*, **23 (2)**, 186--214.

Mitchell, R., R. Platt, J. Lukosius-Sanders, M. Artist-Downey, and S. Moogk-Pickard, 1993: Petrology of syenites from center III of the Coldwell alkaline complex, northwestern Ontario, Canada. *Canadian Journal of Earth Sciences*, **30 (1)**, 145--158.

Mountain, B. and S. Wood, 1988: Chemical Controls on the Solubility, Transport, and Deposition of Platinum and Palladium in Hydrothermal Solutions A Thermodynamic Approach. *Economic Geology*, **83 (3)**, 492--510.

Mulja, T. and R. Mitchell, 1991: The Geordie Lake Intrusion, Coldwell Complex, Ontario; a palladium-and tellurium-rich disseminated sulfide occurrence derived from an evolved tholeiitic magma. *Economic Geology*, **86 (5)**, 1050--1069.

Mungall, J., 2005: Magmatic geochemistry of the platinum-group elements. *Exploration for platinum-group elements deposits*, J. Mungall, Ed., Mineralogical Association of Canada,, London, ON, Canada, 1--34.

Murahwi, C., S. Shoemaker, R. Gowans, J. Lemieux, and C. Jacobs, 2010: Technical report on the updated feasibility study for the Marathon PGM-Cu project, Marathon, Ontario, Canada. Tech. Rep. 1, Marathon-PGM Internal Report.

Naldrett, A., 1992: A model for the Ni-Cu-PGE ores of the Noril'sk region and its application to other areas of flood basalt. *Economic Geology*, **87**, 1945--1962.

Naldrett, A., 2011: Fundamentals of Magmatic Sulfide Deposits. *Reviews in Economic Geology*, **17**, 1--50.

Naldrett, A., M. Asif, S. Krstic, and C. Li, 2000: The Composition of Mineralization at the Voisey's Bay Ni-Cu Sulfide Deposit, with Special Reference to Platinum-Group Elements. *Economic Geology*, **95 (4)**, 845--865.

Naldrett, A. and P. Lightfoot, 1999: Ni-Cu-PGE deposits of Noril'sk region, Siberia: their formation in conduits for flood basalt volcanism. *Geological Assocation of Canada Short Course Notes 13*, R. Keays, M. Lesher, P. Lightfoot, and C. Farrow, Eds., Geological Assocation of Canada, St John's, Vol. 104, 195--249.

Naldrett, A. and E. Ripley, 2009: Anorthosite-related Ni-Cu-Co deposits- Examples from Labrador, Canada. *New developments in magmatic Ni-Cu and PGE deposits*, C. Li and E. Ripley, Eds., Geological Publishing House, Beijing, 192--218.

Nielsen, T., J. Andersen, and C. Brooks, 2005: The platinova reef of the Skaergaard intrusion. *Exploration for platinum-group elements deposits*, J. Mungall, Ed., Mineralogical Association of Canada, London, ON, Canada, 431--455.

Ohnenstetter, D., D. Watkinson, and R. Dahl, 1991: Zoned hollingworthite from the Two Duck Lake intrusion, Coldwell complex, Ontario. *American Mineralogist*, **76 (9-10)**, 1694.

Palmer, H. and D. Davis, 1987: Paleomagnetism and U-Pb geochronology of volcanic rocks from michipicoten island, lake superior, canada: precise calibration of the keweenawan polar wander track. *Precambrian Research*, **37 (2)**, 157--171.

Paster, T., D. Schauwecker, and L. Haskin, 1974: The behavior of some trace elements during solidification of the Skaergaard layered series. *Geochimica et Cosmochimica*, **38**, 1549--1577.

Peach, C., E. Mathez, and R. Keays, 1990: Sulfide melt-silicate melt distribution coefficients for noble metals and other chalcophile elements as deduced from MORB: Implications for partial melting. *Geochimica et Cosmochimica Acta*, **54 (12)**, 3379--3389.

Peach, C., E. Mathez, R. Keays, and S. Reeves, 1994: Experimentally determined sulfide melt-silicate melt partition coefficients for iridium and palladium. *Chemical Geology*, **117 (1-4)**, 361--377.

Pruseth, K. and H. Palme, 2004: The solubility of Pt in liquid Fe-sulfides. *Chemical geology*, **208 (1-4)**, 233--245.

Puritch, E., D. Orava, T. Armstrong, A. Yassa, R. Gowans, I. Wislesky, and C. Jacobs, 2009: Technical report on the updated mineral resource estimate and feasibility study for the marathon PGM-Cu project, Marathon, Ontario, Canada. Tech. Rep. 1, Marathon-PGM Internal Report.

Puskas, F., 1967: Geology of the Port Coldwell Area. *Ontario Dept. Mines, Open File Report 5104*.

Puskas, F., 1970: The Port Coldwell alkalic complex. Tech. rep., Institute of Lake Superior Geology.

Righter, K., A. Campbell, M. Humayun, and R. Hervig, 2004: Partitioning of Ru, Rh, Pd, Re, Ir, and Au between Cr-bearing spinel, olivine, pyroxene and silicate melts1. *Geochimica et Cosmochimica Acta*, **68 (4)**, 867--880.

Ripley, E. and C. Li, 2011: A Review of Conduit-Related Ni-Cu-(PGE) Sulfide Mineralization at the Voisey's Bay Deposit, Labrador, and the Eagle Deposit, Northern Michigan. *Reviews in Economic Geology v. 17*.

Ripley, E., C. Li, and D. Shin, 2002: Paragneiss assimilation in the genesis of magmatic Ni-Cu-Co sulfide mineralization at Voiseys Bay. *Economic Geology*, **97 (6)**, 1307--1318.

Ripley, E., N. Taib, C. Li, and C. Moore, 2007: Chemical and mineralogical heterogeneity in the basal zone of the Partridge River Intrusion: implications for the origin of Cu Ni sulfide mineralization in the Duluth Complex, midcontinent rift system. *Contributions to Mineralogy and Petrology*, **154 (1)**, 35--54.

Samson, I., B. Fryer, and J. Gagnon, 2008: The Marathon Cu-PGE deposit, Ontario: Insights from sulphide chemistry and textures. *Abstracts of the 18th annual V. M. Goldschmidt conference*, 2004--2004.

Shaw, C., 1994: Petrogenesis of the Eastern Gabbro, Coldwell Alkaline Complex, Ontario. M.sc. thesis, University of Western Ontario.

Shaw, C., 1997: The petrology of the layered gabbro intrusion, eastern gabbro, Coldwell alkaline complex, Northwestern Ontario, Canada: evidence for multiple phases of intrusion in a ring dyke. *Lithos*, **40 (2-4)**, 243--259.

Song, X., Y. Wang, and L. Chen, 2011: Magmatic Ni-Cu-(PGE) deposits in magma plumbing systems: Features, formation and exploration. *Geoscience Frontiers*, **2 (3)**, 375--384.

Stone, W., J. Crocket, and M. Fleet, 1990: Partitioning of palladium, iridium, platinum, and gold between sulfide liquid and basalt melt at 1200 C. *Geochimica et Cosmochimica Acta*, **54 (8)**, 2341--2344.

Sun, S.-s. and W. McDonough, 1989: Chemical and isotopic systematics of oceanic basalts: implications for mantle composition and processes. *Geological Society, London, Special Publications*, **42 (1)**, 313--345.

Swanson-Hysell, N. L., A. C. Maloof, B. P. Weiss, and D. a. D. Evans, 2009: No asymmetry in geomagnetic reversals recorded by 1.1-billion-year-old Keweenawan basalts. *Nature Geoscience*, **2 (10)**, 713--717.

Taib, N., 2001: Open System Magmatism, and the Emplacement of the Partridge River Intrusion, Duluth Complex, Minnesota. Phd thesis, Indiana University, 187 pp.

Taylor, S. and S. McLennan, 1985: *The continental crust: its composition and evolution: an examination of the geochemical record preserved in sedimentary rocks*. Blackwell Scientific Publications.

Theriault, R. and S.-J. Barnes, 1999: Compositional variations in Cu-Ni-PGE sulfides of the Dunka Road deposit, Duluth Complex, Minnesota: The importance of combined assimilation and magmatic processes. *Canadian Mineralogist*, **36 (3)**, 869--886.

Thériault, R., S.-J. Barnes, and M. Severson, 2000: Origin of Cu-Ni-PGE Sulfide Mineralization in the Partridge River Intrusion, Duluth Complex, Minnesota. *Economic Geology*, **95 (5)**, 929--944.

Todd, S., D. Keith, L. L. Roy, and D. Schissel, 1982: The JM platinum-palladium reef of the Stillwater Complex, Montana; I, Stratigraphy and petrology. *Economic Geology*, **77**, 1454--1480.

Toplis, M. J., W. L. Brown, and E. Pupier, 2008: Plagioclase in the Skaergaard intrusion Part 1 : Core and rim compositions in the layered series. *Contributions to Mineralogy and Petrology*, **155 (3)**, 329--340.

Van Schmus, W. and M. Bickford, 1981: Proterozoic chronology and evolution of the midcontinent region, North America. *Precambrian Plate Tectonics*, **261**, 296.

Walker, E., R. Sutcliffe, C. Shaw, G. Shore, and R. Penczak, 1993: *Precambrian Geology of the Coldwell Alkalic Complex*. Ontario Geological Survey.

Watkinson, D. and P. Jones, 1996: Platinum-group minerals in fluid inclusions from the Marathon deposit, Coldwell Complex, Canada. *Mineralogy and Petrology*, **57 (1-2)**, 91--96.

Watkinson, D. and D. Ohnenstetter, 1992: Hydrothermal origin of platinum-group mineralization in the Two Duck Lake intrusion, Coldwell Complex, northwestern Ontario. *Canadian Mineralogist*, **30 (1)**, 121.

Weill, D. and M. Drake, 1973: Europium anomaly in plagioclase feldspar: experimental results and semiquantitative model. *Science*, **180 (4090)**, 1059--1060.

Wilkinson, S., 1983: Geology and sulphide mineralization of the marginal phases of the Coldwell Complex, Northwestern Ontario. M.sc. thesis, Carleton University.

Winter, J., 2001: *An introduction to igneous and metamorphic petrology*. Prentice-Hall Inc., Upper Saddle River, New Jersey, 697 pp.

Wood, S., 1987: Thermodynamic calculations of the volatility of the platinum group elements (PGE): The PGE content of fluids at magmatic temperatures. *Geochimica et Cosmochimica Acta*, **51 (11)**, 3041--3050.

Yi, W., A. Halliday, J. Alt, D. Lee, M. Rehkaemper, M. Garcia, C. Langmuir, and Y. Su, 2000: Cadmium, indium, tin, tellurium, and sulfur in oceanic basalts: Implications for chalcophile element fractionation in the Earth. *Journal of Geophysical Research*, **105 (B8)**, 18 927.

Appendix I: Summary of Analyses

This appendix contains a summary of the analyses performed during this study.

This table is also available as an excel file on a CD that can be obtained from the Department of Earth and Environmental Science upon request, and are located in the folder 'Appendix 1 - Summary of Analyses'.

Table: Summary table of samples collected and analyses performed

Sample ID	DDH	Depth [mid-point] (m)	Mineralization	Polished Thin Section	Whole Rock Geochemistry	Electron Microprobe				LA-ICP-MS	
						Olivine	Pyroxene	Plagioclase	Oxide	Olivine	Pyroxene
59411	M-07-306	128.06	unmineralized	X	X	X					
59412	M-07-306	135.23	unmineralized	X	X	X					
59413	M-07-306	143.20	unmineralized	X	X	X					
59414	M-07-306	147.25	unmineralized	X	X	X					
59366	M-07-306	150.18	W-Horizon	X	X	X					
59367	M-07-306	150.53	W-Horizon	X	X	X					
59368	M-07-306	150.80	W-Horizon	X	X	X					
59369	M-07-306	151.50	W-Horizon	X	X	X					
59370	M-07-306	151.82	W-Horizon	X	X	X					
59371	M-07-306	152.06	W-Horizon	X	X	X					
59372	M-07-306	152.39	W-Horizon	X	X	X					
59373	M-07-306	152.80	W-Horizon	X	X	X					
59374	M-07-306	153.69	W-Horizon	X	X	X					
59375	M-07-306	153.97	W-Horizon	X	X	X					
59376	M-07-306	154.26	W-Horizon	X	X	X			X		
59377	M-07-306	154.64	W-Horizon	X	X	X					
59378	M-07-306	155.20	W-Horizon	X	X	X					
59415	M-07-306	155.75	W-Horizon	X	X						
59416	M-07-306	156.24	W-Horizon	X	X	X					
59417	M-07-306	156.76	W-Horizon	X	X	X					
59418	M-07-306	157.31	W-Horizon	X	X	X					
59419	M-07-306	158.25	W-Horizon	X	X	X					
59420	M-07-306	166.20	W-Horizon	X	X	X					
59422	M-07-306	176.31	unmineralized	X	X	X					
59423	M-07-306	185.65	unmineralized	X	X	X					
59424	M-07-306	195.27	Main Zone	X	X	X					
59379	M-07-306	202.15	Main Zone	X	X		X				
59380	M-07-306	202.45	Main Zone	X	X						
59381	M-07-306	202.75	Main Zone	X	X						
59382	M-07-306	203.05	Main Zone	X	X	X					
59383	M-07-306	203.39	Main Zone	X	X						
59384	M-07-306	203.72	Main Zone	X	X				X		
59385	M-07-306	204.02	Main Zone	X	X						
59386	M-07-306	204.40	Main Zone	X	X	X					
59387	M-07-306	204.81	Main Zone	X	X			X			
59388	M-07-306	205.17	Main Zone	X	X						
59389	M-07-306	205.52	Main Zone	X	X	X					
59390	M-07-306	205.85	Main Zone	X	X	X			X		
59425	M-07-306	212.30	unmineralized	X	X						
59426	M-07-306	222.35	unmineralized	X	X						
59427	M-07-306	231.28	unmineralized	X	X	X					
59251	M-07-368	105.45	unmineralized	X	X	X		X			
59252	M-07-368	109.875	unmineralized	X	X	X					
59253	M-07-368	113.375	unmineralized	X	X	X	X			X	X
59254	M-07-368	117.625	unmineralized	X	X	X					
59255	M-07-368	122.2	unmineralized	X	X	X					
59256	M-07-368	126.47	unmineralized	X	X	X					
59257	M-07-368	129.185	unmineralized	X	X	X					
59258	M-07-368	129.495	W-Horizon	X	X	X	X			X	X
59259	M-07-368	129.775	W-Horizon	X	X	X		X	X	X	X
59260	M-07-368	130.1	W-Horizon	X	X	X	X	X		X	X
59261	M-07-368	130.37	W-Horizon	X	X	X				X	X
59262	M-07-368	130.615	unmineralized	X	X	X				X	X
59263	M-07-368	130.91	unmineralized	X	X	X					
59264	M-07-368	131.22	unmineralized	X	X		X				

Sample ID	DDH	Depth [mid-point] (m)	Mineralization	Polished Thin Section	Whole Rock Geochemistry	Electron Microprobe				LA-ICP-MS	
						Olivine	Pyroxene	Plagioclase	Oxide	Olivine	Pyroxene
59265	M-07-368	131.56	unmineralized	X	X						
59266	M-07-368	131.87	unmineralized	X	X	X					
59267	M-07-368	132.2	unmineralized	X	X		X				
59268	M-07-368	132.6	unmineralized	X	X					X	X
59269	M-07-368	132.955	unmineralized	X	X	X					
59270	M-07-368	133.22	unmineralized	X	X			X			
59271	M-07-368	133.485	unmineralized	X	X						
59272	M-07-368	133.795	unmineralized	X	X	X					
59273	M-07-368	134.11	unmineralized	X	X						
59274	M-07-368	134.425	unmineralized	X	X	X		X			
59275	M-07-368	134.735	unmineralized	X	X		X				
59276	M-07-368	135.045	unmineralized	X	X	X				X	X
59277	M-07-368	135.35	unmineralized	X	X						
59278	M-07-368	135.655	unmineralized	X	X						
59279	M-07-368	135.96	unmineralized	X	X	X					
59280	M-07-368	136.26	unmineralized	X	X			X			
59281	M-07-368	136.57	unmineralized	X	X	X	X				
59282	M-07-368	136.885	unmineralized	X	X						
59283	M-07-368	137.19	unmineralized	X	X	X					
59284	M-07-368	137.47	unmineralized	X	X					X	X
59285	M-07-368	137.75	unmineralized	X	X	X					
59286	M-07-368	138.04	unmineralized	X	X						
59287	M-07-368	138.335	unmineralized	X	X	X					
59288	M-07-368	138.72	unmineralized	X	X						
59289	M-07-368	139.125	unmineralized	X	X	X					
59290	M-07-368	139.45	unmineralized	X	X						
59291	M-07-368	139.75	unmineralized	X	X	X				X	X
59292	M-07-368	140.065	unmineralized	X	X	X					
59293	M-07-368	140.35	unmineralized	X	X	X	X				
59294	M-07-368	140.66	unmineralized	X	X	X		X			
59295	M-07-368	140.96	unmineralized	X	X	X					
59296	M-07-368	141.22	unmineralized	X	X	X					
59297	M-07-368	141.485	unmineralized	X	X	X					
59298	M-07-368	141.72	unmineralized	X	X						
59299	M-07-368	141.95	unmineralized	X	X						
59300	M-07-368	142.235	unmineralized	X	X						
59301	M-07-368	142.615	unmineralized	X	X	X				X	X
59302	M-07-368	142.96	unmineralized	X	X					X	X
59303	M-07-368	143.195	unmineralized	X	X	X					
59304	M-07-368	143.525	unmineralized	X	X		X			X	X
59305	M-07-368	143.89	Main Zone-like	X	X	X	X			X	X
59306	M-07-368	144.125	Main Zone-like	X	X						
59307	M-07-368	144.425	Main Zone-like	X	X	X			X	X	X
59308	M-07-368	144.72	Main Zone-like	X	X						
59309	M-07-368	145.02	Main Zone-like	X	X	X					
59310	M-07-368	145.38	Main Zone-like	X	X					X	X
59311	M-07-368	145.655	Main Zone-like	X	X				X		
59312	M-07-368	145.855	Main Zone-like	X	X	X				X	X
59313	M-07-368	146.095	Main Zone-like	X	X		X			X	X
59314	M-07-368	146.33	Main Zone-like	X	X						
59315	M-07-368	146.53	Main Zone-like	X	X						
59316	M-07-368	146.815	Main Zone-like	X	X		X				
59317	M-07-368	151.21	Main Zone-like	X	X		X				
59318	M-07-368	155.75	Main Zone-like	X	X						
59319	M-07-368	161.625	Main Zone-like	X	X	X					
59320	M-07-368	165.6	unmineralized	X	X	X				X	X
59321	M-07-368	170	unmineralized	X	X	X					
59322	M-07-368	174.585	unmineralized	X	X						
59323	M-07-368	178.82	unmineralized	X	X						

Sample ID	DDH	Depth [mid-point] (m)	Mineralization	Polished Thin Section	Whole Rock Geochemistry	Electron Microprobe				LA-ICP-MS	
						Olivine	Pyroxene	Plagioclase	Oxide	Olivine	Pyroxene
59324	M-07-368	183.9	unmineralized	X	X	X	X				
59397	M-07-369	69.20	unmineralized	X	X						
59398	M-07-369	73.23	unmineralized	X	X						
59399	M-07-369	78.20	unmineralized	X	X	X					
59400	M-07-369	81.20	unmineralized	X	X	X					
59325	M-07-369	84.54	unmineralized	X	X						
59326	M-07-369	86.89	unmineralized	X	X						
59327	M-07-369	87.21	unmineralized	X	X	X					
59329	M-07-369	87.25	unmineralized	X	X						
59330	M-07-369	87.48	unmineralized	X	X						
59328	M-07-369	87.49	W-Horizon 1	X	X						
59331	M-07-369	88.23	W-Horizon 1	X	X						
59332	M-07-369	88.49	W-Horizon 1	X	X						
59333	M-07-369	88.75	W-Horizon 1	X	X				X		
59334	M-07-369	89.04	W-Horizon 1	X	X				X		
59335	M-07-369	90.07	unmineralized	X	X						
59401	M-07-369	91.20	unmineralized	X	X	X					
59402	M-07-369	95.55	unmineralized	X	X						
59336	M-07-369	97.41	unmineralized	X	X	X					
59403	M-07-369	101.20	unmineralized	X	X	X					
59404	M-07-369	107.23	unmineralized	X	X						
59405	M-07-369	114.25	unmineralized	X	X	X					
59406	M-07-369	120.58	unmineralized	X	X	X					
59337	M-07-369	123.10	unmineralized	X	X						
59338	M-07-369	123.30	W-Horizon 2	X	X	X					
59339	M-07-369	123.50	W-Horizon 2	X	X	X					
59340	M-07-369	123.70	W-Horizon 2	X	X						
59341	M-07-369	123.90	W-Horizon 2	X	X						
59342	M-07-369	124.10	W-Horizon 2	X	X	X					
59343	M-07-369	124.32	W-Horizon 2	X	X	X					
59344	M-07-369	124.54	W-Horizon 2	X	X	X			X		
59345	M-07-369	124.77	W-Horizon 2	X	X	X			X		
59346	M-07-369	125.05	W-Horizon 2	X	X			X			
59347	M-07-369	125.35	W-Horizon 2	X	X	X					
59348	M-07-369	125.65	W-Horizon 2	X	X						
59349	M-07-369	126.07	W-Horizon 2	X	X						
59407	M-07-369	132.23	unmineralized	X	X						
59408	M-07-369	139.20	unmineralized	X	X						
59409	M-07-369	141.94	unmineralized	X	X						
59428	M-08-441	50.30	unmineralized	X	X	X					
59429	M-08-441	60.21	unmineralized	X	X	X					
59430	M-08-441	70.21	unmineralized	X	X	X					
59431	M-08-441	79.53	unmineralized	X	X	X					
59432	M-08-441	91.42	unmineralized	X	X	X					
59433	M-08-441	99.80	unmineralized	X	X						
59434	M-08-441	109.85	unmineralized	X	X	X					
59435	M-08-441	119.73	unmineralized	X	X	X					
59436	M-08-441	130.23	W-Horizon	X	X	X					
59437	M-08-441	135.25	W-Horizon	X	X	X					
59350	M-08-441	138.25	W-Horizon	X	X	X		X			
59351	M-08-441	138.67	W-Horizon	X	X	X					
59352	M-08-441	138.95	W-Horizon	X	X	X					
59353	M-08-441	139.26	W-Horizon	X	X	X			X		
59354	M-08-441	139.63	W-Horizon	X	X	X					
59355	M-08-441	139.98	W-Horizon	X	X	X					
59356	M-08-441	140.35	W-Horizon	X	X	X					
59357	M-08-441	140.73	W-Horizon	X	X	X			X		
59358	M-08-441	141.21	W-Horizon	X	X	X					
59359	M-08-441	141.66	W-Horizon	X	X						

Sample ID	DDH	Depth [mid-point] (m)	Mineralization	Polished Thin Section	Whole Rock Geochemistry	Electron Microprobe				LA-ICP-MS	
						Olivine	Pyroxene	Plagioclase	Oxide	Olivine	Pyroxene
59360	M-08-441	141.99	W-Horizon	X	X	X					
59361	M-08-441	142.35	W-Horizon	X	X	X					
59362	M-08-441	142.78	W-Horizon	X	X	X					
59363	M-08-441	143.11	W-Horizon	X	X	X					
59364	M-08-441	143.44	W-Horizon	X	X	X					
59365	M-08-441	143.83	W-Horizon	X	X	X					
59438	M-08-441	146.25	W-Horizon	X	X	X					
59439	M-08-441	153.55	unmineralized	X	X	X					
59440	M-08-441	163.25	unmineralized	X	X	X					
59441	M-08-441	173.20	unmineralized	X	X	X					

Appendix II: Drill Core Logs

This appendix contains the drill core logs from the diamond drill holes used in this project.

The drill core logs are also available as an excel file on a CD that can be obtained from the Department of Earth and Environmental Science upon request, and are located in the folder 'Appendix 2 - Drill Core Logs'.

The log of DDH-306 is contained in the tab "DDH-306"

The log of DDH-368 is contained in the tab "DDH-368"

The log of DDH-369 is contained in the tab "DDH-369"

The log of DDH-441 is contained in the tab "DDH-441"

MARATHON PGM CORPORATION - DIAMOND DRILL CORE LOG

DDH-306

NTS: 42 D / 16
UTM Northing 5404392.83
(Nad27) Easting 550045.76
Elevation: 300.56
Dip at Collar: -71
Azimuth: 89.65
Total Depth: 246m
Core Size: NQ
Remarks: Core stored in Marathon PGM Corporation warehouse, Marathon, Ontario

Property: Marathon
Contractor: Chibougamau Diamond Drilling Ltd.
Logged by: Dave Leng
Assistant: Ryan Milne
Relogged by: Ryan Ruthart

GEOLOGY					Mineralization	
From	To	Maj Rock	Min Rock	Comments	Mineraliz	Comments
0	2.00	O/B - Overburden				
2.00	124.15	2a - Fine grained gabbro			Trace to 0.5% disseminated sulphides	
				Intervals of coarser grained differentiates 3.67-3.70, 5.50-5.57, 7.30-7.55, 8.04-8.11,		10.32-10.7very fine gr cpy
				32.90-33.10,	Trace to 0.5% disseminated sulphides	
				Interval of coarser grained pyroxenes 8.27-8.80 that fades		56.95-64.75 dusting of very fine gr cpy, with local blebs at
				Interval of coarse grained pyroxenes with albite replacement on rims 12.40-13.80,		62.64 up to 1cm with po/cpy (1:1). Locally cpy up to 1%
				Intervals of coarse grained gabbro with magnetite <10% <1cm, 19.9-19.16, 21.97-21.74,	Magnetite Cumulate	
				21.30-25.18,		localised band of <30% magnetite (highly magnetic) from
				Olivine cumulates begin at ~25.20 and gradually phase into bands 90CA through to 35.00		66.76-66.8, 68.9-68.96
				then cycle back to cumulates	Trace to 0.5% disseminated sulphides	
				Zone of intense chloritisation and hematisation 29.20-29.76		88.85-95.65 fine gr cpy + minor po (90.47-90.8 up to 2%cpy)
				Interval (45.80-50.28) of pervasive fine grained chlorite alteration, highly fractured, chlorite		(92.18-92.5 up to 1%po)
				present on fracture surfaces, numerous chlorite+carbonate fractures at high angles to CA and	0.5% to 1% disseminated sulphides	
				local olivine cumulates <50%		infrequent patches of fg po from 105.2-
				1cm carbonate breccia at 49.32 @ 60 deg to ca	Magnetite Cumulate	
				Interval (55.18-61.50) of chlorite healed fractures (45-50CA), with localised patches (<10cm)		localised patches of semi-massive to massive magnetite
				of coarse network textured chlorite, from 58.04-58.76m interval of carbonate+chlorite filled		(111.67-112.07)
				fractures 50CA,	Magnetite Cumulate	
				Interval (59.7-60.55) of crs gr gabbro with similar texture to TDL		localised patches of magnetite <25% 123.43-123.60
				Interval (68.90-68.96) of semi-massive magnetite within differentiate		
				Interval (68.96-88.85) of homogeneous gabbro, irr bands of olivine cumulate		
				Interval (98.90-104.87) of regular fracturing (typically 45-60CA) healed with semi-massive		
				chlorite+localised patches of epidote		
				Interval (105.22-106.15) of coarse grains of pyroxene (?) with plag mantles		
				Interval (108.85-116.97) of strong fracturing healed with chlorite, thick intervals of stacked		
				chl healed fractures (112.83-113.27, 114.56-114.69, 115.98-116.97)		
				Interval 116.97-124.15 of homogeneous gabbro, uniform grain size throughout until		
				119.40 then marked decrease in plag,		
			5a - Quartz syenite dikelet			
				Coarse grained kspar+plag+smokey coloured quartz+minor coarse flecks of magnetite		
				Intrusions at 26.36-27.46, 52.3-53.35 with carb+qz fractures 45CA, 62.97-63.30, 63.74-63.82		
				79.36-79.44, 121.59-121.82 (very coarse pyroxenes, strongly altered-sausseritised)		
			3a/3b Fine to medium / coarse grained gabbro			

GEOLOGY						Mineralization
From	To	Maj Rock	Min Rock	Comments	Mineraliz	Comments
				88.85-91.27 Fine-med and coarse grained gabbro alternate. 3b folows increase in chlorite and		
				magnetite		
			2d - Fine grained gabbro with coarse grained gabbro dikelets			
				116.98-119.5		
			3b - Coarse grained gabbro (>5mm)			
				123.15-123.95		
124.15	133.1	2d - Fine grained gabbro with coarse grained gabbro dikelets			Trace to 0.5% disseminated sulphides	
				Coarse Intervals - 124.44-144.80, 126.1-126.59, 127.47-128.11, 128.70-129.84,		130.2-130.5 fine gr cpy
				130.40-131.31, 132.30-132.37		
				Interval (132.37-132.50) 1cm wide massive chl vein 30CA		
124.15	133.1	2d - Fine grained gabbro with coarse grained gabbro dikelets			Trace to 0.5% disseminated sulphides	
				fg plag-ol-pyx cummulate, mod int mt EG. 1-4mm poikilitic mt grains give it a slight spotted appearance.		130.2-130.5 fine gr cpy
				cg intervals are ol-plag-pyx (40%, 40%, 15%, 5% mt) with grain sizes 5mm-1cm average. Minerals are		
				subhedral-anhedral. Bands of cummulate olivine are present throughout the cg interval. Poikilitic magnetite		
				up to 1 cm		
				Coarse Intervals - 124.44-124.80, 126.1-126.59, 127.47-128.11, 128.70-129.84,		
				130.40-131.31,		
				Interval (132.37-132.50) 1cm wide massive chl vein 30CA		
				130.40-131.15 vcg interval, plag rich (60-70%), grains up to 2-3 cm, texturally the same as the cg interval but		
				the grain size is notably larger		
			3b - Coarse grained gabbro (>5mm)			
				132.30-132.37 very felsic rich (70-80% plag) cg subophitic-ophitic plag (euhedral, first formed, elongate laths		
				5mm-2cm), with interstitial angular cpx + olv (subhedral -anhedral interstitial, angular, 2-6mm in size) and		
				mt and bt (anhedral, angular, up to 4mm). Modal abundance 85% plag, 5% ol, 4% pyx, 4% mt, 3% bt		
133.10	150.00	3b - Coarse grained gabbro (>5mm)				
				cg ophitic to subophitic plag (4mm-7mm, euhedral-subhedral (first formed), elongate laths) with		
				cpx (interstitial angular, subhedral-anhedral, 4mm-1cm) and ol (interstitial, angular, subhedral-		
				anhedral, 3-6mm) mt subrounded-subangular, interstitial, 2-5mm. Modal abundance approx 40% plag		
				40% pyx, 15%ol, 2-3% mt, 2% bt		
				Weak patchy chlorite atleration of mafics (5%) to soft green chalky throughout,		
				Unit is homogeneous from 133.10-150.00m		
				144 and on start to get large crystals/cummulations of cpx, 3-6cm in the core		
				Chlorite filled fractures at 149.40 (1cm 60CA), 151.66 (2cm 30CA), 152.10 (1cm 30CA),		
				1404-1407, 137.75 m rep photo of the homogeneous unit (133.10-150.00) rep texture		
				1408-1412, 146.40 showing a large pyroxene crystal in the TDL		
150.00	154.80	3b - Coarse grained gabbro (>5mm)				
				Texture is highly heterogeneous in this section, it ranges from subophitic-cummulate, there are not large		
				bands where the texture is consistent. Throughout the cummulate sections there are euhedral-subhedral		

GEOLOGY						Mineralization
From	To	Maj Rock	Min Rock	Comments	Mineraliz	Comments
				plag laths that look like they formed first (3-6mm, elongate laths) within large zones of subhedral-		
				anhedral pyx (5mm-3cm, typically enclosing plag crystals). And olivine (2-5mm, subhedral-anhedral)		
				leucocratic plag differntitates are also common throughout this section where the rock is ~60-70% plag		
				and has a white apperance with scattered mafic minerals within		
				isome patches where the grain size grades down to fg-mg		
				Weak chlorite patchy chlorite alteration of mafcis (~5-10%) altered to soft green chalky		
				150.00-150.36		
				59366		
				cummulate/subophitic texture as described above. Felsic plag differntiate from 150.12-150.25. other wise		
				this interval is very afic rich, dominated by pyx (from 5mm-2cm in size) and olivine (3mm-6mm) with		
				interstitial plag (slight ophitic texture) subhedral.		
				trace fg cpy (up to <1mm-1mm) disseminated, interstitial in this section		
				1413-1416, 155.05m, mafic rich patch in the above unit, note late large pyroxnes		
				1417-14120 150.20m, felsic differntiate patch, note the opaque white plag in the wet photos, trace cp visible (vfg)		
				150.36-150.69		
				59367		
				dominantly mafic patch (approx 70%pyx, 10% ol, 20% plag), 2-5% mt, (2-5mm) from 150.36-150.52 pyx are		
				5mm-3cm, and the largest minerals present		
				grain size decreases at 135.52m to mg-fg		
				4 chlorite healed fractures at 30 TCA, hairline		
				trace fg-mg cpy (up to 1 mm) in this section		
				1421-1424 150.41m rep texture of the coase grained pyx in this section, note the large pyx grains, trace cpy		
				1425-1428 150.60m, mg-fg section, trace cpy		
				150.59-150.90		
				59368		
				mg (2-5mm average) mafic rich, cummulate/subophitic TDL. felsic plag differntiate patch from		
				150.90-151.05m		
				trace fg diss int cpy (<=1mm)		
				1429-1432 151.05m, rep texture of the interval, showing felsic patch bounded by fg-mg subophitic/subcummulate		
				tdl texture		
				150.90-151.30		
				No Sample, core already quartered, dave already took for sample		
				fg-mg cummulate/subophitic TDL as described above		
				from 151.14-151.20 felsic differentiate patch, grian size increasesw, large pyx, plag are first formed and euhedral		
				trace fg cpy (<=1mm) throughout, at 151.25-151.30 there are 0.5% fg-mg (up to 4mm) cpy subrounded crystals		
				1433-1436, 151.17 rep texture showing felsic differntiate patch, fg cpy grain visible		

GEOLOGY						Mineralization
From	To	Maj Rock	Min Rock	Comments	Mineraliz	Comments
				151.30-151.70		
				59369		
				fg-mg cummulate look with mg (2-5mm euhedral plag crystals within the fg-mg cummulate matrix) TDL gabbro		
				mafic rich (approx 70% pyx+ol (pyx>ol)),		
				trace-0.5% fg cpy (up to 1 mm)		
				1437-1440 151.40m, rep texture of unit, showing cummulate like texture, trace fg cp		
				151.70-151.94		
				59370		
				very felsic patch (approx 70% plag) leucocratic, light greyish white colour. A chlorite fracture with strong		
				chlorite alteration halo (mafics altered to soft black chalky in 2cm buffer) runs at 30 TCA from 151.70-		
				151.82. plag crystals euhedral are elongate laths, 3mm-6mm in size, mafic minerals are subhedral-anhedral.		
				interstitial, cpx 2mm-1cm in size, with lesser oliving 3-6mm.		
				poikilitic magnetite up to 1cm		
				trace-0.5% cpy up to 1mm with trace bornite (<1mm)		
				disseminated interstitial		
				1441-1444, 151.80m, rep texture of unit showing fg cpy + bo		
				151.94-152.17		
				59371		
				SAB, high plag content (less than above interval, 50%) , with 1cm poikilitic mt. mafic minerals are subhedral-anhedral		
				grains from 2mm-1cm, plag are elongate euhedral laths 4mm-10mm.		
				0.5-1% fg diss int cpy (up to 1 mm) + trace bornite (<1mm)		
				1445-1448, 152.10m rep texture of unit showing approx 1% fg diss int cpy + bornite		
				152.17-152.60		
				59372		
				Unit is a 3b with subophitic to cummulate texture. Medium grain size. Patches of leucocratic felsic		
				differntiates		
				mafic minerals are dominant in the non leucocratic patches		
				mg 2-6mm pyx+ol crystals, subhedral-anhedral. With euhedral-subhedral plagioclase (2mm-6mm elongate		
				laths)		
				0.5-1% vfg-fg-mg cpy (up to 2mm) with trace bornite (up to 1mm) dissemintated interstitial throughotu section		
				bornite is commonly associated with cpy		
				1449-1452 152.40m rep texture of unit showing vfg-fg cpy + bo		
				152.60-153.00		
				59373		
				3b, unit is coarsening up, now its cg, subophitic texture is still slightly masked but more well defined now		

GEOLOGY						Mineralization
From	To	Maj Rock	Min Rock	Comments	Mineraliz	Comments
				the plag (subhedral-euhedral, elongate laths, 5mm-1cm) with cpx (subhedral-anhedral, encasing plag crystals		
				4mm-3cm), ol (subhedral, interstitial, angular, 2-6mm), 2-4% mt, 2-5mm angular interstitial.		
				1-2% fg-mg (up to 3mm cpy) + trace bornite (up to 2mm) often associated, bornite also occurs as		
				individual grains		
				1453-1456, 152.70m, rep teture of unit showing cpy + bo and larger cpx crystals		
				153.00-153.57		
				no sample, already quarter core		
				subophitic plag-pyx-ol TDL gabbro, subophitic texture is well defined now		
				1-2% fg-mg (up to 3mm) cpy + bo (up to 2mm) disseminteated interstitial throughout this section		
				1157-1160 153.20m, rep texture of unit, showing 3mm cp+bo crystal		
				153.57-153.80		
				59374		
				Leucocratic plag patch throughout this section, approx 80% plagioclase, (euhedral, elongate laths, 4mm-1cm)		
				with poikilitic mt 3-6mm (5%), cpx + ol (3-7mm, anhedral-subhedral, interstitial, sometimes angular)		
				1-2% fg-mg cpy (up to 3 mm) + trace bornite (up to 2mm), cpy + bo often occur together		
				1161-1164 153.62m rep texture of unit		
				153.80-154.13		
				59375		
				welll defined subophitic-ophitic texture. Plag (elongate laths, 4mm-1cm, euhedral), cpx (subhedral-anhedral,		
				interstitial, angular, up to 2 cm in size, enclose plag crystals), ol (subhedral-anhedral, angular interstitial		
				3-6mm), magnetite angular, subhedral up to 4mm, biotite angular interstitial, up to 3mm.		
				approx 45% pyx, 32% plag, 10% ol, 5%mt, 3% bt, 5-7% sulphides		
				5-7% sulphides		
				5% cpy, fg-mg up to 5 mm, disseminated, interstitial angular		
				1-2% bornite,fg-mg 1-2mm on average, often associated with cpy, very high occurance in this zone		
				1165-1168 1153.90m rep texture showing suphides		
				1169-1172 154.08m, rep photo showing ophitic texture and sulphides		
				154.13-154.39		
				59376		
				well defined ophitic cg texture, plag (elongate euhedral laths, 5mm-1.5 cm) pyx (subhedral-anhedral		
				intestitial angular, 5mm-2cm), ol (subhedral-anhedral, 3-6mm), 3-5% mt 2-5mm angular interstitial		
				trace bt.		
				2-3% fg-mg (up to 3mm) cpy + 0.5% bornite (up to 2mm) disseminated throughout, typically angular inter		

GEOLOGY						Mineralization
From	To	Maj Rock	Min Rock	Comments	Mineraliz	Comments
				stitial		
				1173-1176, 154.23 rep photo showing unit texture and sulphides		
				154.39-154.89		
				59377		
				3b with subophitic/cummulate texture. Texture is poorly defined in this interval		
				mg overall grain size, plag crystals (euhedral, 2-6mm) with cpx+ol,		
				overall very simlar to previous subophitic units		
				3-4% fg-mg cpy (up to 8mm) and 0.5% bornite (up to 4 mm) disseminated throughout		
				from 154.50-154.70 at 30 TCA is a qtz-syenite dike, dominant mineral is orthoclase (90%), with		
				154.45 1477-1480 rep unit texture showing cpx and bo		
				1481-1484 154.60 orthoclase-labradorite dike		
				154.89-155.50		
				59378		
				pegmatitic ophitic plag(1-6cm, elongate laths, euhedral) cpx (subhedral-anhedral, interstitial, 1cm-7cm),		
				1485-1488 155.15m, rep texture of pegmatitic unit		
				1489-1492 155.25m, rep texture showing cg cp with bornite centre		
				mg-cg cp+bo, 2-3% cp (3mm-9mm) + 0.5-1% bo (2mm-5mm) , occurs locally throughotu section not dissemintead throughout typically as coarse grains		
154.80		3b - Coarse grained gabbro (>5mm)				
				cg ophitic-subophitic plag (euhedral, elongate laths, 4mm-10mm), cpx (interstitial, angular, subhedral-		
				anhedral, 5mm-1cm), olivine (subhedral, angular interstitial, 3mm-6mm), 3-5% angular interstitial mt, 3-6mm		
				trace biotite		
				Modal minerals is approx 45% cpx, 43% plag, 5-10% ol, 3-5% mt, 1-2% bt		
				weak patchy (5-15%) variable chlorite alteration of mafic minerals (green, soft chalky) throughout		
				158.20-158.27 small patch where grain size decreases to mg, and it has a cummulate look to it, mafic rich,		
				similar to the ones above, cpx rich, plag euhedral, 2mm-4mm average, cpx 2mm-5mm		
				from 158.30-158.57 slight increase in grain size, plag up to 1.5 cm, cpx up to 3 cm		
				grain size for the most part is consistent, but there are pegmatitc zones (marked out) and zones with a		
				slight grain size increase (plag 5mm-1.5cm, cpx 5mm-2cm)		
				slight increase in grain size from 172.40-175.50,		
				174.34-174.46, 191.56-191.60, 194.12-194.20, 194.28-194.30, 194.70-194.71 carbonate+hem healed fracture zones		
				wide, at 90 TCA		
				198.85-201.70 fault zone within the 3b unit (cg-vcg), intense fracturing, fractures are chlorite/hematite filled,		

GEOLOGY						Mineralization
From	To	Maj Rock	Min Rock	Comments	Mineraliz	Comments
				zones of ground rock. Slickenside chlorite+talc+serpentine surfaces, strong pervasive chlorite		
				blackish green alteration of mafics (essentially all the mafics in this zone), soft, chalky, patchy hematite		
				alteration (overall this looks like the fault zone that was above the first W intersection in hole 369(.		
				201.70-202.89, fracturing is less baundant, carbonate/hematite fractures, chlorite (blackish green) and		
				hematite (dark red) alteration of mafic minerals, strongly altered 3b.		
			3d - Coarse grained to pegmatitic gabbro			
				pegmatitc plag-pyx-ol TDL gabbro		
				from 158.00-158.20m, plag up to 3cm, cpx up to 4 cm.		
				165.55-170.80 pegmatitic band within the 3b unit		
				ophitic plag (euhedral, elongate laths, 1-8cm) cpx (subhedral-anhedral, interstital angular, 1cm-8cm), no ol		
				noted. Mt angular, interstitial, 2mm-1.4 cm), approx 45% plag, 40% cpx, 5% mt.		
				170.25-170.80, 171.15-60, 172.16-172.40, vcg-pegmatitic patches, plag 0.5mm-3cm, cpx 1cm-5cm		
			5a - Quartz syenite dikelet			
				166.73-167.54 of coarse <3-5cm (network of overgrowths) kspar grains and		
				coarse (<0.5-1cm) interstitial pyroxenes (85% ksp, 10% cpx, 5% mt)		
				196.25-198.85 (network of coarse ksp grains, localised patches of coarse magnetite,		
				bands of chlorite rich matrix supporting fragments, patches of smokey quartz		
				200.6-200.8, 207.75-208.2, 216.58-216.85, 219.85-220.23,		
				Main Zone Sampling		
202.00	202.30	3b - Coarse grained gabbro (>5mm)				
				59379		
				cg subophitic plag (euhedral-subhedral, elongate laths, typically encased in cpx grains, approx 3mm-1cm,		
				cpx (subhedral-anheral, interstitial angular, 5mm-2cm), no olivine distinctly noted (would likely be		
				subhedral-anhedral, interstitial angular, 2mm-5mm). 5-8% mt, angular, interstitial, 2mm-1cm.		
				Mod chlorite alteration of mafics (!8-12%) altered to soft pale green-blackish green, chalky and		
				hematite alteration (~5%) to blackish red colour with red streak.		
				no sulphides in this sample		
				1494-1497, 202.10m, rep photo of unit, red is hem, pale green chl alteration.		
202.30	202.60	3b - Coarse grained gabbro (>5mm)				
				59380		
				starting at 202.60 start to get some hairline chlorite fractures at 30-40 TCA		
				SAB, hem alteration 10%, chl 10-15% + light pink staining (ksp?)		
				1-2% fg-mg (up to 2mm) angular, interstitial disseminated cpy		

GEOLOGY						Mineralization
From	To	Maj Rock	Min Rock	Comments	Mineraliz	Comments
				1498-1501, 202.52 rep texture showing strong hem alteration, angular cpy is visible		
202.60	202.90	3b - Coarse grained gabbro (>5mm)				
				59381		
				SAB but the original texture is almost completely annihilated, due to intense fracturing		
				carb+hem fracture and chlorite+-talc+-serpentine fractures in this zone, intense, approx 15 in this section		
				fractures are also overprinted, hematite alteration is approx 15%, chlorite 10-15%, very messy		
				trace cpy		
				1502-1505 202.83, rep photo showing carb+hem fracture, highly distorted texture of unit		
				trace fg cpy noted, difficult to see in intense fractured zones		
202.90	203.20	3b - Coarse grained gabbro (>5mm)				
				59382		
				mg-cg subophitic plag (euhedral-subhedral, elongate laths, typically encased in cpx grains, approx 3mm-1cm,		
				cpx (subhedral-anheral, interstitial angular, 5mm-2cm), no olivine distinctly noted (would likely be		
				subhedral-anhedral, interstitial angular, 2mm-5mm). 5-8% mt, angular, interstitial, 2mm-1cm.		
				Mod chlorite alteration of mafics (5-10%) altered to soft pale green-blackish green, chalky and		
				hematite alteration (~5%) to blackish red colour with red streak.		
				1506-1509, 203.18m, rep texture, showing mineralization		
				3-4% fg-mg (up to 2mm) angular interstitial cpy		
203.20	203.58	3b - Coarse grained gabbro (>5mm)				
				59383		
				SAB, hem alteration patches 4mm-2cm, irregular, dark blackish red		
				3-5% fg-mg-cg (1-3mm average) up to 6mm, interstital angular cpy		
				1510-1513 203.55m, rep texture showing blotches of blackish red hematite and mineralization		
203.58	203.85	3d - Coarse grained to pegmatitic gabbro				
				59384		
				vcg-pegmatitic subophitic-ophitic plag (euhedral, elongate laths, 5mm-3cm, enclosed within cpx crystals		
				[ie the ophitic texture], cpx (subhedral-anhedral, interstitial angular, 5mm-7cm), ol (little is detected,		
				3-5mm, subhedral-anhedral, interstitial angular). Mt angular interstitial, 4mm-1cm. Approx 40%plag, 40% cpx		
				10% ol, 5-7%] mt, 3-5% cpy		
				Mod (5-10%) patchy chlorite altreation of mafics (soft, pale green, chalky to greenish black), weak pink		
				patches (very few, scattered, hem? + hem alteration of mafics (dark reddish black), 3-5%.		
				overall very swimilar to previous unit except with a larger grain size		
				3-5% fg-mg-cg (up to 8mm) interstitial angular disseminated cpy		
				1514-1517 203.65m, rep texture showing 8 cm cpx crystal		
				1518-1521 203.8, rep texture		
203.85	204.18	3d - Coarse grained to pegmatitic gabbro				

GEOLOGY						Mineralization
From	To	Maj Rock	Min Rock	Comments	Mineraliz	Comments
				59385		
				SAB		
				3-5% fg-mg-cg (up to 1cm) diss int angular cpy		
				1522-1525 204.05 , rep texture showing mineralization		
204.18	204.62	3d - Coarse grained to pegmatitic gabbro				
				59386		
				SAB		
				1526-1529 204.55m, rep texture showing mineralization		
				3-5% fg-mg-cg (up to 1cm) diss int angular cpy		
204.62	205.00	3b - Coarse grained gabbro (>5mm)				
				59387		
				mg-cg subophitic plag (euhedral-subhedral, elongate laths, typically encased in cpx grains, approx 3mm-1cm,		
				cpx (subhedral-anheral, interstitial angular, 5mm-2cm), no olivine distinctly noted (would likely be		
				subhedral-anhedral, interstitial angular, 2mm-5mm). 4-6% mt, angular, interstitial, 2mm-1cm.		
				Mod chlorite alteration of mafics (5-10%) altered to soft pale green-blackish green, chalky and		
				hematite alteration (~5%) to blackish red colour with red streak.		
				3-5% fg-mg-cg (up to 1cm) angular interstitial cpy		
				The grain size is decreased relative in this unit to the previous, alteration and fracturing are also more		
				intense		
				1530-1533 204.75m, rep texgture showing increased alteration, 1cm cg cpy + fg-mg diss cpy, pinkish patch		
				the cg cpy in this photo is part of the thin section		
205.00	205.34	3b - Coarse grained gabbro (>5mm)				
				59388		
				SAB		
				hem is as pink patches , chlorite alteration is strong,		
				3-5% cpy, cpy is dominangly mg-cg, up to 2cm,		
				1534-1537, 205.25 rep photo of texture showing pink hem, and cg cpy minerlization, this is where the thin is		
				coming from		
205.34	205.70	3b - Coarse grained gabbro (>5mm)				
				59389		
				as above, contains chlorite fractures, serpentization possible, black specs		
				1-2% fg cpy		
				1538-1541 205.6m, rep texture showign black chlorite alteraiton, some mineralization		
205.70	206.00	3b - Coarse grained gabbro (>5mm)				
				59390		
				coming out of the alteration into a nice looking TDL.		
				mg-cg subophitic-ophitic plag (euhderal laths, 2mm-7mm) cpx (subhedral-anhedral, interstitial angular		

GEOLOGY						Mineralization
From	To	Maj Rock	Min Rock	Comments	Mineraliz	Comments
				typically enclosing plag grains, 2mm-1.5 cm) ol (angular, interstitial, subheral-anhedral, 2mm-5mm)		
				mt angular, interstitial, 2mm-5mm, 3-5%		
				patchy chlorite alteration of mafics (pale green soft), approx <=5%		
				3-5% fg-mg (up to 2mm) disseminated cpy, interstitial, angular		
206.00	235.35	3b - Coarse grained gabbro (>5mm)				
				mg-cg subophitic-ophitic plag (euhderal laths, 2mm-7mm) cpx (subhedral-anhedral, interstitial angular		
				typically enclosing plag grains, 2mm-1.5 cm) ol (angular, interstitial, subheral-anhedral, 2mm-5mm)		
				mt angular, interstitial, 2mm-5mm, 3-5%		
				patchy chlorite alteration of mafics (pale green soft), approx <=5%		
				Unit is fairly consistent and homogeneous down hole from heree		
				no sulphides (ie none after main zone above ended)		
235.35	242.1	5a - Quartz syenite dikelet				
				Network of coarse grained kspar+interstitial plag+quartz, irregular patches of carbonate		
242.1	244.85	2a - Fine grained gabbro				
				fine grained plag+olivine+pyroxene+abundant magnetite (magnetic), minor clots of biotite		
244.85	246	1a - Footwall Breccia (RIB)				
				irr mafic sub-rounded clasts		
246		EOH - End of Hole				

MARATHON PGM CORPORATION - DIAMOND DRILL CORE LOG

DDH-368 Log

NTS: 42 D / 16
UTM Northing 5404392.83
(Nad27) Easting 550045.76
Elevation: 300.56
Dip at Collar: -71
Azimuth: 89.65
Total Depth: 246m
Core Size: NQ
Remarks: Core stored in Marathon PGM Corporation warehouse, Marathon, Ontario

Property: Marathon

Contractor: Chibougamau Diamond Drilling Ltd.
Logged by: Dave Leng
Assistant: Ryan Milne
Relogged by: Ryan Ruthart

GEOLOGY					Mineralization	
From	To	Maj Rock	Min Rock	Comments	Mineraliz	Comments
0.00	1.90	O/B - Overburden				
1.90	13.79	2d - Fine grained gabbro with coarse grained gabbro dikelets				
				Cut surface is medium grey, salt and pepper texture. Fine grained pyx-ol-plag equigranular gabbro. Minerals are all < 1 mm, due to small size difficult to identify. Melanocratic colour, looks more mafic than felsic. The rock exhibits minor magnetism. Unit does not show alteration.. Whole unit is fractured, approx 2-3 chlorite fractures per 20 cm, typically hairline fractures sometimes with chlorite alteration halos (0.5cm thick). These fractures range in angle from parralle to perpendicular. fracture surfaces are irregular to hackled. No sulphides present.		
				Contains irregular stringers and dikelets of a coarse grained 2f, 3b		
			2f - Medium to coarse grained magnetite rich gabbro			
				Medium coarse grained (1-10 mm) olivine (subhedral, rounded) magnetite (subhedral, rounded to massive bands) , plag (subhedral, elongate tabular) cummulate. Contains accessory irregular shaped, interstitial biotite. Colour is a green black (magnetite and olivine contrast). Magnetite rich bands, dominantly magnetite rich unit. Contacts are irregular, typically at 90-80 TCA. Unit is not very consistent, the intrustions are clearly the same and only have one contact, but it can grade from being magnetite + olivine rich (mag 50%, ol 40%) to a more balanced unit of mag, ol and plag (approx 30,30,30). In the more balanced unit there is a mod (10%) chlorite (pale green) alteration of the unit (dominantly the mafics) Contacts between mag+ol rich and the balanced are gradationals contacts leading me to belive that they are the same unit.		
				2.16-2.56 (mag, ol rich), 6.90-8.33.60 (from 6.90-7.15 mag ol rich, after balanced mag, ol, plag), 10.00-10.20 (balanced), 11.45-11.60 (mag+ol rich, top 4 cm is a chlorite gouge) 11.64-13.79 (12.00-12.50 is mag+ol rich, then changes to balanced),		
			3b - Coarse grained gabbro (>5mm)			
				Cg plag rich gabbro. cg plag (80%, 4-6mm, euhedral-subhedral), pyx (10% subhedral , 4-6 mm, subhedral), mt (angular, interstitial, 3-6 mm, 3-5%). Unit is white (plag) with black specs (mag) with a pink tinge to it (ksp?) Dominantly plagioclase. Previously logged as a syenite but does not look like one.		
				Photos:		
				734, 5.70 m, 3b plag rich gabbro		
				735, 6.05 m 3b plag rich unit on the fresh break side		
				736-737, 7.95 m 2f mag + ol rich section		
				738, 8.50 m 2f balanced mag,ol,plag		
				739, 10.00m rep texture of the 2a fg gabbro, with a parallel chlorite fracture		
				740, 12.45m chlorite gouge		
13.79	20.70	2e - Medium to coarse grained gabbro				
				grey with hint of green, salt and pepper texture, mg ol-plag-pyx, moderately magnetic gabbro. This unit is heterogeneous, Grain size is dominantly mg from 13.79-19.20, then it grades to fg, but there are still patches of mg material. Olivine grains are slightly larger than the rest, subrounded subhedral, plag grains are subhedral, and appear interstitial. abundant olivine. contains intrusions of 3b with euhedral plag, subhedral-anhedral pyx+ol, highly irregular stringers.		
			3b - Coarse grained gabbro (>5mm)			
				mg-cg (variable grain size,) plag (euhedral, 2mm-10mm) -pyx (subhedral-anhedral, interstitial to plag 2mm-10mm) - ol (subrounded to angular, interstitial, subhedral. 2-4mm) , minor magnetite (3-4%) and biotite. Irregular contacts. No alteration.		
				18.10-18.46, 18.74-19.20, are the large pockets of it, other wise irregular stringers		

				Photos:		
				741, 17.0m rep texture of the cg gabbro		
				742, 17.0m rep texture of the cg gabbro fresh surface		
				743, 18.10m contact of 3b with 2d		
				744, 18.20 m 3b dikelte rep txture		
20.70	39.52	2a - Fine grained gabbro				
				fg pyx-ol-plag gabbro. Grey colour, salt and pepper texture on cut surface. Salt and pepper texture. Equigranular. Very homogeneous unit		
				fine grained pyx+olv rich, minor mag cummulate		
				- coarse olv cumulate from 19.23-20.72		
				- spotted chl alt, anhedral grains up to 1cm from 21.85-23.75, 25.48-26.57		
				- abundant irregular fractures from 26.37-26.66(@ subparallel to ca. chl alt.), 28.5-28.87(@ subparallel		
				to ca. with chl alt, and pebbled), 29.52-29.86(chl+carb infilling @ 40deg to ca.), 38.20-38.27 (45deg TCA, 2 mm)		
				- homogenous from 28.43-39.52		
				Hairline fractures throughout, domintnat chlorite fill, occasionally carb fill. Approx 1/20 cm on average,, typically 45-60TCA but can change		
				Pocket of pink hem? 38.35-38.40(pocket)		
				Photos:		
				745, 19.90m rep texture of the 2a unit		
				746, 22.30m spotted chlorite texture		
				747, 29.85m chlorite+carb fracture		
				748, 32.70m rep 2a texture		
				749, 38.35 pocket of pink		
39.52	43.19	5a - Quartz syenite dike				
				coarse grained, qtz-syenite dike. Composition is dominantly cg orthoclase (80%, 2-4 cm), qtz (5%) minor mt (rounded, 5%), deep red (hematite) colouring from 39.52-41.00, then it changes to a more grey colour, hematite still visible along grain boundaries.		
				sharp upper and lower contacts at 30 TCA.		
			2a - Fine grained gabbro			
				fine grained pyx+olv rich, homogenous from 41.82-42.13		
				Photos:		
				750, 40.0m , qtz-syenite with red hem staining		
				751, 41.10m, 5a large orthoclase crystals		
				752, 42.80m, white albite crystals with black (Chlorite?) rims		
				753, 43.19 lowre contact of dike with 2a unit		
43.19	51.1	2d - Fine grained gabbro with coarse grained gabbro dikelets				
				fine grained pyx+olv rich cumulate, minor mag with intrusions of 5a, 3b and zones of 2f		
				- abundant fractures from 43.58-43.64 (strong chl alt. and pebbled), 44.95-45.02(chl alt., pebbled)		
				46.44-46.6(chl alt. subparallel to ca.), 49.66-49.8(@45 deg to ca.)		
			2f - Medium to coarse grained magnetite rich gabbro			
				45-45.32 med grained rounded ol-plag-mt-pyx, abun mag (10%) mag cumulate rich , . Equigranular. Olivine and pyx are subhedral, plag is subhedral to anhedral (crystallization of olivine and pyx first to form cummulate) Interstitial magnetite (approx 5-10%)		
			5a - Quartz syenite dike			
				coarse grained qtz-syenite dike, dominant orthoclase,f rom 49.77-50.23(lower contact is assimilated into 2a), 50.46 50.58,		
				50.7-50.75, dominantly orthoclase, 5-10% qtz, lesser labradorite. This one does not have mag		
			3b - Coarse grained gabbro (>5mm)			
				White/green mottled colour (green/grey pyroxenes and olivine with white plag crystals) the unit is patchy and there are zones where the colour is dominantly grey/green and where the colour is dominantly white. This reflects zones of plag rich and mafic rich minerals. Plag grains are euhedral, tabular, size is 5mm-10mm, olivine grains are rounded to interstitial angular and typically only 1-3mm, pyroxenes are angular, anhedral interstitial and 2-4 mm.		
				from 48.07-48.40, 52.10-52.50, 55.24-55.6.30(irregular pockets of 3b)		
				Photos		

				754, 43.20m close up of strong chlorite alteration zone		
				755 43.20m zoom out of clhlorite alteration showing contac		
				755, 50.0m qtz-syenite dike, showing pink orthoclase crystals, highly fractured look		
				756,757 50.20 m lower irregular assimilated contact of dike		
				757, 45.20m 2e cg ol-pyx cummulate		
51.1	57.59	3a - Fine to medium graine		3a mg plag-ol-pyx gabbro. Plag is euhedral to subhedral with subhedral to anhedral (interstitial to plag) pyx + ol. Strong chlorite alteration throughout (pervasive) giving it a pale green colour. Abundant fractures throughout, with zones of anastomizing over lying fractures (looks stripped). Outside of the marked intense fracture zones chlorite fractures are approx 3-4/10 cm. chlorite fractures range from hairline to 2-3mm thick, are 90-70 TCA. Unit is highly distorted due to fracturing and chlorite alteration.		
				- heavily fractured, chl+mag infill,thin anastomosing banding from 52.5-57.3, (stripped look)		
				very dense, anastomising chlorite fractures, > 12/10cm from 52.50-53.70, 54.26-55.00, 56.40-57.30 (looks stripped	1-3% disseminated sulphides	
				Contains a few irregular stringers of 3b, and a 5a qtz syenite dike		from 54-54.23 fine grained cpy up to 1mm
				Mineralization		from 57.46-57.58 fine grained cpy up to 1mm
				53.92-54.24 2-3% fg disseminated interstitial cpy, at 54.18-54.20 there is a small cluster (5 grains) of fg bornite		from 57.14-57.17 fine-med grained 3% cpy up to 2mm
				55.53-53.82, 1-2% fg-mg disseminated interstitial cpy		
			3b - Coarse grained gabbro (>5mm)		0.5% to 1% disseminated sulphides	
				3b, 51.10-51.18, 51.29-51.45, 51.90-52.50, cg overall, variable grain size plag (euhedral, tabular, up to 1.5 cm) with interstitial (subhedral-anhedral, angular, 2-6 mm, interstitial) pyx+ol, mod int mt (angular interstitial). Overall colour is a mottled white/grey with a green tint. Mod chlorite alteration of mafics give the units a green colour.		from 54.88-54.9 fine grained cpy up t 1mm
			2f - Medium to coarse grained magnetite rich gabbro			
				57.3-57.59 Equigranular. Olivine and pyx are subhedral, plag is subhedral to anhedral (crystallization of olivine and pyx first to form cummulate) Interstitial magnetite (approx 5-10%)		from 57.29-57.42 fine grained cpy up to 1mm
				coarse grained from 49.77-50.23(lower contact is assimilated into 2a), 50.46-50.58,		
				Photos		
				754, 43.20m close up of strong chlorite alteration zone		
				755 43.20m zoom out of clhlorite alteration showing contac		
				755, 50.0m qtz-syenite dike, showing pink orthoclase crystals, highly fractured look		
				756,757 50.20 m lower irregular assimilated contact of dike		
				757, 45.20m 2e cg ol-pyx cummulate		
				758, 51.10m, 3b showing patch of white (plag) and patch of green (cpx+ol)		
				759, 52.60 anastomiozing chlorite veins, stripped look		
				760, 52.70 thick band of chlorite		
				761, 52.90m stipped look of anastomizing chlorite veins		
				762, 763, 57.40m, 2f cg olivine rich unit		
				784-786, 54.18, bornite in the 3a unit, second picture is right centre under the white band (hard to see in photo)		
				787, 54.10 2-3% fg cp in 3a unit		
				786, 54.18 bornite as in 784, this time with sample wetted down		
				786, 55.60 1-2% fg-mg cpy in 3a		
57.59	63.90	3b - Coarse grained gabbro (>5mm)				
				Greenish grey colour, leucocratic gabbro. Plag (euhedral, elongate laths, up to 2 0 mm, 5-6 mm average) with interstitial angular anhedral olivine (occurs as clumps up to 10 mm, but on fresh broken surface appears to be multiple grains, average 2-5mm) and pyroxene (2-10mm) Grain size is highly variable . Olv is greater occurance than pyx. Modal mineral percent is highly variable, plag>ol>pyx. Trace mt (1-2%) , grains are also anhedral and angular. Chlorite alteration is patchy (0-5%) and mafic minerals become a dull greenish colour. Patches of white leucocratic felsic pods occur.(<1% of total section). Low amount of chlorite healed fractures (1/30cm) hairline, at variable angles approx 90-70 TCA		
				Upper contact with 2d is irregular, looks like a mixed zone.		
				Mineralization:		
				57.59-57.90, trace fg-mg interstitial cpy		
				58.90-59.10, 1-2% fg cp + bo, bo occurs as part of cp grains, (cp:bo 15:1)		
				59.40-60 2-3% fg-mg-cg cpy, trace bo occuring on rims and centres of cpy grains, there is a single po grain that appears to be being replaced by cp		
				778, 57.6m contact between 2e and 3b, contains cp		
				789, 58.8m, rep unit texture, of 3b, plag rich, can see int olivine, mod chlorite alteration,		

				788-789, 59.60, po and cp grain, cp appears to be replacing po		
				790-791, 59.65m, mg-cg cpy in 3b, grain of bornite		
				792, 59.70m, cg cpy in 3b, patchy white looking plag		
63.9	65	3d - Coarse grained to pegmatitic gabbro				
				above unit grades into a pegmatitic grain size. Euhedral plag crystals, variable grain size, (5mm-4 cm, euhedral, first to form), ol (interstitial, angular, several mm-2 cm), cpx (interstitila, angular, 5mm-8 cm). Unit has a blue grey colour. Moderate silicification, mod patchy chlorite alteration (approx 5%), 2-3% angular interstitial magnetite. Unit shows a very nice ophitic texture (giant pyroxene encasing euhedral plag laths)		
				795, 64.0m, large 8 cm cpx grian encasing euhedral plag alths (ophitic texture)		
				796, 64.50m, 3d showing leucocratic plag patch (greenish tinge)		
				797, 65.0m, rep texture of unit, showing pegmatitc plag and interstitial ol+pyx		
				No mineralization		
65.00	67.22	3b - Coarse grained gabbro (>5mm)				
				cg-vcg plag (euhedral) with interstitial pyx+olv (anhedral, angular interstitial). Grain size is highly variable throughout, maximum grain size of 2.5 cm (for plag, pyx, ol). Colour is blue grey, indicating moderate silicification. Scattered 1-2 cm felsic pods in this unit. Modal percentage of minerals is variable, approx plag 50%, cpx + olv 45 %. 1-2 % angular, interstitial mt, up to 1cm, typically rare in this section.		
				66.65-66.68, band of magnetite+biotite at 90 TCA, biotite appears interstitila to magnetite		
				lower contact is gradational into a pegmatitic unit		
				798, 65.75m rep texture of unit, showing blue grey colour and felsic pods of materia		
				799, 66.67m, band of magnetite+biotite at 90 TCA, biotite appears interstitila to magnetite		
				800, 66.80, biotite crystal that has elongate tabular shape (ie looks like plag lath was repalced		
67.22	67.70	3d - Coarse grained to pegmatitic gabbro				
				vcg-pegmatitic plag (euhedral, up to 4 cm) with interstitial cpx+ol (angular, interstitial, 2-5 cm). Blue grey colour, well defined ophitic texture. Mod silicification, blue grey colour.		
				801-802, 67.22m, gradation between coarse grained and pegmatitic		
				803, 67.60, 3d pegmatitic texture		
67.20		3b - Coarse grained gabbro (>5mm)				
				cg plag (euhedral-subhedral, first formed, elongate laths up , 2-4mm up to 1.5 cm, variable grain size) with pyx+ol (interstitial, angular, variable grain size, mm-scale to 2 cm, average 1 cm). Trace angular anhedral interstitial magnetite, variable, sometimes occurs in clumps, for the most part absent from unit. Pockets of pegmatitc grain size, gradational change in grain size, no contacts visible. Variable modal mineral percentage, overall approx 40-50% plag, 40% pyx+ol, approx 1:1 pyx:ol on average, varies locally		
				Moderately silicified from 67.20 - (blue grey colour)		
				Unit for the most part shows only trace chlorite alteration of mafics (pale green), however there are patches of moderate chlorite alteration marked out below.		
				moderate chlorite alteration, approx 10-15% pale green alteration of mafic minerals from 68.80-69.00, 72.72.25, 72.85 72.99, 74.10-74.50, 75.94-76.05, 77.85-78.00 (with hairline chlorite fracture), 78.65-78.80 (with hairline chlorite fracture, approx 60 TCA), 79.06-79.15 (with hairline chlorite fracture), 79.90-80.40,		
				78.30-78.55 leucocratic abundant plag zone, almost entirely opaque white, interstitial mafics are all chloritized., contains a coarse grain of cpy. Bounded on top and bottom by coarse grained magnetite		
				Photos		
				804, 68.90 m, patch of moderate chlorite altreation, 10-15%, pale green mafics		
				805, 69.95, 3d pegmatitic ophiitc texture		
			3d - Coarse grained to pegmatitic gabbro			
				vcg-pegmatitic plag (euhedral, up to 4 cm) with interstitial cpx+ol (angular, interstitial, 2-5 cm). Blue grey colour, well defined ophitic texture. Mod silicification, blue grey colour. From 69.20-69.94, 76.32-76.5		
				Photos		
				804, 68.90 m, patch of moderate chlorite altreation, 10-15%, pale green mafics		
				805, 69.95, 3d pegmatitic ophiitc texture		
				806, 7290, rep texture of zone of strong chlorite alteration, chlrotie is pale green,		
				807, 73.10m, rep texture of unaltered unit, white plag, grey is pyx, green is olv,		
				808, 78.40m, leucoratic plag zone as described above, opaque white, one grain of cpy		
				809, 78.55, coarse grained magnetite below leucocratic plagioclase zone		
				810-811, 80.55, rep texture of 3b unit, unaltered, wet and dry		

82.53	90.25	2g - Anorthositic gabbro with poikilitic magnetite				
				Unit is grey coloured with irregular lenses and patches of white felsic material. Overall unit is fg-mg (1-2mm average grain size). Composed of approx 40% plag, 30% pyx, 15% olv. Contains white patches of felsic material that are dominantly white, with a hint of green and pink, entirely feldspar material. Contains poikkilitic magnetite, 3mm-2 cm in size scattered throughout the unit. Unit appears moderately silicified, giving it a blue grey colour.		
			5a - Quartz syenite dikelet			
				82.74-82.89 cg qtz syenite dike, contact is at approx 60 TCA, sharp and distinct. Approx 80% orthoclase feldspar, 5% labradorite, 5% qtz, no magnetite		
				Photos:		
				812-813, 82.53m contact between 3b and the fg felsic uni		
				814, 82.80m qtz-syenite dike at		
				815, 84.14m, rep unit texture with poikilitic magnetite, with inclusions of feldspars.		
				816 87.80m, rep texture of unit showing the felsic banding within the fg grey gabbro uni		
90.25	100.99	3b - Coarse grained gabbro (>5mm)				
				medium to coarse grained plag (euhedral-subhedral) pyx-olv (subhedral-anhedral, interstitial to plag), grain size is variable, but on average 4-6 mm grain size. Unit is highly heterogeneous and messy looking. Contains irregular leucocratic patches of felsic material (dominantly plag). Olv and pyx form clumps up to (1-2 cm). Occasional large pyroxene crystals 5-8 cm at 92.38-93.42, 93.80, 94.00-94.05, 96.10-96.15, but these are the largest crystals, every other grain size stays in the mg grain range, so it is not the pegmatitic unit. Moderate silicification gives the core a blue-grey colour. Chlorite alteration is generally absent from this section but is present in patches up to 10%. Interstitial magnetite approx 2-3%, is scattered throughout, angular interstitial to other minerals. Trace amounts of biotite, interstitial, often occurs with magnetite. Mt can be 1-4 mm, or up to 1 cm poikilitc with fine grained plag crystals contained within. This unit has a modal percentage bias of pyx>plag>ol, ol+pyx approx >80%, variable composition., in small patches ol+pyx decreases to 60%, pyx to 40%		
				Upper contact is difficult to define between the previous unit due to strong silicification, lack of poikilitic magnetite, and coarse grain size highlight the change in units but no clear contact was found.		
				Chlorite alteration, 10-15% pale green to dark black-green colour from 94.80-95.00, 95.30-95.40, 96.00-96.05, 98.20-98.60, . Other than these sections there is only trace grains of chlorite alteration, very fresh look.		
				817, 91.85m rep texture of unit		
				818, 92.95m felsic leucocratic patch of plagioclase as described above		
				819, 93.38 large pyroxene crystal surrounded by leucocratic patches		
				820, 94.90 chlorite alteration patch showing plae green minerals		
				821, 98.40 abundant pyroxene zone with chlorite alteration		
				822, 99.70, felsic rich patch, with poikilitic magnetite		
				823, 100.99 contact between 2c and 3b		
100.99	105.10	2e - Medium to coarse grained gabbro				
				fine grained-mg (<1mm-1mm) olivine-pyx-plag equigranular gabbro. Green-grey colour with grey spots. Spots are subrounded 3-6 mm porphyroblasts of magnetite and pyroxene.		
				Strong pervasive chlorite alteration (almost completely dark greenish black from 104.60-104.75		
				Unit contains about 12 hairline chlorite fractures, at 70-90 TCA and parallel.		
				Upper contact is distinct with slight intermixing.		
				fine grained olv rich green colouring with undefined pyx porphyroblast (3-6mm) becoming more		
				defined and rounded downhole		
				Strong chlorite alteration (almost completely black, soft chalky) from 104.60-104.75m, this is right above a qtz-syenite dike		
				has a few mm-scale stringers of coarser grained material		
				Photos		
				824, 102.60m rep texture showing mt porphyroblasts (dark grey) and cpx (light grey) green colour is from abundant olivine, white patches are plag		
				825, 101.75m rep texture again showing sub parallel chlorite fracture		
				826, 104.60m zone of chlorite alteration mentioned above		
				827, 104.85m upper contact with qtz-syentite diek		
				828, 105.10m lower contact of qtz syenite dike with 3b uni		
			5a - Quartz syenite dikelet			
				104.85-105.10, qtz-syenite dike, 80% orthoclase (5mm-1.5cm), grey colour, heavily fractured look. Intrestitial mafics to the orthoclase crystals. Contact is irregular, approx 60 TCA, and lower contact is also irregular		
				Trace cpy in the mixing zones above and below the dike		
105.10	108.10	3b - Coarse grained gabbro (>5mm)				

				blue-grey mg-cg plag (subhedral-euhedral, elongate laths, 5mm average, 1cm maximum), pyx-olv (subhedral-anhedral, angular interstitial 2mm-5 mm, this unit lacks the clumps of olinvine and large pyx crystals),, magnetite (less than to about 1%, angular, interstitial, very low amount). Chlorite alteration throughout, approx 10-15% of mafics have a pale green colour, soft to them. Plag is approx 50%, cpx approx 30%, olv 10% or less, variable modal mineral percentages. pyx>ol throughout section.		
			3d - Coarse grained to pegmatitic gabbro			
				107.70-108.10 cg-pegmatitc grain size, plag (euhedral, elongate laths up to 3 cm, 1cm on average), pyx-olv (pyx>olv, grain size 1cm-5cm). Grain size on average in this unit is in the coarse grained (1cm-2cm) range but there are large pegmatitic size >3cm crystals, this is typical for the pegmatitic unit.		
				107.92-108.05, 6 chlorite healed fractures, approx 80TCA, strong zone of pervasive chlorite alteration. Abundant (approx 5-10%) subrounded to subangular magnetite.		
				Small zones 1-3 cm, scattered throughout of leucocratic feldspar, much smaller than the previous 3b unit. Patches are highly irregular, no normal grain boundaries, look kind of all over the place		
				Photos		
				837-838, 105.40m, rep texture of unit, showing chlorite alteration, white is plag, green is olv, grey is pyx, medium grained size		
				839, 106.75m rep texture of unit, showing chlorite alteration and plag rich leuoccratic patch		
				840, 107.80m pegmatitic zone in the unit, large pyx and cpx crystals shown		
				841, 108.00m, strong chlorite alteration in the pegmatitic zone, plag crystals are opaque white		
108.10	108.53	3a - Fine to medium grained gabbro (<5mm)				
				fg-mg plag (euhedral-subhedral, 1mm average, up to 2 mm) with ophitic cpx enclosing plag grains, (subhedral, interstitial and enclosing plag laths, occasional ophitic grains up to 5 mm, typical grains are on the mm scale), olivine (interstitial, 1 mm average). Weak-mod pink patches (ksp) and wisps throughout unit. Unit is a grey-green colour, mod (10%) chlorite alteration throughout unit. Plag crystals are opaque white (due to ksp? alteration). plag>cpx>ol. Moderate interstitial angular magnetite. veyr minor biotite.		
				upper contact is well defined after zone of chlorite alteration in the pegmatitc unit, lower contact is diffuse into a 3b		
				Photos:		
				842-844, 108.20m, rep texture of unit, both sides of core dry and wet, white opaque plag, difficult ot see ophitic pyx		
108.53	109.09	3d - Coarse grained to pegmatitic gabbro				
				cg-pegmatitic, variable grain size, grain size is increasing down hole. Plag (euhedral to subhedral, 5mm-3cm) with interstitial cpx (5mm-5cm, large grains encase feldspar crystals, defining ophitic texture), and olivine (2mm-1cm, subhedral-anhedral, angular, interstitial). abundant magnetite approx 5-10% magnetite, subrounded to subangular grains, form magnetite rich bands in the unit.		
				845-848 108.90m rep texture of the pegmatitic unit, shown wet dry, and both sides of core		
				849-850 109.09 contact between pegmatitic unit and 3c		
				lower contact is well defined, approx 60TCA with a unit of 2c.		
109.09	109.66	2e - Medium to coarse grained gabbro				
				mg (1-2mm, equigranular), olivine - pyx-plag gabbro. Olivine and pyx approximately equal modal percentage, lesser plag. With larger phenocrysts of (3-6mm) of pyx and magnetite. Overall colour is grey with dark grey spots (phenocrysts). Lower contact is approx 40 TCA, well defined but not a straight line, it is more wavy.		
109.09	109.67	2e - Medium to coarse grained gabbro				
				mg (1-2mm) olivine-pyx-plag equigranular gabbro. Green-grey colour with grey spots. Spots are subrounded 3-6 mm phenocrysts of magnetite. Magnetite crystals often haeve thin biotite rims.		
				Fresh unaltered look. Contains 5 hairline chlorite fractures.		
				Photos:		
				851, 109.40m Rep texture of unit showning dark grey mt phenocrysts		
				852, 109.67m lower contact with 3b		
109.67	127.60	3b - Coarse grained gabbro (>5mm)				
				Generally very homogeneous unit		

				Plag (euhedral-subhedral, 5mm average, up to 1 cm) with interstitial cpx (subhedral-anhedral, interstitial angular) and olivine (subhedral-anhedral, interstitial, angular). Apprximately 40%plag, 40% pyx, 10% olv, composition is relatively stable, but difficult to determine exact percentages.. Blue grey colour. Moderately silicified. Magnetite present throughout, typically subrounded to subangular, interstitial to other minerals, percentage varies from 1%-5%, variable throughout the unit.		
				Chlorite alteration is variable throughout the unit.		
				109.67-111.50, mod chlorite alteration, approx 5-10% pale green alteration of mafics		
				111.50-117.0m chlorite alteration is absent (trace rare mafic grains are pale green, but more or less not present)		
				117.00-120.00 5-10% variable chlorite pale green alteration of mafics., 118.00-118.20 strong chlorite alteration, approx 30% pale green, with dark green black phenos (soft chalky)		
				120.00-XXXX chlorite alteration is absent, trace rare mafics may be altered but esseiantlaly unaltered		
				23.55-123.80 10% chlorite alteration of mafics pale green		
				128.70-128.90, 5% chlorite alteraiton of mafics		
				Leucocratic Patches (dominantly white colour, plagioclase rich patches, irregular boundaries, lenses etc, plag becomes opaque white.)		
				from 111.20-111.30, 117.80-1118.00		
				123.50-124.20 leucocratic patch, with 10% chlorite alteration from 123.55-123.80		
				123.98-124.05 pinkish white ball, irregular, 5 cm across, plag appears to be altered to opaque white with hint of pink (ksp?) at 12.05 there is a band of coarse grained (1-2cm) magnetite		
				Photos		
				853, 110.90m rep texture of chlorite altered section, pale green mafic minerals		
				854-855, 111.15 m leucocratic patch white colour		
				856-857, rep texture of unit with no chlorite alteration		
				858-159, 117.85 leucocratic patch, with white plag and dark grey mafics,		
				860-861, 118.10m, strong chlorite alteration patch		
				862, 123.50 leucocratic patch + chlorite alteration		
				863-864, 124.00m pinkish white ball with band of magnetite described above		
127.60	129.00	3d - Coarse grained to pegmatitic gabbro				
				coarse grained to pegmatitic variable grain size plag (euhedral to subhedral, 1cm-4cm), with interstitial typically angular subhedral to anhedral pyx + olv. Cpx grains up to 8 cm encasing plag crystals (ophitic texture). Moderate magnetite (1-3%, 1-3mm, angular interstitial).		
				at 128.70 band of cg 1-2 cm magnetite looksl ike it is replacing biotite		
				lower contact grades back into mg-cg unit		
				856-867, rep texture of ophitic unit, also showing magnetite band with biotite replacement by mt		
129.00		3b - Coarse grained gabbro (>5mm)				
				medium grey, when wet plag have a transulcentpartially opaque look with mottled grain boundaries. Mg-cg plag (euhedral-subhedral, 5mm-10mm, 5 mm is average, elongate laths), pyx-olv (subhedral-anhedral, interstitial angular, 5mm-10mm). Mod magnetite, angular, interstitial, 1mm-5mm, approx 1-5%, approx 40% plag, 60% mafics, with cpx>ol. Mod silicification, giving core a blue grey colour. Patches of weak chlorite alteration (approx 5% of mafic minerals exhibiting a pale green colour), will be noted when they occur, otherwise no chlorite alteration.. Unit for the most part is homogeneous.		
				129.00-129.37,		
				59257		
				magnetite 5-7%, from 129.10-129.18 mod chlorite alteration, approx 10% of mafics pale green, soft		
				Thin section in zone of chlorite alteration		
				no sulphides		
				868-870, chlorite alteration zone		
				871-874 rep texture, no chlorrite alteration		
				129.37-129.62		
				59258		
				as described, pyx up to 3cm, (only large mineral), well defined ophitic texture		
				no chlorite		
				no sulphides		
				129.50-129.75 leucocratic plag zone, approx 70% plag		
				875-876 rep texture well defined ophitic texture		

				877, 129.75 plag rich leucocratic zone		
				129.62-129.93		
				59259		
				as described		
				no chlorite alteration		
				2-3% fg (1mm average) dissimated, interstitial cpy		
				878-879, rep texture showing sulphides		
				129.93-130.27		
				59260		
				as described, no chlorite alteration		
				1-2% fg disseminated interstitial cpy, 1 spec bornite		
				880-881, rep texture showing cp		
				130.27-130.47		
				59261		
				as described, 1% interstitial angular 1-5mm magnetite		
				1-2% fg-mg (1-2 mm) disseminated interstitial cpy		
				882-885, rep texture showing cpy		
				130.47-130.76		
				59262		
				as described, 1% angular interstitial mt, approx 60%mafics, 40% plag, dominant mafic mineral is cpx		
				886-888, rep texture showing magnetite grain		
				no sulphides		
				130.76-131.06		
				59263		
				as described, 1% mt		
				no sulphides		
				889-890		
				131.06-131.38		
				59264		
				as described, 1% mt,		
				no sulphides		
				891-892, rep texture		
				131.38-131.74		
				59265		
				from 131.38-131.42 very coarse grained (3cm pyx, and 2 cm plag), no clear contact, grain size just increaseds for a 5 cm section and is then back to the cg as described, beyond this part the unit other wise unit is as described as described, 1% mt		
				no sulphides		
				893-894, rep texture		
				895-897 very coarse grained section,		
				131.74-132.00		
				59266		
				as described, 1% mt,		
				no sulphides		
				897-898 rep texture		
				132.00-132.40		
				59267		
				as described, 1% mt,		
				this one I think was at the water table and it is very nice to look at, plag is bone white, approx 50% , cpx > olv, but ratio is hard to determine, <1% mt, trace bt		
				nice ophitic texture displayed,		
				counted 5 plag crystals that are elongate up to 2 cm, irregular for this unit, or ust because we can see clearly here		
				899-903, rep texture of unit		
				no sulphides		
				132.40-132.80		
				59268		
				very coarse grained unit, crystals average 1-1.5cm up to 3 cm in size, plag is euhedral, pyx+olv are interstitial angular and subhedral-anhedral		
				a single grain of 1 mm cpy was noted		

				904-905 rep text + cpy grain		
				906-907, 907-909, rep texture of unit, still has bone white plag as before, making texture very easy to se		
				132.80-133.11		
				59269		
				coarse grained, 1cm-2cm average crystal size, but as is usual for this unit, there is no minimun on grain size, crystals can still be down to a 1-2mm. Plag is euhedral, formed first, with interstitial angular subhedral-anhedral pyx+olv (pyx>olv), 1-2% mt,angular, interstitial no chlorite alteration,		
				no sulphides		
				910-911, rep texture of unit		
				133.11-133.33		
				59270		
				coarser grained unit as above, loses the white bone white plag, and the unit is a blue-grey again masking individual minerals, 1-2% interstital angular mt		
				no sulphides		
				no chlorite		
				912-913, rep texture, showing change between bone white and bluegrey silicified loo		
				133.33-133.64		
				59271		
				Unit is back to the cg unit as described originally, 1-2% mt		
				2-4% of mafics are altered to soft black-green chlorite		
				no sulphides		
				914-915, chlorite grain encircled, dark black is chlorite, dark grey is magnetite, brown is biotite		
				133.64-133.95		
				59272		
				as described, 1-2% mt, no sulphides		
				no sulphides		
				no chlorite alteration		
				916-917 rep texture		
				133.95-134.27		
				59273		
				unit same as above, 1-2% mt, spot of chlorite alteration described below		
				134.10-134.19 clot of chlorite alteration + bone white feldspar (albite?) mixed in with magnetite and albite		
				918-919 photo of chlorite clot		
				134.27-134.58		
				59274		
				coarse grained, 1cm-2cm average crystal size, but as is usual for this unit, there is no minimun on grain size, crystals can still be down to a 1-2mm. Plag is euhedral, formed first, with interstitial angular subhedral-anhedral pyx+olv (pyx>olv), 1-2% mt,angular, interstitial		
				trace chllrite pale green alteration of mafics		
				no sulphides		
				steel blue grey, mod silicification		
				920-921, rep texture of unit		
				134.58-134.89		
				59275		
				main unit described, coarser grained as above is no longer present		
				mod chlorite alteration, 10-15% of unit is chlorite altered, altered to pale green or dark greenish-black, sof		
				no sulphides		
				922-923, rep texture showing large chlorite grain		
				134.89-135.20		
				59276		
				as main unit described, 1% mt		
				1-2% chlorite alteration of mafics		
				steel blue grey colour		
				924-925, rep texture		
				no sulphides		

				135.20-135.50		
				59277		
				as main unit described, 1% mt		target 931
				1-2% chlorite alteration of mafics		
				steel blue grey colour		
				926-927, rep texture		
				no sulphides		
				135.50-135.81		
				59278		
				as main unit described, 1% mt		
				1-2% chlorite alteration of mafics		
				steel blue grey colour		
				928-929, rep texture		
				no sulphides		
				135.81-136.11		
				59279		
				as main unit described, 1% mt		
				3-4% chlorite alteration of mafics		
				steel blue grey colour		
				930-931		
				no sulphides		
				136.11-136.41		
				59280		
				as main unit described, 1% mt		
				1-2% chlorite alteration of mafics		
				steel blue grey colour		
				no sulphides		
				932-933		target 941
				136.41-136.73		
				59281		
				SAB, except mt is up to 2-3% now		
				(note to self, 135-140 is very homogeneous)		
				934-935		
				136.73-137.04		
				59282		
				SAB		
				936-937		
				137.04-137.34		
				59283		
				SAB		
				938-939		
				137.34-137.60		
				59284		
				SAB		
				940-941		
				137.60-137.90		
				59285		
				SAB		
				942-943		
				137.90-138.18		
				59286		
				SAB		
				944-945		
				138.18-138.49		
				59287		

				SAB		
				946-947		
				138.49-138.95		
				59288		
				SAB, has a 2cm thick qtz-syenite stringer at 20 TCA		
				948-949		
				138.95-139.30		
				59289		
				SAB		
				950-951		
				139.30-139.60		
				59290		
				SAB		
				952-953		
				139.60-139.90		
				59291		
				SAB		
				954-955		
				139.90-140.23		
				59292		
				957-958		
				SAB		
				140.23-140.47		
				59293		
				SAB, 2-3% interstitial, 2-4mm angular, anhedral magnetite crystals. Grey colour. Mod chlorite alteration (pale green blackgren mafics, approx 2-3%).		
				958-959 rep texture		
				960, showing magnetite crystals		
				140.47-140.85		
				59294		
				medium grey, when wet plag have a transulcentpartially opaque look with mottled grain boundaries. Mg-cg plag (euhedral-subhedral, 5mm-10mm, 5 mm is average, elongate laths), pyx-olv (subhedral-anhedral, interstitial angular, 5mm-10mm). Mod magnetite, angular, interstitial, 1mm-5mm, approx 2-3%, approx 40% plag, 60% mafics, with cpx>ol. weak-mod silicification, giving core a blue grey colour.		
				two 1 mm grains of cpy at 147.63m, interstitial,		
				weak chlorite alteration (2-3%) of mafics, pale green to dark greenish black, sof		
				961, rep texture showing chlorite alteration		
				962 rep texutre showing 1 mm grain of cpy		
				140.85-141.07		
				59295		
				SAB. 3-4% mt, 3-4% chlorite alteration		
				no sulphides		
				141.07-141.37		
				59296		
				cg-pegmatitic, plag is 2-3cm on average, up to 5 cm, elongate laths, cpx is 2-3 cm on average, up to 5 cm, ol is still cg only up to 5mm grains noted. Approx modal percentage 40%plag, 40% cpx, 7%ol, 3% mt, trace bt. Magnetite is angular to subrounded. The upper contact has a band of chlorite altered mafics, possibly olivine. The lower contact is gradational and is not well defined.		
				963-964, rep texture, showing upper contact defined by band of mafics, and large pyroxne crystal		

				trace sulphides, 1 mm grain size, interstitial disseminated (5 grains counted in section)		
				141.37-141.60		
				59297		
				medium grey, when wet plag have a transulcentpartially opaque look with mottled grain boundaries. Mg-cg plag (euhedral-subhedral, 5mm-10mm, 5 mm is average, elongate laths), pyx-olv (subhedral-anhedral, interstitial angular, 5mm-10mm). Mod magnetite, angular, interstitial, 1mm-5mm, approx 5-7%, approx 30% plag, 70% mafics, with cpx>ol..		
				chlorite alteration of mafics, pale green, approx 2-3%		
				965-966 rep texture		
				no sulphides		
				141.60-141.84		
				59298		
				SAB		
				trace sulphides, 2 1 mm grains of cpy		
				967-969 rep texture of unit		
				141.84-142.04		
				59299		
				SAB, but with a slightly coarser grain size, average grain size is 7mm-10mm, with 5-7% angular interstitial mt, up to 5 mm in size, mt forms bands		
				contains a small xenolith of 2a at 141.90-141.96, 6 cm in length, 3 cm in width		
				pyx crystals are larger in this zone, up to 1 cm in size (three crystals of this size noted		
				969-970, showing magnetite rich bands, and rep texture with slightly coarser grain size		
				971-972 showing 2a xenolith within unit		
				no sulphides		
				142.04-142.43		
				59300		
				SAB, at 143.35 clorite alteration becomes mod-strong with approx 20% of core showing altreation to pale green/dark black green		
				973-974 rep texture, no alteration		
				975-976 strong alteration		
				no sulphides		
				142.43-142.80		
				59301		
				SAB, but grain size of pyx is up to 2 cm, other minerals average around 1 cm, plag is still euhedral, elongate laths, cpx +ol anhedral-subhedral, interstitial, larger cpx grains enclose plag crystals		
				5% pale green chlorite alteration throughout section		
				trace cpy, 1-2 mm grains (about 5 total) , with a smeared appearance		
				977-978 rep texure showing smeared cp		
				979-980 rep texture of unit		
				142.80-143.12		
				59302		
				SAB., with coarser grain size,		
				trace cpy, 1-2mm grains		
				chlorite alteration stops at 142.90, and the rock appears very fresh		
				981-982, rep texture in chlorite alteration zone with fg <1 mm cpy		
				143.12-143.27		
				59303		
				plag is euhedral 1-2cm (1 cm on average) with interstitial/angular subhedral to anhedral pyx up to 3 cm, highly irregular shapes, ol crystals are 2-3 mm. approx 60% cpx, 30% plag, 5% mt, 5% ol. Patchy grey colour due to grey cpx		
				trace sulphides, at 143.20-143.27, fg interstitial <1mm-1 mm		
				983-984, rep texture		
				985-987 rep texture showing sulphides		
				143.27-143.78		
				59304		

				cg, euhedral-subhedral plag (5mm-10mm) in size, this section lookis almost like a cummulate, abundant mafic minerals, aprox 70% of the interval. The mafics have a rounded look to the grain edges. 8 chlorite fractures at 80-90TCA, individual fractures look like they have been refractured multiple times. The mafics are formed together in large clumps. While the plag crystals can be seen to be euhedral on the broken surface of the rock, on the cut surface they have very hazy grain boundaries (hackled?). Approx 80% mafics 20% plag in this unit. Strong chlorite alteration throughout section. Alteration is pervasive (essentially all of the mafics are soft and pale green and appear to be chlorite altered). Due to alteration cannot discern the pyx:olv ratio. cpx>>olv.		
				0.5-1% fg (1mm and less) cpy disseminated throughout the unit		
				Unit contacts are the sampling interval		
				989-992 showing rep texture, chlorite alteration, cpy grains, and chlorite fractures		
				143.78-144.0		
				59305		
				plag is euhedral 1-2cm (1 cm on average) with interstitial/angular subhedral to anhedral pyx up to 1-2 cm average, up to 3 cm, highly irregular shapes, ol crystals are 2-3 mm. approx 50% cpx, 40% plag, , 7% ol. Patchy grey colour due to grey cpx . Variable grain size, ie. as usual grains can go down to 2 mm. approx 1-2% intestitial angular mt		
				2-3% chlorite alteration		
				3-4% fg-mg (1-2mm average, up to 4 mm) disseminted interstital cp		
				993-998 rep textures showing mineralization		
				144.0-144.25		
				59306		
				SAB		
				mineralization is much lower, approx 1% fg (1mm) cpy interstitial, disseminated		
				999-1000, rep texture		
				144.25-144.60		
				59307		
				SAB		
				5% fg-mg (1mm-5mm, 3mm average), interstitial angular cpy. One 1 mm spec of bornite noted.		
				at 144.40 there is a band of magnetite with fine grained cpy occuring within		
				1002-1003 rep texture showing mg cpy		
				1004-1005 mt band with fg disseminated cpy occuring within		
				144.60-144.84		
				59308		
				This section is a partially digested 2a pyx-ol-plag fg gabbro xenolith (approx 75%) with stringers of the 3b running through it. In the stringers plag is euhedral 5 mm average, up to 1 cm, with interstitial cpx (up to 1cm average)-olv, (2-3mm). Approx 50% cpx, 40% plag, 10% ol, 1-2% interstitla irregular mt grains. Patchy chlorite alteration of mafics, approx 3% pale green.		
				upper and lower contacts are diffuse but visible, irregular		
				2-3% fg-mg (1mm-4mm, 3mm average) cpy occurs within the bands of TDL stringers		
				1006-1009 upper contact of unit, can distinguish previous 3b and the 2a xenolith		
				1110 is the lower contact of the unit with td		
				144.84-145.15		
				59309		
				cg-vcg plag (euhedral, elongate laths, 1-2 cm in size), pyx is 1-2 cm, olv is 2-5 mm. grey colour pyx+olv interstitial, angular, irregular.. Approx 2-4% chlorite alteaiton of mafics, pale green colour to greenish black.		
				a 1 mm chlorite fracture runs through the middle of this piece of core, sub parallel, irregular		
				3-5% sulphides, mineralization appears to occur on surfaces perpendicular to the core axis		
				fg-mg (1mm-5mm) dominant mineral is cpy, cpy is tarnished to, blue-green-aquamarine, and brilliant metallic purple (not the same as the dull purple bornite). There are also a few (4) grains of 1 mm bornite as well as 2-3mm pyrrhotite grains associated with cp (possible replacement texture)		
				1111-1114 broken surface showing above described mineralizaiton		
				1015-1016 rep texture, showing cpy mineralization		
				1017 lower contact with xenolith, chlorite fracture is clearly visible		
				1018-1021 145.12m cpy+bornite replacement texture		
				145.20-145.56		
				59310		
				2a xenolith		

				Xenolith of 2a, fg pyx-ol-plag gabbro. Approx 70% 2a, with 20% 3b stringers as above with cpy. Partially digested xenolith by 2a. Irregular intertwined boundaries,. Chlorite fracture approx 1 mm, irregular fracture, about 20 TCA		
				2-3% fg-mg (2mm average) cpy , appears to be in sections of tdl stringers in the 2a, however thhere are some cpy grains within the xenolith and do not appear to be connected to TDL stringers		
				1022-1023, 145.3m rep texture of xenolith		
				1024-1025, 145.5m, rep texture of xenolith, lower part of the picture has cg cpy, likely contained within 3b stringer		
				145.56-145.75		
				59311		
				vcg, plag (euhedral, elongate laths, 2 cm average, 3 cm maximum) with cpx (interstitial, angular, average 2 cm, up to 3 cm), olv 2-3 mm. Mottled look. Strong chlorite alteration of mafics (10-15% pale green + dark greenish black phenos). Colour is a greenish grey, unit has a mottled look due to strong chlorite alteration. Ophitic texture is well defined. 2-3% mt, angular interstitial.		
				2-3% fg-mg cpy (2mm average), a few grains of po noted (2mm) with replacement textures with the cpy.		
				1026-1027, 145.66m ophitic texture with interstitial cpy grain wedged between plag crystals (has triangular look)		
				145.70-145.96		
				59312		
				SAB		
				1-2% fg-mg (2mm average) cpy + trace amounts of po, 1 grain of bornite intermixed with cpy		
				1028-1029 145.75m rep texture, + cpy/po grain replacement texture		
				1030-1031, 145.90m, cpy grain with bornite intermixed		
				145.96-146.23		
				59313		
				This unit is likely still TDL, but has a more mafic rich cummulate look to it. plag crystals are (subhedral, 5 mm average where visible, which is very rare due to large amount of mottled mafics) Green mottled colour. Approx 80-90% mafic minerals. Mafics have a rounded look to them and form in large clumpsl, with small patches of white material showing through. Strong pervasive chlroite alteration throughout the mafic clumps(ie all of the mafics are chlorite altered). 1-2% mt, 2-5mm grain size, approx 3-4%, seem to form in bands.		
				4 chlorite fractures in the unit, one at 80 TCA, the others are sub parallel, highly irregular hackled look		
				Stringer of white felsic material, running at approx 30TCA, highly irregular cross cutting the core, possible 5a stringer?		
				0.5-1% cpy, interstitial disseminated, 2-3mm average grain size, one 3 mm grain of pyrrhotite intermixed with cpy		
				1032-1033, rep texture of unit, can see band of mt on the far right of image		
				1034-1035, showing rep texture with white felsic stringer, chlorite fractures and po/cp grain		
				146.23-146.43		
				59314		
				plag crystals are (subhedral, 5 mm average where visible, which is very rare due to large amount of mottled mafics) Green mottled colour. Approx 80-90% mafic minerals. Mafics have a rounded look to them and form in large clumpsl, with small patches of white material showing through. Strong pervasive chlroite alteration throughout the mafic clumps (ie all of the mafics are chlorite altered). 1-2% mt, 2-5mm grain size, approx 3-4%, seem to form in bands.		
				White stringer runs through the section, aprox 30 TCA, has a slight pink tinge, at one point expands into a clump		
				1-2% fg disseminated interstitial cpy		
				1036-1037 146.33 rep texture showing felsic band		
				1		
				146.43-146.63		
				59315		
				SAB, mottled green mafic rich unit, with rounded mafic clasts, difficult to discern grain size		
				1038-1039, rep texture		
				1040-1041 fg disseminated cpy		
				146.63-147.00		
				59316		

				Gradational change out of the previous unit into a 3d (good 3d starts by 146.70m) This is a pegmatitic TDL gabbro. Plag (euhedral, 2 cm average, up to 4 cm), with cpx (interstitial, angular, 3cm average, up to 5 cm), ol (1-10mm, 5 mm average). As usual the grain size is highly variable, and all crystals minimum grain size is around 2 mm. Well developed ophitic texture. 3-5% mt, mt forms in clumps or bands together.		
				no visible sulphides		
				1042 showing change from previous unit into 3d,		
				1043-1044 rep texture of 3d, nice ophitic texture		
147.00	166.60	3b - Coarse grained gabbro (>5mm)				
				green-grey coarse grained TDL gabbro. Plag (euhedral, 1 cm average, up to 2 cm), with pyx+ol (interstitial, anhedral, angular, 1 cm average, up to 2 cm). Moderate chlorite altreation (pale green mafics to dark blackish green) approx 10% of mafics are affected. Unit has a mottled fuzzy look. pyx approx 60-70%, plag 10-15%, very mafic rich		
				From 147.10-147.50 and 147.60-147.90, looks like the unit is intermixed with qtz syenite. There are large patches o white material that has a pinkish hue.contains labradorite and quartz. These are highly irregular patches with no margins, intermixed with chunks of the tdl contained within.		
				variable magnetite, 2-4% mt, 2mm-8mm, angular, interstitial		
				from 155-162, chlorite alteration is strong, and mafics have a subrounded look to them (similar to the fuzzy green unit in the w horizon)		
			3d - Coarse grained to pegmatitic gabbro			
				164.60-164.80 pegmatitic, plag (euhedral, 3-4cm average, up to 5 cm average), with cpx (interstitial, angular, grains, 3-4 cm average,l up for 5 mm), ol, (diffiicult to reckognize, few grains, 2-4mm size, may be masked). Approx 5-10% angular interstitial magnetite. Modal percentage approx 45% plag, 35% cpx, 10% mt, 5% ol		
				trace fg (1-2mm) cpy		
				1053-1054, 147.25m rep texture showing white felsic bands in the unit		
				1055-1056, 147.95m, 5a irregular dikelte, with labradorite. Mafic chunks in the middle		
				1057, 149.30m patch of pink felsic material		
				1058, 155.70m, rep texture without felsic 5a patches		
				1059, 156.75m, large 5a patch, blue colour ot the right is labradorite		
				160-162, 150.10m, rep texture with no alteratior		
				1063-1064, 156.50m upper contact of 2a xenolith		
				1065-1066, 166.25 5a dike showing upper contact and rep texture		
				From 152-165 there is approx 5-10% highly variable patches of pink felsic material, looksl ike small pieces of qtz syenite, but very irregular, no well defined contacts, possibly just alteration, highly irregular and sporadic. The qtz syenite patches are continusou throughout the unit, approximately 5-10% variable, patches range from a few mm to 5 cm bands, always highly irregular. Labradorite commonly visible. Colour ranges from opaque white, to white with a slight pinkish tinge, to pink		
				trace sulphides throughout the unit, cpy, fg-mg (2mm typical grain size).		
			2a - Fine grained gabbro			
				156.40-156.64 2a xenolith, irregular boundaries. Partially diffuse contact but still noticable. fg gabbro, pyx-ol-mag plag, mag rich (approx 30%) xenolith		
			5a - Quartz syenite dikelet			
				166.25-166.85, clear contacts approx 30 TCA, cg qtz-syenite dike		
166.60	187.62	3a - Fine to medium grained gabbro (<5mm)				
				fg-mg tdl gabbro. Euhedral plag, 1mm-4mm, 2mm average, with interstitial pyx+ol. Abundant magnetite approx 5-10% (per\haps up to 15% in some areas) interstitial, angular typically. Chlorite alteration throughout, patchy, approx 5-10% of mafics to a pale green colour.		
			5a - Quartz syenite dike			
				coarse grained from 176.14-176.53, 181.67-182.07, contacts approx 30 TCA		
			3b - Coarse grained gabbro (>5mm)			
				coarse ophitic pocket of 3b from 176.53-177.12(green alt. colouring), 179.49-179.56		
			2a - Fine grained gabbro			
				177.20-178.34m partially digested 2a xenolith, approx 80% 2a, 20% 3a		

				1067-1068, 172.0m, rep texture of 3a unit		
				1069-1070, 176.14 5a dike upper contac		
				1071-1072, 177.5m partially digested 2a xenolith		
				1073-1074, 180.90m, rep texture of 3a uni		
				1075-1078, 187.62m, contact between 3a and 1a		
187.62	192	1a - Footwall Breccia (RIB)				
				very fine grained silicified with felsic differentiated bands (variably angled),		
				- slight increase in graine size from 191.27-192		
			2a - Fine grained gabbro			
				189.6-189.80 , 191.28-192 2a xenoliths, vfg pyx-ol-plag gabbros		
				1079-1080, 187.50m, rep texture		
				1081-1082, 189.06 m, contact between 1a dn 2a xenolith		
192	192	EOH - End of Hole				

MARATHON PGM CORPORATION - DIAMOND DRILL CORE LOG

DDH-369

NTS:		42 D / 16				
UTM	Northing	4200	M-07-369			
(Nad27)	Easting	50			Property:	Marathon
Elevation:						
Dip at Collar:		-75				
Azimuth:		90				
Total Depth:		168			Contractor:	Chibougamau Diamond Drilling Ltd.
Core Size:		NQ			Logged by:	John McBride
Remarks:		Core stored in Marathon PGM Corporation warehouse, Marathon, Ontario			Assistant:	Stephan Besner
					Relogged by:	Ryan Ruthart

GEOLOGY					Mineralization	
From	To	Maj Rock	Min Rock	Comments	Mineraliz	Comments
0.00	3.00	O/B - Overburden				
3.00	7.60	2a - Fine grained gabbro				
				fine grained pyx+olv rich cumulate		
				- bands of mag up to 1cm thick from 5.49-5.63, mag cumulate from 7.15-7.36(2f?)		
				- extensive chl alt. along all fracture surfaces.		
				- dark black/green chl alt. colouring, soft chalky of complete core with minor carb veining		
				from 3.37-4.25, 6.73-6.93		
7.60	18.58	2f - Medium to coarse grained magnetite rich gabbro			Trace to 0.5% disseminated sulphides	
				med-crs grained pyx+olv cumulate and rounded cumulate mag rich. Mod bio		from 7.6-10.6 trace cpy <1mm
				- heavily fracture often pebbled, with extensive chl alt.		from 18.29-18.42 fine grained cpy up to 1mm
				- plag shows alignment @ 70-80deg to ca. from 10.09-12.24		
				- abundant Fe-carb and serp alt of grains both spotted and along calcite veins, deep red		
				rust colour from 12.24-16.1 (possibly 2i?)		
18.58	52.10	2d - Fine grained gabbro with coarse grained gabbro dikelets			Trace to 0.5% disseminated sulphides	
				fine grained pyx+olv rich, mod mag,		from 39.11-42.87 trace cpy <1mm
				- chl alt of pyx grains, anhedral soft/flat black, chalky		
				- zones of hematization, deep red alt colouring from 21.62-21.88, 22.06-22.6, 26.34-27.39,		
				28.26-30.79		
				- carb veining soft white, from 23.26-23.34(@65deg to ca.), 26.37-26.42(@ 70deg to ca.),		
				26.49-26.55(@ 70deg to ca.), 26.89-26.93, 50.34-50.41(@ 45deg to ca.)		
				- extremely alt+fractured from 28.37-33.57 Fe-carb alt red colouring of grains and carb veining		
				chl alt soft chalky black colour. Pebbled and fractures subparallel to ca. originally 2f(mag rich)?		
				37.36-38.26(chl+hem alt)		
				- abundant healed chl fractures from 43.84-44.75		
			2f - Medium to coarse grained magnetite rich gabbro			
				med-crs grained pyx+olv+mag rich		
				from 30.75-32.57(heavily alt 2f?), 32.76-33.41, 34.04-34.16, 34.96-35.11, 42.82-43.63,		
				- plag show a minor alignment @ 75deg to ca.		
			3b - Coarse grained gabbro (>5mm)			
				coarse grained, angular pyx+olv+mag, ophitic texture difficult to see.		
				from 38.26-42.63(heavily alt.), 42.68-42.82, 45.39-45.68, 46.17-49.49(pockets of 2a)		
52.10	72.48	Fault or shear zone				
				heavily fracture and pebbled zones with extensive hematite (deep red/brown colouring),		
				carb (cementing breccia zones) and serpentine alt. green colour and soft pebbling		
				- parent rock was a coarse grained 3b (remnant ophitic texture and minor amounts of 5a.,		
				abundant breccia zones with carb matrix		
			5a - Quartz syenite dike			
				alt coarse grained 5a from 67.1-75.11 (solid deep red)		
72.48	144.92	3b - Coarse grained gabbro (>5mm)				
				coarse grained subophitic-ophitic very mafic and alt. abundant pyx+olv interstitial		
				core as a foggy appearance, minor mag		
				- gradational grain size increase from 78.23-81.91		
				- abundant chl alt, flat black, soft.		
				- abundant hematite+carb alt, carb banding from 87.94-87.99, 88.87-88.91, 94.51-94.69,		
				94.87-94.9,		
				- highly fractured from 82-82.15(@ 45deg to ca.), 82.66-82.93(@ 35deg to ca.), 83.62-83.79		
				(pebbled), 89.18-89.71(subparallel to ca. and pebbled), 99.87-99.95(pebbled)		
				- gradational grain size increase from 3a to 3b from 120.28-121.76		
				- thin layered pyx+plag+mag @ 50deg to ca.		

72.48	87.08	3d - Coarse grained to pegmatitic gabbro				
				Greenish-grey colour due to strong chlorite presence. cg plag (euhedral-subhedral, elongate laths, variable size, 2mmx0.5mm to 5mmx2mm), with interstitial olivine (subhedral-anhedral, interstitial and angular dominantly 2mm-6mm), pyx (subhedral-anhedral, interstitial, 2mm-10mm), subophitic texture (implied by using 3b). 2-3% interstitial magnetite (2mm-8mm). Abundant chlorite fractures, variable density, 1/10 cm average. Hairline fractures at 80-90TCA, while there are subparallel (form u shape) 3mm-10mm fractures, anastomising (look like U's) with carbonate within the chlorite, sometimes with red hematite. These fractures have alteration halos of chlorite and hematite that extend 1-3 cm from the fractures. The chlorite alteratoin is strongest around these fractures, but where there are no fractures mafics (2-3% weak) are altered to a pale green soft (chlorite). Due to strong alteration it is difficult to determine modal mineral percentages, it is approximately 30-40% plag, 60-70% mafic minerals, with cpx:ol approx 1:1.		
				From 81.40-81.80, anastomising u shaped chlorite fracture, with carbonate infill. 2-5 cm of strong chlorite alteration of phenocrysts occurs around this (dark , black soft)		
				From 81.80-83.50 intense zone of chlorite fractures, anastomizing fractures, with carb+- hem, 3cm - 5cm intense alteratoin bands, very fractured. Chlrotie atleration in this zone is 10-20% of mafics (soft pale green) on top o fthe intense blackish green alteration around the fractures.		
				83.50-87.55m strong chlorite alteratoin of mafics, approx 30% of rock is pale green colour, strong alteration of phenocrsyts to soft dark blackish green (pale green streak) as well as hematite blackish red (red streak, hematite) also occurs. Approx 1-2/10 cm fractures, ahrirline fractures, chlorite+-carb+-hem		
				87.55-87.08m mod pink alteration (looks like ksp crystals, 5mm-1cm with hairline hematite alteration). Mafics are still strongly chlorite altered and look subrounded on their grain boundaries. Fractured abou 1-3/10cm, chl+-carb+-hem (mostly +) fractures, irregular boundaries. , 60-90TCA and subparallel, irregular always hackly (ie not straight lines). 5-8% interstitial mt, subangular to subrounded, 2-7mm.		
				Photos:		
				1115-1118 81.20m rep texture of the unit for the weakly altered part (ie typical description		
				1119-1122 81.60m, photo showing a anastomizing chlorite fracture with 3 cm band of chlrotie alteration		
				1123-1124 82.05 m, very intense chlorite fracture with 5 cm band of strong pervasive chlorite alteration of mafics		
				1125-1126 82.50m, more chlorite altreation fractures, in the intense chlorite alteration zone		
				1127-1130 rep texture of strong chlorite atlteration zone, redish black is hem alteration, greenish black is chlorite alteration of phenocrysts, fracture contains carb.		
				11131-11134, 86.80m, rep texture of the mod pink alteration, showing pink ksp? And hairline red hem?		
87.08	87.34	3d - Coarse grained to pegmatitic gabbro				
				grey-green, ophitic-subophitic pegmatitic. Plag (euhedral-subhedral, 2cm-4 cm, elongate laths), cpx (2-5cm, subherla-anhedral, interstitial), ol (4mm-2cm, interstitial, subhedral-anhedral). Strong chlorite altreation throughout (20-30%, affecting mafics, with mafics being altered to pale green as well as greenish black		
				faint hint of pink in small patches (similar to the previous unit, <2% of the whole)		
				lower contact grain size grades down from pegmatitic,		
				1135-1138, 87.25m, rep texture of the unit, strong chlorite alteration, black phenos as well as pale green altreation. chlorite alteration, faint hint of pink, rep of ophitic texture in the pegmatitic unit		
87.34	97.00	3c - Coarse grained gabbro with leuco pods				
	note unit continues past 93.00 but that is outside of the w horizon study zone			grey green, with black spots due to chlorite altreation of mafics, subophitic.cg-vcg, Plag (euhedral-subhedral, elongate laths, 2mm-1cm, 0.5mm-1 cm average, occasionally up to 2 cm), cpx (subhedral-anhedral, interstitial, 2mm-4cm rarely, typically around 5mm-1mm), ol (subhedral-anhedral, intestiital, 2mm-5mm, difficult to detect due to strong chlorite alteration). Strong chlorite alteration (30% altered to pale green to blackish green phenocrysts, mafics affected). Mafic rich, hard to tell through alteration, but possibly around 30-40% plag, the rest mafics. Other than the magnetite bnad mentioned below, mt is very low in this section, approx 1-3%, 2mm-4mm, interstitial, angular. Small patches (5%) of weak pink alteration, similar to the previous strong band but in very small patches. Around the carb/hem/chl fractures the mafic phenos are also altered to hematite (reddish black, along with the greenishb lack chlorite)		
				Abundantly fracture, approx 1-3/10cm, chlorite fractures, irregular, ranging from 60-90TCA, as well as subparllel.		
				From 87.70-87-80, vcg-pegmatitic band of pegmatitc material, magnetite crystals which are 2-4cm, along with a 5 cm cpx grain, magnetite exhibits a replacement texture (has lines wihin the inside, thin section taken)		
				From 87.92-88.10, vcg again, 1 cm average plag, 4-5cm cpx. Very small band,		

				87.95-87.98, 3 cm at 60 TCA, 3 cm wide carbonate gouge with brecciated look, also occuring within are hematite (pink) and chlorite.		
				88.16-88.21, 3 mm carbonate+hem+chl fracture, anastomizing looik, at 60 TCA		
				88.85-88.89, carb+hem+chl fracture, 2 cm wide, at 75 TCA.		
				From 96.00-97.00 there is a weakiening of the chlorite altration, it becomes more patchy		
				1139-1142, 87.4m rep texture of this interval, showing chlorite alteraiton as well as the black chlorite phenocrysts.		
				1143-1146, 87.77m the above mentioned coarse grained band with 1cm mt crystals showing some sort of replacement texture		
				1147-1150, 87.95 3cm carb fracture, described above		
				1151-1153, 88.18 hairline carb fracture		
				1154-1157, 88.38m rep texture with a single grain of cpy, interstitial, 1mm		
				1158-1160,88.88m, 3 cm carb fracture as mentioned above		
				1161-1162, 90.07m strong pink alteration in the pegmatitic uni		
				11631166, 90.57m weak ksp alteration in the pegmatitc unit, rep texture of this unit, pegmatitic crystal size		
				1167-1170 90.8m, lower contact between pegmatitic unit and the typical section unit. Very strong chlorite alteration of mafics (greenish black, soft).		
				1171-1174 92.50m rep texture of the unit after the strong ksp alteration, looks like the original description but this one doesn't hve quite as intense anastomizing chlorite fractures.		
				From 89.20-89.80, rock is intensely chlorite altered, and pebbled about 50%		
			3d - Coarse grained to pegmatitic gabbro			
				from 89.70-90.80 the unit is pegmatitic grain size, plag is euhedral, 2-4 cm, cpx, is angular interstitial, subhedral-anhedral, 2cm-8cm, 2-4cm average, ol is 2mm-7mm, subhedral-anhedral, intestitial. Strong chlorite alteration throughout this section, abundantly fractured, irregular fractures, 60-90TCA, irregular boundaries, very low mt (1-2% mt, 2-5mm angular interstitial),		
				From 89.70- 90.20 strong pink alteration (possible ksp+hem), approx 50% pink.		
				From 90.20-90.60, mod pink alteration (hem+ksp),		
				trace cpy, fg 1mm (very trace, few scant grains)		
				After 90.80 the unit retuns to the typical unit described above		
97.00	98.12	3d - Coarse grained to pegmatitic gabbro				
				pegmatitic,ophitic, plag (euhedral-subhedral, elongate laths, 2cm-5cm in size) with interstitial cpx (subhedral-anhedral, angular, interstitial), with leucocratic felsic patches where the mineralogy is completley masked it is opaque white. Weak chlorite altration patchy (1-2%) patchy weak pink alteration, throughout section plag crystals have a pink tinge to them . Mt is trace, only a few 2-5mm grtains noted through the this section. Olivine wasw also not noted. Modal mineral percentages approx 50% plag, 50% cpx		
				97.15 1175-1178 rep texture of 3d unit with felsic white opaque annihilation patch		
				97.5 1179-1182 rep texture of the 3d unit showing the felsic patch (this is where the thin section will be taken from)		
98.12	144.92	3b - Coarse grained gabbro (>5mm)				
				grey-blueish grey (weak-mod silicified) colour that masks the minerals. cg plag (euhedral-subhedra, 2-7mm) pyx + (interstitial, subhedral-anhedral, angular2-8mm averages). Core has a foggy appearance. Leucocratic (approx 5-10% of total core in this range) patches are common throughout this section, highly irregular, ranging in size from a few cm to spanning 10 cm, varible. This section of core is highly variable, not consistent. Weak-mod patchy chlorite alteration throughout (approx 5-10%, variable) mafics are altered to a pale green mineral. Variable magnetite, present throughout, 1-6mm in size, anhedral interstitial, 2-5% variable		
				Overall grey colour with patches of opaque white (hints of green and pink, very slight) due to leucocratic plag patches		
				108.60-108.70 hairline pink fracture (looks refractured, not a single thin line but several overlayered lines) at approx 60TCA. Looks like carb+hem, surrounding this area the minerals have a pink staining colour to them (possibly hem?)		
				5a assimilation: these look like possible 5a mixing with 3b zones or are simply alteratoin zones. The core has a mottled pink colour. The mafics are subrounded, occur in clumps. Magnetite rich (approx 10-15%) 2-6mm in size, range from subrounded to angular, look sinterstitial. Still contains euhedral plag crystals (3-7mm). everything else in these units is subhedral-anhedral. rounded mafics also appear to have chlorite alteration (approx 5-20% highly variable. The pink mineral is likely ksp, this looks distinctly differnt than the pink ksp+hem alteation noted earlier in the core. also contains milky white quartz.		
				The above described zones are prominent from: 102.56-103.60, 117.20-120.18, 126.20-129.30 (this one has very mag rich bands, approx 20-30% in some sections, other wise 10% is typical), 129.10-144.92		
				from about 114 the blue grey colour appears stronger, looks like going from weak silcification to mod silicification		
				114-118m, 121.0-122.50m increase in chlorite altreation approx 5-10% of mafics are a pale green soft minera		

				98.20- 101.2 Strong chlorite alteration (pale green, soft) approx 10-15% of mafic minerals, approx 1/10cm average fractures, some zones increase in fracutring. Hairline chlorite fractures, typically at 70-90TCA, irregaulr hackeled surface.		
				1182-1186, 99.75m rep texture the the fractured chlorite zone described above		
				1187-1191, 102.80 rep texture of the ksp rich 5a? Assimilation zone		
				1192-1195, 105.20 m, rep texture in in a large leucocratic patch in the uni		
				1196-1199, 106.10m, rep texture showing faint leucocratic patch, plag are opaque milky white		
				1200-1203, 109 m, rep texture showing opaque white plag, typical look of this uni		
				1204-1206, 108.65m, hairline carb+hem fracture with surrounding pink staining of minerals		
				1207-1210, 119.00m, the 5a assimilation unit, showing a pegmatiic grtain size (2-4cm on the plag crystals etc.)		
				1211-1214 121.10m rep texture in the zone with increased chlorite alteration described above, about 10% chlorite altered, targets the mafics.		
				Detailed sampling notes		
		3b - Coarse grained gabbro (>5mm)				
				123.00-123.20		
				59337		
				blue grey colour (mod silicified), with approx 10-25% irregular wisps of white material, these are the typical leucocratic cg felsic patches of plagcioclase. Weak chlorite alteration (2-5%) mafics affected, altered to a pale green to greenish black colour, soft. Plag (euhedral, elongate laths, 2mm-1cm) with cpx (subhedrla-anhedral, interstitial,a ngular, 2mm-1cm). olivine is not distinctly noted, but it becomes very hard to see in the silicified unit. wll need to check thin sections to confirm presence. low mt, 2-3%.		
				no sulphides noted,		
				1215-1218, rep texture showing white felsic bands		
		3b - Coarse grained gabbro (>5mm)				
				123.20-123.40		
				59338		
				vcg (1-2cm average crystals zie) blue grey colour (mod silicified), with approx 10-15% irregular wisps of white material, these are the typical leucocratic felsic patches of plagcioclase. Weak chlorite alteration (2-5%) mafics affected, altered to a pale green to greenish black colour, soft. Plag (euhedral, elongate laths, 5mm-2cm) with cpx (subhedrla-anhedral, interstitial,a ngular, 5mm-2cm). ol (subhedral-anhedlra, interstitial, angular, 3mm-2cm. low mt, 2-3%.		
				no well defined contact, unit grades up in grain size		
				trace-0.5% vfg-fg cpy (<1mm-1mm)		
				1219-1222, 123.25m rep texture showing white felsic bands, + fg cpy interstital, angular this is what the thin secditon should catch		
		3b - Coarse grained gabbro (>5mm)				
				123.40-123.60		
				59339		
				Same unit as above, vcg, 1-2cm average crystals. Only 5% felsic patches irregular		
				1-2% vfg-mg-cg cpy, cpy up to 1 cm occurs (2 large grains) grains are mm scale on average		
				1223-1226 123.42m rep texture of unit showing 1 cm cpy crystals shoujld have a thin section of this		
		3b - Coarse grained gabbro (>5mm)				
				59340		
				123.60-123.80		
				same unit as above, 1-2cm average crystals, only approx 5% white opaque felsic whisps		
				no sulphies detected		
				1227-1230, 123.70m, rep texture of unit, nothing specia		
		3b - Coarse grained gabbro (>5mm)				
				123.80-124.00		

				59341		
				blue grey colour (mod silicified), with approx 5% irregular wisps of white material, these are the typical leucocratic cg felsic patches of plagcioclase. Weak chlorite alteration (2-5%) mafics affected, altered to a pale green to greenish black colour, soft. Plag (euhedral, elongate laths, 2mm-1cm) with cpx (subhedrla-anhedral, interstitial,a ngular, 2mm-1cm). ol (anhedral, interstitial, angular). low mt, 2-3%.		
				1231-1234, 122.90m, rep texture of uni		
				no sulphides		
		3b - Coarse grained gabbro (>5mm)				
				124.00-124.20m		
				59342		
				Same unit as above		
				no sulphdies		
				124.00-124.05 slight increase in grain size, up to 2 cm is common, small band no contacts discontinuou		
				1235-1238, rep texture, left edge is the vcg part of the section, fades away quickly going ot the righ		
		3b - Coarse grained gabbro (>5mm)				
				59343		
				124.20-124.44		
				SAB, without the vcg sectoin, all just cg, up to aobut 1cm average grain size		
				no sulphides		
				1239-1242, 124.30m, rep texture, nothing specia		
		3b - Coarse grained gabbro (>5mm)				
				124.44-124.64		
				59344		
				SAB but with a 2a xenolith in the section. The xenolith is only caught shallowly (ie, it was mostly on the other half o the core, its fg, ol-pyx-plag mod mag, EG, equigranular etc.. Aprox 30-40% EG xenolith		
				1243-1246, rep texture showing 2a xenolith, and vfg cpy along contact with xenc		
				at approx 124.60 grain size increases to 2-3cm average crystal sizes, very small band, continues to about 124.66 on the next section		
				1243-1246 rep texture showing the xenolith in the unit, contact is highlighted in red crayoi		
				1-2% fg-mg interstitial dissemianted cpy, cpy is in the 3b and around the edges of the 2a xenolith, but does not appea to be inside the core of the xenolith		
		3b - Coarse grained gabbro (>5mm)				
				124.64-124.90		
				59345		
				cg blue grey colour (mod silicified), with approx 5% irregular wisps of white material, these are the typical leucocratic cg felsic patches of plagcioclase. Weak chlorite alteration (2-5%) mafics affected, altered to a pale green to greenish black colour, soft. Plag (euhedral, elongate laths, 2mm-1cm) with cpx (subhedrla-anhedral, interstitial,a ngular, 2mm-1cm). ol (anhedral, interstitial, angular). low mt, 2-3%.		
				1-2% fg-mg (1mm-3mm) interstitial disseminated cpy,		
				1247-1250, rep texture showing fg-mg cpy		
		3b - Coarse grained gabbro (>5mm)				
				124.90-125.20		
				59346		
				SAB		
				about 5% of crystals are 2cm large, majority are the cg grain size (2mm-10mm)		
				2-3% fg-mg disseminated, interstitial cpy. 1mm-2mm average, elongate grain 8 mm long		
				1251-1255, rep photos showing interstitial cpy		
		3a - Fine to medium grained gabbro (<5mm)				
				125.20-125.50		
				59347		
				mg-cg (some parts of it the average grain size is around 2mm, some parts its more like 6mm, intermixed unit, no contacts) blue grey colour (mod silicified), with approx 5% irregular wisps of white material, these are the typical leucocratic cg felsic patches of plagcioclase. Weak chlorite alteration (2-5%) mafics affected, altered to a pale green to greenish black colour, soft. Plag (euhedral, elongate laths, 2mm-5mm) with cpx (subhedrla-anhedral, interstitial,a ngular, 2mm-5mm). ol (anhedral, interstitial, angular). low mt, 2-3%.		
				0.5-1.5% fg-mg interstitial disseminated cpy (1m-2mm average)		
				1256-1259, 125.35m, rep texture of this unit showing some fg cpy		
		3d - Coarse grained to pegmatitic gabbro				
				125.50-125.80		

				59348		
				vcg-pegmatitic. blue grey colour (mod silicified), with approx 5% irregular wisps of white material, these are the typical leucocratic cg felsic patches of plagcioclase. Weak chlorite alteration (2-5%) mafics affected, altered to a pale green to greenish black colour, soft. Plag (euhedral, elongate laths, 5mm-4cm with cpx (subhedrla-anhedral, interstitial,a ngular, 5mm-8cm). ol (anhedral, interstitial, angular, 4mm-1cm). low mt, 2-3%.		
				ophitic texture well developed in the pegmatitic grain size sections as is per usual, grain size is still highly variable, but dominantly on the vcg-pegmatitic stze, but you will still find the occasional smaller crystal		
				0.5-1.5% fg-mg cpy (1mm-2mm average).		
				at the loast 10 cm of this section start to get wisps of the pink material from the 5a assimiliation dikes		
				1260-1263, 125.65 rep texture pegmatitic unit, 1 grain cpy visible		
				1264-1267, 125.75 rep tetxture of 3d uni		
		3b - Coarse grained gabbro (>5mm)				
				125.80-126.33		
				59349		
				blue grey colour (mod silicified), with approx 10-25% irregular wisps of white material, these are the typical leucocratic cg felsic patches of plagcioclase. Weak chlorite alteration (2-5%) mafics affected, altered to a pale green to greenish black colour, soft. Plag (euhedral, elongate laths, 2mm-1cm) with cpx (subhedrla-anhedral, interstitial,a ngular, 2mm-1cm). olivine is not distinctly noted, but it becomes very hard to see in the silicified unit. wll need to check thin sections to confirm presence. low mt, 2-3%.		
				this unit hits the 5a assimilation, ksp rich, mag rich unit at 126.00, it has irregular boundaries, parts still look like good TDL, but with ksp alteration, mag is up around 10%, mafics have a roundd lok to them, chlorite alteration prevalent, etc.		
				1268-1271, 125.95m, rep texture of unit, weak pink colour due to proxmity to 5a intermixed zone		
				1272-1275, 126.30m, mixing of 3b and 5a		
				1276-1279, XXX m, rep shot of the 5a mixing unit		
144.92	148.75	2a - Fine grained gabbro			Trace to 0.5% disseminated sulphides	
				fine grained pyx+olv rich cumulate, homogenous with syenite mixing from 144.92-147.08		from 147.48-147.53 trace po>cpy <1mm
148.75	168.00	1a - Footwall Breccia (RIB)			Trace to 0.5% disseminated sulphides	
				very fine grained light grey, silicified with felsic banding @ variable angles,		from 151.85-153.86 trace po <1mm
				- syenite assimilation from 155.09-157.14, 157.6-158.04, 159.18-159.43(@ 25deg to ca.		
			2a - Fine grained gabbro			
				fine grained homogenous pyx+olv cumulate from 161.48-162.10		
168.00	168.00	EOH - End of Hole				

MARATHON PGM CORPORATION - DIAMOND DRILL CORE LOG

DDH-441

NTS: 42 D / 16
UTM Northing 5404063
(Nad27) Easting 550022
Elevation (m):
Dip at Collar: -70
Azimuth: 90
Total Depth: 203
Core Size: NQ
Remarks: Core stored in Marathon PGM Corporation warehouse, Marathon, Ontario

Property: Marathon

Contractor: CABO Drilling Ltd.
Logged by: John McBride
Assistant: Adrian Meyer
Relogged by: Ryan Ruthart

GEOLOGY					Mineralization	
From	To	Maj Rock	Min Rock	Comments	Mineraliz	Comments
0.00	1.85	O/B - Overburden				
1.85	28.05	2a - Fine grained gabbro			0.5% to 1% disseminated sulphides	
				Fine grained pyx+olv cumulate minor mag+biotite, with intrusive fingers of 2f and 5a.		From 3.40-3.48 1% cpy up to 3mm
				- 2a unit coarsens to a 2e, pyx+olv with mottled plag, gradatinoal contacts		From 4.09-4.32 fine to very fine grained cpy up to 1mm
				- rubble from 1.85-2.03,		
				- heavily fractured with chl+talc infilling from 10.24-10.78 (subparallel to ca.), 13.29-13.49 (@ 30deg to ca.),		
				- spotted pyx in fine grained core (not a 2c) up to 3mm from 18.24-20.22,		
				- minor irregular pockets of kspar differentiation with a ophitic texture, pink colouring		
				- spotted felsic rounded alteration from 21.77-22.59,		
			2f - Medium to coarse grained magnetite rich gabbro			
				medium grained mag rich up to 85% irregular thin to thick 10cm finger like intrusions into 2a		
				From 2.23-2.34, 2.52-2.58, 2.61-3.49 (multiple pockets of 2f), 3.71-3.78, 3.82-3.97, 4.82-4.33,		
				4.73-4.83 (85% mag), 27.29-27.45,		
			5a - Quartz syenite dikelet			
				coarse grained with spotted chl alt along contacts		
				From 6.19-6.27, 11.63-11.82, 12.59-12.79, 14.65-14.97, 16.19-16.22 (@ 70deg to ca.), 16.32-16.79 (subparallel to ca.)		
			2e - Medium to coarse grained gabbro			
				Coarse grained pyx+olv with mottled plag moderate rounded to subhedral magnetite grains, minor biotite		
				From 6.27-7.55, 8.21-8.42, 8.62-9.42, 17.22-17.48 (mafic rich with minor chl alteration moderate interstital		
				phases),		
28.05	47.27	3b - Coarse grained gabbro (>5mm)				
				mg-cg subophitic plag with interstitial cpx+olv, mod chloriate alteration TDL gabbro with		
				5a xenoliths within		
				(note john below called it a 2e, I think it's a 3b)		
28.05	47.27	2e - Medium to coarse grained gabbro			Trace to 0.5% disseminated sulphides	
				medium-to-coarse grained olv+pyx cumulate with semi planer plag @ 45 deg to ca., with fragments of 2a		From 36.19-36.20 trace cpy <1mm
				with sharp contacts.		
				- fractures are commonly infilled with chlorite,		
			2a - Fine grained gabbro			
				fine grained light grey, olv+pyx cumulate		
				From 33.33-33.44, 33.7-33.73, 33.95-34.12, 34.88-36.16, 36.37-36.48, 36.66-41.0 (heavily altered by thin		
				chlorite bands, up to 1cm, dark green), 41.26-41.43, 43.13-44.3 (heavily chl banding from 44.0-44.3), anastomising over printed fractures giving it a stripped look		
47.27	132.90	3b - Coarse grained gabbro (>5mm)			Trace to 0.5% disseminated sulphides	
				coarse grained ophitic to subophiitc (along contacts) diffuse contacts with interstitial pyx+olv		From 50.35-50.36 trace cpy up to 1mm associated to 5a
				with fragments of 2e		From 72.92-73.08 trace cpy associated to mag, <1mm
				- fracture from 74.57-74.77 (subparallel to ca, with chl+talc infilling), 104.47-105.02 (chl+talc infilling		From 75.41-75.90 fine-med grained po+cpy 5:1 up to 3mm
				- becomes homogenous 3b from 98.81->115.07 with no 2e xenoliths.		From 88.16-88.22 trace cpy <1mm
				- felsic differentiates with minor chl alteration of mafics from 119.14-119.32, minor pockets of felsic diff with		From 108.52-108.54 trace cpy <1mm
				chl+ep alteration around mafics		From 110.02-110.03 trace cpy <1mm
			2e - Medium to coarse grained gabbro			From 111.73-111.77 fine grained cpy up to 2mm
				coarse grained with rounded pyx+olv grains and mottled plag cumulates		
				From 47.57-47.8 (chl alteration along upper contact), 48.84-48.91, 49.55-51.58 (Thin 5a intrusion from		
				50-3-50.39 @ 30deg to ca.), 51.8-52.46, 52.63-52.72, 53.42-55.0, 56.79-57.09, 60.56-61.82 (felsic		
				cumulate along upper contact), 63.26-63.91, 73.02-73.4 (grading into a 2a), 76.71-77.67, 78.3-78.84,		
				78.97-81.10, 81.24-32.77, 84.06-87.35, 87.68-88.16, 96.23-96.81 (mafic rich very crs grained), 117.83-118.12		
			2a - Fine grained gabbro			

				fine grained pyx+olv cumulate with felsic differentiates with poikilitic magnetite		
				From 73.4-74.78, 90.17-91.12,		
			5a - Quartz syenite dikelet			
				coarse grained dark pink with chlorite alteration along contacts, coarse vugs with crs crystals with good		
				habit,		
				From 74.78-75.21 (with a medium grained mixed zone up to 75.88 overprinting primary textures)		
				96.81-98.81, 101.86-101.96 (@ 45deg to ca.), 131.73-132 (with mixed zone starting from 131.56),		
			3d - Coarse grained to pegmatitic gabbro			
				Very coarse grained pyx+plag up to 4cm from 118.55-118.82,		
132.70	132.90	3d - Coarse grained to pegmatitic gabbro				
				pegmatitic, ophitic plag (euhedral-subhedral, elongate laths, 3-5cm) with interstitial cpx (subhedral-anhedral, interstitial angular, 2-10cm), and olivine (subhedral-anhedral, 2mm-1cm). Interstitial magnetite, approx 5%, angular, commonly occurs enclosing other crystals. Weak chlorite alteration, 2-3% alterd to pale green colour soft, only affects mafic minerals. When dry colour is pegmatitic with grey cpx and white plag laths clearly visible. When wet the rock is a dark grey, and the plag cyrstals have a slight green colouration to them.		
				1 grain of 2 mm interstitial cpy noted at upper contact		
				1329-1332, 132.78m, rep texture of the unit showing pegmatitic ohitic TDL. The bottom left of the first photo is a good shot of the magnetitei replacement texture		
132.90	136.53	3b - Coarse grained gabbro (>5mm)				
				cg, subophitic plag (2mm-8mm, elongate laths, euhedral-subhedral) with cpx (subhedral-anhedral, interstitial angular, 2mm-1.5cm) and oliving (subhedral-anhedral, interstitial angular, 1mm-6mm). Magnetite approx 5%, interstitial angular, 2mm-1.5cm). Weak patchy chlroite alteration, mafics altered to a pale green colour, aroudn <1-3% of rock affected (ie very fresh and unaltered). Modal mineral abundance approx 40% plag, 55% cpx+ol (with cpx>>ol), and 5% mt, trace biotite. Grey colour when dry, plag is masked (detectable through cleavage), dark grey when wet, some plag crystals have an opaque green colour to them (5% of total rock)		
				trace fg-mg cpy (1mm-2mm) throughout this section		
				1333-1336, 133.50m rep texture of unit,nothing specia		
			3d - Coarse grained to pegmatitic gabbro			
				134.65-134.75, pegmatitic patch as described above		
				136.35-136.52m pegmatitic patch as described above, 1% fg-mg (1-3mm) disseminated interstitial cpy		
			2e - Medium to coarse grained gabbro			
				135.50-135.70 coarse grained with rounded pyx+olv grains and mottled plag cumulates, (this is like the green unit in the previous whole, but we still called it two duck then, this time it is a disctinct band. Well defined contacts. Approx 90% mafic minerals, with faint plag crystals showing through		
				5-10%plag, 3-5% mt, the rest are all mafics. Grey green colour. Mafics have a rounded look to them		
				135.75-135.80 patch of caorse grained (3-4cm plag crystals within the above describ ed unit, looks like the coarser grained unit has been over printed by the above described unit		
			2a - Fine grained gabbro			
				135.90-136.10 2a ol-plag-cpx xenolith. Partially digestged, faint stringers of 3b within i		
				from 1365.70-126.20 1-2% fg-mg dissemianted interstitial cpy		
				1341-1344, 136m, showing 2a xenolith and lower contact with 3b		
136.52	139.40	3b - Coarse grained gabbro (>5mm)				
				cg, subophitic plag (2mm-8mm, elongate laths, euhedral-subhedral) with cpx (subhedral-anhedral, interstitial angular, 2mm-1cm) and olivine (subhedral-anhedral, interstitial angular, 1mm-6mm). Magnetite approx 5%, interstitial angular, 2mm-1cm). Weak patchy chlroite alteration, mafics altered to a pale green colour, aroudn <1-3% of rock affected (ie very fresh and unaltered). Modal mineral abundance approx 40% plag, 55% cpx+ol (with ol>=cpx (definate increase in ol relative to cpx compared to previous unitl), and 5% mt, trace biotite. Grey colour when dry, plag is masked (detectable through cleavage), dark grey when wet, some plag crystals have an opaque green colour to them (5% of total rock)	3-5% disseminated sulphides	
						136.53-137..50 3-5% fg-mg (<1mm-1mm dominant grain size, up to 3mm but much less common) disseminated interstitial cpy
				1345-1348, rep texture of unit, showing 3-5% fg disseminated insterstitial cpy	Trace to 0.5% disseminated sulphides	
						137.50-138.40 trace fg dissemianted interstitial cp,
				137.98-138.02 opaque white with greenish hint plagioclase pod? Photos 1349-1352	0.5% to 1% disseminated sulphides	
						138.40-139.40 1-2% fg-mg (<1mm-2mm grain size) disseminate
				138.23-138.33 patch of strong chlorite alteration, turns black, soft, mafic minerals aff4ected		at 138.75 2 1mm specs of bornite

				138.50-139.00 decrease in grain size, medium grained dominant, (2-5mm grain size on average)		
				1353-1356, 138.75m rep fineer grained section, showing a patch of opaque white plagioclase and a 1mm bornite grain		
139.40	144.00	3b - Coarse grained gabbro (>5mm)			0.5% to 1% disseminated sulphides	
				cg-vcg subophitic plag (euhedral-subhedral, elongate laths, 5mm-1.5cm), with cpx (subhedral-anhedral, interstitial, angular, 5mm-3cm, rarely 4-5 cm, but these are the only crystals of this size)., olivine (anhedral, 2-5mm, angular, interstitial). Approx 35%plag, 40% cpx, 5%ol, 3-5% mt, 3% sulphides. Patchy mod chlorite alteration of mafics throughout section, approx 5-10% of total rock altered. compared to above unit olivine content has decreased to almost non detecteable. 3-5% 2mm-1.2 cm interstitial angular mt., occasionally with skeletal structure		139.40-140.0 fg-mg (<1mm-5mm, 2-3mm average), interstitial disseminated angular cpy
				from 143.00-144.00 approx 1/25 cm chlorite fractures at approx 60-80 TCA		140.00-140.25 no sulphides
					3-5% disseminated sulphides	
						140.25-141.00 3-5% fg-cg (1mm-7mm, 2-5mm average) cp disseminated, interstitial, angular, with trace (trace-0.5%) po, po typically occurs within cp grains in the cores or on the rims.
			3a - Fine to medium grained gabbro (<5mm)			
				141.52-141.83 medium grained subophitic texture with abundant sulphides, increased abundance of solid white plag	0.5% to 1% disseminated sulphides	
				mafic minerals appear rounded, approx 5-10% mt, subangular to subrounded to rounded		141.00-141.52 1-2% fg-mg cp disseminated, interstitial, angular, trace po associated with cp, 2-3mm average
					0.5% to 1% disseminated sulphides	
			3d - Coarse grained to pegmatitic gabbro			141.52-141.83 1-2% fg-mg cp dissemianted interstitial, up to 2 mm, po is absent except for very trace spec
				142.55-142.95 vcg ophitic-subophitic plag (euhedral-subhedral, elongate laths, 5mm-3cm, 2-3cm average), with cpx (subhedral-anhedral, interstitial angular, 5mm-4cm range, 2cm-4cm average, up to 8 cm)	1-2% disseminated sulphides	
						141.83-142.55 1-2% fg-mg disseminated, interstitial, cp with trace po associated with cp
			2a - Fine grained gabbro			
				143.75-143.78, 143.92-144.05, fine grained pyx+olv cumulate with felsic differentiates with poikilitic magnetite, still c	Trace to 0.5% disseminated sulphides	
						142.55-142.95 trace-0.5% fg-mg up to 5 mm, angular, itnerstitial disseminated cpy, no po noted
				1356-1360, 139.70m, rep unit texture showing sulphides and large cpx grains	0.5% to 1% disseminated sulphides	
				1361-1364 140.50m, 3-5% fg-mg cpy showing the po and cp replacement texture		142.95-143.85 fg-mg (disseminated, interstitial) cpy with trace po associated with cp (up to 3 mm in size, 1-2mm average)
				1365-1369, 140.72m, 3-5% fg-mg cpy showing the cp and po replacement? Texture		
				1370-1373 141.30m, rep texture, 1-2% sulphides, no po, good rep of unit showing large plag crystals		
				1374-1377 141.5 rep text of 3a unit with rounded mafics described above		143.85-144.00 trace fg disseminated interstitial cpy
				1378-1381, 141.65m, 3a unit as described above		
				1382-1385, 142.15m, rep texture of main described unit, showing cp and po sulphides		
				1386-1389, 142.82 rep texture of the 3d unit described above, note the pyroxene in the bottom corner is 7 cm large		
				1390-1393 143.38 rep texture showing cp+po and chlorite fracture in the main unit (weakly fractured zone		
				143.75, 1394-1397, 2a xenolith as described above		
144.00	164.41	3b - Coarse grained gabbro (>5mm)			Trace to 0.5% disseminated sulphides	
				coarse grained ophitic to subophiitc (along contacts) diffuse contacts with interstitial pyx+olv		From 153.24-153.4 fine grained specs of cpy up to 1mm
				with fragments of 2e		From 157.2-157.28 fine grained trace cpy <1mm
					1-3% disseminated sulphides	
			2e - Medium to coarse grained gabbro			From 145.11-145.67 1-2% fine-med cpy+ trace po up to 3mm
				coarse grained with rounded pyx+olv grains and mottled plag cumulates	0.5% to 1% disseminated sulphides	
				158.08-158.32 (crs mafics), 158.96-159.61		From 144.11-144.2 1% fine grained cpy up to 2mm
					Local blebs to 2-4% sulphides	
			2a - Fine grained gabbro			147-147.07 4% cpy blebs up to 12mm
				fine grained pyx+olv cumulate with felsic differentiates with poikilitic magnetite	Trace to 0.5% disseminated sulphides	
				From 43.75-143.78, 143.92-144.05,		From 174.51-176.68 fine grained po+cpy 4:1 up to 1mm
			5a - Quartz syenite dikelet			
				coarse grained dark pink with chlorite alteration along contacts, coarse vugs with crs crystals with good		
				habit,		
				148.08-150.82, 152.51-153.37 (mixed zone with 3b, looks like it is mixed in with the 2e described above		

				159.61-160.61 (crs-med grained intermixed with 2e+3b)		
			3d - Coarse grained to pegmatitic gabbro			
				Very coarse grained pyx+plag up to 4cm from 154.2-154.69,		
			3d - Coarse grained to pegmatitic gabbro			
				Very coarse grained pyx+plag up to 4cm from 154.2-154.69,		
			3a - Fine to medium grained gabbro (<5mm)			
				medium grained subophitic texture with abundant sulphides, increased abundance of solid white plag		
				From 141.52-141.83,		
164.41	176.74	2e - Medium to coarse grained gabbro			Trace to 0.5% disseminated sulphides	
				Medium to coarse grained with fragments of 2a and intrusions of 3b. 2e texture is an olv+pyx cumulate		From 174.51-176.68 fine grained po+cpy 4:1 up to 1mm
				and moderate mag. Moderate chl+ep alteration to mafics.		
			2a - Fine grained gabbro			
				fine grained homogenous light grey olv+pyx+plag cumulate		
				From 165.18-166.64 (multiple pockets of 2a within 2e felsic rich zones), 168.43-168.48,		
			3b - Coarse grained gabbro (>5mm)			
				medium-to-coarse grained ophitic intrusions with interstitial pyx+olv		
				From 169.22-169.76, 171.68-171.95, 173.06-176.68		
			5a - Quartz syenite dikelet			
				Medium grained intrusion from 16903-160.22,		
176.74	185.88	2a - Fine grained gabbro				
				fine grained pyx+olv cumulate, homogenous with intrusions of 1a and 3b and 5a		
			1a - Footwall Breccia (RIB)			
				very fine grained, light grey and silicified from 176.71-179.88		
			5a - Quartz syenite dikelet			
				irregular intrusion, medium-crs grained form 182.69-183.15		
			3b - Coarse grained gabbro (>5mm)			
				with undefined contacts, subophitic with interstitial pyx		
				From 183.79-184.47, 185.5-185.88		
185.88	203.00	1a - Footwall Breccia (RIB)				
				very fine grained, light grey extremely silicified with felsic banding (randomly orientated), thin 5a intrusions		
			5a - Quartz syenite dikelet			
				Coarse grained large intrusion from 189.11-189.45, 195.89-196.01		
203.00	203.00	EOH - End of Hole				

Appendix III: Thin Section Descriptions

This appendix contains descriptions of the thin sections studied in this project.

The thin section descriptions are also available as an excel file on a CD that can be obtained from the Department of Earth and Environmental Science upon request, and are located in the folder 'Appendix 3 - Thin Section Descriptions'.

Hole	Thin	Box	From	To	ID	Sample Description	Description	Alteration (pristine, low, Moderate)	Alteration Desc	Sulphide Mineralogy
M-05-077	59391	1			H-70		Plagioclase, clinopyroxene, minor apatite, chlorite.	Low, No olivine	Chlorite going to inverted pigeonite in some areas, dusting of the plagioclaseioclas (sericite) chlorite alteration kicking around.	Semi massive pyrrhotite+chalcopyrite and minor amounts of pn exsolution flames witin pyrrhotite. Pyrrhotite>>chalcopyrite (5:1). Some pyrrhotite is intruding along cleavage in clinopyroxene. pyrrhotite+chalcopyrite filled fractures in plagioclase. Sulphides occur as semi massive and have clear boundaries against gangue minearals, and also disseminated in large grains of clinopyroxene-inverted
M-05-077	59392	1			H-71		Plagioclase, clinopyroxene, inverted pigeonite, chlorite.	No olivine	Chlorite replacement along edges of pyrrhotite+chalcopyrite.	Pyrrhotite+chalcopyrite, trace amounts of pn (much lower than 59391). Sulphides dominantly occur as net-textured-disseminated. One zone of multiple grains of pyrite. Ppyrrhotite>>chalcopyrite (5:1), chalcopyrite is dominantly along pyrrhotite edges. Within chalcopyrite found a relict pyrrhotite grain, which also contained pentlandite. Sulphides formed after plagioclase, and have well defined grain boundaries around it, except
M-05-077	59393	1			H-72		Clinopyroxene(with inverted pigenoite)-dark brown to green colour, plagioclase, clinopyroxene, chlorite,	Moderate	Clinopyroxene going to inverted pigeonite, hydrous minerals along edges of sulphides, sulphide replacement of inverted pigeonite.	Semi massive pyrrhotite+chalcopyrite with pentlandite exsolution flames in the pyrrhotite. Lesser amounts disseminated within clinopyroxene(with inverted pigeonite). In one area chalcopyrite is replacing pyrrhotite. Sulphides are shredded by chlorite in some places.

M-05-077	59394	1	H-73	Plagioclase (euhedral-subhedral)-dark brown fractures throughout, clinopyroxene(inverted pigeonite)-dark coloured, with angular edges near plagioclase or rounded, chlorite zones replacing (shredded) sulphides.	Moderate	Semi-massive to net textured pyrrhotite + chalcopyrite + pn. Pn occurs as exsolution within the pyrrhotite and in zones with chalcopyrite replacing pyrrhotite it is alone the edges/inside of the chalcopyrite. Dominantly sulphides have nice grain edges where they are along the edges of plagioclase. Zones of chlorite replacing along edges of pyrrhotite are present. Chalcopyrite containing pentlandite.
M-05-077	59395a	1	H-74	Plagioclase (euhedral-subhedral)-dark brown fractures throughout, clinopyroxene(lined)-dark coloured, with angular edges near plagioclase or rounded, apatite small euhedral grains within plagioclase), graphic qtz-ksp intergrowths, chlorite zones replacing (shredded) sulphides, magnetite	Moderate	Net-textured-disseminated sulphides. pyrrhotite + chalcopyrite (dominantly as rims on pyrrhotite grains) and mt intergrown throughout the sulfides (the previous slides did not have this much mt). Also abundant apatite xls trapped encased by the mt and sulphides. Minor amount sof pn within the pyrrhotite. nice zones of sulphides being shredded by chalcopyrite
M-05-077	59395b	1	H-75	Plagioclase (euhedral-subhedral, with brown stained fractures along), clinopyroxene(altering to inverted pigeonite, with dark colour in general, have angular boundaries along plagioclase, also rounded grains which are dominantly trapped within sulphides), apatite (abundant throughout, euhedral grains, encased in plagioclase, clinopyroxene, a bit in sulphides), minor zones of chlorite.	low	Semimassive-net-textured pyrrhotite+chalcopyrite+pentlandite. Pentlandite is large grains in pyrrhotite compared to previous slides, also it can be along the edges of chalcopyrite grains. Have an interesting stripped pattern of chalcopyrite bands within pyrrhotite, also first seen here. Sulphides have nice grain boundaries showing they wrapped around euhedral plagioclase and subrounded clinopyroxene grains. Local fractures filled by

M-05-077	59396a	1			H-76	This slide is composed of a xenolith and a dominantly mafic section. Xenolith is very fine grained, intercumulus plagioclase (euhedral-subhedral), clinopyroxene and magnetite (with ilmenite exsolution). The other half is dominantly mafic, clinopyroxene(inverted pigeonite,, rounded, not networked) surrounded by sulphides. small zones of chlorite alteration	low		Very little sulphides in the xenolith. In the other half pyrrhotite+chalcopyrite+pn exsolution are networked and surround the rounded grains of clinopyroxene
M-05-077	59396b	1			H-77	Dominantly very fine grained cumulate xenolith composed of plagioclase+clinopyroxene. Within this there are stringers of mafic rich clinopyroxene (dark brown, lined, rounded) with sulpihide inclusions.	low		Pyrrhotite+chalcopyrite+pentlandite. Well defined pentlandite grainswithin the pyrrhotite. They have a weak anisotrophism.
M-07-306	59411	1	127.78	127.82	A-15	Plagioclase (euhedral to subhedral, scalloped edges common with olivine and clinopyroxene), olivine (individual grains to poikilitic large single grains , subhedral, subrounded), minor bt (surrounding mt), minor mt	Pristine.	Pristine	Very trace, a few grains of chalcopyrite, 100-200um. Smalll amount of fine grained mineral around edge (chlorite?).
M-07-306	59412	1	135.1	135.14	A-16				
M-07-306	59413	1	143.22	143.26	A-17	Major elements are plagioclase (euhedral to subhedral, scalloped edges common, formed first), olivine (subhedral subrounded, common throughout) and clinopyroxene, large ophitic grains surrounding other minerals. Minor minerals are biotite, hornblende and apatite (euhedral)	No alteration	Pristine sample, all grains are very fresh.	About 5 grains of chalcopyrite, some of them have FeO magnetite rims (does not appear to have ilmenite exsolution). One grain also has bornite exsolution. Also a grain of pyrrhotite with pentlandite within it. Sulphides are within plagioclase (controlled by cleavage) and within olivine grains.
M-07-306	59414	1	147.3	147.34	A-18	plagioclase (euhedral, subhedral, first formed), olivine (subhedral-subrounded) and clinopyroxene oikiocrysta encasing both olivine and clinopyroxene, minor amount of biotite and magnetite. A few small grains of apatite.	Low.	Alteration of olivine by serpentine. A fine grained zone of chlorite alteration within plagioclase.	A few small grains of chalcopyrite, within plagioclase and one grain within a zone of chlorite in plagioclase.

M-07-306	59366	1	150.23	150.27	H-45		Plagioclase, olivine, clinopyroxene, minor biotite and chlorite,	Low		Minor serp of some olivine, over all very fresh. Small cm-scale alteration zone with abundandant tremolite/chlorite/sericite alteration, makes chalcopyrite very ragged in areas, sericite rich matrix.	Trace very fine grained chalcopyrite, chalcopyrite is very common, some small pieces of white mineral present as well (pentlandite?). Thick Fe-rims on sulphide minerals.
M-07-306	59367	1	150.58	150.62	H-46		Plagioclase, olv, clinopyroxene, minor bt, chlorite,	Low		Minor serp of some olivine, overall very fresh, some small zones of chlorite alteration	Trace fg chalcopyrite+bornite exsolution and abundant pentlandite. Sulphide fractures in silictes, sulphides in plagioclase, olivine, chlorite alteration.
M-07-306	59368	1	150.86	150.9	H-47	3b with cummulate fg-mg texture, ns.	Fine grained overall plagioclase, clinopyroxene, trace olivine, minor magnetite, trace biotite and chlorite. Dominantly clinopyroxene, with subrounded to anuglar boundaries, and plagioclase typically encased by clinopyroxene. A few scattered grains of olivine.	Low		Small zones of chlorite alteration, serpentinization of the olivine	3 grains of vfg chalcopyrite, no PGM no bornite.
M-07-306	59369	1	151.3	151.35	H-48	3b with cumulate texture, trace - 0.5% fg chalcopyrite	Plagioclase, clinopyroxene, olivine, with minor magnetite, biotite, chlorite.	Low		Small zones of chlorite alteration, serpentinization of the olivine	Trace to 0.5% chalcopyrite + bornite exsolution, pentlandite, PGM?
M-07-306	59370	1	151.8	151.84	H-49	3b plagioclase rich, trace-0.5 fg chalcopyrite + tr fg bornite, should be in this sample	Plagioclase (80%) olivine, clinopyroxene	Low.		Fresh, weak serpentinization of olivine in small chlorite patches.	Trace -0.5% chalcopyrite + bornite exsolution (bordering on bornite>chalcopyrite), pentlandite grains,. The chalcopyrite is dominantly in the plagioclase, good slide to show the plagioclase cleavage control on sulphide shape

M-07-306	59371	1	152.13	152.17	H-50	3b cummulate with plagioclase rich patches, medium to coarse grained, catches 1% chalcopyrite + trace bornite, (<1mm).	Plagioclase, clinopyroxene, olivine, minor chlorite, biotite, magnetite.	moderate.	Moderate-strong sericitization of plagioclase throughout, chlorite alteration fo clinopyroxene	0.5-1% fg-mg chalcopyrite+ bornite exsolution (some grains bn>chalcopyrite, one or two all bn grains), pentlandite. Sulphides occur within plagioclase, within clinopyroxene and within the alteratoin zones (chlorite+tremolite)
M-07-306	59372	1	152.42	152.46	H-51	3b cummulate, 1-2% vfg chalcopyrite + bornite.	Plagioclase, clinopyroxene, olivine, minor chlorite and biotite, magnetite.	Low.	Zones of chlorite alteration, otherwise pretty good	1-2% very fine grained chalcopyrite + bornite.
M-07-306	59373	1	153.03	153.07	H-52	3b, subophitc texture, becoming more well defined, chalcopyrite + bornite	Plagioclase, clinopyroxene, ol, minor chlorite and bt, mag/ilm	Low	Small mm-scale zones of chlorite.	1-1.5% fine to mediuim grained chalcopyrite+bornite exsolution (variable ratio of chalcopyrite:bornite), pentlandite.
M-07-306	59374	1	153.64	153.68	H-53	3b leucocratic plagioclase patch, very felsic rich, (~60%) catches fg up to 2 mm chalcopyrite + bornite	Plagioclase >80%, ol (poikilitic), clinopyroxene, minor bt, chlorite, mag/ilm (poikilitic)	Pristine.	Fresh for the most part	Only a small patch with very fine grained chalcopyrite+bornite exsolution + pentlandite, possible PGM grains. Within plagioclase sulphide shape is controlled by plagioclase cleavage.
M-07-306	59375	1	153.92	153.96	H-54	3b, well defined subophitic-ophitic texture, 5-7% chalcopyrite + bornite.	Plagioclase, clinopyroxene, olivine, minor biotite, magnetite, chlorite	low-local	Strong serp of some olivine, they are altered to the brown remnant colour, there is a fracture along which the alteration occurs.	1-1.5% fine to coarse grained chalcopyrite+bornite exsolution, pentlandite. Fe-rims on some of the chalcopyrite.

M-07-306	59376	1	154.21	154.25	H-55	3b, well defined ophitic texture, 3% fine to medium grained chalcopyrite, up to 0.5% bornite.	Plagioclase and olivine predominantly.	Low	Minor chlorite alteration and serpentinization of olivine.	trace to 0.5% chalcopyrite+bornite exsolution + pentlandite (contains chalcopyrite fractures), PGM grains.
M-07-306	59377	1	154.7	154.74	H-56	3b with cumulate look, medium grained, contains fine grained bornite.	Dominantly clinopyroxene (dark green, rounded crystals, none really have the chadacryst texture to them), plagioclase, mostly fine grained, subhedral to anhedral shape is common, rarely euhedral, minor amounts of bt, some pyrrhotiteikilitic magnetite,	Low-moderate.	Minor sericitization or plagioclase, strong local serpentinization of olivine.	1-1.5% vfg-fg disseminated chalcopyrite+bornite + trace pentlandite, PGM grains. Sulphides are dominantly in clinopyroxene (although this could be because there is more clinopyroxene), in plagioclase the sulphide shape is controlled by grain boundaries and along cleavage.
M-07-306	59377b	1	154.7	154.74	A-58		Clinopyroxene (dominantly subhedral rounded grains within plagioclase, there is a zone rich in these and then the other area plagioclase is more dominant.). Plagioclase is subhedral to subrounded, scattered througout, a few grains of hornblende and biotite, some rounded olivine grains, encased in clinopyroxene, can be highlyi irregular, small amount of poikilitic magnetite.	Low		Trace very fine to fine grained chalcopyrite with bornite exsolution, minor pentlandite, PGM?. Sulphides occur within plagioclase controlled by cleavage and grain boundaries, within clinopyroxene where it is disseminated throughout a larger ophitic grain and surrounded by biotite.
M-07-306	59378	1	155.25	155.29	H-57	3d, coarse grained pegmatitic unit, catches a bit of a coarse grained bornite + chalcopyrite.	Dominantnly coarse grained to pegmatitic plagioclase, with minor amounts of clinopyroxene (nice ophitic texture), minor hornblende, biotite, magnetite, chlorite.	Low	Mild sericitization, small amount of patchy chlorite.	Trace very fine grained to coarse grained chalcopyrite with bornite exsolution and trace pentlandite. Bright white PGM rim on one chalcopyrite grain in a zone of chlorite.

M-07-306	59378b	1	155.25	155.29	A-59	Coarse grained plagioclaseare euhedral to subhedral, clinopyroxene grains show ophitic texture, olivine, minor biotite, magnetite, and scattered zones of chlorite and hornblende.	Low-moderate		Chalcopyrite with bornite exsolution and pentlandite. PGM grains. Grains occur in clinopyroxene as fine disseminated grains, in plagioclase weakly controlled by cleavage, surrounded by biotite/chlorite, and one round grain with FeO rims is encased within a large grain of olivine.
M-07-306	59415a	1	155.5	155.54	A-19	Plagioclase, clinopyroxene (dark coloured, altered), abundant hornblende, (dark green, very altered looking), zones of chlorite alteration, large grains of calcite	Moderate-strong	Alteration of clinopyroxene to chlorite and inverted pigeonite, zones of chlorite alteration, secondary calcite grains.	Dominantly bornite, small amounts of chalcopyrite + pentlandite. PGM? grains within the bornite. Occur predominantly within plagioclase, and the local zones of chlorite-hornblende.
M-07-306	59415b	1	155.6	155.64	A-20	Very coarse grained plagioclase, with dark brown fractures, clinopyroxene is almost entirely altered to dark green hornblende, calcite is intergrown with the hornblende some zones of chlorite alteration, a few apatite crystals.	Moderate	Replacement of sulphides by hornblende.	Sulphides are chalcopyrite, bornite and pentlandite. Sulphides in zone of hornblende are ragged/replaced by the hornblende, in the other areas they are presnt in plagioclase, with some shape controlled by the grains. Sulphides also controled shape by the hornblende and apatite, PGM rim on one large sulphide grain within the chlorite.
M-07-306	59415c	1	155.7	155.74	A-21	Plagioclase (dark brown fractures running throughout) clinopyroxene (also dustry looking), minor magnetite (large magnetite crystals), hornblende and biotite.	Moderate	Sericite alteration of plagioclase.	Chalcopyrite with minor amounts of bornite exsolution within the centres of the grain, a few pieces pentlandite. Sulphides occur within plagioclase, and appear at least partially controled by grain boundaries and fractures, smaller disseminated grains within clinopyroxene and a a few rounded grains within magnetite.

M-07-306	59416	1	156.1	156.14	A-22	Excellent texture, plagioclase dominantes, euhedral to subhedral, mild amount of dark staining on fractures. Olivine second formed, subhedral sub-rounded crystals, boundaries controlled by plagioclase when close to grain boundary. Last formed ophitic clinopyroxene encases both olivine and plagioclase. Minor amounts of biotite, apatite, magnetite	Pristine		Sulphides are chalcopyrite with bornite exsolution as well as pentlandite. The sulphides are dominantly within plagioclase and controled by grain boundaries as well as penetrating along cleavage. Some chalcopyrite grains within clinopyroxene, associated with biotite, and within olivine.
M-07-306	59417	1	156.45	156.49	A-23	Another sample with well developed texture, nice euhedral to subhedral plagioclase, ophitic clinopyroxne and olivine. Minor amounts of biotite and magnetite.	Pristine	Trace serpentine alteration of olivine and trace chlorite.	Dominantly chalcopyrite, with lesser amounts of bornite exsolution and pentlandite. Sulphides commonly have Fe rims. The sulphides are dominantly in plagioclase and controlled by grain shape/cleavage. There is a zone within a strongly serpentinized olivine that has been altered to magnetite.
M-07-306	59418	1	157.4	157.44	A-24				
M-07-306	59419	1	158.2	158.24	A-25	Very coarse grained sample. Contains plagioclase, olivine and clinopyroxene. There are strong zones of alteration, olv-serp, abundant apatite throughout the slide, magnetite, minor amounts of biotite, hornblende alteration of clinopyroxene.	Moderate to strong	There are strong zones of alteration with olivine being altered to serpentine. Clinopyroxene being altered to hornblende.	Chalcopyrite+pyrrhotite exsolution within the chalcopyrite grains, ragged, small zones of the pentlandite. Mineral grains are very coarse grained, up to 1 cm in length, dominantly occurs between plagioclase and clinopyroxene grains. A zone of dusty fine grained disseminated chalcopyrite near a zone of strong chlroite/actinolite alteration.

M-07-306	59420	1	166.2	166.24	A-26		Very good sample. plagioclase+clinopyroxene+olv, mostly pristine, minor amounts of magnetite and biotite.	Pristine		Very few sulphide, some small scattered grains of chalcopyrite within both plagioclase and clinopyroxene. Grains do not show any control by grain boundaries
M-07-306	59421	1	169	169.04	A-27		Plagioclase (dust brown colour, abundant areas of chlorite/serircite alteration), ophitic clinopyroxene, minor amounts of apatite and chlorite,	Moderate-strong	Strong serpentinization of of olivine, completely dark brown in some areas. Dusty brown fractures within plagioclase, large zones of chlorite alteration.	Chalcopyrite, a few 1 cm grians, with no bornite, small amounts pentlandite Sulphides are dominantly in plagioclase however they are encased in fine alteration zones of chlorite? Not much into the cleavage of the grains.
M-07-306	59422	1	176.36	176.4	A-28		Pristine, plagioclase, ophitic clinopyroxene, olivine, minor magnetite, biotite and apatite	Low	Some minor alteration of olivine to serpentine, light dusting of plagioclase	Pyrrhotite+chalcopyrite, very fine grained, scattered, plagioclase and clinopyroxene. Trace amounts of pentlandite.
M-07-306	59423	1	185.6	185.64	A-29					
M-07-306	59424	1	195.22	195.26	A-30		Plagioclase, ophitic clinopyroxene, olivine, minor chlorite, biotite and magnetite	Low	Minor local chlorite.	Trace chalcopyrite, fine grained and scattererd, minor amounts of pyrrhotite. Located within plagioclase, associated with magnetite, and within local chlorite alteration zones.
M-07-306	59379	1	202.18	202.22	H-58	3b, chlorite + hem alteration, just below fracture zone, rep sample, ns	Clinopyroxene (altering to inverted pigeonite, very altered looking throughout, grains are typically subrounded and squished together looking, dusty apeparance were there is no inverted pigeonite), plagioclase, minor magnetite, chlorite.	Strong	Strong zones of sericite alteration of plagioclase, all of clinopyroxene is going to inverted pigeonite, with zones of intense alteration. Mafics have a mottled rounded look to them.	Trace-0.5 very fine to fine grained chalcopyrite, trace bornite. One larger grain of chalcopyrite was found to have a cubic white mineral in the centre (pyrite?).

M-07-306	59380	1	202.4	202.44	H-59	3b, hematite + chlorite, alteration, apatitic clinopyroxenite.	Clinopyroxene (going to inverted pigeonite), plagioclase, chlorite, minor magnetite and apatite.	Strong	Strong alteration throughout, very storng zones of chlorite alteration (approx 40% of slide is chlorite), strong zones of a dark brown alteration, different than the olivine, visible on the slide, possibly K-feldspar, good amount of apaite kicking around	Trace very fine grained to fine grained chalcopyrite, containing trace amounts of bornite and pentlandite. Sulphide grains are located in plagioclase, associated with chlorite alteration and in clinopyroxene/inverted pigeonite.
M-07-306	59381	1	202.75	202.79	H-60	Highly fractured unit, strong hematization + chlorite alteration, catches chlorite frac + red hematite alteration,	Plagioclase (all altered), minor clinopyroxene, mag/ilm,	Strong	Strongly altered, associated with syenite dike, contains abundant K-feldspar and hematite.	Trace very fine grained chalcopyrite+bornite exsolution, pentlandite.
M-07-306	59382	1	203.18	203.22	H-61	3b with chlorite alteraiton, catches 2-3% fine to medium grained chalcopyrite (angular interstiital)	Plagioclase, olivine, clinopyroxene minor biotite and chlorite.	Moderate alteration locally.	Plagioclase shows moderate-strong alteration to sericite / the dark brown alteration that accompanies dark brown sepentinized olivine. Olivine is strongly altered to dark brown serpentine. Clinopyroxene is generally messy, with pieces of biotite within it	1-2% fg-mg chalcopyrite and pyrite. Fe-rims on sulphide grains.

M-07-306	59383	1	203.59	203.63	H-62	3b with chlorite alteraiton, catches 2-3% fine to medium grained chalcopyrite (angular interstiital).	Plagioclase (has a cubic fractured look to it), clinopyroxene, olivine (completely serpentinized to dark brown colour) minor chlorite and biotite.	Moderate.	Plagioclase is sericitized and it has the dark brown fracture lines. All of the olivien has been completely altered to dark brown. Dusty alteration of chalcopyrite. Secondary biotite. Chlorite alteration locally strong.	1-2% very fine to coarse grained chalcopyrite, pyrite. Sulphides are observed encasing hydrous minerals (chlorite, and altered brown olivine), sulphides have a ragged appearance.
M-07-306	59384	1	203.72	203.76	H-63	3d, coarse grained to pegmatitic, catches 2-5% medium to coarse grained chalcopyrite.	Plagioclase, clinopyroxene (some altering to inverted pigeonite), olivine, minor chlorite, magnetite, apatite.	Moderate.	Plagioclase has brown dusty alteration and zones of strong sericitization. Olivine is completely altered to brown serpentine. Clinopyroxene is being replaced by biotite, edges are often chloritic. Chlorite associated with magnetite.	2-3% fine to coarse grained chalcopyrite. Sulphides are often replaced by chlorite in patches of stronger alteration. Sulphide filled fractures in silicate grains. Sulphides are located in plagioclase, often in zones of chlorite alteration and less commonly in clinopyroxene.
M-07-306	59385	1	203.85	203.89	H-64	Pegmatitic gabbro, catches a 1 cm chalcopyrite grain.	90% plagioclase, altered clinopyroxene (altering to inverted pigeonite) minor magnetite and chlorite.	Strong alteration.	Plag is altered to a brown dusty colour, olivine grains have been completely altered to serpentine, clinopyroxene has been altered completely (amphibole?).	1-2% fine to medium grained chalcopyrite.

M-07-306	59385b	1	203.85	203.89	A-60	Plagioclase, fine to coarse grained, with clinopyroxene (some altering to inverted pigeonite), olvine altered to serpentine, chlorite.	Moderate-strong	Clinopyroxene altered to inverted pigeonite, olivine is serpentinized.	Fine grained disseminated chalcopyrite, scattered within the chlorite alteration zones, within plagioclase and within clinopyroxene. Fe-rims on chalcopyrite are common.
M-07-306	59386	1	204.54	204.58	H-65	Pegmatitic TDLG, small stringer of syenite causing plagioclase alteration to K-sp. Lots of chlorite and serpentinization of olivine.	Strong	Strong alteration, serpentinization of olivine, chlorite, K-feldspar replacing plagioclase.	2-3% fine to coarse grained chalcopyrite, sulphides were plucked in polishing.
M-07-306	59386b	1	204.54	204.58	A-61	Plagioclase, clinopyroxene, olivine, minor biotite.	Moderate	Olivine is altered to serpentine.	Scattered grains of chalcopyrite within plagioclase and clinopyroxene.
M-07-306	59387	1	204.75	204.79	H-66	Plagioclase, clinopyroxene (half is altered to inverted pigeonite), chlorite, minor magnetite, biotite.	Strong	Sericite alteration of plagioclase, has a brown dusty colour. Chlorite is replacing inverted pigeonite. Zones of chloirte alteration.	1-2% fine to medium grained chalcopyrite.
M-07-306	59387b	1	204.75	204.79	A-62	Plagioclase, clinopyroxene (altered to inverted pigeonite), olivine (altered to serpentine), hornblende, chlorite.	Moderate	Olvine is all strongly altered to brown serpentine.	1-2% fine to medium grained chalcopyrite.
M-07-306	59388	1	205.22	205.26	H-67	Plagioclase, clinopyroxene (completely altered to inverted pigeonite, minor magnetite and chlorite.	Strong	Clinopyroxene altered to inverted pigeonite and chlorite/actinolite and plagioclase to sericite.	2-3% fg-mg-cg chalcopyrite.
M-07-306	59388b	1	205.22	205.26	A-63				

M-07-306	59389	1	205.65	205.69	H-68	3b, just comingo ut of the altered zone, 2% fine grained chalcopyrite	Plagioclase, clinopyroxene (some altering to inverted pigeonite), olivine, minor magnetite, biotite, chlorite.	Low-Moderate.	Small zones of clinopyroxene are altering to inverted pigeonite, olivine is partially altered to serpentine and sericite and brown fractures occur in plagioclase.	2% chalcopyrite and pyrrhotite.
M-07-306	59390	1	205.86	205.9	H-69	3b, out of previous alteration zone, 5% fine grained chalcopyrite, well developed ophitic texture.	Plagioclase, clinopyroxene, olivine, minor chlorite and biotite.	Low	Minor amounts of clinopyroxene are being altered to inverted pigeonite. A fracture cuts the thin section with chlorite and biotite associated with it. Minor serpentinization of olivine.	1-2% fg-mg chalcopyrite + pyrrhotite. Fe-rims on the chalcopyrite. Some chalcopyrite is associated with chlorite.
M-07-306	59425	1	212.16	212.2	A-31		Nice texture, first formed euhedral to subhedral plagioclase, subhedral subrounded olivine, ophitic clinopyroxene, small amounts of biotite and magnetite. Some small amounts fo chloritelorite surrounding olivine grains. Doesn't really appear to be to much serpentinization of olivine	Low amount, just some chlorite		Small scattered grains of sulphides. Also a bit of tabular whiteish pink mineral within olivine, possibly millerite? At the junction of olivine and millerite. one of the grains is pyrrhotite + pyrite.

M-07-306	59426	1	222	222.04	A-32		Plagioclase, first formed, euhedral to subhedral, olivine, subrounded all dark brown to serpentine, ophitic clinopyroxene, minor biotite, and magnetite (3%).	Olivine has been strongly serpentinized, dark brown fractures thoruhgout plagioclase, chlorite in plagioclase, clinopyroxene is a brown colour and has pervsive fine lines throughotu it as well as darkgrey filled fractures	0.5-1% sulphides are vfg and scattered throughout the slide. Mineral asemblatge is chalcopyrite+pyrrhotite+py. chalcopyrite+chalcopyrite occur in the same grain, looks like a replacement texture, py is ragged and contains exsolution of the dark grey streaks again. A few independent blebs of pyrrhotite. Within chalcopyrite grains of pyrite grains have cubic shape. Sulphides occur within plagioclase grains controled by cleavage , within and on
M-07-306	59427	1	231.05	231.09	A-33				
M-07-368	59251	1	105.36	105.4	T-1	Representative texture, NS			
M-07-368	59252	1	109.9	109.95	T-2	Representative texture, NS			
M-07-368	59253	1	113.36	113.4	T-3	Representative texture, NS			
M-07-368	59254 A	1	117.41	117.45	T-4	Representative texture, NS			
M-07-368	59254 B	1	117.6	117.64	T-5	Catches felsic leucocratic patch, try to describe			
M-07-368	59255	1	122.15	122.19	T-6	Representative texture, NS			
M-07-368	59256	1	126.26	126.3	T-7	Representative texture, NS with pyrrhotiteikilitc magnetite			
M-07-368	59257	1	129.1	129.14	T-8	Representative texture, NS with felsic patch	Strongly altered. Lots of mg chlorite, large patches of green, looks like some fine grained needle like tremolite as well.		

M-07-368	59258	1	129.49	129.53	T-9	Representative texture, NS		Trace vfg chalcopyrite, with small specs of pn? (less white than white mineral)
M-07-368	59259	1	129.76	129.8	T-10	2% fg -mg chalcopyrite	Good pile of mg cpy. Contains abundant bornite. Cpy grains are present which have a deeper purple opaque mineral. Cpy contains pentlandite within it	Chalcopyrite+bn + trace amount sof the white mineral (pn?)
M-07-368	59260a	1	130.01	130.02	T-11	2% fp chalcopyrite		Chalcopyrite+bn + trace amount of white mineral (pn?)
M-07-368	59260b	1	130.14	130.18	T-12	Representative texture, NS		Trace chalcopyrite + bn + trace white mineral (pn?)
M-07-368	59261	1	130.3	130.34	T-13	Trace fg chalcopyrite	Vfg cpy with bornite, within cpx and plag. There are some nice big cpy crystals within this slide.	Trace-0.5% vfg-fg chalcopyrite+bn+pn
M-07-368	59262	1	130.6	130.64	T-14	Representative texture, NS	Very fine grained cpy with bornite within. Typically within plagioclase along fractures and often with fine grained alteration products.	
M-07-368	59263	1	130.83	130.87	T-15	Representative texture, NS	Typical rep texture, ophitic plag+cpx+olv.	
M-07-368	59264	1	131.14	131.18	T-16	Representative texture, NS	Typical texture, ophitic plag+cpx+ol. Minor amounts of bt. Plag is dominantly Carlsbad twins. Minor zones of chlorite/sericite alteration. Some zones of interstitial mt, showing ilmenite exsolution and ilmenite zones in the grains, small amounts of cpy are associated along the grain boundaries of the magnetite. Vfg cpy scattered throughout the slide, dominantly occurs as interstitial mineral to plag grains. The cpx occasionally is in association with pyrite. This is one of the slides where cpx and olivine show the same birefringence but are clearly different grains.	

M-07-368	59265	1	131.38	131.42	T-17	Representative texture, NS increase in grain size (2cm)	Ophitic texture, vcg-pegmatitic. Plag+cpx+olivine, (40,50,10),. Minor amount of bt within the cpx grain. Plag shows Carlsbad and rare crosshatched twinning. Bt is present within cpx and small amounts rim the interstitial mt. Very small amount of mt <1% within the slide, interstitial exhibits ilmenite exsolution and ilmenite zones. Minor amounts of cpy dominantly within grains, very small amount overall.
M-07-368	59266	1	131.8	131.84	T-18	Representative texture, NS	Typical texture, ophitic plag + cpx + olivine TDL gabbro. Plag shows Carlsbad twinning with occasional cross hatched twinning. Minor amounts of bt in association with mafic grains or magnetite. Minor zones of chlorite alteration. Serpentine alteration of olivine, as well as alteration to fine grained magnetite. Mt is the dominant opaque, small zones of interstitial mt. mt has ilmenite exsolution lamella and ilmenitezones. Minor amounts of cpy associated with interstitial mt. typically along grian boundaries. Most of the cp is associated with the olivine alteration to vfg mt+-cp (approx 20%
M-07-368	59267	1	132.2	132.24	T-19	Representative texture, NS	Typical texture, relatively unaltered. Vcg ophitic plag + cpx+olv TDL gabbro. Biotite often rims magnetite grains and is also prsetn as indclusions within cpx
M-07-368	59268	1	132.57	132.61	T-20	Representative texture, NS vcg peg, trace chalcopyrite in area	Vcg-ophitic grain size. Typical ophitic plag+cpx+olv (50,30,20). All grains are monster sized in this sample. Relatively little alteration. Decent amount of biotite, sometimes with mt sometimes not. Olivine is altering to serpentine. Plag crystals show Carlsbad twinning and a decent amount (~20%) with crosshatched twinning.
M-07-368	59269	1	132.98	133.04	T-21	Representative texture, NS	Minor amonts of interstitial mt, showing ilmenite exsolution and ilmenite zones within the grians. Minor maounts of interstitial cpy within the slide.

M-07-368	59270	1	133.17	133.21	T-22	Representative texture, NS	Vcg typical ophitic plag+cpx+olv (50, 30, 15) TDL gabbro. With minor maounts of biotite. Zoens of chlorite alteration +- sericite scattered throughout. Plag is dominantly Carlsbad twinnign with lesser amounts (~15%) of cross hatched twinning. Plag show minor maounts of light brown alteration (sericite?). Olivine is strongly altered to serpentine and to opaque magnetite. Not very much interstitial magnetite in this slide, very little. Mt is dominantly present along fractures and in zones of intense olivine alteration (ie the olivine is altering to magnetite). One crystal in particular
M-07-368	59271	1	133.25	133.56	T-23	Representative texture, NS, chlorite alteration, ns	VCG-pegmatitic, plag+ol+cpx (60, 25, 20).plag is vcg, dominantly subhedral, grain ends are typically irregaular and end truncating onto other plag grains. Mod sericite alteration prevalent throughout the plag. Plag are dominantly Carlsbad twinned but there is also a fair amount (~10%) showing cross hatched twins. Biotite commonly rims interstitial magnetite. Large mt crystals are dominantly in interstitial to grain boundaries.Mt shows typical ilmenite exsolution and zones of ilmenite within the grains. Tehre are also some vfg mt +- cp that are present along grain boundaries. Minor amounts of mt+cp traped
M-07-368	59272	1	133.79	133.83	T-24	Representative texture, NS	Ophitic plag + cpx + olivine TDL gabbro. 35, 35, 20. Abundant biotite, rimming almost all of the interstitial magnetite within the slide. Plag grians are dominantly euhedral with some subhedral, all exhibiting Carlsbad twinning with a few showing cross hatched twinning. Olivine grains are intimeately linked with cpx grains, often rimmed by cpx or contained as inclusions within the cpx. Biotite iss also seen rimming cpx and olivine grians. One zone of large interstitial magnetite. Mt occurs as interstiail grains withininclusions of plag and biotite rims.mt contains ilmenite exsoluiton lamella and zones of

M-07-368	59273	1	134.04	134.08	T-25	chlorite alteration, blocky biotite rich	Ophitic plag+cpx+olv TDL gabbro. Zones of intense alteration scattered throughout the slide, fine grained alteration product effects the cpx and olivine dominantanly. Light brown sericitE? Alteration of the plagioclase. Cpx grains are vcg, up to 5 mm and greater. Olivine is strongly altered to serpentine in some areas (upt o 100% in some grians). Fine grained black alteration product of olivines (mt) rimming most of the olivine grians in the slide. Small amount of carbonate noted. Approx 15% mt is in the slide. Mt shows exsolution ilmenite lamella and zones of ilmenite within the grains. Dominanlty occurs as
M-07-368	59274	1	134.3	134.34	T-26	Representative texture, NS	Typical ophitic texture, plag + cpx + olivine. 40, 40, 15. Cpx crystals are vcg, up to 5 mm and larger in some rare cases. Plag grians are subhedral to euhedral and pretty looking. Plag all show Carlsbad twinning. Olivine crystals are only 0.5-1mm in size and distinctly smaller than the other minerals in the thin section. Small amounts of biotite within the gange. Oloivine shows alteration to serpentine. Large cpx grains appear to be composed of distinct grains (do not all have the same birefringence on XPL) Needle like tremolite alteration of cpx. Mt is relatively low amounts in this slidke <0.5%. Some occur as
M-07-368	59275	1	134.75	134.79	T-27	Representative texture, NS, chlorite alteration, ns	Increase in the alteration. Fine grained alteration products surroudnign grains of cpx and olivine. Increase in the amount of biotite. Chlorite alteration is present throughout the slide. Some grains of amphibole and calcite are also present. Abundant sericite alteration throughout. Biotite often rims mt grains. Cpx and Olivine become difficult to distinguish using the colour method in this thin section. Mt is the dominant opaque with ilmenite exsolution lamella and zones of ilmenite. Associated in interstitial sites as well as present as fineg rained magnetite in alteration zones of olivine and cpx. Vfg cpx +/- pyrite are

M-07-368	59276	1	135	135.04	T-28	Representative texture, NS	Typical texture. Ophitic plag + cpx + olivine 40, 40, 15. Plag is euhedral first formed laths, up to vcg, with interstitial cpx encasing it and last formed olivine near euhedral plag laths and encased within anhedral cpx grains. Minor amounts of highly irregular biotite typically associated with magnetite. Fine grained opaque alteration of olivine (dominantly mt, hard to discern). Fien grained brown alteration of the plag crystals. Patchy zones of fine grained alteration fo the mafic grians as well. Mt is the dominant opaque, typically contains ilmenite exsolution lamella and zones of ilmenite. Typically occurs
M-07-368	59277	1	135.38	135.34	T-29	Representative texture, NS	Typical texture for the most part. Ophitic plag (chadacrysts) + cpx (oikiocrysts), + olivine, approx 50, 30, 15 respectively. Plag crystals are dominantly euhedralgrains well defined grain boundaries encased by large cpx grains. Olivine crystals are subhedral to anhedral and are often on grain boundaries with plag grains showing straight edges indicating that olivine formation was after plagioclase. Minor amounts of biotite, typically formed around the cpx. Small zones of chlorite+sericite alteration of the cpx and plag (respectively. The bottom of the slide has the pebble like subhedral cpx? Grains within a matrix
M-07-368	59278	1	135.6	135.64	T-30	Representative texture, NS	Very fresh sample. Ophitic plag (chadacrysts) + cpx (oikiocrysts) + olivine, 45, 30, 10. Minor sericite alteration of the plag, and some zones of chlorite alteration of the cpx. Dominant opaque is mt,interstitial to gangue minerals. Commonly contains ilmenite exsolution lamella. Fg cpy is scattered throughout the slide. Occurs both interstitial to gangue, as inclusions within gangue and in association with the magnetite. Upon close inspection fine grianed cpy grians can be seen to have both po or pyrite in the core.

M-07-368	59279	1	135.9	135.95	T-31	Representative texture, NS, possibly fg chalcopyrite near bt but not in sample	This slide is approx 50% unaltered, and 50% strong alteration of the mafics predominantly. Typical ophitic plag (chadacrysts), + cpx (oikiocrysts) + olivine, 40, 35, 15. Zones of intense alteration to fine grained sericite and chlroite. Alteration fo cpx to amphibole (likely hornblende, green, cleavage at 60 deg. Biotite is associated with magnetite. Has a zone of the pebbly like cpx, where the grains are approx 0.2 mm in size, subhedral sub rounded and individual. In this zone of pebbly like grians there is a matrix of magnetite in a few zones which encases the rounded cpx grains. Biotite and amphibole are commonly
M-07-368	59280	1	136.26	136.3	T-32	chlorite alteration + mt, ns	Overall slide has a dirty sandty texture to all the minerals present, likely some sort of artifact from the polishing process. Ophitic Plag + cpx + olv 40, 30, 25. Zones of intense chlorite alteration of the mafics ina ssociation with plagioclase. Olivine is strongly altered to serpentine and fine grained opaque (mt + unknown). Strong association of opaques with olivine, turns out to be cp more often than mt. Cpy grains are associated with pyrrhotite and pyrite. Some small grains of possibly cubanite (perfect polish) are also present. Abundant vfg mt + cp inclusions within magnetite. Mt has ilmenite exsolution lamella
M-07-368	59281	1	136.6	136.64	T-33	chloritet alteratio = Mt NS	Overall fresh sample, but there is a zone (approx 40% of slide) where the cpx is strongly altered to a fine grained needle like lath material. Plag + cpx + olivine subophitic TDL gabbro. Olivine is strongly altered to serpentine and to fine grained black opaque (includes mt). minor sericite alteration of the plagioclase. Looks like we have some KSP within the thin section as well. Aprox 5% mt within the thin section, forms ophitic texture. Minor amounts of cpy in interstitial sites within the gangue minerals and in association with the magnetite. No other opaque minerals noted.

M-07-368	59282	1	136.94	136.98	T-34	Representative texture, NS	Ophitic plag (chadacrsyts) + cpx + olivine TDL gabbro. Nice ophitic texture defined in this sample. Relatively fresh over all, small zones of sericite alteration of the plag, and chlorite+tremolite alteration of the cpx + olv. Olivine is altering to a fine grained opaque mineral and to serpentine. The fine grained material definitely includes somme magnetite but not all of it is reflective. Olvine crystals typically have vfg inclusions of mt + cp within them. Ophitic magnetite (oikiocrysts with plag inclusions) is common in theis slide. Approx 10% mt overall. Mt has ilmenite exsolution lamella as well as
M-07-368	59283	1	137.3	137.34	T-35	Rep + chlorite alteration	Mg-cg varitextured, melanocratic subophitic plag (chadacrysts) + cpx (oikiocrysts) + olv TDL gabbro. Relatively fresh and unaltered. Minor sericite alteration of the plagioclase. Approx 50, 40, 20%. Minor amounts of biotite are present typically associated with opaques or olivine. Minor zones of chlorite alteration of cpx and olivine. Fine grained opaque alteration of olivine appears to involve some magnetite, most of it is not reflective however. Minor (<1%) mt, contains ilmenite exsolution lamella. Minor amount sof cpy, typically interstitial to gangue minerals. One of the olivines that is highly altered to
M-07-368	59284	1	137.56	137.6	T-36	Mt unaltered, ns	Leucocratic unaltered sample. Plag (chadacrysts) + cpx (oikiocrysts) + olivine, 55, 25, 20 (olivine slightly less than cpx). Minor sericite alteration fo the plagioclase. Fine grained alteration of a few olivine grains. Olivine shows typical serpentine alteration. Overall fresh slide. Minor amounts of biotite, occasionally encasing magnetite. Magnetite is the dominant opauq mineral, approx 6% of thin section, large zone of mt form ophitic texture surrounding first formed plagioclase laths. Minor amounts of chalcopyrite dominantly occur within the interstitial spaces of the gangue minerals (olivine and

M-07-368	59285	1	137.8	137.84	T-37	Representative texture, NS	Relatively unaltered slide. Ophitic plag (chadarysts) + olivine + cpx (oikiocrysts), 60, 20, 20 Leucocratic slide. Plag has slight fine grianed alteration product (likely sericite). Olivine crystals have minor serpentine alteration, otherwise are very fresh. More olivine than cpx in this thin section. Olivine crystals are seen to be entrained within cpx crystals. Crystallization order Plag > olivine > cpx. Minor amounts of biotite (8%) typically enclosing or near olivine grains. <2% opauqes, dominantly mt with ilmenite exsolution lamella. Trace vfg cpy within interstitial gangue sites, a few grains as inclusions within
M-07-368	59286	1	138	138.04	T-38	Representative texture, NS	Beautiful ophitic texture, plag + cpx + olv 40, 40, 10, almost no opaques. Minor alteration to the minerals. There are a few nice biotite grains that are surrounding a core of pyrite with minor amounts of chalcopyrite. Olivine is strongly altered to serpentine in some grains. Some chlorite alteration of pyroxene. Dominant opaque is mt with ilmenite exsolution lamella. Some grains of pyrite (unusual because there is usually more cpy with a minor pyrite core). These grains are typically surrounded by biotite. Minor amounts of vfg cpy scattered throughout the rest of the slide
M-07-368	59287	1	138.3	138.34	T-39	chlorite alteration, blocky biotite rich	Subophitic Plag (chadacrysts) + cpx (oikiocrysts) + olivine 40, 30, 15, 5% mt. Mod alteration throughout the slide. There are some zones of very intense alteration that are altered to a fine grained high birefringence mineral. Olivines are often altered to fine grained opaque material (appears to be magnetite). There is a zone of biotite + cpy crystals and they are associated with a 1mm grain of cpy. This association maybe should be analyzed. Dominant opaque is magnetite in this slide. Mt shows ilmenite exsolution lamella. Within a zone of intense fine grained alteration with high second to third order

M-07-368	59288	1	138.8	138.84	T-40	Catches syenite stringer	This slide is kinda interesting as it has a syenite? Stringer going through the centre of it according to my core log. Contacts of this stringer are kinda messy. Other than the stringer it would be a typical subophitic plag + cpx + olivine, no olivine withing the syenite stringer zone. TDL gabbro. Syenite stringer has calcite within it, crazyness. Very little opaques within this thin section. What little there is is dominantly mt, with very little cpx.	
M-07-368	59289	2	139.12	139.16	T-41	Weak chlorite altreation, catches mt, nice plagioclase crystals, NS	Subophitic plag (chadacrysts) + cpx (oikiocrysts) + olivine, 50, 40, 5. Minor fine grained sericite? Alteration of the plagioclase. Fine grained chlorite? Alteration of the cpx. Olivine is altered to serpentine, and often to a fine grained opaque material (probably magnetite? SEM will have to confirm). Minor amount sof biotite throughout the slide, sometimes rimming mt grains. Chlorite alteration and chlorite needle like laths are also present. <1% opaque minerals, dominantly mt with ilmenite exsolution lamella. Mt form ophitic texture with plagioclase chadacrysts.	Trace vfg chalcopyrite + pyrrhotite
M-07-368	59290	2	139.32	139.36	T-82	Magnetite rich, NS	Plag (altered to sericite) + cpx. Although this is the intense alteration slide it is interesting that the cpx does not have the lineations that typically accompany the intense alteration. Cpx is altered to chlorite + tremolite+ sericite. Large zones of intense chlorite alteration, needle like, anomalous bluey birefringence colour. Approx 5-10% amphibole (beautiful 60 degree cleavage). Also interesting is that this slide lacks the typical graphic qtz+ksp intergrowths I have come to expect on this slide, as well it lacks quartz in general and has no apatite that I could see. Dominant opaque is mt, approx 8% of the thin	Has SEM confirmed py

M-07-368	59291	2	139.55	139.59	T-83	chlorite fracture, NS	Fine grained (<1mm) relatively equigranular. Subophitic plag + cpx + olv, 50, 30, 10, approx 10% mt. cpx crystals can be seen to exhibit ophitic texture if you stretch the imagination a little bit, how ever magnetite is clearly the dominant ophitic mineral (with plag chadacrysts). Mt is the dominant opaque, approx 10% of the slide, shows ilmenite exsolution lamella. Trace amounts of cp (vfg) scattered throughout the gangue and mt.		Trace vfg chalcopyrite + trace pyrrhotite
M-07-368	59292	2	139.86	139.9	T-84	Representative texture, NS	Fg-mg, gradational increase in grain size is noticeable traversing the slide. Subophitic plag + cpx + olivine 55, 35, 5, approximate ratios. Some of the cpx grains (<30%) exhibit the perfect lineations along their surface. Patchy chlorite (weak) alteration throughout the slide, plag grains appear relatively fresh. Olivine grains show strong serpentine alteration and typically contain symplectic worm like intergrowths of opaque magnetite within the grains. Similar to previous slide. Mt is the major opaque (approx 5% opaques overall), and contains ilmenite exsolution lamella. Trace fg cpy is throughout the slide within		Trace vfg chalcopyrite+pyrrhotite (~2:1)
M-07-368	59293	2	140.24	140.28	T-85	chlorite alteration, patch NS	Fine grained to medium grained, plag (chada) + cpx (oikiocrysts) + olivine, 40, 30, 15 approx. Approx 10% mt, mt often forms subophitic texture with plag chadacrysts. Olivine often has symplectic mt worm like intergrowths within the grains. Actually quite interesting. ?Overall grain size is quite uniform throughout the slide, very few larger plag phenocrysts. Almost equigranular! Interesting. Very fresh sample over all, next to no alteration at all, no biotite or chlorite of any abundance noticed. About 10% mt, trhoughtout the slide, occurs as interstitial growths between the plag crystals. Also commonly symplectici		Trace vfg chalcopyrite + pyrrhotite (almost 1:1)

M-07-368	59294	2	140.6	140.64	T-42	Rep texcture, trace fg chalcopyrite, 2-4% chlorite, 2-5% mt	Nice texture, low amount of alteration. Subophitic plag (chadacrysts) + cpx + olivine, 60, 30, 10, leucocratic overall. Fine grained alteration of the oliviens, unknown, olvine often has fine grained disseminated mt around the boundaries. Patchy zones of chlorite +- tremolite alteration throughout. Mt crystals are also oikiocrysts showing the ophitic texture. Major opaque is mt with ilmenite exsolution texture. Minor amounts of vfg cpy throughout the gangue and the mt.		Trace vfg chalcopyrite+pyrrhotite
M-07-368	59295	2	140.96	141	T-43	Rep texture, chloriteirote, NS, trace MT	Well defined texture, subophitic plag (chadacrysts) + cpx (oikiocrysts) + olivine. Leucocratic sample, plag ~ 70% cpx <= olivine, at 30%. Minor sericite alteration of the plag, patchy zones of chlorite +- tremolite alteration throughout the slide. Minor amounts of biotite rimming magnetite crystals, bt has srange looking altered zones. Nice texture showing that olivine formed after pyroxene (rounded grains with straight edges along the plag also in connection with cpx grains. Cpx grains have fractures that mildly remind me of amphibole cleavage, but this shouldn't be possible. Dominant opaque is mt. The		Trace vfg chalcopyrite + trace pyrrhotite, a few grains of white? Pn?
M-07-368	59296 A	2	141.08	141.12	T-44	Catches felsic leucocratic patch, through mafics mottled rounded look, NS	Very nice texture, ophitic Plag (chadacrysts) + cpx (oikiocrsyts) + olivine, approx 50, 30, 20 ratio. Minor-mod patchy sericite alteration of plagioclase (fine grained, brown), minor-mod chlorite alteration (dominantly on the cpx) throughout, fine grained, green needle like laths. Olivine grains often have fine grain disseminated rims of magnetite. Noted an olivine grain with a quartz inclusion in it, on the middle left hadn side of the thin section near some magnetite. Dominant opaque is mt with ilmenite exsolution lammea. Minor amounts of fg cpy throughout.		

M-07-368	59296 B	2	141.18	141.22	T-45	Vcg pegmatitic, fuzzy look to unit	Leucocratic, plag rich, plag (chadacrysts) + cpx (oikiocrysts, looks normal, without the lineations), + olivine (strongly atlered to serpentine). Mod alteration throughout the slide, abundant fine grained (sericite?) alteration of the plagioclase crystals. Mod amounts of amphibole (light brown and green) thorughotu the slide, showing perfect 60 degree cleavage. Minor mt (<1%), with ilmenite exsolution lamella.	
M-07-368	59297	2	141.5	141.55	T-46	Representative texture, NS, cg	Relatively fresh sample, still contains some of the cpx with perfect lineations within it. As a note I tried buffing the sample incase this got rid of the lineations, and no it did not. Subophitic-ophitic plag (chadacrysts) + cpx (oikiocrysts) and olivine. Cpx is approx 60% regular and 40% the one with strange lineations. Near the dead centre of the slide there is one large cpx grain that is optically continuous and on the one end of it it looks normal, and then on the other it has the lineations, so the grain is most certainly the same. Very good candidate for Seming this phenomenon. Some of the olivine is	
M-07-368	59298	2	141.77	141.81	T-47	Rep text, 2-3% chlorite alteration, NS	Plag (chadacrysts) + cpx (oikiocrysts) + olivine TDL gabbro. Mod patchy zones of alteration (chlorite+sericite, minor tremolite?) throughout the slide. Alteration is dominantly on the cpx, mild sericite on the plag. Minor amounts of biotite along rims of mt grains. Dominant opaque is magnetite, contains exsolution lamella of ilmenite. Possibly some cubanite. Trace amounts of cpy, occasionally with pyrite within the grain boundary.	

M-07-368	59299	2	141.96	142	T-48	Representative texture, NS mt band (~8% of sample) with interstitial irregular look	Crazy alteration slide, cpx with lineaations, graphic/symplectic qtz+ksp intergrowths. Abundant sericite + chlorite + tremolite. Abundant quartz thorughotu the slide. Mt + ilmenite exsolution. Possibly some cubanite on this slide (perfect polish). Minor amounts of cpy associated with gange and mt.
M-07-368	59300	2	142.36	142.4	T-49	chlorite band, ~20% chlorite, large mtcrystals (4-6mm) NS w spec chalcopyrite in mt	This is a weak version of the crazy alteration. Actually a very good border line case. Mod alteration, chlorite + sericite + tremolite. This slide has cpx grains that show the irregular cleavage lining. Mionor amounts of graphic quartz + ksp intergrowths (regular angular ksp). Plag + cpx + olivine. Mt + ilmenite exsolution. Trace fg cp in the mt and gangue.
M-07-368	59301	2	142.6	142.64	T-50	Rep tecture, 2-3% chloriteroite, contains smeared chalcopyrite (trace-0.5%)	Plag (60%), cpx (oikiocrysts)|, olinvine, very plag dominant. Mod alteration to sericite + chlorite + amphibole. Minor amount sof bt, in the cpx, and as rims on the mt. Mt is the dominant opaque, with ilmenite exsolution laemma, well developed cleavage in a few of the grains, very minor amonts of cp in the gangue and the mt.
M-07-368	59302	2	142.88	142.92	T-51	Rep texturte, no chlorite, NS spec cp)	Perfect ophitic texture, one of the best ones seen to date, nice large grains of cpx with perfect euhedral fine laths of plag trapped within them, A+ texture, (world class) Plag + cpx + olv TDL gabbro, ophitic texture. Minor sericite + chlorite alteration. Minor amounts of biotite. Cpxc also traps anhedral subrounded grains of olivine within them. Mt with ilmenite exsolution,. Mt grains with rounded cpx inclusions. Very minor amounts of cpy in the gange and as inclusions within the mt.

M-07-368	59303	2	143.12	143.16	T-52	Vcg rep tecxtur, tr fg chalcopyrite	This is an interesting slide, as it catches a zone of the fine grained, subhedral to euhedral thing that I think is all cpx, from slide 59313B, this slide has parts that are definitely containing of olivine, but there is none in that middle sections I really think that it is all cpx, so this is like the 4th time that I am becoming sure that it is cpx. Plag (chada) with cpx (oikiocrysts) and olivine. Mod alteration to chlorite and sericite. Mt with ilmenite exsolution lamella and minor amounts of cpx.	
M-07-368	59304 A	2	143.4	143.44	T-53	Pervasive chlorite alteration rounded mafic grains look, rep text of that unit	Moderately altered slide. Altration is chlorite and fine grained sericite. Plag + cpx + olv (plag chada, cpx oikiocrysts). Large mt grain with circular inclusions of cpywith pyrrhotite cores, minor amounts of pyrite within the poo as well. Mt has illmenite exsolution . Inclusions of circular cpx within the mt grain as well. I believe this one must be secondary mt based on this relationship. Small fine grained remnant mt + cp within the strong alteration zone.	Trace chalcopyrite+pyrrhotite+pn
M-07-368	59304 B	2	143.57	143.61	T-54	chlorite fractures (2) + chalcopyrite + pyrrhotite grain, look for replacement texture	Unaltered slide. Ophitic (plag chada, cpx oikiocrysts), + olivine. Minor zones of alteration (sericite + chlorite). Lots of the olivine crystals are fully altered to serpentine (opaque dark green colour). Minor amount sof biotite associated with mt,a nd within olivine grains. Mt with ilmenite exoslution lamella. Cpy grains with cores of po? + minor amounts py within. Cpy rimmed by biotite.	Trace-0.5% chalcopyrite+pyrrhotite+pn(white?) (chalcopyrite>pyrrhotite>pn)

M-07-368	59305 A	2	143.82	143.86	T-55	Rep text, with 2-5% fg-mg chalcopyrite this is sulphides contining	Unaltered slide, dominantly plag + cpx + olivine. Minor amounts of biotite, typically associated with magnetite. About 5-10% of a green pleochroic, anomalous interference colour mineral. A few patchy zones of strong alteration, abundant chlorite?. Minor amounts of calcite in the alteration zones. <3% opaques, mt+cpy. Mt has exsolution lamella.	Tace chalcopyrite+pn(white)
M-07-368	59305 B	2	143.96	144	T-56	Rep text 2-3% fg cp, 2cm average grain size, up to 2 cm in leucocratic patch	Not altered slide (note that the slide before this one about 20 cm away was strongly altered. Subophitic with plag chadacrysts, cpx oikiocrysts, and abundant olivine (20%). Minor amounts of biottie typically surround magnetite. Mt with ilmenite exsolution lamella. Anisotropic other mineral, possibly cubanite (perfect polish, possible cleavage). Fg mt+ cp in fracgtures of olivine crystals. Rare amounts of pyrite on edges of cpy grains. Digested cpy grain contained with a plagc rystal.	Trace chalcopyrite+pyrrhotite+pn(white)
M-07-368	59306	2	144.12	144.16	T-57	Vcg, 1 cm, up to 3 cm grain size, NS-> very trace	Strongly altered slide again, similar to previous. Dominantly cpx with the cleavage lineations, amphiboles, large plagioclase grains, strongly altered. Apatite and quartz are somewhat common. Tremolite is also common, zones of graphic quartz + ksp graphic intergroth (regular with almost corner like edges). Minor amounts of biotite rimming mt dominantly, also occurs within the cpx grains. Likely toss some sericite alteration in the mix as well. No olivine detected. Dominant opaque is mt. one very interesting grain in the north east corner, with some sort of alteration product, can clearly see the nice lamella of ilmenite	Trace-0.5% fg-mg chalcopyrite+ pyrrhotite/pn? Not sure likelier pn

M-07-368	59307 A	2	144.3	144.34	T-58	Rep text, vcg, 2-5% mg 2-3m chalcopyrite +bornite (if I took sample right)	Some minor amount of cpx Dominantly the altered lineated cpx is the dominant mineral in the slide, typically large, anhedral grain. Minealogy contains a fair (10%) amount of amphibole (well defined 2 at 60 degree cleavage), some minor amounts of biotite, large zones of quartz, apatite crystals within the quartz. Graphic qtz + ksp intergrowth texture, with apaite (clear colourless, euhedral octagonal crystal shape, length ? look into that technique, uniaxial negative). Ksp has brown alteration on it. Minor amounts of calcite. Doesns't look like very much chlroite, but there is a fine grained	Chalcopyrite+white pn? Mineral, no pyrrhotite found
M-07-368	59307 B	2	144.37	144.41	T-59	Fg chalcopyrite in a mt band	CG-VCG, plag + cpx (large oikiocrysts, contain both plag and olv) + ol (cpx~=olv). Well developed subophitic texture. Olivine shows good fractures with serpentization within them. Some tremolite? Alteration of the pyx crystals. Cpy looks digested and is in association with plagioclase. Bornite is commonly associated with the cpy. Rare amounts of py are with the cpy. Not too bad mineralization overall.	Fg-mg chalcopyrite+bn exsolution, a few grains with large Pn cores
M-07-368	59307 C	2	144.46	144.5	T-60	Rep text, 2-3% chalcopyrite + trying to grab some pyrrhotite - lost pyrrhotite I think	Plag, olivine, cpx (olv >> cpx). Subophitic TDL gabbro. Zone of strong pervasive alteration through the centre of the slide in the plag grain, looks dirty kaolininte+sericite+-chlorite. Around the zone of strong alteration there is more or less no alteration. There are a few grains of cpx, and they are oikiocrysts, and are optically contiuous with plag chadacrysts contained within. Trace cpy, typically associated with worm like intergrowths of bornite. Little amount of magnetite. Sulphides are interstitial to silicates.	Fg-m,g chalcopyrite+lots of bn exsolution, a few grains have the white pn? Mineral associated

M-07-368	59308	2	144.66	144.7	T-61	2-3% fg chalcopyrite (2mm max) right before xeno, pyrrhotitessible stringer or bits of xeno	Subophitic cg plag (chadacrysts) with oikiocrysts of cpx. No olivine detected. Cpx has a very distinct dark rim not seen in any other slides to date. Very little opaques, small amount of magnetite, often rimmed by biotite. Some scatterd fg cpy, typically contained with the cpx phenocrysts. There is an interesting mt crystal which has 360 degree lines of something going through it (photo 1) in the middle left top of the slide.	Trace chalcopyrite + trace bn
M-07-368	59309 A	2	144.84	144.88	T-62	Cp+pyrrhotite replacement texture, cp+pyrrhotite occcur in some grain - don't get it :(	Plag + ol + cpx (ol >> cpx). Cg-vcg sample. None of the grains are really euhedral, does not display subophititc texture. Weak alteration overall, a few patchy zones of chlorite+biotite alteration associated with magnetite. In the same assemblage there is a 100% amphibolte (nice cleavages at 60 degrees. Cpy+bornite throughout the slide. Dominantly cpy > mt. bornite usually occurs with cpy, a few grains of pure bornite. Cpy commonly has pyrite associated with it.	Trace-0.5% fg-mg chalcopyrite+bn exsolution + pn? (white)
M-07-368	59309 B	2	144.96	145	T-63	Rep text right after the xeno from previous, 1 spec of bornite, this is where brilliant aquamarine chalcopyrite (bright metallic purple)	Plag + cpx + olivine, olivne is in a good amount approx 40, 35, 35, 10% accessory. Mod alteration throughout the slide, zones of intense chlorite+tremolite+sericite alteration of the plag phenos. Cpx shows alteration around edges. Lots of cpy + mt. small amounts of bornite within the cpy. Trace amounts of pyrite, pyrite grains show exsolution to ?? mineral.	1-3% fg-mg chalcopyrite + bn exsolution + white pn?

M-07-368	59309 C	2	145.14	145.18	T-64	In large 2-3cm grain of clinopyroxene a chalcopyrite / pyrrhotite grain with replacement texture is occuring in this sample	Vcg-pegmatitic. Plag with cpx + olivine. Subophitic textgure with cpx oikocrysts and plag chadacrysts. Little alteration, patchy zones of chlorite+ sericite alteration + biotite. There are some biotite grains that appear green in colour but in XPL the grains look optically continuous. Good amount of olivine. Relict wedges of cpx within grains of plagioclase. Dominant mineral is chalcopyrite. Trace amounts of bornite in cpy, there is also trace amounts of pyrite.	1-2% fg-mg chalcopyrite + trace tiny bit of bn exsolution
M-07-368	59310	2	145.48	145.52	T-65	Large 2a xeno, sample should grab both TDL stringer + xeno, chlorite frac + 3 mm chalcopyrite grain (1-2% chalcopyrite)	This is another slide that has fine grained minerals and is similar in appearance to 59313B ? the one that I had a lot of trouble with telling if there were olv + pyx because the contrast looked so similar. I am not on the band wagon again that it had NO olivine, as this one there is a distinct clear olivine in it, and it has a huge contrast compared to the pyroxne. I am starting to think that no contrast means no olivine. Logically this should be aite. Overall weak alteration. Cpx + plag + olv (<5%), with minor biotite and chlorite. Subophitic with cpx oikocrysts and plag chadacrysts. There is a zoned plag crystal (kinda like a	Trace-1% fg-mg chalcopyrite + bn exsolution, tiny bit of white pn?, sulphides are dominantly in the TDL not the fine grained cumulate, has a lot of hydrous silicates that truncate the sulphides. GOOD SHREDED
M-07-368	59311	2	145.48	145.52	T-66	Strange chlorite alteration (green) cp grain with clorite black ish green w fracts that appear to be pyrrhotite (2% 2 mm chalcopyrite)	Mg-cg, subophitic with plag (chadacrysts) and pyx (oikiocrysts), olivine up to 15% of the slide. Overall weak alteration. Patches of mod sericite (brown, fine grained) alteration of the plagioclase. Very little chlorite and biotite. Mt is dominant opaque, commonly with ilmenite exsolution. Mt is commonly associated with olivine. Trace cp throughout the slide. Cp rarely has pyrite in it. One grain in the top centre has rounded medium brown grain within it, unknown mineral. SEM!	Trace-0.5% chalcopyrite + bn exsolution,

M-07-368	59312	2	145.88	145.92	T-67	Vcg 1-2% chalcopyrite, should have a grain of chalcopyrite +pyrrhotite about 2mm	Vcg cpx (50%), plag (40%), olv (<5%), TDL gabbro. Plag chadacrysts with cpx oikiocrysts, subophitic texture overall. Minor alteration present, some small zones of chlorite alteration, plag has a slight dusty appearance to the crystals. Also some zones of intense alteration (sericite), fine grained alteration product. Minor amounts of biotite (typically with chlorite, rimming cpy grains.) Contains mt and cpy, mt has ilmenite exsolution lamelle. There is a nice grain of cpy in the centre which half is perfect cp, and the other half is partially digested mt, with fien grained cp within the grain. Vfg cpy disseminated		0.5-1% chalcopyrite+ pn? (white), pretty big pn grains within chalcopyrite,. Nice shredded
M-07-368	59313 A	2	146.18	146.22	T-68	Strong chlorite alteration, + 5a stringer, mottled green cummulate look to TDL, contains 2 grains of blackish pyrrhotite + chlorite fracture	VCG – pegmatitic, cpx (oikiocrysts) plag (chadacrysts), olv, Dominantly cpx and pyroxene. Sample is relative fresh and unaltered overall. Very coarse grains of cpx and plag. Minor amounts of olivine (<5%). Weak fine grained sericite? Alteration of plagioclase grains. Some small grains of biotite included within the cpx crystals. Contains mt with ilmenite exsolution, minor amount sof cpy associated with mt and with gangue minerals.		
M-07-368	59313 B	2	146.22	146.26	T-69	Same but @ qtz sytenite chlorite fracture, backup for first one due to breaking	Very low amount of alteration, fresh looking sample. This one it is hard to discern, between the cpx and the olivine due to a low contrast in the colour and reflectiveity? (the solidness of the grain boundaries) Mg-fg (<1mm-2mm) average grain size. This sample the cpx turns back into the cpx that we are used to from before the strong alteration of the rocks, it is approx 40% cpx, 40% plag, 10% accessory minerals (like 5% olv possibly). The olivine grains are suhedral to anhedral, and tent to occur in clumps, there are two distinct zones where the olivines occur with a change in average grain size. Interstitial to the		Trace-0.5% fg-mg chalcopyrite + a little bit of the white pn? Mineral… (possibly py this time?)

M-07-368	59314	2	146.28	146.32	T-70	Rep text of mottle green chlorite rich unit, plus captures the felsic 5a stringer, mentioned in log, looks like the same as the two lareg 'blowouts' mentioned in log for 147.0- + 147.35 those	This one has some of the best sulphides in my thin sections, but the cores have been plucked out of the grains. Slide is highly altered, chlorite and biotite alteration of cpx, cpx typically has the fine lined cleavage and mid 2nd order birefringence. Strong chlorite alteration and biotite alteration products. Strong chlorite and biotite alteration of the cpx. There are zones of intense alteration of the main minerals, altered to a fine grained alteration product. A couple nice olivine grains, near centre right edge, show chlorite? Altreatio along the grain boundary. One nice large pyroxene grain near upper left corner	
M-07-368	59314	2	146.28	146.32	T-70	Rep text of mottle green chlorite rich unit, plus captures the felsic 5a stringer, mentioned in log, looks like the same as the two lareg 'blowouts' mentioned in log for 147.0- + 147.35 those	Dominantly plagioclase, huge plag crystals (4-5mm in size). Altered cpx with fine lines, mid 2nd order birefringence. Graphic qtz + ksp intergrowths (qtz is clear in ppl, ksp has dirty brown colour in ppl). There are perfect hexagonal grains, that are almost isotropic (are if it is cut just perfectly), very difficult to get optic axis figure, still undertermined at this time. Strong alteration, bt and chlorite are within the cpx grains, as alteration product? Mt is the dominant opaque mineral, commonly associated with ilmenite. Mt is commonly more pock marked and ragged compared to ilmenite, commonly has triangular	0.5-1% fg-mg chalcopyrite + pyrrhotite (the pyrrhotite looks white in this sample but is clearly anisotropic and contains pentlandite flames) plus a little bit of cubic mineral that looks like py
M-07-368	59315	2	146.47	146.51	T-71	Catches the sane like ol rich part of the uni. Should be able to tell if this is TDL or not (ie this unit started at 145.96) fg, diss sulphides	This one is slightly different than the usual slides. There are 4+mm plagioclase grains, but this time instead of the plag being encased within pyroxene grains the place crystals are encasing cpx (mod altered, 2nd order birefringence, perfect cleavage in one direction, possibly cleavage in another dirction, looks more like fractures, irregular grain boundaries, the altered cpx?). Mod alteration throughout the slide. Plag crystals are weakly altered, show a slight brown tinge. Cpx crystals are mod-strongly alterd, contain frequent inclusions of biotite. Zones of graphic magnetite + cpx intergrowth (two	

M-07-368	59316 A	2	146.82	146.86	T-72	Unit changes back into 3d, the crazy strong chlorite alteration from before is gone, sample of mt w/ associated chlorite alteration	This is supposed to have been an ophitic sample from the hand sample description, however it appears more to be a mod-strongly altered sample and the ophitic texture is ____. Subophitic with plag chadacrysts and cpx oikocrysts. The cpx is the altered variety with strong well developed cleavage, mid 2nd order birefringence, pleochroic in ppl with a brown – slightly greenish brown colour. Contains several 4-6 mm large sutured quartz phenocrysts. Cpx is strongly altered to chlorite + biotite + finer grained material. Dominantly mineralogy is cpx (70%), plag (20%), accessories (bt, chl) and quartz is
M-07-368	59316 B	2	146.94	146.98	T-73	Rep texture of pegmatitic ophitic texture	
M-07-368	59317	2	151.2	151.24	T-74	Rep texture, cg, 5mm average, chlorite alteration, TDL	Similar to previous slide. Dominant mineral is perfect cleavage pleochroic Cpx, secondadry is plagioclase. No olivine detected. Strong alteration throughout the slide. Plag is altered to fg material. Contains ~5% quartz, as well as the hexagonal isotropic mineral that is unknown at present. The cpx is strongly altered throughout the slide to a fine grained mineral. Biotite occurs within the cpx? And chlorite and biotite appear int eh strongly altered zones (which appear to be focused on the cpx?). Mt is the dominant opaque, contains typical twinning as well as the ilmenite? Association. Cpx is the dominant

M-07-368	59318	2	155.56	155.6	T-75	Rep texture, contains qtz syenite stringer, the irregular pink ones in the log	We are back to the altered looking slide, with the graphic qtz+ksp intergrowth (BURP confirmed qtz), the perfect cleavage cpx? Or whatever it is that is slightly pleochoric and has a million lines through it. Overall very chaotic look to the thin section, looks like 323 and 322 more than the previous two which were actually nice gabbros. Dominant mineralogy is unknown, mostly it is that well defined linear cleavage mineral of which I am a little bit unsure. In addition to that. I am getting pretty convinced that it is CPX with really well defined cleavage, and htat the cleavage is giving it an apparent
M-07-368	59319	2	161.7	161.74	T-76	Rep texture, 3b chlorite atleration, trace fg + mt (3-5%) contains pinkish bleb (5a?)	Coarse grained (2-3cm largest grains) ophitic plag (40%), olivine (35%), cpx (10%), with accessory biotite and chlorite. Overall slide is mod-strongly altered. Plag crystals have ubiquitous alteration, to dirty brown staining throughtouslide and in zones the alteration is much stronger and the minerals are altered to a fine grained sericite? Alteration, difficult to discern anything. Chlorite alteration throughout the slide, concentrated in the fine grained alteration product mentioned above. It still seems like the strongest alteration is of the plagioclase grains, cpx and olv in the slide appear unaltered. Tehre are
M-07-368	59320	2	165.6	165.64	T-77	3a rep texture, 5% chlorite, 5% mt	Coarse grained (ol, plag, and cpx are ~3 cm large) Plag (30%), cpx (40%), ol (25%), coarse grained, up to 3 cm. Minor amounts of biotite and chlorite + weak sericitic alteration (fine grained, dusty looking) alteration of the cpx. Overall plag looks slightly altered, fine grained rims of chlorite and biotite alteration along some of the grain boundaries. Biotite occurs within the cpx, and as an alteration/replacement on the edges of cpx and olivine. Pyroxene grains show ophitic texture. Even the olivine grain which is very large contains inclusions of plagioclase within it. A thin qtz vein cuts across the sample

M-07-368	59321	2	169.9	169.94	T-78	3a rep twith bits of leucocratic patches + 5% chlorite, 5% mt	This one looks more like a typical gabbro we expect from the suite, lacks the graphic intergrowth texture, and the cpx? That has the very fine regular cleavage within it. Dominant mineralogy is Plag (45%), cpx (35%), olv (8%), and minor biotite with lesser chlorite (weak alteration of the XX). Olivine crystals show very nice fractures infilled with a green material, look up what this material is, of note in this slide some of the olivine is more of the fracture fill material than it is olivine itself, could be of note. Mt, cpy, and possible pyrite (associated with the cpy) are the main opaques within the section
M-07-368	59322	2	174.6	174.64	T-79	3a, 5-7% mt, + tr chlorite	Large zone of graphic qtz+feldspar intergrowth, very large, approx 1 cm by 1 cm large. The clear colourless, with low low first order interference is uniaxial positive (BURP) with altered dirty looking feldspar. Very coarse grained plag, with typical twinning, 1cm-2cm large, making up approx 40% of the thin section. Approx 30% is that pleochroic brown mineral with very fine lines going throughout it, with upper 2-lower 3rd order birefringence. The lines do not look like twins and appear to be perfect cleavage, very evenly spaced, give the mineral pleochroism, typically light brown to clear and colourless. The
M-07-368	59323	2	178.76	178.8	T-80	3a fg, rep	Contains graphic qtz+fsp intergrowth texture. In one small section there is graphic magnetite + other mineral, difficult to make out due to strong alteration of the gangue mineral, but the magnetite is definitely magnetite, also minor amounts of cpy within this zone. Slide overall shows high degrees of alteration, alteration is to chlorite and a foggy dusty looking mineral, sericitization?. Abundnat biotite (20%), has a strange look to it, like it has striped lines going through, but is still pleochroic, not sure if it is birds eye extinction. Contains a very large oikiocryst? Of plag which has inclusions of other minerals within

M-07-368	59324	2	183.86	183.9	T-81	3a rep texture				
M-07-369	59397	2	69	69.04	A-1		TDLG with strong alteration, plagioclase crystals where visible are euhedral-subhedral, encased in pyroxene grains, minor amount of biotite, very large amounts of chlorite and tremolite (fibrous, radiating)	Strong	Lots of chlorite alteration pervasive thorougout plagioclase, fibrous tremolite is also abundant, strong dustry grey alteration of plagioclase, no olivine grains.	No sulphides
M-07-369	59398	2	73	73.04	A-2		Strongly altered slide, dominantly compsoed of K-feldspar. Looks pink in hand sample, but is very dark grey on thin section, abundant amounts of tremolite, zones of strong chlorite and calcite. Fault related.	Very strong		One fine grain of chalcopyrite, also there is the tabular within a zone of strong chlorite alteration, calcite and bladed tremolite.
M-07-369	59399	2	78	78.04	A-3		Strongly altered on half of the slide, the other half is relatively fresh TDLG. Plagioclase formed first, subrounded olivine, and large ophitic clinopyroxene. Olivine grains are entrained within clinopyroxene. Olivine grains are commonly rimed by fine green chlorite. The alteration zone appearas to be a strongly chloriteoritizied/amphibolized clinopyroxene grain, with bits of biotite scattered trhoughout.	Strongly altered		Chalcopyrite occurs within olivine, plagioclase, clinopyroxene. Trace pyrite occurs within strong olivine alteration zones.
M-07-369	59400	2	81.32	81.36	A-4		Well formed ophitic texture, plagioclase first formed, olivine subrounded and clinopyroxene forms ophitic texture, minor amounts of magnetite, biotite.	Low	Prisitne, a bit of serpentinization of olivine and a bit of chlorite alteration.	Trace amounts, very fine grained disseminted chalcopyrite + ultra-trace bornite. Occurs dominantly within plagioclase and minor amounts along contact with olivine grains. FeO rimming observed in one area.

M-07-369	59325	2	84.38	84.7	H-1	Rep texture of unit, strong pervasive chlorite alteration, chlorite is black-green with hematite staining (black red) alteration of phenos, no sulphides	Plagioclase, clinopyroxene, hornblende (dark brown colour, cleavage at 90/120, birefringence looks highly altered and is not a solid colour for the grain).	Strong.	Strong, chlorite alteration, fine grained opaques replacing hornblende and plagioclase. Brown fractures all through the plagioclase and a dusty brown look to them.	Trace amounts of very fine grained disseminated chalcopyrite and small amount of pyrite within havily altered olivine.
M-07-369	59326	2	86.9	86.96	H-2	Pink (K-feldspar and hematite) alteration zone, mafics strongly chlorite altered.	Plagioclase K-feldspar (with perthite exsolution), clinopyroxene, hornblende (green and brown with green altering to brown), inverted pigeonite, apatite, calcite, magnetite, K-feldspar intergrowth with quartz. Abundant magnetite (>10%).	Strong.	Strongly altered, chlorite alteration throughout, brown sericite alteration of the plagioclase, hornblende altering into a different colour.	Trace to 0.5% sulphides, composed of chalcopyrite, trace pyrite. Occurs as small fine grained, dissemianted, dominantly as small subrounded nuggets within clinopyroxene and more ragged grains within zones of chlorite alteration.
M-07-369	59327	2	87.24	87.28	FAIL	Pegmatitic band with black chlorite alteration of phenocrysts, no sulfides	No thin section.			
M-07-369	59327b	2	87.24	87.28	A-48		Slide composed of plagioclase (60%), and olivine (40%), thin rims of pyroxene around olivine, minor amounts of biotite and chlorite.	Pristine	Small zones of chloriteroite, olivine has very dark fractures but doesnot appear extensively altered. Some chlorite penetrating along plagioclase cleavage.	Trace (<0.5%) sulphides, the dominant sulphide is chalcopyrite, there are trace amounts of bn, + trace amounts of pn. PGM grains? FeO rims on sulphides. The sulphides are present within plagioclase, and are controeld by clevage or on grain boundaries within olivine.

M-07-369	59328	2	87.6	87.64	H-4	3b, strong chlorite alteration (30-40%) pale green and blackish green	Plagioclase, clinopyroxene (with and without inverted pigeonite), hornblende (dark brown, opaque) replacing large olivine, minor magnetite and apatite.	Strong	Brown fracture alteration of plagioclase (looks like it is working on 60/120 angles), as well as dusty grey alteration, strong chlorite throughout, large zones of chlorite, also replacing plagioclase and clinopyroxene. Olivine is all altering strongly to dark brown	Trace amounts of chalcopyrite, within plagioclase, clinopyroxene and chlorite alteration zones of plagioclase.
M-07-369	59329	2	87.75	87.79	H-5	3d, coarse grained with a magnetite band. Magnetite has replacement texture, 1 cm - 2 cm.	Dominantly magnetite, very large coarse grained grains, cross cutting clinopyroxene and plagioclase grain cleavage. The plagioclase is strongly altered to chlorite, as well the clinopyroxene (inverted pigeonite) also shows alteration. minor amounts of apatite, biotite and hornblende.	Moderate-strong.	Moderate-strong zones of chlorite throughout slide. Clinopyroxene being replaced by inverted pigeonite and hornblende. Dusty sericite alteration of plagioclase. Biotite rims on magnetite.	Trace very fine grained chalcopyrite in the plagioclase and clinopyroxene as well as chlorite alteration of plagioclase, commonly occurs with FeO rims and associated with magnetite.
M-07-369	59330	2	88.06	88.1	H-6	3b, coarse to very coarse grained, with hematite altered phenocrysts .	Clinopyroxene(almost all of it has the inverted pigeonite lines throughout), and plagioclase, very fine grained apatite, trace biotite within clinopyroxene and minor amounts of magnetite.	Moderate	Moderate, brown fracture cleavage alteration of plagioclase and dusty sericite altreation. Strong inverted pigeonite alteration of clinopyroxene.	Trace very fine to fine grained chalcopyrite (about a dozen grains), within clinopyroxene, lesser amounts in plagioclase, a few grains have bornite exsolution, and accompaniying that is some possible PGM minerals

M-07-369	59331	2	88.3	88.34	H-7	3b, very coarse grained, rep texture, still in w horizon, 20% chlorite + black chlorite alteration of phenos	Plagioclase, clinopyroxene (lots of inverted pigeonite) hornblende (dark brown opaque), minor biotite and magnetite.	Moderate.	Moderate (still some fresh clinopyroxene and plagioclase). Plagioclase has brown alteration along fractures, as well as dusty grey sericite and chlorite throughout. Dark brown hornblende was also observed replacing clinopyroxene.	Trace, very fine grained chalcopyrite + trace amount of pn (white with chalcopyrite fractures) There are also a few possible grains of pgm within this thin section.
M-07-369	59332	2	88.4	88.44	H-8	Typical unit, coarse grained strong chlorite alteration and patchy pinkish alteration should be in thin section.	Plagioclase, hornblende and clinopyroxene.	Strong	Plagioclase is all altered to sericite, with dark brown hornblende and the light grey dusting, Chlorite throughout. Magnetite alteration.	A few scattered grains of chalcopyrite, dominantly within clinopyroxene and chlorite alteration zones of plagioclase.
M-07-369	59333	2	88.7	88.74	H-9		Plagioclase, clinopyroxene, hornblende, minor apatite.	Moderate	Plagioclase is strongly altered with dark brown alteration products, and grey dusting of sericite. Chlorite is present in large zones of fibrous minerals.	Up to 0.5% chalcopyrite, sulphide trails going through clinopyroxene, main chalcopyrite zone is associated with clinopyroxene and plagioclase in a chlorite alteration zone

M-07-369	59334	2	89.08	89.12	H-10	End of strong w horizon, sample in very strong hematite/chlorite alteration (50%) + blackish + 30% pale green.	Plagioclase, and pervasively serpentinzied (brown) olivine.	Moderate	Plagioclase is all altered with dark brown (hbl?) alteration and dusty grey. Olivine are completely altered to brown/black, no clinopyroxene. Approx 10% chlorite total.	Trace sulphides, fine grains of chalcopyrite, dominantly within plagioclase, some minor amounts in chlorite zone.
M-07-369	59334b	2	89.08	89.12	A-49					
M-07-369	59335	2	90.15	90.19	H-11	Just after w horizon, strong pink K-feldspar and hematite.	Plagioclase/K-feldspar, hornblende (dark brown opaque), minor apatite and inverted pigeonite.	Strong	Plagioclase is altered with the dark borwn fractures, fine grey dusting, abundant chlorite	Trace sulphides, chalcopyrite and trace pyrite Pyrite is associated with highly altered olivine. Chalcopyrite occurs within clinopyroxene, alteration zones of chlorite, and within a few apatite grains.
M-07-369	59401	2	91.06	91.1	A-5		The textre is well developed, but there are zones of alteration throughout. Plagioclase first formed, sub to euhedral, olivine grains subrounded and rimed by clinopyroxene and large ophitic clinopyroxene grains encasing chlorite, minor amounts of hornblende, actinolite and biote	Moderate-strong in zones	Olivine altered to serpentine, clinopyroxeneto hornblende-tremolite and plagioclase has zones of sericite.	Trace-0.5% very fine grained scattered chalcopyrite + trace pyrite domiantnly within clinopyroxene, alteration zones and lesser amounts within plagioclase.
M-07-369	59402	2	95.44	95.48	A-6		Plagioclase euhedral-subhedral, clinopyroxene and olivine(completely altered to brown serpentine).	Moderate-strong.	Olivine is completely altered to dark brown, plagioclase is altered to sericite, clinopyroxene has dusty brown alteration within it as well.	Trace very fine grained chalcopyrite, with FeO rims, possibly a small amount of pyrite. Chalcopyrite is located within plagioclase and clinopyroxene.

M-07-369	59336	2	97.61	97.65	H-12	3d, sampling of felsic leucocratic patch with a hint of pink in the plagioclase crystals.	Plagioclase, clinopyroxene (some alteration to inverted pigeonite)t, olivine (the olivine is altering into the dark serpentine).	Strong	Moderate-strong brown frac alt of pl, as well as abundant dusting of pl, olivine is altering to dark opaque brown, clinopyroxene is going to ipgt	Trace chalcopyrite within clinopyroxene and plagioclase
M-07-369	59336b	2	97.61	97.65	A-50		Well developed texture, plagioclase, pyroxene, and olivine. Minor amonts of magnetite and biotite, as well as chlorite and a bit of tremolite	Moderate	Olivine is altering to dark brown serpentine alteration, some alteration of plagioclase to sericite	Trace very fine to fine grained chalcopyrite, within clinopyroxene, along alteration to magnetite, edge of olivine grains and within plagioclase.
M-07-369	59403	2	101.28	101.32	A-7		Well developed texture, plagioclase and clinopyroxene, no olivine, minor magnetite and hornblende.	Moderate alteration	Some olivine is going to dark brown serpentine, some chlorite in plagioclase and some hornblende within clinopyroxene.	Trace very fine to fine grained chalcopyrite within clinopyroxene and plagioclase.
M-07-369	59404	2	107.26	107.3	A-8		Plagioclase, clinopyroxene(lined common), minor magnetite, hornblende, calcite and quartz.	Moderate-strong	Strong sericitzation of plagioclase, hornblende alteration of clinopyroxene, some fibrous tremolite and chlorite	Trace-0.5% very fine grained disseminated chalcopyrite within plagioclase, clinopyroxene and zones of strong chlorite
M-07-369	59405	2	114.26	114.3	A-9		Well developed texture, plagioclase + clinopyroxene, a bit of olivine but its mostly altered, minor bt and chlorite	Low	Minor biotite and chlorite patches.	Trace very fine to fine grained chalcopyrite + possibly a few pgm grains? Chalcopyrite occurs disseminated, within plagioclase, clinopyroxene and chlorite alteration

M-07-369	59406	2	120.5	120.54	A-10		Well developed texture, plagioclase, clinopyroxene, minor magnetite and chlorite.	Moderate	Zones of chlorite and weak sericite alteration of plagioclase.	Trace to 0.5% chalcopyrite, in chlorite altered zones, possibly PGMs pyrrhotitessible PGM (white), or in sericite altered zone of plagioclase,
M-07-369	59337	2	123	123.04	H-13		Plagioclase, clinopyroxene, trace magnetite, biotite and green hornblende.	Moderate	Plagioclase is all strongly sericitized, clinopyroxene is mildly chloriteoritized	Trace very fine grained chalcopyrite and trace bornite, possibly PGM. Sulphides occur dominantly in the plagioclase
M-07-369	59338	2	123.28	123.32	H-14	3b very coarse grained felsic patch, should catch some very fine to fine grained chalcopyrite	Plagioclase, clinopyroxene, trace magnetite.	Moderate	Plagioclase is strongly sericitized (fine grey dusting) throughout, large chlorite crystals, clinopyroxene is relatively fresh.	Trace very fine grained chalcopyrite + pyrrhotite
M-07-369	59338b	2	123.28	123.32	A-51					Trace chalcopyrite, 3 grains that are 2-3 mm and look like they may have PGM grains.
M-07-369	59339	2	123.4	123.44	H-15	Very coarse grained, catches mg-cg chalcopyrite.	Plagioclase, clinopyroxene, magnetite, trace calcite.	Moderate	Clinopyroxene altering to inverted pigeonite. Plagioclase altering to sericite (light grey dusting throughout plagioclase crystals) Chlorite present in large crystals, and replacing mafic minerals.	Two grains of chalcopyrite, almost 1 cm large, irregular edges, and some fine grianed trace scattered chalcopyrite. Trace amounts of pyrrhotite.
M-07-369	59339b	2	123.4	123.44	A-52					Trace chalcopyrite, very good PGM potential (4-5 grains) possibly some pentlandite with chalcopyrite. Sulphides occur within plagioclase and in chlorite

M-07-369	59340	2	123.74	123.78	H-16	Representative text, very coarse grained unit.	Plagioclase, clinopyroxene, olivine, minor apatite.	Moderate-strong	Lots of chlorite, plagioclase altering to sericite, clinopyroxene is fresh	Trace very fine grained chalcopyrite.
M-07-369	59341	2	123.92	123.96	H-17		Plagioclase, clinopyroxene, chlorite, trace bt, mag/ilm	Moderate.	Lots of chlorite, plagioclase is altered to sericite clinopyroxene has some altered patches, mostly to chlorite.	Trace very fine grained chalcopyrite, in plagioclase and clinopyroxene. Trails of sulphide blebs in clinopyroxene. Fe rimmed chalcopyrite.
M-07-369	59342	2	124.04	124.08	H-18	Representative text, very coarse grained.	Plagioclase, clinopyroxene, olivine, trace biotite and magnetite.	Moderate	Moderate altered overall, chlorite throughout, strong altreation of plagioclase and clinopyroxene in some zones.	2-3% fine to coarse grained chalcopyrite, with bornite exsolution common, trace pentlandite.
M-07-369	59345b	2	124.1	124.14	H-22	Coarse grained (1cm average) with 1-2% fine to medium grained chalcopyrite.	Plagioclase, clinopyroxene, olivine, chlorite, magnetite, minor hornblende (green, nice cleavage), calcite, biotite, apatite.	Good, plagioclase, clinopyroxene, ol find some fresh pieces to sample, over all pretty altered	Moderate-strong altered throughout, chlorite throughout, plagioclase has abundant sericite alteraiton, strong serpentinzation of olivine, green colour, also strong fine grained olivine, clinopyroxene shows alteration throughout as well	Trace vfg chalcopyrite, excellemt PGM grain potetential, Fe? Rimming of chalcopyrite. Sulphides are dominantly in the plagioclase,

M-07-369	59343	2	124.36	124.4	H-19	Rep text, contains pale green chlorite alteration	Plagioclase, clinopyroxene, ol, chlorite, mag/ilm,	Good, decent amount of fresh amongst the alterations	Strong zones of chlorite alteration, olivine crystal is seen being altered by chlorite and then turning into the fine grain mag mess with sulphides in the destroied zone	Tr-0.5% vfg chalcopyrite +pnt?, EXCELLENT potential for PGM as well, there is a cloud near the centre in a field of clinopyroxene that has good pgm potential. Good sulphide trails cutting across olivine grain
M-07-369	59344	2	124.5	124.54	H-20	Unit w/ 2a xenolith, sample catches 2a/3b with fg chalcopyrite mineralzation	Sand like unit, fg, plagioclase, clinopyroxene, olv, chlorite (one grain) mag/ilm, tr, bt, ap,	Good, plagioclase, clinopyroxene, 1 olv, fresh for sampling	Moderate-strong chlorite zones thoughtout, zones with fresh zones as well	Tr-0.5% vfg-fg chalcopyrite, + pn? Good potential for PGM grains, in plagioclase, as well as sulphide trails in grains, chalcopyrite with Fe? Rims, interesting dusting of light grey-white vfg opaques within the brown altered olivine crystal
M-07-369	59345a	2	124.64	124.68	H-21	Vcg, 2-3cm grain zie, 3b/3d, no visible sulfides	Pl, clinopyroxene, ol, chlorite, trace bt, mt,ilm, cal, hbl (green), ap,	Good, plagioclase, clinopyroxene, olv ,fresh for sampling	Patches of chlorite alteration throughout, the dark opaque brown alt of ol, sericite alt of pl,	Fg-mg-cg chalcopyrite, chalcopyrite is getting shreaded by chlorite into ragged bands. Excellent PGM potential. No bn noted.
M-07-369	59346	2	125.13	125.17	H-23	2-3% fg-mg chalcopyrite, should have a bit of chalcopyrite growing next to a 1 cm plagioclase crystal	Pl, clinopyroxene, chlorite, mag/ilm, tr bt,	Good pieces of plagioclase and clinopyroxene, no OLIVINE	Strong alteration throughout, sericitization of pl, chloriteoritization throughout of the mag/clinopyroxene, ragged chlorite alteration of sulphides as well	2-3% fg-mg chalcopyrite + lots of white material within the chalcopyrite, (pentlandite?) There is also magamtic sulphide seeping into cracks in gangue minerals. chalcopyrite is in plagioclase and clinopyroxene, no preference noted, lots of Fe? associated with chalcopyrite, and lots of sulphide bleb trails in gangue minerals

M-07-369	59347a	2	125.3	125.4	H-24	Same rep unit of 3b, (3-5 mm avg grian zise) but ocntains trace fg-mg chalcopyrite,	Pl, clinopyroxene, ol, trace chlorite, bt, mag/ilm	Good pieces of plagioclase, clinopyroxene, and olivine	Sepentinization of olivine, goes to dark brown/green, opaue fine grain alteration of olivines as well. chlorite is throughout slide affecting, plagioclase, clinopyroxene and olivine, ragged chalcopyrite from chlorite alteration	1-2% vfg-fg chalcopyrite + pn (white isotropic with exsoluitiopn lamlella of chalcopyrite), there is also a zone of py? Within a strongly altered olivine, most pn?
M-07-369	59347b	2	125.4	124.44	H-25	Mg (2-5mm) average grain zie, may catches bit of fg chalcopyrite, should be able to see a distinct grain size decrease for this section	Plagioclase, clinopyroxene, chlorite, ol, trace cal, hbl,	Good, there are a few unaltered plagioclase, clinopyroxene and 2 ol grains to use	Sepentinization of olivine (goes to green and also completely dark brown grains), strong chlorite altreaiton throughout, instense alteriaotn of clinopyroxene, to the pyrrhotiteint that only ragged remants in a sea of alteration remain, chlorite and calcite are	Trace chalcopyrite, some areas ragged due to chlorite. A few white grains with pgm potential, also good amount of sulphide blebs cutting across grains. This time the white mineral is anisotropic, but still doesn't have the pink pyrrhotite colour
M-07-369	59348	2	125.7	125.75	H-26	3d pegmatitic, fg-mg chalcopyrite in this section,	Pl, clinopyroxene, chlorite, mag/ilm, tr bt, ap	Moderate- enough clinopyroxene and plagioclase grains to get a few samples NO OLIVINE	There are a few of the opaque brown grains which are likely once olivine, strong dark brown alt of plagioclase, and strong sericitiization, clinopyroxene is going to ipgt in a lot of place, strong chlorite alteration of mag and sulfides,	Trace vfg-fg chalcopyrite, in clinopyroxene NO potential for PGM

M-07-369	59349a	2	126	126	H-27	3b unit, in a patch that looiks very mafic, lets see what is going on	Clinopyroxene/ipgt, chlorite, pl, minor bt, calcite, completely messed	Very strong	Clinopyroxene going to ipgt, chlorite all over, weird things with completely random interference pattersn, mottled small mt grains all oer the place as well	Trace vfg chalcopyrite, a small patch of py
M-07-369	59349b	2	126.28	126.32	H-28	Good piece of the 5a mixing unit, find out what this stuff is	Plagioclase, some sort of dark brown unit, trace ap, chlorite, cal, brown hbl, mag/ilm(all crusty and digested looking),	Very strong	Similar to above but plus 'syenite' stringer running through making for some more messedupness!	
M-07-369	59407	2	132.18	132.22	A-11					
M-07-369	59408	2	139.36	139.4	A-12					
M-07-369	59409	2	141.76	141.8	A-13					
M-07-369	59410	2	147.4	147.44	A-14					
M-08-441	59428	2	50.2	50.24	A-34		Very nice well developed texture. First formed euhedral to subhedral plagioclase, olivine is > clinopyroxene, olivine ranges from subhedral to subrounded and also includes some larger pyrrhotiteikilitic grains encasing plagioclase (but not clinopyroxene), and then a few large ophitic clinopyroxene grains and clinopyroxene rims on olivien grains. minor amounts of magnetite, biotite and chlorite, tremolite		Minor areas of chlorite lateration within plagioclase, serpentinization/ tremolite of olivine, dark green serp fractures into olivine	Tracre amount of chalcopyrite+pyrrhotite. Dominantly within plagioclase grains and showing control by cleavage, and smaller amounts on plagioclase-olivine (more abundant) and plagioclase-clinopyroxene grain contacts.

M-08-441	59429	3	60.2	60.24	A-35	Cg, plagioclase, olivine is pyrrhotiteikilitic and very large grains, small amount of clinopyroxene, clinopyroxene rims olivine. Minor amounts of biotite, magnetite and chlorite/serpentine		chloriteoritization/sericitization within plagioclase, serpentinization of oliiine, bit of chlorite in olivine and clinopyroxene as well. Biotite appears to be replacing magnetite in a	Trace amounts of chalcopyrite+pyrrhotite + trace pn. Dominantly occurs within olivine, lesser amounts within clinopyroxene and plagioclase (cleavage controlled).
M-08-441	59430	3	70.2	70.24	A-36				Trace vfg chalcopyrite
M-08-441	59431	3	79.6	79.64	A-37	Plagioclase + olivine, almost no clinopyroxene, olivine grains are large and pyrrhotiteikilitic, encasing plagioclase grains. Minor amounts of biotite and magnetite and chloriteroirte		Minor amount of chlorite alteraiton of plagioclase and olivine, small zones of sericite, serpentinization of olivine	Trace amount of chalcopyrite + minor pyrrhotite. Dominantly within plagioclase, minor amounts on plagioclase-olv boundaries
M-08-441	59432	3	91.4	91.44	A-38	Nice texture, clinopyroxene is back. plagioclase nice first formed euhedral to subhedral, olivine grains subhedral to subrounded, irregular in shape, no longer pyrrhotiteikilitic. Large clinopyroxene grains partially encase olivien and plagioclase.		Very fresh overall, minor zones of serp of olivine, sericite of plagioclase and chloritization of plagioclase	Trace amount of chalcopyrite+minor pyrrhotite, dominantly within plagioclase secondarily within olivine
M-08-441	59433	3	99.7	99.74	A-39	Large first formed euhedral-subhedral plagioclase, encased in clinopyroxene, clinopyroxene is strongly altering to hbld throughout slide, zones of calcite grains are commonly associated with hornblend. Minor amounts of magnetite.		Strong sericitization of plagioclase, dirty brown cloudyness, intense hbld alteration of the clinopyroxene, large grains are completely to hbld	1 vfg chalcopyrite grain within plagioclase
M-08-441	59434	3	109.9	109.94	A-40	Nice texture, ahlf is olivien rich, the other half is clinopyroxene rich. plagioclase + olivine subrounded to subhedral, and clinopyroxene chadacrysts encasing the olivine grians, minor amounts of biotite and magnetite,	Very fresh	Few zones of serp of olv, + chloriteoritization of plagioclase	Trace chalcopyrite + bn exsolution, within plagioclase and olivine

M-08-441	59435	3	119.6	119.64	A-41		Plagioclase, olivine, clinopyroxene, hbld replacing clinopyroxene, minor amounts of biotite and mt,	Moderate-strong	Pervasive hbld altreation of clinopyroxene, serp of olivine and strong zones of chlorite/sericitie/ tremolite alteration. Some of the original grains are fresh but there is decent alteration all throughout.	Trace vfg chalcopyrite + trace pyrrhotite, all in serpentinization/chlorite alteration zones of olivine (original olivine grain is completely destroyed)
M-08-441	59436	3	130.2	130.24	A-42					Trace vfg chalcopyrite with minor amounts of pyrrhotite + white mineral (also some zones of white mineral + streaked grey mineral). Dominantly in plagioclase and some in olivine as well
M-08-441	59437	3	135	135.04	A-43		Fairly good texture, plagioclase, oliviune (small amount) and clinopyroxene, minor bt, mt, etc	Moderate-strong	Alteration throughout, olv to serp, chlorite/tremolit e alteration within plagioclase, and around	Trace scattered fg chalcopyrite+minor pyrrhotite. Occurs within plagioclase, clinopyroxene and olivine, no dominant host minearl
M-08-441	59350	3	138.15	138.19	H-29	Rep unit, ns, chck to see if ol	Pl, ol, clinopyroxene, tr bt, chlorite,, mag/ilm	PERFECT	A little bit of sericite dusting on the plagioclase, otherwise perfect	Trace vfg chalcopyrite, one grain has bornite , scattered throughout the slide, dominantly within plagioclase, and along cleavage, one grain within olivine, and two grains within chlorite alteration in the plagioclase.

M-08-441	59351	3	138.5	138.54	H-30	Rep unit, 1-2% fg chalcopyrite arnishes to blue and purple) rep texture with mineralizatio n	Pl (80%), clinopyroxene, ol, tr, bt, mag/ilm, chlorite, hbl (greenm, good cleavage)	Pristine	Dusting of sericite Moderateerately throughout the plagioclase in the thin section, small zones of chlorite alteration	1-2% fg-mg chalcopyrite + bn exsolution, bn grains, several white grains. Sulfides are dominantly in plagioclase, also associated on plagioclase/ol grain boundaries, it is in fresh plagioclase and equally or more so in altered plagioclase, Fe-Rims are common. The 'bn' grain still has some cdcp on the rim, it also looks like it is being digested by the altration within what was once plagioclase but is now very strongly altered, prismatic
M-08-441	59352	3	138.84	138.88	H-31	Big opaque white patch, has 2 grains of bo, see photo	Pl (90%), ol, clinopyroxene (only 1 grain), trace mag/ilm, chlorite, alt products	Good there is 1 grain of each mineral that is unaltered	Strong sericite alteration throughotu the plagioclase (this slide was from an opaque white zone of alteration, sericite), approx 70% of the plagioclase is destroied, there re good areas of destroied olivine by chlorite and the olivine goes into fine grained	
M-08-441	59353	3	139.33	139.37	FAIL	Patch of cholrite alteration, approx 40% of thin section, 0.5% chalcopyrite, looking at min in chlorite alteration				3-5% chalcopyrite with trace bn exsolution, good amount of whit egrains within the chalcopyrite GOOD PGM potential. Sulphides are dominantly within the plagioclase (most oten the heavily sericitized plagioclase) hhowever it is also seen within clinopyroxene, and in alteration zones,

M-08-441	59353b	3	136.33	136.37	A-53					Tr-1% vfg chalcopyrite + trace bornite bn exsolution, dominantly in plagioclase. 1 white grain in chalcopyrite near label (5). Dominantly in plagioclase, and has some very nice grains showing clevage control
M-08-441	59354	3	139.7	139.74	H-33	3-5% mg 2-3 mm chalcopyrite, one grain is tarnished rep texture looking at sulphide zone	Plagioclase, clinopyroxene, ol, trace chlorite, cal, ap, NO MAG/ILM, all sulfides	Moderate-OK, got 1 grian of pl, clinopyroxene, ol. Pl is pretty altered	Strong alteration throughout, zones of intense sericitization, chlorite is completely obliterating olivine and sulphides, calcite is kicking about inside of plagioclase	3-5% fg-mg (up to 7mm), trace amounts of bornite and pn? (white, isotropic with chalcopyrite exsotluion lamella) and a few grains around of a white mineral that is anisotropic, would be a good slide to confirm this mineral
M-08-441	59354b	3	139.7	139.74	A-54					Ultra trace vfg chalcopyrite,+ trace bn, + trace white mineral (pn? Isotropic) within plagioclase grains, sometimes in association with clinopyroxene/olv grains. SOME white mineral within the chalcopyrite (PGE GOOD potential for a few)
M-08-441	59355	3	139.96	140	H-34	Rep texture, slightly coarser grained, 1 cm average, plagioclase to clinopyroxene, trace fg chalcopyrite	Plagioclase, clinopyroxene, ol, trace chlorite, mag/ilm, bt	Perfect, have pl, clinopyroxene, ol and several grains of each completely unaltered	Overall fresh, zones of serpenintinized olivine, sericitization of plagioclase, clinopyroxene is also altered by unknown,	3-5% chalcopyrite + trace bn exsolution, there is also abundant amounts of a white mineral within the chalcopyrite, Very well developed Fe rims on some of the chalcopyrite that is enveloped by bt. PGM are in pl, clinopyroxene, also associated with bt, often rimmed by dark green chlorite?

M-08-441	59356	3	140.47	140.51	H-35	3-5% fg-mg chalcopyrite +pyrrhotite looking for cp + pyrrhotite replacmeent texture	Plagioclase, clinopyroxene, ol, minor chlorite, bt, mag/ilm	Perfect has lots of pl, clinopyroxene and 3 grains of ol for testing	There is abundant zones of sepentinization of ol, sericitiazation of pl,	2-3% fg-mg (up to 5 mm) chalcopyrite + same white mineral as before, (often has chalcopyrite exsolution within it) One chalcopyrite grain has whiteish granular grains that are anisotropic. Sulphides are dominantly associated with alteration and have a ragged appearance due to it. Sulphides are in plagioclase, one case of a clinopyroxene grain encased by sulphides (ragged and altered)
M-08-441	59357	3	140.7	140.74	H-36	3-5% fg-mg chalcopyrite + pyrrhotite looking for cp + pyrrhotite replacement textures, otheriwse rep unit texture	Pl, clinopyroxene, ol, minor chlorite, bt,	PERFECT, lots of unaltered of each grain	Sericite alteration of plagioclase in areas thorughout, chlorite alt of olivine completely in some areas, variable serp of ol (from small bits to entire grains)	1-3% chalcopyrite . There are also a small grains within chalcopyrite of the white mineral that has chalcopyrite exsolution. A few grains of the other white mineral, which is white-yelow, pleochroic in ppl, highly anisotropic in cpl, and looks granular, as within the previous slide). Some of the sulphides have been altered by chlorite and have a ragged appearance. sulphides are in plagioclase alteration zones, on grain boundary of mag and
M-08-441	59358	3	141.04	141.08	H-37	Rep unit texture, trace-0.5% fg diss chalcopyrite, skeletal mt, nothing too fancy	Pl, clinopyroxene, ol, minor bt, chlorite, cal,	PERFECT, 2 grains ol, 2 grains clinopyroxene and plenty of pl that have unaltered zones	Strong sericitization of the pl, chlorite alteration is present, ol is altered byserp going othe dark brown alteration product as well.	Tr-1% vfg-fg-mg chalcopyrite, with white mineral within, as well as what looks good to be pyrrhotite, in the mafics and associated on the boundaries with mag/ilm, sulphides are silhouetting the hbld,

M-08-441	59359	3	141.67	141.71	H-38	3a unit with rounded mafics and mt chlorite al, 1-2% fg diss chalcopyrite opaque white plagioclase, chalcopyrite is tarnished to purple	Mottled mafic hydrous unit, ipgt, heavily altered plagioclase, graphjic qtz-ksp intergrowths, mag/ilm, hbl, ap, minor bt	Highly altered	Mottled mafic unit, completely altered	0.5-1% chalcopyrite+trace py (pretty sure pyrite) throughtout the whole unit, in all of the minerals
M-08-441	59360b	3	142.08	142.12	A-55					2-3% chalcopyrite + white(isotropic) + pyrrhotite (definitely pyrrhotite) in one grain they are all together and can see a definate change in reflectance, the white mineral has the nice exsolution of chalcopyrite bands in it that are characterisitic of it, there is no oxidation associated with the chalcopyrite.
M-08-441	59360	3	142.08	142.12	H-39	2-3% chalcopyrite in opaque white plagioclase zone, may catch pyrrhotite but unliklely	Plagioclase, clinopyroxene, minor bt, mag/ilm, chlorite, cal + weird radiating spherical things, no clue what they are?	Moderate, plagioclase is all altered, one grain of clinopyroxene has clean spots to run on, no olivine	Super strongly sericitized plagioclase throughout barely any spyrrhotitets of unaltered plagioclase anywhere. clinopyroxene is full of random spyrrhotitets of bt ,	1-2% fg-mg (up to 10 mm) chalcopyrite + trace (pyrrhotite + pn). chalcopyrite is dominant, one grain has some ragged pyrrhotite that looks like chalcopyrite has replaced it (all the pyrrhotite goes extinct at the same time).

M-08-441	59361b	3	142.18	142.22	A-56					2-3% fg-mg-cg chalcopyrite + pyrrhotite + white (isotropic) another good grain where both pyrrhotite and the white ? mineral are in the same chalcopyrite grain. The cp in this slide are highly airregular grain boundaries aand being destroied by chlorite, chlorite needs are bounding and within chalcopyrite. excellent PGM potential
M-08-441	59361	3	142.18	142.22	H-40	Rep unit with chalcopyrite/ pyrrhotite/bo? Replacmeent ,	Plagioclase, clinopyroxene, chlorite, minor	Good for plagioclase and clinopyroxene, one grain of olv that has been heavily serpentinized but has a few 'fresh' looking spyrrhotitets	Sericitization of plagioclase, ctp going to ipgt, serpentinization/ chlorite obliterating most of the olivines in the slide, leaving a few remnant grains,	0.5-1% fg-mg chalcopyrite+ pyrrhotite (definate, pink, anisotropic), + white ?grian isotropic (pn? With chalcopyrite exoslution streaks within the grain) --> these two are in the same chalcopyrite grain, in plagioclase (including altered) and on grain boundary of mag and within mag as small circular blebs
M-08-441	59362	3	142.82	142.86	H-41	3d unit, getting large mt + chalcopyrite trace sulphides, 1400-1401	Plagioclase, clinopyroxene, ol, minor mag/ilm, chlorite, bt	Perfect, got a grain or two of all, unaltered	Moderate chlorite throughout, zones of stronglysricitized plagioclase, ol shows some serpentinization	Fg-mg-cg chalcopyrite and pyrrhotite (good pyrrhotite), excellent PGM potential (a few small grains of pn? With chalcopyrite exoslution streaks through it in a grain with pyrrhotite)

M-08-441	59363	3	143.1	143.14	H-42	Weak chlorite. Frac zone, otherwise rep unit, 2-3% fg-mg cp+pyrrhotite (look for replacmeent textures)	Plagioclase, clinopyroxene, ol, minor chlorite, bt, mag/ilm	GOOD for plagioclase and clinopyroxene, 1 grain of ol with heavily serpentinized margins	All of the olivine but one grain has been completely serpentininzed (brown) colour, strong chloriteroite thorughout, sericitization of the plagioclase, as well as dark brown fractures that seem related to the brown olivine,	2-3% fg-mg-cg (afew grains > 1 cm) chalcopyrite+pyrrhotite (pyrrhotite is pink, anisotropic , typically ias core of chalcopyrite grains) and a small amount of the pn? White isotropic mineral with chalcopyrite streaks within it
M-08-441	59363b	3	143.1	143.14	A-57					Chalcopyrite+pyrrhotite (very good pyrrhotite, pink, anisotropic) in the same grain, sulphides ar every very raged and chaotic, looks like a lot of things were plucked from the grains, Ap is closely associated with the [illegible]
M-08-441	59364	3	143.36	143.4	H-43	Rep text, 1-2% fg-mg chalcopyrite +pyrrhotite (look for replacmenet textures)	Plagioclase, clinopyroxene, ol, minor cbt, chlorite, mag/ilm, ap, . It is interesting as clinopyroxene and ol have trapped small crystals of plagioclase within them, I have not seen this so prevalently before.	PERFECT, unalterd multiple grains of all types	Zones of Moderate chloriteoritization about, olivine is fresh to strongly serpeninitzed, when serp it is altered to fine grained Fe remnants,	Fine grained chalcopyrite + pyrrhotite in the grains, (very nice pyrrhotite, anisotropic), found within all of the different gangue minerals.
M-08-441	59365	3	143.74	143.78	H-44	This is the part with the 2a xenolith containing vfg-fg chalcopyrite,	This is a suposed '2a xenolith' it seems that every time we have a xenolith it is a change in the grain size of the gabbro, but it never look like there is a xenolith contact, it is more like there is just a zone of finer grained gabbro, but xenolith? I am skeptical of this, it coudl jsut be chaotic grain size change. Fg plagioclase, clinopyroxene, ol gabbro, minor chlorite and biotite, all of the grains in this are msaller than is usual	Perfect, lots of small grains of all the minerals we might want to take a look at	Serp of ol, weak serc of plagioclase, prety fresh overall, some of the ol grains are to dark reen-dark brown,	

M-08-441	59438	3	146.2	146.24	A-44		Nice typical texture plagioclase, clinopyroxene, olv			Trace vfg chalcopyrite+-pyrrhotite, within plagioclase the most, olv, and clinopyroxene.
M-08-441	59439	3	153.5	153.54	A-45					
M-08-441	59440	3	163.2	163.24	A-46		Plagioclase, clinopyroxene, hbld, minor calcite, mt, bt	Moderate-strong zones, clinopyroxene is prety altered	Olv to serp pretty strong in areas, hbld over taking clinopyroxene, strong chlorite/tremo/seriicite within plagioclase	Very trace vfg chalcopyrite
M-08-441	59441	3	173.1	173.14	A-47		Plagioclase, clinopyroxene, minor olivine, minor amounts of mt, and bt		Not very altered, small amounts of chlorite in plagioclase, some serpentinization of olivine etc	Trace vfg chalcopyrite +- minor pyrrhotite, and white mineral I cannot identify. In the usual places, plagioclase, clinopyroxene, olv and hbld alteration zones (which can shred the chalcopyrite)

Appendix IV: Whole Rock Geochemistry

This appendix contains contains an excel spread sheet with results of whole rock geochemistry assays for DDH-306, DDH-368, DDH-369 and DDH-441.

The excel file is available on a CD that can be obtained from the Department of Earth and Environmental Science upon request, and are located in the folder 'Appendix 4 - Whole Rock Geochemistry'.

The results of DDH-306 is contained in the tab "DDH-306" The results of DDH-306 is contained in the tab "DDH-368" The results of DDH-306 is contained in the tab "DDH-369" The results of DDH-306 is contained in the tab "DDH-441"

Appendix V: Electron Microprobe

This appendix contains excel spreadsheets with the electron microprobe results from this study. Each spreadsheet contains tabs for the results from each drill hole.

The excel files are available on a CD that can be obtained from the Department of Earth and Environmental Science upon request, and are located in the folder 'Appendix 5 - Electron Microprobe'.

The results for olivine analyses are contained in ''Appendix 5-A- Olivine Microprobe.xlsx''

The results for pyroxene analyses are contained in ''Appendix 5-B- Pyroxene Microprobe.xlsx''

The results for plagioclase analyses are contained in ''Appendix 5-C- Plagioclase Microprobe.xlsx''

The results for oxide analyses are contained in ''Appendix 5-D- Oxide Microprobe.xlsx''

Appendix VI: LA-ICP-MS

This appendix contains contains excel spreadsheets containing the LA-ICP-MS results. Each spreadsheet contains tabs for the results from each drill hole.

The excel files are available on a CD that can be obtained from the Department of Earth and Environmental Science upon request, and are located in the folder 'Appendix 6 - LA-ICP-MS'.

The results for olivine analyses are contained in ''Appendix 6-A- Olivine LA-ICP-MS.xlsx''

The results for pyroxene analyses are contained in ''Appendix 6-A- Pyroxene LA-ICP-MS.xlsx''